

**SYNTHESIS OF IONIC BORON AMPHIPHILIC DIBLOCK  
COPOLYMERS AND PYRIDYLBORATE LIGANDS FOR  
TRANSITION METAL COMPLEXES**

*By Chengzhong Cui*

A dissertation submitted to

the Graduate school – Newark Rutgers, The State University of New Jersey

in partial fulfillment of requirements for the degree of Doctor of Philosophy

Graduate Program in Chemistry

Written under the direction of Professor Frieder Jäkle

and approved by

---

---

---

---

Newark, New Jersey

January, 2010

**ABSTRACT OF THE THESIS**

**SYNTHESIS OF IONIC BORON AMPHIPHILIC DIBLOCK  
COPOLYMERS AND PYRIDYLBORATE LIGANDS FOR  
TRANSITION METAL COMPLEXES**

*By Chengzhong Cui*

**Thesis Director: Professor Frieder Jäkle**

Atom transfer radical polymerization (ATRP) has been successfully used to prepare well-defined poly(trimethylsilyl)styrenes and the diblock copolymers, poly(trimethylsilyl)styrene-*b*-polystyrene, with controlled molecular weight and low polydispersity. Quantitative replacement of trimethylsilyl groups with boron tribromide in dichloromethane provided an important highly Lewis acidic intermediate that have allowed for the preparation of novel boron containing borate and boronium types of homopolymers and amphiphilic diblock copolymers with different post-polymerization modification processes. Characterizations including NMR spectroscopy, gel permeation chromatography (GPC) and the representative elemental analysis have been applied to confirm the quantitative transformations from the silylated polymers to the boron

containing ionic polymers. The self-assembly properties in block selective solvents of the amphiphilic block copolymers were extensively studied. Most importantly, through an electro-static interaction, the weakly coordinating pentafluorophenyl borate block copolymers were successfully used to attach an organo-rhodium catalyst and then underwent self-assembly in selective solvent to give rise to transition metal containing micelles with well-defined nanostructures.

In the last chapter, synthesis and characterizations of a variety of novel multidentate pyridylborate ligands are described. An appropriate procedure for synthesis of 2-pyridyl magnesium chloride in a usual dimeric structure was developed. The 2-pyridyl magnesium chloride was then used to react with different arylbromoboranes in dichloromethane or toluene affording different multidentate ligands. The tris(2-pyridyl)borate ligands were the first pyridine based tripod ligands with a boron atom as the bridging head and their complexation with Fe(II) was studied by cyclic voltammetry (CV) and UV-vis spectroscopy. All the structures of the ligands and metal complexes were determined by single crystal X-ray spectroscopy. The styryltris(2-pyridyl)borate monomer was successfully polymerized in a free radical polymerization to give a polymer with good yield and high molecular weight. NMR analysis was used to confirm the formation of this novel polydentate polymer.

## Acknowledgments

I wish to express my deepest gratitude to my supervisor and mentor, Prof. Frieder Jäkle, for his kind support, guidance and encouragement throughout my Ph.D. study, for his meticulous and rigorous attitude toward science which I will never forget and has been the most valuable education of life I received in Rutgers University.

I would like to thank my committee members, Prof. Roger Lalancette, Prof. John B. Sheridan and Prof. Brent S. Sumerlin of Southern Methodist University, for spending their time reading and correcting my thesis, and for their helpful advice and encouragement. I also thank Dr. Piotr Piotrowiak for his kind help and encouragement during my Ph.D. study. I would also like to thank Judith Slocum, Louise Curry, Monica Dabrowski, Lorraine McLendon, Maria Arujo and Paulo Vares for their assistance. In addition, I would like to thank all the former group members and current group members for their help and support. I would especially like to thank Dr. Yang Qin for sharing his research experience with me and giving me supportive help, including instrument training at my early reach stage.

I would also like to thank Dr. Roger Lalancette for helping me with single crystal X-ray for the structure determination of all the pyridyl borate compounds. His encouraging work has been critically important to for the research described in the last chapter of my

thesis. I would like to thank Dr. Edward M. Bonder of Department of Biology for helping me in the characterization of the micellar solutions of the diblock copolymers with TEM. Thanks to Dr. Huixin He and Dr. Yufeng Ma for helping me with AFM. Thanks to Dr. Lazaros Kakalis for helping me with NMR measurements. Thanks to Haiyan Li for helping me with MALDI-TOF characterizations.

Finally, I am very grateful to my family and friends for giving me continuous support and encouragement. I would like to dedicate this thesis to my mother Mrs. Jinfeng Wang, my father Mr. Shushen Cui, my wife Aiqin Jiang and my son Ricky Cui, my brothers Huanzhong Cui and Huizhong Cui; who gave me strength and enthusiasm to pursue my dreams.

# Table of Content

Abstract of Thesis	ii
Acknowledgments	iv
Table of Content	vi
List of Schemes	xi
List of Figures	xvi
List of Tables	xxii
List of Abbreviations	xxiv
Chapter A Introduction	1
A.1 Definition of Block Copolymers	1
A.2 Synthesis of Block Copolymers	1
A.2.1 Living Anionic Polymerization	2
A.2.2 Controlled/living Cationic Polymerization	8
A.2.3 Ring Opening Metathesis Polymerization	12
A.2.4 Controlled Free Radical Polymerization	23
A.2.4.1 Nitroxide Mediated Radical Polymerization (NMP)	24
A.2.4.2 Atom Transfer Radical Polymerization (ATRP)	29
A.2.4.3 Reversible Addition-Fragmentation Chain Transfer (RAFT)	34
A.3 Phase Segregation of Block Copolymers	39

A.3.1 Phase Segregation in Melts of Block Copolymers	39
A.3.2 Block Copolymer Micelles	43
A.4 Boron Containing Block Copolymers	47
A.4.1 Introduction of Organoboron Chemistry	47
A.4.1.1 Applications in Organic Chemistry	47
A.4.1.2 Applications of Lewis Acidity	47
A.4.2 Building Blocks of Polymeric Materials	49
A.5 References	64
Chapter B. Synthesis of Organoboronium-functionalized Polystyrene Homopolymers and Amphiphilic Block Copolymers	69
B.1 Introduction	69
B.2 Organoboronium-Functionalized Polystyrenes	72
B.2.1 Synthesis of Organoboronium-Functionalized Polystyrenes	73
B.2.2 Characterization of Organoboronium-Functionalized Polystyrenes	74
B.3 Synthesis and Characterization of Organoboronium Amphiphilic Block Copolymers	77
B.3.1 Synthesis of Organoboronium Amphiphilic Block Copolymers	78
B.3.2 Characterization of Organoboronium Amphiphilic Block Copolymers	80
B.3.3 Micellizations in Selective Solvents	82
B.4 Thermal Properties of Boronium Homo- and Diblock Copolymers	87

B.5 Conclusions	88
B.6 Experimental Section	89
B.6.1 Materials and General Methods	89
B.6.2 Synthesis of Organoboronium Polymers and Block Copolymers	92
B.6.3 Synthesis of Model Compounds	99
B.7 References	101
Chapter C. Synthesis of Weakly-Coordinating Organoborate-Functionalized Styrene Homopolymers and Amphiphilic Block Copolymers	104
C.1 Introduction	104
C.2 Weakly Coordinating Organoborate Anions	105
C.3 Immobilization of Organometallic Catalysts onto Ionic Polymers via Electrostatic Interactions	110
C.4 Synthesis and Characterization of Organoborate-Functionalized Homo and Amphiphilic Block Copolymers	116
C.4.1 Synthesis of Organoborate-Functionalized Polystyrenes	116
C.4.2 Characterizations of Amphiphilic Organoborate Block Copolymers	119
C.4.3 Micellization in Selective Solvents	123
C.4.4 Immobilization of a Rhodium Complex	125
C.5 Conclusions	128
C.6 Experimental Part	128

C.6.1 Materials and General Methods.	128
C.6.2 Synthesis of Organoborate Polymers and Block Copolymers	130
C.6.3 Micellization Experiments of Organoborate Polymers	139
C.6.4 Synthesis of Model Compounds	140
C.7 References	145
Chapter D. Synthesis of Polymerizable Tris(2-pyridyl)borate Ligands and Their Metal Complexes	155
D.1 Introduction	155
D.1.1 Pyrazolylborate and Pyridylborate Ligands	155
D.1.2 Pyrazolylborates and Polypyridyl Ligands in Supramolecular Chemistry and Polymer Science	162
D.2 Synthesis and Characterization of Polypyridylborate Ligands and Their Metal Complexes	168
D.2.1 Synthesis of 2-Pyridyl Grignard Reagent	168
D.2.2 Tris(2-pyridyl)borate Ligands and Their Magnesium Complexes	171
D.2.2.1 Synthesis of Polypyridylborate Ligands and Magnesium Complexes	171
D.2.2.2 NMR Characterizations	176
D.2.3 Synthesis of Bis(2-pyridyl)borate Ligands	179
D.2.4 Synthesis and Characterization of Fe(II) Complexes with Tris(2-pyridyl)borate Ligands	182

D.2.5 Cyclic Voltammetry and UV-visible spectroscopy data of Fe(II) complexes	186
D.2.6 Single Crystal X-ray Diffraction Analysis of the Pyridylborate Ligands	190
D.3 Free Radical Polymerizations of Styryltris(2-pyridyl)borate Free Acid (D39)	206
D.4 Conclusions	210
D.5 Experimental Part	211
D.6 References	227
Appendix	230
List of Publications	298
VITA	300

## List of Schemes

<b>Scheme A1.</b>	General reaction scheme of living anionic polymerization of an olefin.	2
<b>Scheme A2.</b>	Side reactions of acrylate monomers in anionic polymerization.	6
<b>Scheme A3.</b>	Synthesis of the diblock copolymer <b>A1</b> by sequential living anionic polymerization using a combination of anion transformation with 1, 2-diphenylethylene and complexation with LiCl.	8
<b>Scheme A4.</b>	General reaction mechanism of a cationic polymerization.	9
<b>Scheme A5.</b>	Mechanism of chain transfer reaction in the cationic polymerizations.	9
<b>Scheme A6.</b>	Mechanism of controlled cationic polymerizations of a Lewis acid as cocatalyst.	11
<b>Scheme A7.</b>	Mechanism of ring opening metathesis polymerization.	13
<b>Scheme A8.</b>	Synthesis of a triblock copolymer using titanacyclobutane <b>A5</b> as catalyst.	15
<b>Scheme A9.</b>	The first well-defined ruthenium alkylidene catalyst ( <b>A13</b> ) and its conversion into <b>A14</b> by exchange of triphenyl phosphine ligands (PPh <sub>3</sub> ) with tricyclohexylphosphine ligands (PCy <sub>3</sub> ).	19

<b>Scheme A10.</b>	Vinylcarbene Ruthenium catalyst ( <b>A14</b> ) used to synthesize functional diblock copolymers ( <b>A17</b> ).	20
<b>Scheme A11.</b>	Mechanism of the Nitroxide (TEMPO) Mediated radical Polymerization (NMP).	26
<b>Scheme A12.</b>	Preparation of diblock copolymers, <b>A24</b> and <b>A25</b> , through sequential controlled free radical polymerization.	29
<b>Scheme A13.</b>	Mechanism of Atom Transfer Radical Polymerization (ATRP).	30
<b>Scheme A14.</b>	ATRP of the diblock copolymer, <b>A26</b> , through a mixed halide initiating system.	33
<b>Scheme A15.</b>	Mechanism of Reversible Addition-Fragmentation Chain Transfer (RAFT).	37
<b>Scheme A16.</b>	Growth mechanism of a well defined amphiphilic diblock copolymer, poly(ethylene- <i>alt</i> -propylene)-block- poly(ethylene oxide) ( <b>A31</b> ), in a mixture of water and DMF.	45
<b>Scheme A17.</b>	Mechanism of the selective sensing of fluoride or cyanide with water soluble borane sensors.	49
<b>Scheme A18.</b>	Examples of the synthesis of highly Lewis acidic organoboron polymers via post-polymerization modification.	50

<b>Scheme A19.</b>	The equilibrium of the complexation between a phenylboronic acid polymer and glucose.	52
<b>Scheme A20.</b>	Preparation of diblock copolymer <b>A35</b> through RAFT.	54
<b>Scheme A21.</b>	The triply-responsive boronic acid block copolymers can undergo reversible micellizations triggered by heat, base or glucose.	55
<b>Scheme A22.</b>	Encapsulation of an enzyme in vesicles with controllable permeability to form bioreactors.	56
<b>Scheme A23.</b>	Preparation of the diblock copolymer ( <b>A36</b> ) containing carborane units.	57
<b>Scheme A24.</b>	Preparation of amphiphilic diblock copolymers ( <b>A37</b> ) functionalized with carborane groups through ROMP.	58
<b>Scheme A25.</b>	Preparation of a diblock copolymer having a norbornene block and decaborane functionalized norbornene block through ROMP.	60
<b>Scheme A26.</b>	Preparation of a diblock copolymer block copolymers ( <b>A39</b> ) with BODIPY dyes in their side chain through RAFT.	62
<b>Scheme A27.</b>	Synthesis of diblock copolymers of boron dye head group, BF <sub>2</sub> dbm.	64

<b>Scheme B1.</b>	Synthesis of ferrocenylboronium salts <b>B2</b> and <b>B3</b> .	70
<b>Scheme B2.</b>	Synthesis of "boronium-type" polyelectrolytes ( <b>B10-B13</b> ) and molecular model systems ( <b>B14 &amp; B15</b> ).	73
<b>Scheme B3.</b>	Synthesis of Boronium-Functionalized Amphiphilic Block Copolymers.	79
<b>Scheme C1.</b>	Synthesis of <b>C1</b> containing a very reactive three coordinate silylium cation stabilized with weakly-coordinating $B(C_6F_5)_4^-$ .	106
<b>Scheme C2.</b>	Synthesis of an ionic liquid ( <b>C2</b> ) of a weakly-coordinating borate moiety and an imidazolium cation; the IL can further react with LiTFSI providing anions of strong ion pairing interaction with the imidazolium cations.	110
<b>Scheme C3.</b>	Preparation of dendrimers <b>C4</b> and <b>C5</b> featuring weakly-coordinating borate anions.	112
<b>Scheme C4.</b>	Synthesis of ammonium borate functionalized polymers ( <b>C7</b> ); Electrostatic attachment of active metallocene catalyst to <b>C7</b> .	114
<b>Scheme C5.</b>	Immobilization of a catalytically active rhodium complex with a soluble quaternary ammonium polyelectrolyte by electrostatic interactions between ammonium and a multiple charged phosphine ligand on the rhodium complex.	115

<b>Scheme C6.</b>	Synthesis of organoborate-functionalized homopolymers and block copolymers.	117
<b>Scheme D1.</b>	Preparation of dimethylbis(2-pyridyl)borate ligand ( <b>D9</b> ) from pyridyllithium ( <b>D4</b> ) reagent.	159
<b>Scheme D2.</b>	Application of the dimethylbis(2-pyridyl)borate platinum complex ( <b>D11</b> ) in C-H activation reactions.	160
<b>Scheme D3.</b>	Preparation of Fe(II) complex ( <b>D16</b> ) with lithium methyltris(2-pyridyl)aluminate ( <b>D14</b> ).	161
<b>Scheme D4.</b>	Preparation of a diblock copolymer (PFS- <i>block</i> -PEO) ( <b>D22</b> ) through the strong metal complexation of the end terpyridine ligand group.	164
<b>Scheme D5.</b>	Synthesis of a terpyridine functionalized polymer ( <b>D24</b> ) through post-polymerization modification.	165
<b>Scheme D6.</b>	Free radical polymerization of a terpyridine functionalized styrene ( <b>D26</b> ).	165
<b>Scheme D7.</b>	Tris(pyrazolyl)borate ligands are attached to a styrenic polymer via a post modification procedure ( <b>D32</b> ); and the ligand functionalized polymer can be further complexed with organotransition metals, such as CpRu ( <b>D33</b> ).	167

<b>Scheme D8.</b>	Synthesis of dimeric 2-pyridylmagnesium chloride ( <b>D34</b> ).	169
<b>Scheme D9.</b>	Synthesis of (2-pyridyl)borate free acids ( <b>D37 and D39</b> ) in CH <sub>2</sub> Cl <sub>2</sub> ; The magnesium complexes were found to be the only side product in trace amount.	173
<b>Scheme D10.</b>	One pot synthesis of styryltris(2-pyridyl)borate free acid monomer ( <b>D39</b> ) in toluene; using toluene as solvent, the magnesium complex ( <b>D40</b> ) was generated in moderate yield (9.4% isolated yield).	175
<b>Scheme D11.</b>	Toluene was used to achieve in high conversion to the magnesium complexes ( <b>D38 and D40</b> ).	176
<b>Scheme D12.</b>	Synthesis of bis(2-pyridyl)borate ligands: <b>D41, D42 and D43</b> .	181
<b>Scheme D13.</b>	Synthesis of Fe(II) complexes: <b>D45 and D46</b> .	183

### List of Figures

<b>Figure A1.</b>	Titanacyclobutanes, <b>A5 and A6</b> , used as ROMP catalysts.	14
<b>Figure A2.</b>	Tungsten alkylidene complexes as ROMP catalysts.	16
<b>Figure A3.</b>	Molybdenum alkylidene complexes as ROMP catalysts.	18
<b>Figure A4.</b>	Three generations of Grubbs catalysts.	21
<b>Figure A5.</b>	A triblock copolymer ( <b>A22</b> ) synthesized by ROMP with the 3 <sup>rd</sup> generation of Grubbs catalysts.	23

<b>Figure A6.</b>	Structures of example nitroxides used for NMP.	26
<b>Figure A7.</b>	A general composition of RAFT agents.	38
<b>Figure A8.</b>	Phase diagram as calculated using self-consistent mean-field theory of the AB diblock copolymer.	41
<b>Figure A9.</b>	Schematic diagram of the fabrication process for Cr dot arrays (upper pictures) and height images of tapping mode atomic force microscope (AFM) of each step (lower pictures): (a) nanoscopic holes in cross-linked PS matrix, (b) evaporated Cr onto the PS template, and (c) Cr nanodot arrays.	42
<b>Figure A10.</b>	Determining factors for the size of polymeric micelles from block copolymers.	46
<b>Figure A11.</b>	Preparation of different nanostructured ceramic materials through pyrolysis of the same diblock copolymer ( <b>A38</b> ) cast from different solvents.	60
<b>Figure B1.</b>	a) The quaternary ammonium polysulphone (QAPS) polymer ( <b>B4</b> ) is hydroxide ion conductive; b) the Nafion polymer ( <b>B5</b> ) is proton conductive requiring low pH environment.	72
<b>Figure B2.</b>	Comparison of the $^1\text{H}$ and $^{11}\text{B}$ NMR spectra of <b>B10</b> with those of the molecular species <b>B14</b> in DMSO- $d_6$ ( $\text{Br}^-$ counterion).	75

<b>Figure B3.</b>	Representative GPC-UV traces for the boronium-functionalized polymers (recorded in DMF/20mM NH <sub>4</sub> [PF <sub>6</sub> ] at 60 °C).	76
<b>Figure B4.</b>	<sup>11</sup> B NMR spectra of block copolymer <b>B19</b> and homopolymer <b>B10</b> .	80
<b>Figure B5.</b>	GPC traces for boronium-functionalized block copolymers <b>B21</b> and <b>B22</b> (recorded in DMF/20mM NH <sub>4</sub> [PF <sub>6</sub> ] at 60 °C).	80
<b>Figure B6.</b>	Comparison of the NMR spectra of <b>B19</b> in different solvents, (a) CDCl <sub>3</sub> :CD <sub>3</sub> OD=5:1; (b) CDCl <sub>3</sub> (PS selective solvent); (c) CD <sub>3</sub> OD (boronium-selective solvent).	83
<b>Figure B7.</b>	a) Size distribution histogram of a solution of <b>B20</b> in MeOH (1.4 mg mL <sup>-1</sup> ; n = 33, m = 120). b) TEM images of <b>B20</b> (micellization in MeOH; negative staining with uranyl acetate).	85
<b>Figure B8.</b>	a) Size distribution histograms of a solution of <b>B19</b> in MeOH (0.2 mg mL <sup>-1</sup> ; n = 33, m = 120). b) Size distribution histogram of a solution of <b>B19</b> in toluene (0.5 mg mL <sup>-1</sup> ; n = 33, m = 120).	86
<b>Figure B9.</b>	TGA results of <b>B10</b> and <b>B19</b> in air.	88

<b>Figure C1.</b>	Immobilization of weakly coordinating borate anions into polymers gives rise to polymeric electrolytes having the lithium cation as the unique mobile charge carrier.	108
<b>Figure C2.</b>	Comparison of the $^{11}\text{B}$ NMR spectrum of the block copolymer PSBPh <sub>3</sub> - <i>b</i> -PS with those of the homopolymer PSBPh <sub>3</sub> and the molecular species MBPh <sub>3</sub> .	120
<b>Figure C3.</b>	Comparison of the $^{19}\text{F}$ NMR spectra of the block copolymer PSBPf <sub>3</sub> - <i>b</i> -PS with those of PSBPf <sub>3</sub> and the molecular species Na[ <sup>t</sup> BuC <sub>6</sub> H <sub>4</sub> BPh <sub>3</sub> ].	121
<b>Figure C4.</b>	Comparison of the $^{13}\text{C}$ NMR spectrum of the organoborate-functionalized block copolymer PSBPh <sub>3</sub> - <i>b</i> -PS with those of the homopolymer PSBPh <sub>3</sub> (green), polystyrene (PS, blue), and the molecular species MBPh <sub>3</sub> .	121
<b>Figure C5.</b>	GPC traces for the organoborate-functionalized homopolymers and block copolymers.	122
<b>Figure C6.</b>	Size distribution histogram of a solution of PSBPf <sub>3</sub> - <i>b</i> -PS in toluene; $n = 33$ , $m = 120$ .	124
<b>Figure C7.</b>	Schematic illustration of the block copolymer assembly of PSBR <sub>3</sub> - <i>b</i> -PS in toluene.	125

- Figure C8.** Size distribution histogram of a solution of PSBPf<sub>3</sub>-*b*-PS 126  
loaded with [Rh(cod)(dppb)]<sup>+</sup> (a) after dialysis from THF to  
toluene (1 mg mL<sup>-1</sup>; n = 33, m = 120) and (b) in THF/ MeOH  
(1:4) (1 mg mL<sup>-1</sup>; n = 33, m = 120).
- Figure C9.** TEM image of PSBPf<sub>3</sub>-*b*-PS after loading with 127  
[Rh(cod)(dppb)]<sup>+</sup> and subsequent micellization in toluene  
(top) and MeOH:THF = 4:1 (bottom).
- Figure D1.** A) X-ray structure of [PhB(pz)<sub>3</sub>]Fe (**D1**); B) X-ray structure of 157  
[HB(3,5-Me<sub>2</sub>pz)<sub>3</sub>]<sub>2</sub>Fe (**D2**).
- Figure D2.** A metal-containing macrocycle (**D19**) prepared through 163  
complexation of a terpyridine ligand and Fe (II) ion.
- Figure D3.** Metal complexes (**D28**) formed by complexation between a 166  
ferrocene-based tris(pyrazolyl)borate ligand (**D27**) and  
divalent metal ions.
- Figure D4.** Tentative view from “diamond” of the dimeric structure of 170  
2-PyMgCl (**D34**) with three coordinating THF (0.5 equivalent  
disordered THF is omitted for clarity) (50% probability).
- Figure D5.** Numbering scheme of the protons in the pyridine and 177  
t-butylphenyl rings.

<b>Figure D6.</b>	<sup>1</sup> H NMR spectrum of t-butylphenyltris(2-pyridyl)borate free acid ( <b>D37</b> ) in CDCl <sub>3</sub> .	177
<b>Figure D7.</b>	<sup>13</sup> C NMR of t-butylphenyltris(2-pyridyl)borate free acid ( <b>D37</b> ) in CDCl <sub>3</sub> .	178
<b>Figure D8.</b>	An overlaid <sup>1</sup> H NMR spectra of t-butylphenyltris(2-pyridyl)borate ligand ( <b>D37</b> ) and its Fe(II) complex ( <b>D46</b> ).	184
<b>Figure D9.</b>	Cyclic voltammograms of Fe(II) complexes: (a) <b>D46</b> (1 x 10 <sup>-3</sup> M) and (b) <b>D45</b> (1 x 10 <sup>-3</sup> M) with 0.1M [Bu <sub>4</sub> N]PF <sub>6</sub> in CH <sub>2</sub> Cl <sub>2</sub> as the supporting electrolyte for anionic scans.	187
<b>Figure D10.</b>	UV-vis spectrum of Fe(II) complex <b>D46</b> .	189
<b>Figure D11.</b>	UV-vis spectra of Fe(III) complex <b>D47</b> .	189
<b>Figure D12.</b>	ORTEP view of the independent molecules of t-butylphenyltris(2-pyridyl) borate free acid ( <b>D37</b> ) (50% probability).	191
<b>Figure D13.</b>	ORTEP view of styryltris(2-pyridyl) borate free acid ( <b>D39</b> ) (50% probability).	191
<b>Figure D14.</b>	ORTEP view of Mg(II) complex ( <b>D38</b> ) (50% probability).	194
<b>Figure D15.</b>	ORTEP view of Mg(II) complex ( <b>D40</b> ) (50% probability).	194

<b>Figure D16.</b>	ORTEP view of diarylbis(2-pyridyl)borate free acids (50% probability). (a) <b>D41</b> ; (b) <b>D42</b> ; (c) <b>D43</b> .	197
<b>Figure D17.</b>	ORTEP view of Fe (II) complex <b>D46</b> (40% probability).	201
<b>Figure D18.</b>	ORTEP view of Fe (II) complex <b>D45</b> (50% probability).	201
<b>Figure D19.</b>	ORTEP view of Fe(III) complex <b>D47</b> (40% probability).	205
<b>Figure D20.</b>	An overlay of <sup>1</sup> H NMR of the homopolymer ( <b>D48</b> ) and model compound ( <b>D37</b> ).	207
<b>Figure D21.</b>	An overlay of <sup>13</sup> C NMR of the homopolymer ( <b>D48</b> ) and model compound ( <b>D37</b> ).	208
<b>Figure D22.</b>	GPC trace for polymer ( <b>D48</b> ) (recorded in DMF/20mM NH <sub>4</sub> [PF <sub>6</sub> ] at 60 °C).	209

### List of Tables

<b>Table B1.</b>	GPC-UV results and yields for organoboronium polymers (DMF/20mM NH <sub>4</sub> [PF <sub>6</sub> ] at 60 °C, polystyrene standards)	77
<b>Table B2.</b>	GPC-RI results and yields for organoboronium polymers <b>B21</b> and <b>B22</b> (DMF/20mM NH <sub>4</sub> [PF <sub>6</sub> ] at 60 °C, PS standards).	81
<b>Table C1.</b>	Results for polymer modification procedures.	123
<b>Table D1.</b>	<sup>1</sup> H NMR assignments of polypyridylborate ligands and metal complexes.	184

<b>Table D2.</b>	Selected bond lengths (Å) and angles (deg) for <b>D37</b> and <b>D39</b> .	192
<b>Table D3.</b>	Selected bond lengths (Å) and angles (deg) for the magnesium complexes <b>D38</b> and <b>D40</b> .	195
<b>Table D4.</b>	Selected bond lengths (Å) and angles (deg) for diarylbis(2-pyridyl)borate free acids of <b>D41</b> , <b>D42</b> and <b>D43</b> .	198
<b>Table D5.</b>	Selected bond lengths (Å) and angles (deg) for Fe (II) complexes of <b>D46</b> and <b>D45</b> .	202
<b>Table D6.</b>	Selected bond lengths (Å) and angles (deg) for Fe(III) complex <b>D47</b> .	205

## List of Abbreviations

Bipy	bipyridine
COSY	correlation spectroscopy
Cp	cyclopentadienyl
CT	charge transfer
CV	cyclic voltammetry
DMF	dimethylformamide
Fc	ferrocene
HMQC	hetero-nuclear multiple quantum coherence
Mes	2,4,6-trimethylphenyl
NMR	nuclear magnetic resonance
Py	pyridine
Ph	phenyl
THF	tetrahydrofuran
Pf	$C_6F_5$
UV-vis	Ultraviolet-visible
GPC	gel permeation chromatography
PDI	polydispersity index
Maldi-tof	matrix-assisted laser desorption ionization time of flight

## **Chapter A. Introduction**

### **A.1 Definition of Block Copolymers**

Block copolymers are made by connecting two or more polymeric chains that, in most cases, are thermodynamically incompatible, giving rise to a rich variety of microstructures in bulk and in solution.<sup>1</sup>

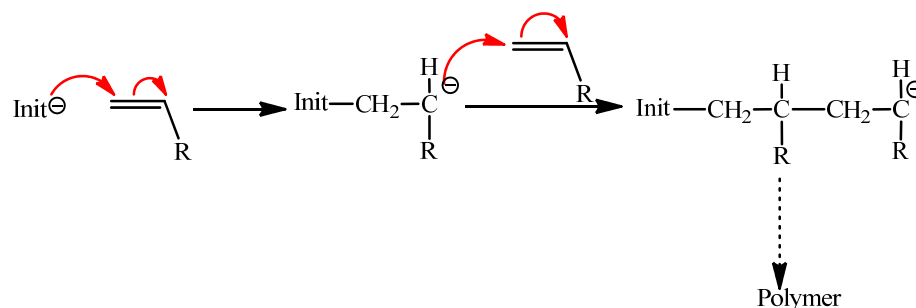
### **A.2 Synthesis of Block Copolymers**

Different polymerization mechanisms have been developed for the synthesis of block copolymers. They consist of living anionic polymerization, ring opening metathesis polymerization, group transfer polymerization, controlled/living cationic polymerization, and controlled/living free radical polymerization. The living character associated with these polymerization techniques has allowed synthetic polymer chemists to prepare a realm of new structures inspiring polymer physicists to create and test new theories. The new well-defined polymers synthesized through these techniques have tremendous impact on polymer and materials science, which are deeply related to modern life and will certainly become more and more important for human society in future in areas such as medicine, energy and so on.

### A.2.1 Living Anionic Polymerization

Living polymerizations were first disclosed during the invention of anionic polymerization.<sup>2</sup> In 1956, Michael Szwarc and coworkers reported the discovery of living anionic polymerization, which was the first polymerization mechanism allowing the synthesis of block copolymers.<sup>3</sup>

Szwarc used sodium naphthalenide as the initiator through an electron transfer mechanism. Anionic polymerizations are usually initiated by strong carbanions, among which organolithium initiators have been most widely employed and commercially useful. They are primarily used for polymerization of styrenes and dienes.<sup>4</sup> The carbanions are strong nucleophiles and able to attack the polymerizable double bond of olefin monomers bearing an electron withdrawing substituent (Scheme A1) or an electron deficient atom of a ring in the case of ring opening polymerization, such as the carbon atom in the ethylene oxide monomer. Other species such as organosodium and organopotassium compounds have also been used.



**Scheme A1.** General reaction scheme of living anionic polymerization of an olefin.

In a typical living anionic polymerization, polymerization occurs by consecutive addition of monomer to an alkyl lithium initiator without chain transfer and termination. The number of polymer chains remains constant during the transferless polymerization, and active chain ends are still intact after all of the monomer has been polymerized. In addition to these living characteristics, the initiation of living anionic polymerization is extremely fast, and the following propagation of the growing polymer chain should be ideally slower than initiation. All the growing polymer chains grow at an equal opportunity of adding units; as a result, the molecular weight has a very narrow distribution and can be predicted based on the amount of monomer and initiator used. The good control over molecular weight and distribution is a great advantage of living anionic polymerization over other traditional polymerization techniques. The polydispersity index ( $M_w/M_n$ ) from a living anionic polymerization is typically less than 1.1.

The propagation rate can be dramatically changed by changing the solvent conditions. For example, the propagation rate of polystyryllithium can be increased hundreds of times when the solvent is changed from a hydrocarbon to a mixture with a little tetrahydrofuran. Early studies have proved that an equilibrium exists between tight (contact) ion pairs and loose (solvent-separated) ion pairs (free carbanion) at the ionic polymer chain ends.<sup>5</sup> The chain ends with a loose ion pair (or free carbanion) exhibit much higher reactivity and propagate much faster than the tight ones. Both types of ionic

species will contribute to the propagation but at a very different rate. One might think the molecular weight distribution would become broad due to the unequal rates of polymerization. However, in a living anionic polymerization, the exchange between these two ionic species is fast so that all the polymer chains have an equal chance to possess very active loose ion pair chain ends and relatively inactive tight ion pair chain ends.<sup>6</sup> That means the polymer chains may have different propagation rates at any given time but the average propagation rate is equal over a certain length of time. Therefore, different propagation rates of the ionic species in a living anionic polymerization do not negatively affect the control of molecular weight and polydispersity of the final product. Donor solvents like tetrahydrofuran can drastically increase the propagation rate by shifting the equilibrium to the side of the loose ion pair and therefore increase the overall polymerization rate.

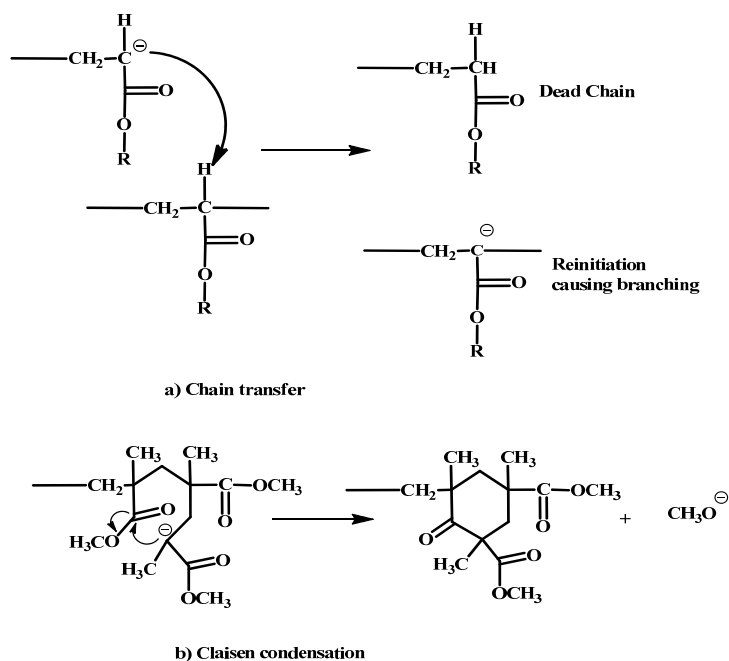
Since the active anionic end groups of polymer chains are well retained after monomers are fully consumed, another monomer can be simply introduced into the polymerization reaction mixture to prepare a diblock copolymer. In this sequential copolymerization, extra attention should be paid to the second monomer: it must be able to form carbanions of more or at least equal stability to the one derived from the first monomer to assure a high initiation rate, i.e., high cross-over rate; to realize good control over the molecular weight distribution, the initiation rate of the second monomer should be also higher than or comparable to its propagation rate; high purity monomers are also required. Monomer

purity is always important for living anionic polymerization because the initiators are usually very active organoalkali species, and loss of initiator will inevitably impact the predictability of molecular weight. The purity of the second monomer is even more important because the loss of carbanion end groups can generate homo polymer impurity that may be hard to remove in the final block copolymer product.

Symmetrical triblock (ABA) copolymers can be prepared by using difunctional initiators which can polymerize the first monomer (B) in opposite directions with two end groups in the polymer product and subsequently be extended with "A" units at each end by adding the second monomer (A).<sup>7</sup> Block copolymers with more than three blocks can also be synthesized in this way, for example, pentablock terpolymers were successfully synthesized.<sup>8</sup> Coupling of the preformed living block copolymers can also be used to obtain block copolymers. However, because the efficiency of coupling is not unity, one of the polymer reagents has to be used in excess. Usually the one that is relatively easier to remove is used in excess in order to achieve a block copolymer product with high purity.

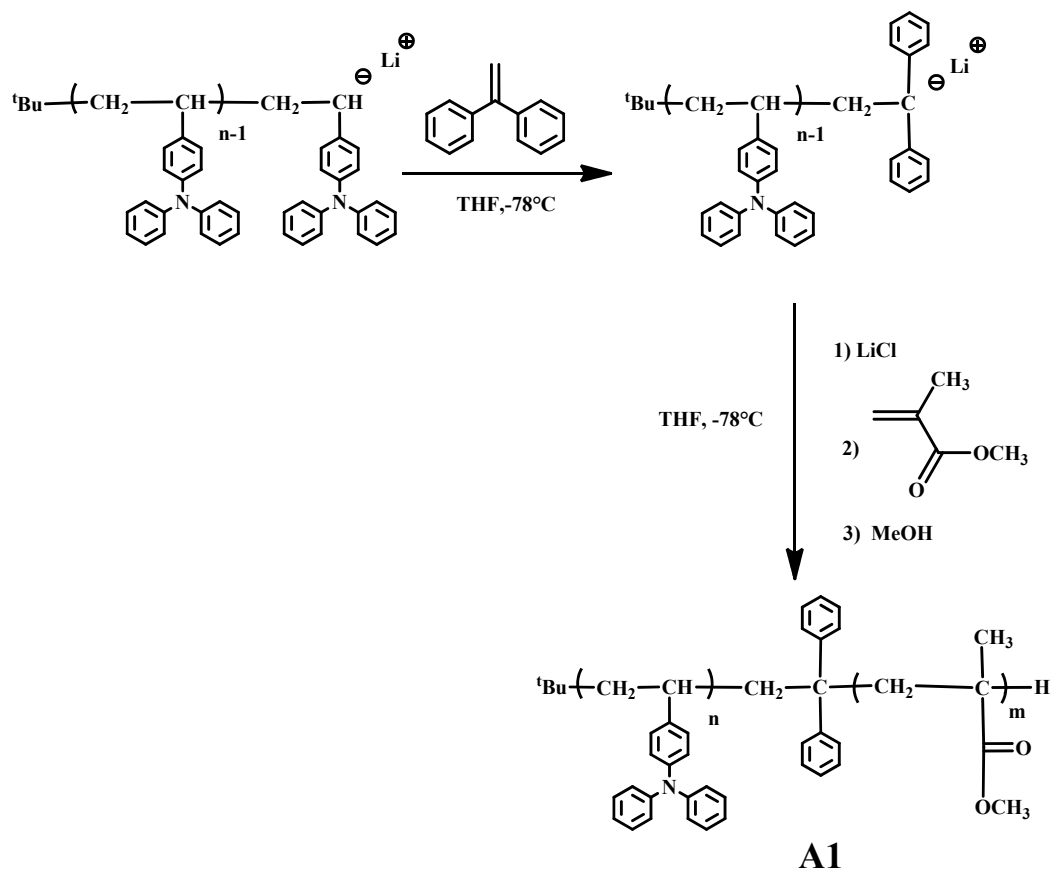
Living anionic polymerizations of acrylate and methacrylate monomers can be associated with serious side reactions. The propagating polymer anions in an anionic polymerization of an acrylate monomer can potentially abstract  $\alpha$ -protons from the backbone resulting in termination of the propagating chains and reinitiation from sites along the backbone to form branched polymers. This chain transfer side reaction is difficult to suppress. Proton

abstraction is absent in the anionic polymerization of methacrylate monomers because there is a methyl group in the  $\alpha$  position. However, polymerizations of both acrylate and methacrylate monomers may suffer from side reactions between the anion and the ester group, which is called the Claisen condensation in organic chemistry. The most common circumstance is intramolecular reaction with the ester two repeat units back, because the transition state is a six-membered ring (entropically favorable). The reaction causes a cyclization and ejects an alkoxide as a leaving group. The alkoxide is too weak of a nucleophile to reinitiate, so this process leads to termination. The activation energy of cyclization is greater than that of propagation, so the former is affected more by temperature than the latter. Therefore, undesired cyclization reaction can be suppressed by using low temperatures. The side reactions are depicted in Scheme A2.



**Scheme A2.** Side reactions of acrylate monomers in anionic polymerization.

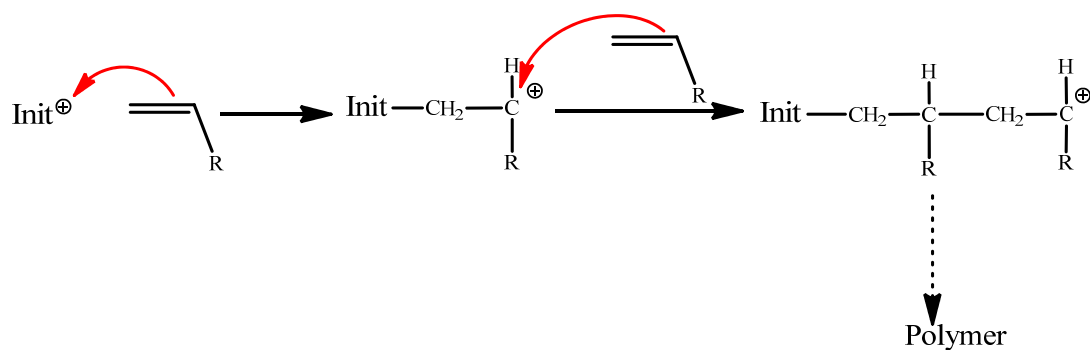
In addition to using low temperature to prevent side reactions in anionic polymerizations of acrylate and methacrylate monomers, relatively low reactive and sterically hindered initiators are required. For this reason, the more reactive anion initiator, for example, styrenic or dienic anion is commonly transformed to a less reactive and more sterically hindered one by reaction with 1, 2-diphenylethylene, a non-homopolymerizable monomer. With an efficient cross-over initiation, the sequential copolymerization of these monomers can therefore proceed in a controlled fashion. The use of LiCl as additive has been proven to enhance control of the anionic polymerization of methacrylate and acrylate monomers by complexation of LiCl to the active anion chain ends. For example, a diblock copolymer (A1) with poly(4-vinyltriphenylamine) and poly(methylmethacrylate) segments has been successfully synthesized via living anionic polymerization by sequential addition of 4-vinyltriphenylamine and methylmethacrylate. The combination of anion transformation with 1, 2-diphenylethylene and complexation with LiCl was applied to achieve excellent control over the molecular weight and distribution with PDIs as low as 1.04 (Scheme A3).<sup>9</sup>



**Scheme A3.** Synthesis of the diblock copolymer **A1** by sequential living anionic polymerization using a combination of anion transformation with 1, 2-diphenylethylene and complexation with LiCl.

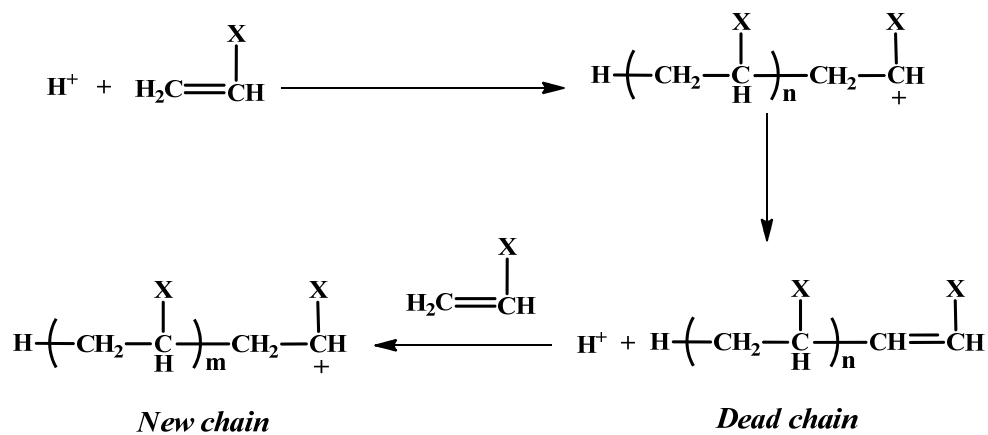
### A.2.2 Controlled/living Cationic Polymerization

Cationic polymerization refers to a polymerization reaction where the chain propagation is achieved through a carbocation, which can be generated by a cationic initiator and a vinyl monomer (Scheme A4).<sup>10,11</sup>



**Scheme A4.** General reaction mechanism of a cationic polymerization.

However, the carbocation chain end produced by initiation of electron-rich monomers with a strong protic acid can transfer its  $\beta$  proton to start a new chain (Scheme A5). The extensive chain transfer may therefore result in low molecular weight with a broader distribution.<sup>12</sup>



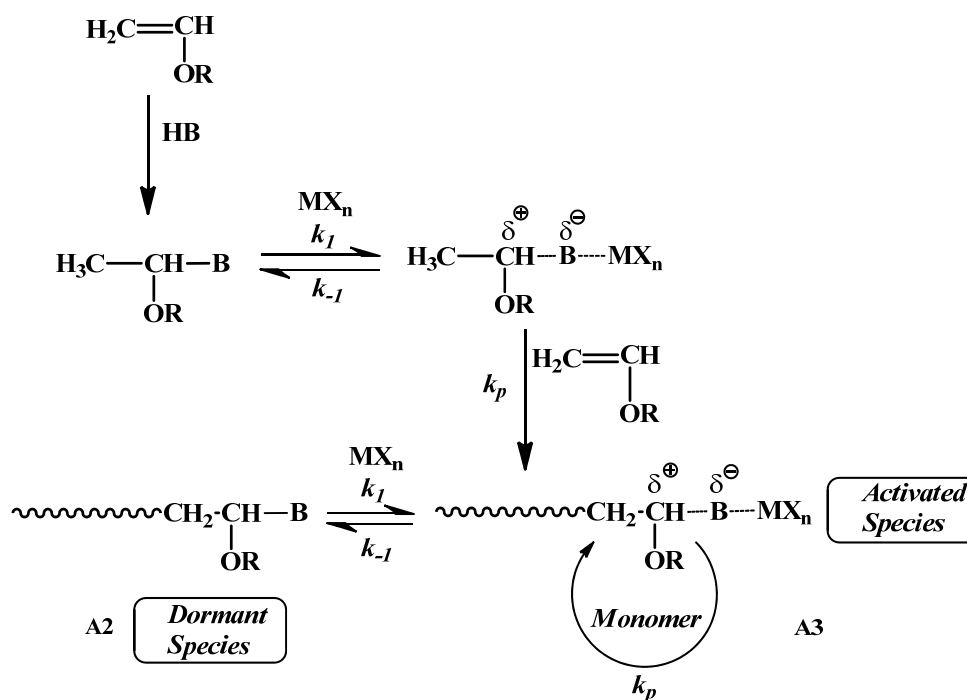
**Scheme A5.** Mechanism of chain transfer reaction in the cationic polymerizations.

To make cationic polymerization a controlled living polymerization, binary initiating systems have been used which usually consist of a protic acid HB and a weak Lewis acid  $MX_n$  (Scheme A6). As shown in Scheme A6, the protic acid HB adds to the monomer

prior to polymerization to give an adduct with an inert C-B bond, and then the C-B bond is subsequently activated by the weak Lewis acid  $\text{MX}_n$  to commence living propagation. The nucleophilicity of the anionic  $\text{B}^{\delta-}$  as well as the Lewis acidity and concentration of  $\text{MX}_n$  play important roles to enable living cationic polymerizations. The Lewis acid  $\text{MX}_n$  can bind onto  $\text{B}^{\delta-}$  so as to activate the dormant species (**A2**), which has an inert C-B bond, in order to undergo fast propagation. Meanwhile, because the binding is reversible and the interconversion between activated species (**A3**) with a  $\text{C}^{\delta+} \cdots \text{B}^{\delta-} \cdots \text{MX}_n$  bond and dormant species is very fast, all the polymer chains can still possess the same polymerization rate. In an appropriately designed living cationic polymerization reaction, the equilibrium lies to the side of the dormant species, and the chain transfer reactions can be suppressed to a negligible level. On the other hand, the average propagation rate can also be attenuated, which is advantageous to achieve a narrow molecular weight distribution. Less nucleophilic anions, strong Lewis acids and low concentration of Lewis acids will all help to shift the equilibrium toward the side of activated species. Careful choice of the combination of initiator and Lewis acid should be critical to avoid loss of control in the cationic polymerization.

The initiation rate can be improved by adopting a carefully designed molecule as the initiator with a C-B bond of anticipated bond energy for successful activation. The initiation system precludes the step of the addition of protic acids to the monomer so that an efficient and fast initiation can therefore be achieved.

Kinetic studies and  $^1\text{H}$  NMR analysis<sup>13</sup> of model reactions have suggested that the dormant species (**A2**) and activated species (**A3**) bond coexist in an equilibrium. If the carbocation is properly stabilized by the anionic  $\text{B}^{\delta-}$  of moderate nucleophilicity to prevent its chain transfer, living cationic polymerizations can be realized. However, interconversion between activated and dormant species should be fast to avoid a broader distribution.



**Scheme A6.** Mechanism of controlled cationic polymerizations of a Lewis acid as cocatalyst.

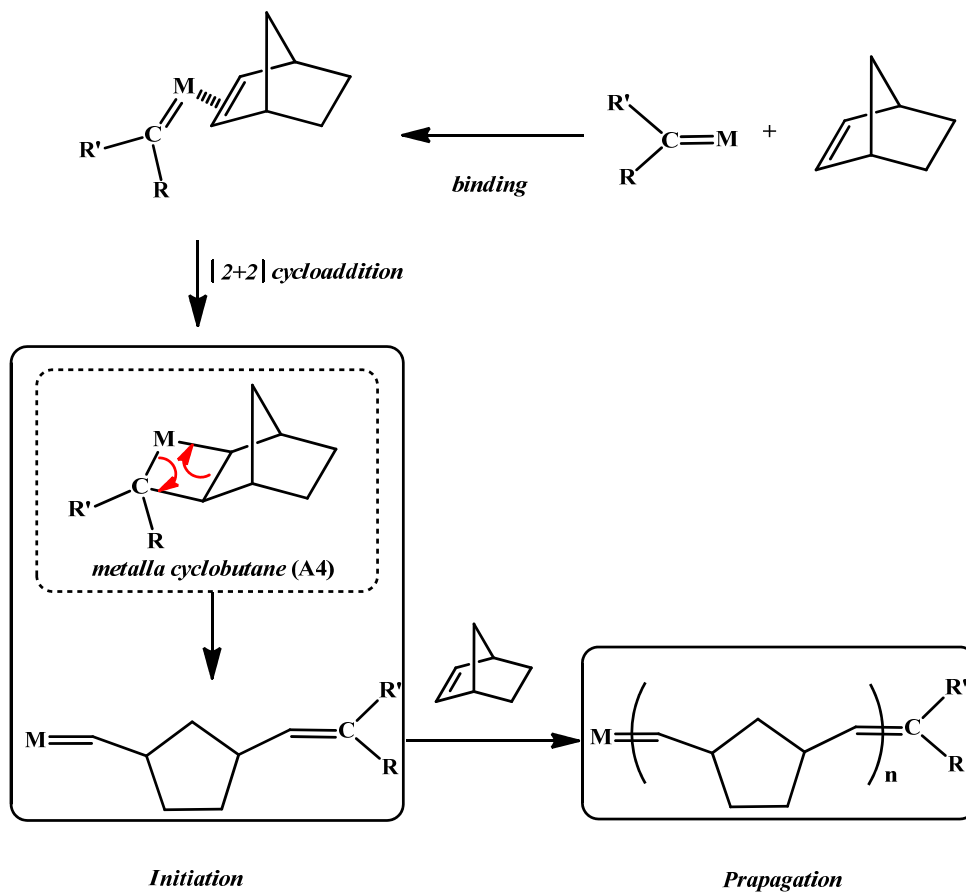
After quantitative conversion of the monomer, sequential addition of the comonomers can be applied to synthesize block copolymers. To achieve a well defined block

copolymer, variation of the binary catalysis system might be needed by changing Lewis acidity and/or concentration of the Lewis acid cocatalyst.

### **A.2.3 Ring Opening Metathesis Polymerization**

Ring Opening Metathesis Polymerization (ROMP) has become an efficient tool for the preparation of a variety of macromolecular architectures with a unique feature of preservation of carbon-carbon double bonds during the polymerization step.<sup>14</sup> Cyclic olefins such as norbornenes, cyclooctenes, cyclobutadienes and many other substituted derivatives with a large range of functional groups can be polymerized with appropriate organometallic metathesis catalysts, giving rise to a variety of highly functional polymers with otherwise inaccessible structures and properties. Titanium, molybdenum and ruthenium carbene complexes with a metal-carbon double bond have been commonly used in metathesis polymerization.

The mechanism of metathesis, which is now generally accepted, was first described by Chauvin and proposes a metalla-cyclobutane transition state (Scheme A7).<sup>15</sup> The metalla-cyclobutane (**A4**) is formed by a [2+2] cycloaddition of the metal-carbon double bond to an olefin. A better understanding of olefin coordination and transition state stability has been the focus of recent catalyst developments and has led to the latest generation of highly reactive catalysts.



**Scheme A7.** Mechanism of ring opening metathesis polymerization.

Transition metal carbene catalyst systems based on different metals such as titanium, tungsten, molybdenum and ruthenium have been extensively studied since Chauvin first described the generally accepted mechanism of metathesis and proposed the metalla-cyclobutane transition state. Early explorations of the ROMP were related to highly reactive metal complexes.

Norbornene has been an important cyclic olefin for ROMP. It has high ring strain being readily polymerized by active catalysts. However, it lacks bulky substituents to prevent

chain transfer, because the double bonds in the growing polymer norbornene chain could be accessible by the catalytically active centers to undergo secondary metathesis. These characteristics of norbornene enable evaluation of the capability of a catalytic system for living ring opening metathesis polymerization.

In 1986, the first living polymerization of norbornene was reported by Grubbs and coworker with two similar titanacyclobutane compounds (Figure A1) as ROMP catalysts.

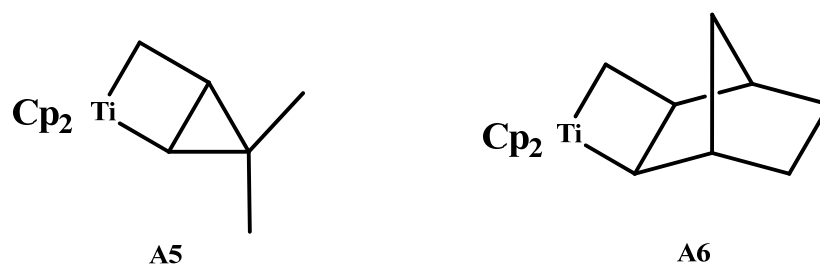
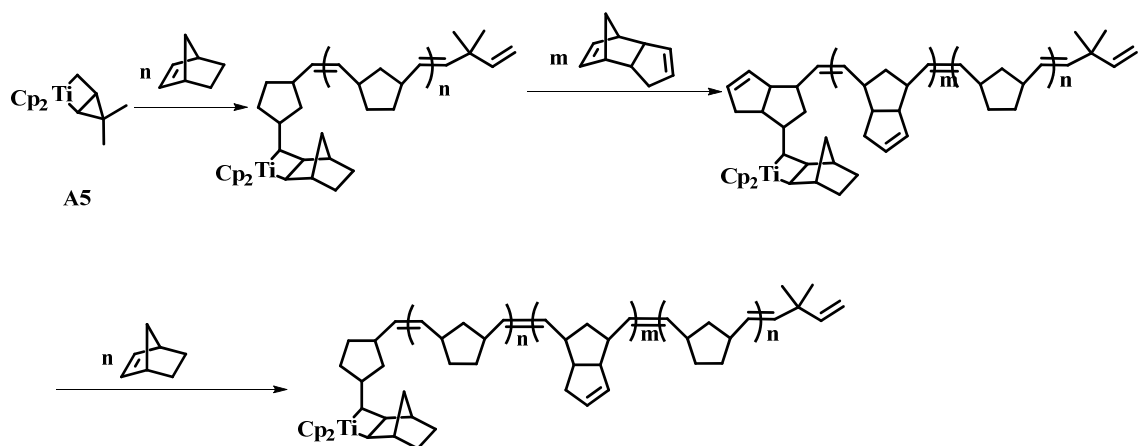


**Figure A1.** Titanacyclobutanes, **A5** and **A6**, used as ROMP catalysts

The polymerizations only occur at elevated temperature ( $\geq 65^\circ\text{C}$ ), leading to cleavage of the metallacycles followed by rapid trapping of the resultant carbene with norbornene. The metallacycle cleavage was identified as rate determining step, giving rise to an unusual zero-order dependence of polymerization rate on monomer concentration. The polymerizations were living with absence of termination and chain transfer up to complete conversion of monomer, but rapid degradation of the polymer occurred with a color change from red to brown. Upon cooling the reaction mixture to room temperature before complete conversion, the end groups of living polymers were all converted into

the stable titanacyclobutane. A polydispersity index as low as 1.08 was achieved when **A5** was used, and the initiation step was so fast that no induction period was observed. Polymerizations initiated with **A6** were also living with molecular weights that increased linearly with the amount of monomer consumed, although they gave an induction period because of slow initiation which slightly broadened the molecular weight distribution when preparing polynorbornenes with low molecular weights.

By sequential addition of various norbornene derivatives to catalyst **A5**, di- and triblock copolymers were prepared with very low polydispersities (Scheme A8).<sup>16</sup>



**Scheme A8.** Synthesis of a triblock copolymer using titanacyclobutane **A5** as catalyst.

Tungsten metathesis catalysts are much more active than the titanium catalysts and show a higher tolerance of polar functional groups.<sup>17</sup> The first successful living polymerization of norbornene with a tungsten alkylidene catalyst was reported by Schrock and Grubbs et al.<sup>18</sup> These well-defined tungsten alkylidene complexes exhibit a four-coordinate

geometry (Figure A2). Typically, bulky alkoxide and imido ligands are used to prevent intermolecular reaction that would result in ligand scrambling to give inactive complexes and decomposition reactions that would destroy the alkylidene ligand.<sup>19</sup>

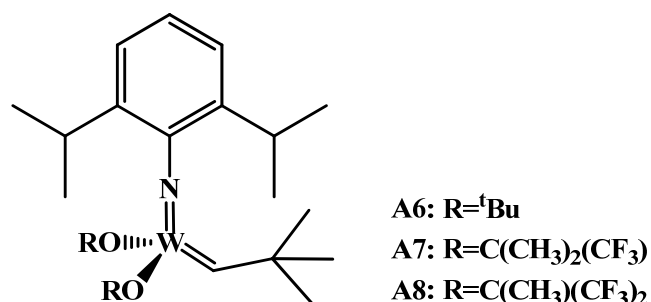


**Figure A2.** Tungsten alkylidene complexes as ROMP catalysts.

A particularly useful feature of these catalysts is that the alkoxide ligands can modulate the activity of the corresponding catalysts over an impressive range. For example,  $W(\text{CH}^t\text{Bu})(\text{NAr})(\text{OCMe}_2(\text{CF}_3))_2$  (Ar = 2, 6- diisopropylphenyl) (**A8**), an active tungsten alkylidene for the metathesis and isomerization of cis-2-pentene, was used for metathesis polymerization of norbornene. No decomposition of the initial and newly generated alkylidene was detected. However, according to <sup>1</sup>H NMR analysis only about 50% of the resultant polymers had tungsten alkylidene groups at the chain end and the cis content of the polymer decreased with time indicating that the tungsten alkylidene at the chain end reacted with double bonds in the growing chains, i.e. secondary metathesis took place. However, when  $W(\text{CH}^t\text{Bu})(\text{NAr})(\text{O}^t\text{Bu})_2$  (**A6**) with relative lower activity, not reacting

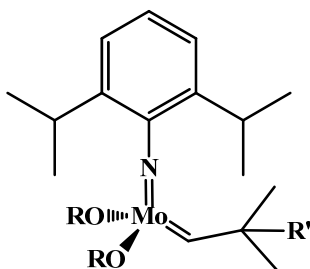
with *cis*-2-pentene appreciably in 24h, was chosen for metathesis polymerization of norbornene, it produced almost monodisperse polymers of PDIs lower than 1.1.

Extensive work on the development of suitable organometallic catalysts for living ring opening metathesis of norbornene has been useful for the elucidation of a myriad of mechanistic aspects of metathesis polymerizations. However, metathesis catalysts that will tolerate more functionalities have been sought ever since the discovery of olefin metathesis reactions. Development of catalysts for polymerizations of functional cyclic olefins has been always important to expand the realm of metathesis polymerization and establish it as a most powerful tool for preparation of specialty polymers.

Tungsten alkylidene complex (**A6**) can be used for polymerization of endo-5,6-dicarbomethoxynorbornene, an ester functional norbornene, but this catalyst is destroyed rapidly and therefore loses its control over molecular weight and distribution.<sup>20</sup>

In analogy to **A6**, Mo(CH<sup>t</sup>Bu)(NAr)(O<sup>t</sup>Bu)<sub>2</sub> (Ar = 2,6-diisopropylphenyl) (**A9**) (Figure A3) has less polarized metal-carbon bond and therefore lower reactivity to react with ester functionality as tungsten complexes. For the first time, living ring opening metathesis polymerizations of a norbornene with reactive functional substituent was realized with good control of molecular weight and low polydispersity. Well defined diblock copolymers (PDIs <1.1) have been also synthesized by sequential addition of the functional monomer. Actually, this molybdenum catalyst later was proved to be also a

capable catalyst for living ROMP of monomers containing a variety of functional groups including ester, amide, imide, ketal, ether, cyano, trifluoromethyl and primary halogen.<sup>21</sup>



**A9:** R=<sup>t</sup>Bu, R'=CH<sub>3</sub>

**A10:** R=Ph, R'=CH<sub>3</sub>

**A11:** R=C(CH<sub>3</sub>)<sub>2</sub>(CF<sub>3</sub>), R'= CH<sub>3</sub> or Ph

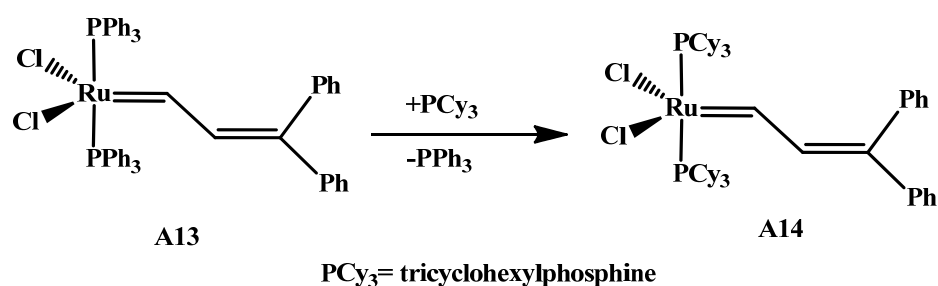
**A12:** R=C(CH<sub>3</sub>)(CF<sub>3</sub>)<sub>2</sub>, R'= CH<sub>3</sub> or Ph

**Figure A3.** Molybdenum alkylidene complexes as ROMP catalysts.

On the contrary, the relatively active tungsten alkylidenes tend to react more readily with the functionalities in the polymer chain, and are more sensitive to low levels of impurities than molybdenum alkylidenes.

In addition to norbornene, molybdenum catalysts can also be used to polymerize a variety of cyclic olefin with varying degrees of ring strain and functionalities. Catalyst **A10**, i.e. Mo(CHC(CH<sub>3</sub>)<sub>2</sub>Ph)(NAr)(O<sup>t</sup>Bu)<sub>2</sub>, was used to synthesize the polymer precursor of a rubbery-crystalline block copolymer with one block polymerized from highly strained cyclopentene. Subsequent copolymerization of ethylenenorbornene and cyclopentene afforded a well defined diblock copolymer with PDI of 1.07.<sup>22</sup>

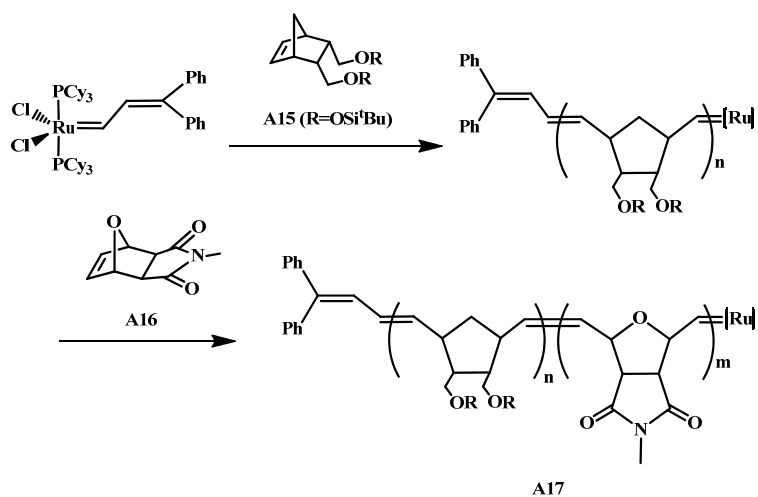
Ruthenium compounds show low oxophilicity and therefore high stability toward a variety of polar functional groups. Early efforts on polymerization of derivatives of 7-oxanobornene showed that in organic solvents a simple inorganic ruthenium salt,  $\text{RuCl}_3$ , without specially designed protecting groups and controllable labile groups, gave high yield (95%) and high molecular weight ( $> 10^5$ ).



**Scheme A9.** The first well-defined ruthenium alkylidene catalyst (**A13**) and its conversion into **A14** by exchange of triphenyl phosphine ligands ( $\text{PPh}_3$ ) with tricyclohexylphosphine ligands ( $\text{PCy}_3$ ).

The first well-defined ruthenium alkylidene catalyst (**A13**) (Scheme A9) for ring opening metathesis was reported by Grubbs and coworkers in 1992.<sup>23</sup> Possessing a vinylcarbene ligand, the ruthenium catalyst can polymerize norbornene in a mixture of dichloromethane and benzene and subsequent additions of 2, 3-dideuterionorbornene and norbornene gave rise to a triblock copolymer indicating the living characteristics of the polymerization. Surprisingly, this catalyst is stable in the organic solvent mixture in the

presence of water, alcohol or even a diethyl ether solution of HCl. Unfortunately, the catalyst is not soluble in water or alcohol and even though complete initiation can be achieved, the initiation rate is much slower than the propagation. Further increase of the reactivity of **A13** was achieved by exchange of triphenylphosphine ligands with bulky and electron rich alkylphosphines such as tricyclohexylphosphine (Cy). The resulting catalyst, **A14**, is more stable and exhibits a broader range of tolerance toward functionalities than **A13**. **A14** does enable good control over the polymerization of norbornene. Of increased reactivity, it increases propagation more than initiation and also induces chain transfer.<sup>24</sup> However, it can be used to polymerize less reactive monomers. The catalyst **A14** was successfully used for polymerization of the silicon containing norbornene (**A15**) (Scheme A10) in a living fashion, and subsequent polymerization of a functional monomer (**A16**) afforded a block copolymer (**A17**).



**Scheme A10.** Vinylcarbene Ruthenium catalyst (**A14**) used to synthesize functional diblock copolymers (**A17**).

Design of ruthenium catalysts with improved initiation ability has been driving fast-paced development. Basically, the advances within this group of catalysts are represented by the three generations of Grubbs catalysts. All three generations of the Grubbs catalysts possess the same benzylidene ligand (Figure A4).

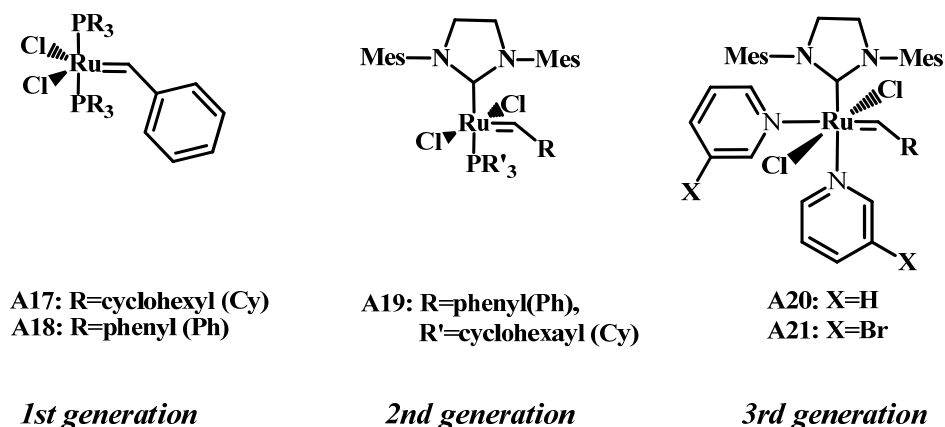


**Figure A4.** Three generations of Grubbs catalysts.

The 1<sup>st</sup> generation of Grubbs catalysts has two phosphine ligands and two chlorides. Comparison had been made between 1<sup>st</sup> generation catalysts containing two different phosphine ligands which showed very distinct ability for the ROMP of norbornene. The slow initiation rate of the cyclohexyl phosphine ruthenium catalyst (**A17**) led to poor control over the molecular weight and distribution. On the contrary, the analogous phenyl phosphine substituted ruthenium catalyst (**A18**) allowed a fast initiation and the ratio of initiation and propagation ( $k_i/k_p$ ) was up to 9.0, resulting in excellent living ring opening metathesis polymerization of norbornene. However, **A18** shows instability in solution

whereas **A17** is much more stable. **A17** did not show any sign of decomposition in a solvent mixture of dichloromethane and benzene heated at 60 °C or in the presence of alcohols, amines or water.<sup>25</sup> As reported later, the half life time of **A17** was up to 8 days in benzene at 55 °C, which indicates its exceptional thermal stability.<sup>26</sup>

The 2<sup>nd</sup> generation of Grubbs catalysts feature N-heterocyclic carbenes (NHCs) known to be strong  $\sigma$  donors yet less labile than phosphines.<sup>27</sup> NHC ligands can stabilize the unsaturated intermediate to achieve exceptional activities in ROMP. However, it generally provides polymers with broad polydispersities, attributed to the relatively slow initiation rate and secondary chain transfer reactions. The 3<sup>rd</sup> generation of Grubbs catalysts is derived from the 2<sup>nd</sup> generation of Grubbs catalysts which have two pyridine ligands instead of one phosphine ligand. Containing strongly ligating NHCs with weakly coordinating pyridine ligands, the 3<sup>rd</sup> generation of Grubbs catalysts displays not only high reactivity but also exceptionally fast initiation kinetics as a result of the labile nature of the pyridine ligands. A wide range of monomers have been polymerized in a living fashion to provide polymers of extremely low PDIs. In fact, the propagation rate of the 3<sup>rd</sup> generation of Grubbs catalysts is much larger than the one of the 2<sup>nd</sup> generation of Grubbs catalysts, meanwhile, the initiation rate of the former is more than ten thousands times higher than the one of the latter which is far more than enough to override their increased propagation rate.<sup>28</sup> With the 3<sup>rd</sup> generation of Grubbs catalysts, living ROMP of norbornene was also achieved at -20 °C when chain transfer reactions were suppressed at

low temperature and initiation was still rapid and efficient.<sup>29</sup> Moreover, diblock copolymers and even a triblock copolymer (**A22**) was prepared by sequential polymerization of different monomers with various functionalities (Figure A5).

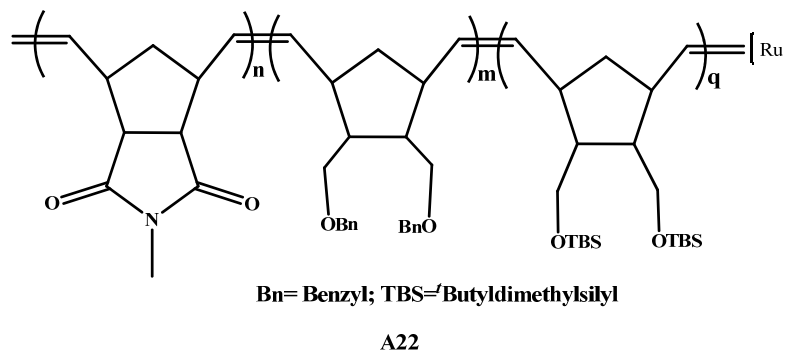


**Figure A5.** A triblock copolymer (**A22**) synthesized by ROMP with the 3<sup>rd</sup> generation of Grubbs catalysts.

#### A.2.4 Controlled Free Radical Polymerization

As the oldest mechanism for polymerization of olefin monomers, free radical polymerization is widely used for industrial preparation of a large number of materials. Free radical polymerizations are intrinsically tolerant of protic and aqueous solvent media and certain functional monomers. A large range of monomers can be polymerized and copolymerized by free radical polymerization, under less rigorous experimental conditions compared with ionic polymerizations. However, facile termination and chain transfers are disadvantageous and prevent polymerization with controlled molecular weight.

Recently, different methods have been developed to suppress the undesired termination

and chain transfer reactions associated with free radical polymerization. The most important methods are Stable Free Radical Polymerization (SFRP), Atom Transfer Radical Polymerization (ATRP) and Reversible Addition Fragmentation Chain Transfer (RAFT).

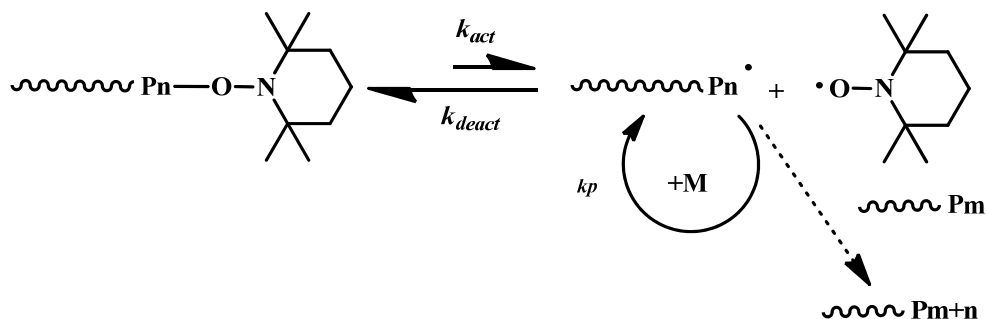
Unlike conventional radical polymerization, in which growing radical chains have a lifetime of only  $\sim 0.1\text{--}1$  s before they undergo irreversible bimolecular radical–radical terminations, in controlled living radical polymerizations the chains are reversibly deactivated and add monomer throughout the polymerization. Irreversible termination does occur to a limited extent, but most of the chains remain ‘living,’ thereby enabling the synthesis of polymers with narrower molecular weight distributions and better control of the microstructure in comparison to conventional radical polymerization. The "livingness" of this polymerization process can be ascertained from a linear first-order kinetic plot, accompanied by a linear increase in number average polymer molecular weights with conversion, with a value of the number-average degree of polymerization (DP) determined by the ratio of reacted monomer to initially introduced initiator. Plenty of well-defined polymers such as block copolymers, star and comb polymers have been prepared by using controlled/living radical polymerizations.

#### **A.2.4.1 Nitroxide Mediated Radical Polymerization (NMP)**

The reversible end-capping of propagating polystyrene by a stable nitroxide free radical,

2,2,6,6-tetramethylpiperidiny1-1-oxy (TEMPO), was originally reported by Moad and coworkers.<sup>30</sup> Years later the TEMPO mediated free radical polymerizations were eventually refined by using bulk polymerization conditions to enable a real “living” free radical polymerization of styrene by Georges and coworkers.<sup>31</sup>

As one of the most important controlled living radical polymerization methods, NMP, also known as Stable Free Radical Polymerization (SFRP), employs stable nitroxides such as TEMPO to reversibly terminate growing polymer chains (Scheme A11), yielding dormant species. The equilibrium is shifted strongly toward the dormant species so that the active (propagating) radical concentration is much lower than in conventional radical polymerization. Since propagation is first order with respect to radical concentration, while irreversible radical coupling termination is second order, the lower radical concentration results in a significantly reduced termination rate that preserves the living character of the chains. Irreversible termination also leads to higher nitroxide concentration, which forces the equilibrium to shift toward the dormant state, thereby further lowering the active radical concentration and reaction rate.<sup>32</sup>



**Scheme A11.** Mechanism of the Nitroxide (TEMPO) Mediated radical Polymerization (NMP).

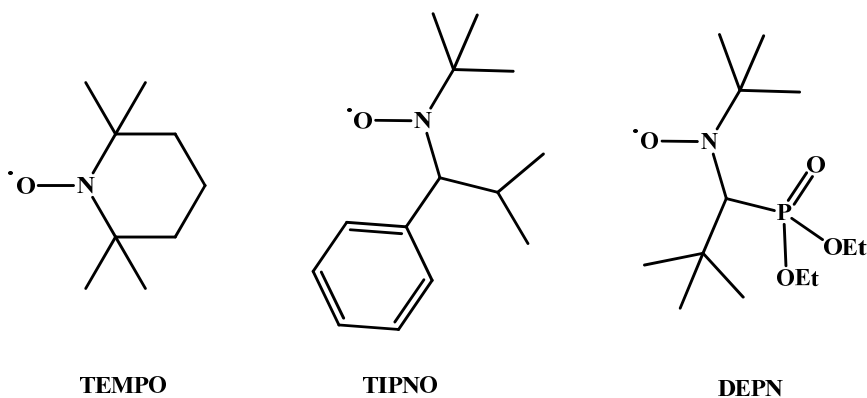


**Figure A6.** Structures of example nitroxides used for NMP.

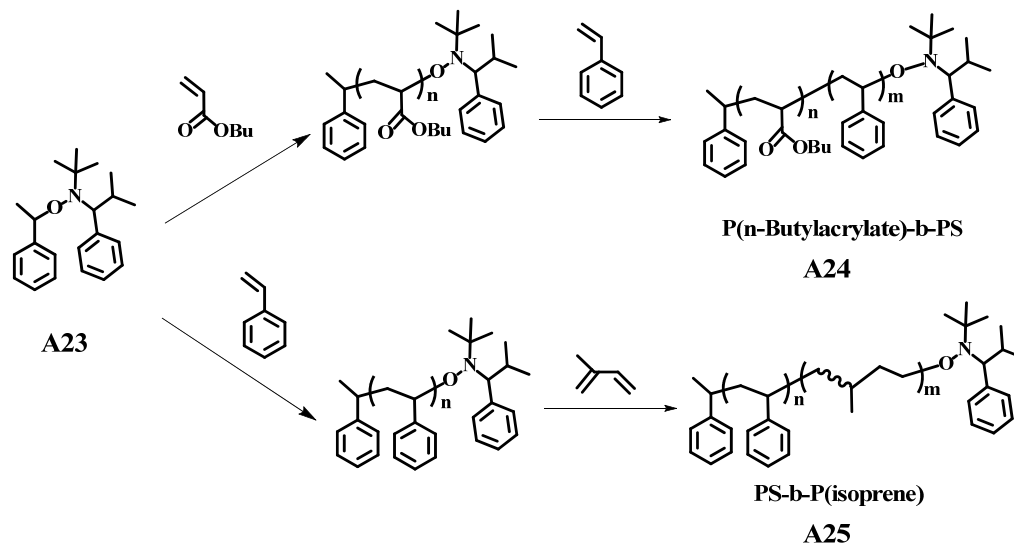
The TEMPO strongly binds to the free radical polymer chains so that the polymerization rates are usually slow. The irreversible chain terminations, being significant at the beginning of the polymerization, always build up excess TEMPO which can increasingly deactivate the growing polymer chains resulting in low conversion. Via self initiation, styrene monomers can be polymerized in a living fashion in the presence of TEMPO. The self initiated polymer chains can work as scavengers of the TEMPO to avoid the

accumulation of free TEMPO in the reaction mixture giving rise to an effective self regulating mechanism. The TEMPO mediated radical polymerization of styrene gives low fidelity of the end groups but typically good control over the polydispersity.

Well-controlled polymerization of a wider range of monomers was successfully enabled by the later developed acyclic nitroxides including DEPN (N-tert-butyl-N-(1-diethylphosphono-2,2-dimethylpropyl)-N-oxyl) and TIPNO (2,2,5-trimethyl-4-phenyl-3-azahexane-3-nitroxide) (Figure A6).<sup>33</sup> Both DEPN and TIPNO are acyclic nitroxides that are sterically bulky, so that their NO-C bonds can be more readily thermally cleaved giving a high dissociation rate and increased polymerization rates. In the beginning of the polymerization, excess of nitroxide is also built up due to the significant radical coupling termination; however, the initiation is so fast and efficient enough to enable chain growth. The probability for irreversible termination eventually decreases as the chain is getting longer and the reaction solution is becoming more viscous (bulk polymerization).<sup>34</sup> The propagating radical concentration will eventually become constant with a decreasing propagation rate.<sup>35</sup> Fast and efficient initiation is significant for achieving a controlled living radical polymerization.

Bicomponent systems in nitroxide mediated polymerizations are easy to use. However, it is difficult to control chain ends, molecular weight, and macromolecular architecture with such systems. By using unimer initiators, initiation efficiency can be increased and therefore better control of molecular weight distribution and predictability of molecular

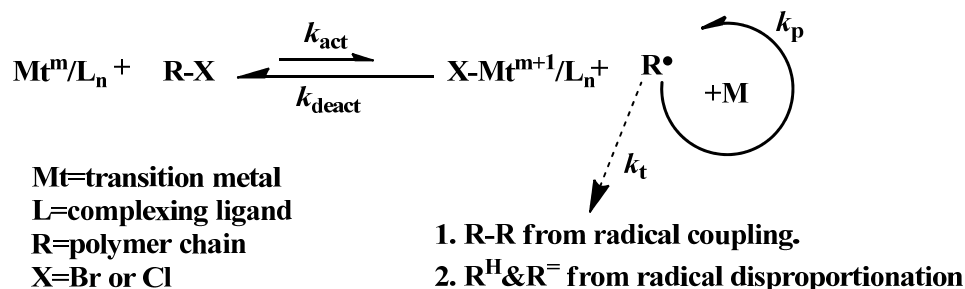
weight can be obtained. One such alkoxyamine unimolecular initiators, **A23** (Figure A7), derived from TIPNO has proven to be a potent initiator with improved performance in controlled living radical polymerization of a variety of monomers including acrylates, acrylamides, acrylonitrile, and 1,3-dienes.<sup>33</sup> Better fidelity of the end group can be achieved by using 0.05 extra equivalents of TIPNO along with the unimolecular initiator, **A23**. Due to the high end group fidelity and capability with a wide range of monomers, **A23** has been successfully used to prepare a number of diblock copolymers (Scheme A12). The efficiency of cross-initiation has to be taken into account, in relation to the propagation reaction of the second monomer, a common feature in all living polymerization to prepare block copolymers. For example, when polystyrene was synthesized as the first block, the following growth of the second polyacrylate block was found to be difficult. But well-defined diblock copolymers have been prepared in the reverse strategy; the PDI of the resulting diblock copolymer was almost the same as for the parent polyacrylate initiator indicating fast initiation of the second monomer.



**Scheme A12.** Preparation of diblock copolymers, **A24** and **A25**, through sequential controlled free radical polymerization.

#### A.2.4.2 Atom Transfer Radical Polymerization (ATRP)

Based on transition metal catalysts, ATRP was independently reported in 1995 by Matyjaszewski<sup>36</sup> and Sawamoto<sup>37</sup> as a method to mediate a controlled living radical polymerization. With the ability of polymerizing a variety of monomers in a living fashion, ATRP is one of the most powerful synthetic techniques that allow the synthesis of polymeric materials with predetermined molecular weight, composition, and molecular architecture derived from styrenics, methacrylates, acrylates or acrylonitrile.



**Scheme A13.** Mechanism of Atom Transfer Radical Polymerization (ATRP).

In a well-controlled ATRP (Scheme A13), the radicals or the active species are generated through a reversible redox process catalyzed by a transition metal complex ( $\text{Mt}^m/\text{L}_n$ ) which undergoes a one electron oxidation with concomitant abstraction of a halogen atom, X, from a dormant species, R-X, with a rate constant of activation,  $k_{\text{act}}$ . Polymer chains grow by the addition of the intermediate radicals to monomers in a manner similar to a conventional radical polymerization, with the rate constant of propagation  $k_p$ . The activation generates not only active species but also oxidized metal complexes,  $\text{X-Mt}^{m+1}/\text{L}_n$ , which deactivate the propagating polymer chains with a higher constant,  $k_{\text{deact}}$ , effectively shifting the equilibrium to the side of the dormant species. A low concentration of growing radicals can be achieved in the stationary stage of the polymerization. Fast initiation and rapid reversible deactivation are essential to accomplish uniform growth of all the chains. Like in other controlled living radical polymerizations, termination reactions ( $k_t$ ) also occur in ATRP mainly through radical coupling and disproportionation. The contribution of termination is minimized in

accordance to the low concentration of radicals in the stationary stage of the polymerization.

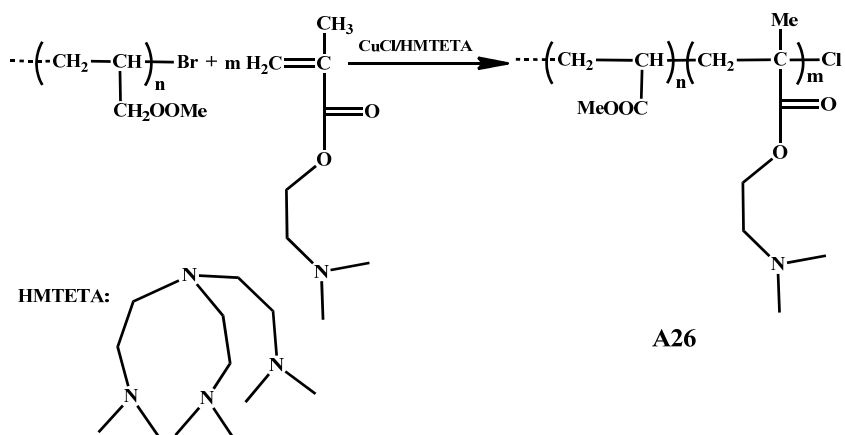
Copper based transition metal catalysts have been the most successful catalytic system for controlled living radical polymerizations. The system can be adjusted flexibly according to different polymerizable monomers, and a large variety of diblock copolymers have therefore been synthesized by ATRP.

As in the nitroxide mediated radical polymerizations, fidelity of chain end groups and efficiency of cross-propagation in ATRP have to be considered in order to prepare well-defined block copolymers. Fidelity of the end groups can be improved by varying reaction conditions, i.e. initiating system, reaction temperature and reaction time. The rate of polymerization increases with increasing temperature due to the increase of propagation rate and equilibrium constant of atom transfer. However, side reactions including chain transfer and termination become more pronounced at elevated temperature. To avoid end group loss, reasonable reaction time for a moderate conversion is preferred. With increased conversion, the polymerization rate becomes slow due to the decreased monomer concentration; meanwhile, side reactions become more competitive than the propagation.

In ATRP, alkyl halides are typically used as the initiator. To obtain well-defined polymers with narrow molecular weight distributions, the halide groups must rapidly and selectively migrate between the growing chain and the transition-metal complex.

Bromine and chlorine are usually used for a high level of control over molecular weight. Initiation should be fast and quantitative with a good initiator. In general, alkyl halides with activating substituents on the  $\alpha$ -carbon, such as aryl, carbonyl, or allyl groups, can potentially be used as ATRP initiators. The initiation rate depends strongly on the alkyl halide structure and increases in the order: primary < secondary < tertiary. Since the general order of bond strength in the alkyl halides is R-Cl > R-Br, alkyl chlorides should be less efficient than alkyl bromides. In general, the same halogen is used in the initiator and the metal salt; however, mixed halide initiating system can sometimes be used to obtain better polymerization control.<sup>38</sup> For example, combination of an alkyl bromide initiator and CuCl metal salt can give better polymerization control. The weaker carbon bromide is replaced by a stronger carbon chloride bond after initiation. As a result, the initiation from homolytic cleavage of an alkylbromide is faster than the propagation where the homolytic cleavage of carbon chloride bond is needed. Thus, the polymerization can be better controlled. The efficiency of cross-over propagation for the synthesis of block copolymers can also be improved by using mixed halide initiating system.<sup>39</sup> For examples, block copolymers of polymethacrylate-*b*-poly(2-(dimethylamino) ethyl methacrylate) (PMA-*b*-PDMAEMA) (**A26**) (Scheme A14) were successfully prepared by using a mixed halide initiating system. The initiation from PMA with a Br end group is relatively slow compared to the propagation of the second block, PDMAEMA, since halogen abstraction from secondary C-Br in the cross-over initiation

is slower than the propagation of PDMAEMA from its tertiary C-Br. Therefore, the synthesis of block copolymers with DMAEMA has a potential problem of slow initiation which may lead to incomplete block copolymer formation. The preparation of the block copolymer was carried by using PMA-Br as the macroinitiator and CuCl/HMTETA (1,1,4,7,10,10-hexamethyltriethylenetetramine) as the catalyst. HMTETA was used as a strong complexing ligand to prevent interference of the amino groups of the monomer. In the initiation step, the C-Br bonds were broken. As the reaction proceeded, chlorine quickly exchanged with bromine, and most chain ends were terminated with chlorine. The propagation rate was decreased since cleavage of stronger C-Cl bonds needed to occur during the propagation.



**Scheme A14.** ATRP of the diblock copolymer, **A26**, through a mixed halide initiating system.

Nitrogen based ligands are used as metal complexing agents in ATRP to solubilize the

transition-metal salt in the organic media and to adjust the redox potential of the metal center for appropriate reactivity and dynamics for the atom transfer. Copper complexes with a number of nitrogen based ligands can have distinct catalytic activities that make ATRP a flexible controlled living polymerization technique. The general order of activities of Cu complexes is related to their structure in accordance with the following order: tetradentate (cyclic-bridged) > tetradentate (branched) > tetradentate (cyclic) > tridentate > tetradentate (linear) > bidentate ligands. The nature of N atoms of the ligands is also important and follows the order pyridine  $\geq$  aliphatic amine > imine.<sup>39b, 40</sup>

#### **A.2.4.3 Reversible Addition-Fragmentation Chain Transfer (RAFT)**

In the late 1990s, Reversible Addition-Fragmentation Chain Transfer (RAFT) was reported by a group of scientists from CSIRO Molecular Science in Australia as a new method of living free radical polymerization with exceptional versatility in providing polymers of predetermined molecular weight and very narrow distribution. The polymerization can be performed by introducing a suitable chain transfer agent (CTA) into the conventional free radical polymerization reaction. The CTAs, also known as RAFT agents, are generally dithioester or trithiocarbonate compounds. Control in RAFT polymerization (Scheme A15) is achieved in a far more complicated manner than the homolytic bond formation and bond cleavage of SFRP and ATRP. The CTA for RAFT polymerization must be cautiously chosen because it has an effect on polymer length,

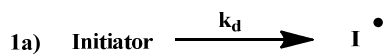
chemical composition, rate of the reaction and the number of side reactions that may occur.

The reaction mechanism consists of a series of steps and is shown in Scheme A15. The first reaction step is the fragmentation of an initiator molecule into radical fragments (1a). The initiator derived radicals subsequently initiate polymerization by reaction with a monomer molecule (1b). The next sequence of reaction steps constitutes the pre-equilibrium involving the reactions of macroradicals, leaving group radicals, and initial RAFT agent. Reaction step (2a) illustrates the equilibrium between initial RAFT agent and radicals. Reaction step (2b) gives the reaction of a leaving group radical with the initial RAFT agent. The next sequence of reaction steps constitutes the propagation reaction of the macroradicals (3a) and re-initiation (3b) reaction of the leaving group radicals. The following sequence is the core of the RAFT process termed the “core equilibrium,” which involves the equilibration between macroradicals. In a controlled living radical polymerization reaction, bimolecular termination reactions such as radical coupling and radical disproportionation reactions can be suppressed to a negligible extent and this also applies to RAFT polymerization.<sup>41</sup> Either the slow fragmentation of the intermediate RAFT radicals, **A27** and **A29**, in the pre-equilibrium or the slow re-initiation of the leaving group radical of the initial RAFT agent in the propagation can cause an inhibition period of considerable length before a RAFT polymerization takes place. In the core equilibrium, a fast interchange can effect a narrow molecular weight distribution. A

high rate coefficient of the formation of the intermediate RAFT radicals (**A30**) is crucial to the control of molecular weight. That means, if the propagating radicals preferably add to the polymeric RAFT agent, living radical polymerization can be expected. In contrast, the fragmentation rate of the intermediate (4) mainly controls the rate of polymerization and may effect retardation phenomena when it is too low.

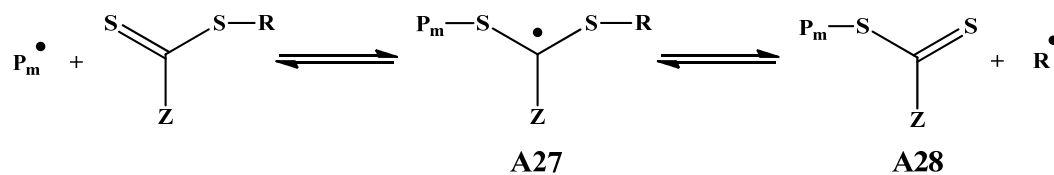
Based on the mechanism of RAFT polymerization, there should be a fraction of dead chains formed, which is directly related to the number of the initiator derived radicals.<sup>42</sup> To achieve maximum purity of the polymers, as low a concentration of initiator as possible is used, although this determines the rate of the radically driven polymerization. Especially, in a sequential polymerization, the initiator derived homopolymer chain will be inevitably present as an impurity. However, the radical derived chains are not discernable or of significance when a high ratio of RAFT agent and initiator is used in a well-designed experiment.

## 1. Initiation

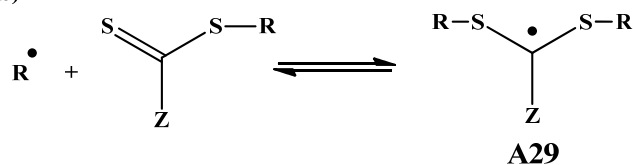


## 2. Pre-equilibrium

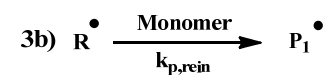
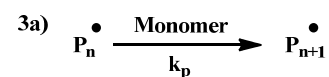
2a)



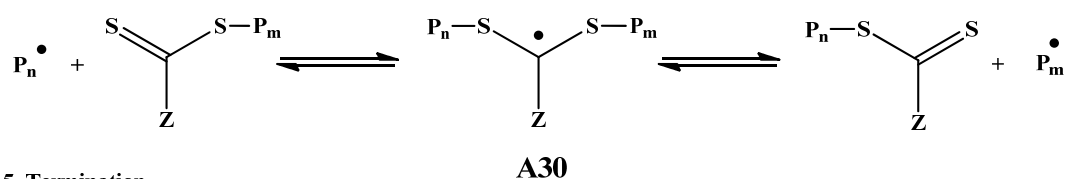
2b)



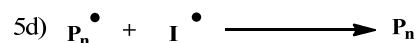
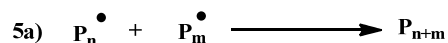
## 3. Propagation



## 4. Core equilibrium



## 5. Termination



**Scheme A15.** Mechanism of Reversible Addition-Fragmentation chain Transfer (RAFT).

Since RAFT polymerizations have a complex mechanism that is not fully understood, it is particularly important to choose an appropriate RAFT agent for a typical monomer. Design and synthesis might be necessary for a suitable RAFT agent. A typical structure of a RAFT agent is shown in Figure A7.

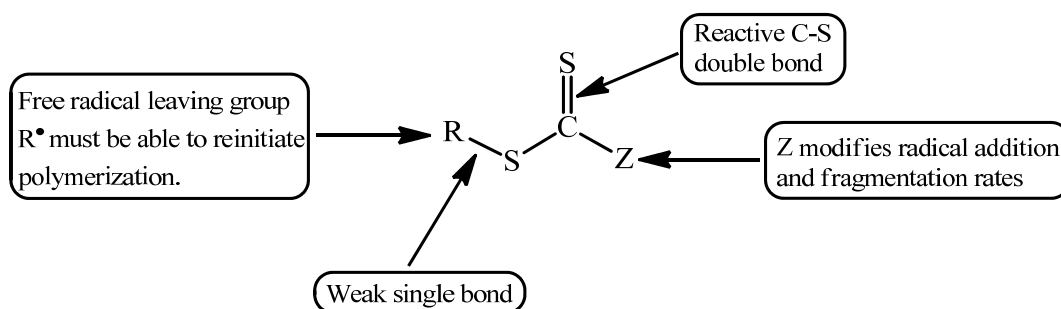


**Figure A7.** A general composition of RAFT agents.

An important component in a RAFT agent is the leaving group, R, which binds to the thiol group weakly, and its radical generated by fragmentation should be able to reinitiate polymerization.<sup>43</sup> In a sequential initiation and propagation of a macromolecular RAFT agent to obtain a block copolymer, the macromolecular initiator works as leaving group, and its ability to reinitiate the comonomers is essential for preparation of well-defined block copolymers. For example, reinitiation of styrene from a poly(methyl methacrylate) RAFT agent is usually effective to obtain well-defined block copolymers because of the fast transfer coefficient. The thiocarbonyl has a reactive double bond that is ready to form an adduct with radical species. The Z group usually attaches strongly to the thiocarbonyl

carbon and can affect the radical addition to the thiocarbonyl bond and also the fragmentation rates of the resulting radical intermediate adduct.

Trithiocarbonates with two thiol groups are also used with one thiol group working as Z group which forms stronger carbon sulfur bonds than the leaving thiol group. However, sometimes two leaving thiol groups are used in RAFT agent. These bifunctional trithiocarbonates can be used for preparation of di-telechelic polymers and multi-block copolymers<sup>44</sup> with a reductive cleavable trithiocarbonate unit in the middle block.

The ability of making well-defined polymers from the largest range of monomers<sup>45</sup> including ionic and even acidic monomers<sup>42</sup> has made RAFT an increasingly attractive method in comparison with other living free radical polymerizations.

### **A.3 Phase Segregation of Block Copolymers**

#### **A.3.1 Phase Segregation in Melts of Block Copolymers**

Some of the most intriguing properties and thereby associated applications of block copolymers are related to the mesoscopic phase segregation in their molten and solid states.<sup>46</sup> The microphase segregation is driven by the chemical incompatibilities between different blocks. Unlike binary mixtures of low molecular weight fluids, the entropy of mixing per unit volume of dissimilar polymers is small.<sup>47</sup> Therefore the mixing process of the different polymers is more dependent on the enthalpy. Thus, even minor chemical or structural differences between two different polymers can produce excess free energy that

disfavors mixing. In the case of block copolymers, the dissimilar constituting blocks are covalently joined together and can not undergo macroscopic phase separation. Instead, phase segregation of the different constituting blocks occurs to form domains of a mesoscopic dimension.

In the simplest case of a well-defined diblock copolymer with dissimilar block A and B, the mesoscopic phase segregation is driven by the repulsion of A and B blocks into a variety of ordered structures. The phase behavior may be controlled by three experimental parameters<sup>48</sup>: the degree of the polymerization,  $N$ ; the block fraction,  $f$ ; and the Flory-Huggins interaction parameter,  $\chi$ . The mixing free energy is affected by these parameters through the Flory-Huggins equation (A.1):

$$\Delta G_{mix}/(k_B T) = (1/N_A) \ln(f_A) + (1/N_B) \ln(f_B) + f_A f_B \chi \quad (\text{A.1})$$

The first two terms correspond to the configurational entropy of the system, which is small for high values of  $N_A$  and  $N_B$ , which may be the reason for the small contribution to the phase segregation from entropy. In the third term,  $\chi$  is the Flory-Huggins interaction parameter, which is associated with the enthalpic penalty of A-B monomer contact and is a function of both the interactions of the molecules and temperature (A.2):

$$\chi = a/T + b \quad (\text{A.2})$$

where  $a$  and  $b$  are experimentally obtained constants for a given composition of a particular polymer pair. Experimentally,  $\chi$  can be controlled through temperature. Positive  $\chi$  indicates net repulsion between A and B blocks, whereas a negative value

indicates a free-energy driving force towards mixing. Unlike macrophase separation in blends, the connectivity of the dissimilar constituting blocks prevents complete separation, and instead the chains organize to put the A and B portions on opposite sides of an interface. The equilibrium mesoscopic domain structures must minimize the unfavorable A-B contact without overstretching the polymer chains.

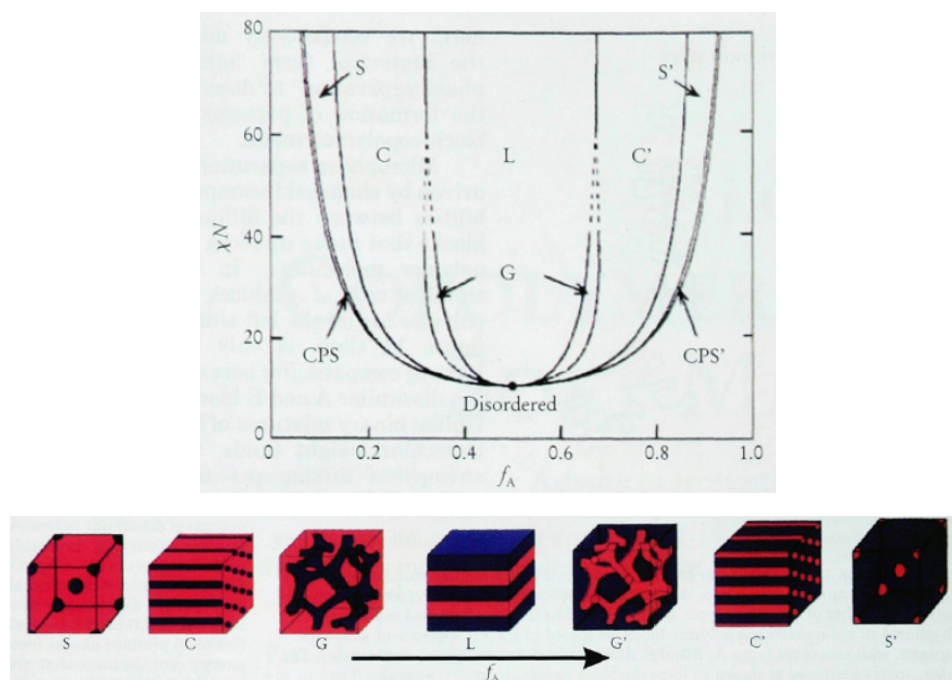


**Figure A8.** Phase diagram as calculated using self-consistent mean-field theory of the AB diblock copolymer.<sup>46, 49</sup> Reprinted in part with permission from *Physics Today* 1999, 52, 32-38, Copyright 1999 American Institute of Physics.

Self-consistent mean-field theory was used to predict the equilibrium morphologies of block copolymers.<sup>50</sup> The calculated diagram for an AB diblock copolymer is shown in

(Figure A8), where  $f_A$  is the block fraction of block A,  $\chi$  is the Flory-Huggins interaction parameter, and  $N$  is the degree of polymerization (number of monomers of all types per macromolecule); Four equilibrium morphologies have been predicted: spherical (S), cylindrical (C), Gyroid (G), Lamella (L), depending on the composition  $f$  and combinational parameter  $\chi N$ .

The morphologies obtained from the block copolymers can be thermodynamically very stable. Thus, monodisperse block copolymers can give a rich variety of well-defined periodic nanostructures offering the potential to fabricate high density arrays for use in data storage, electronics, molecular separation and for combinatorial chemistry and DNA screening.<sup>51</sup>

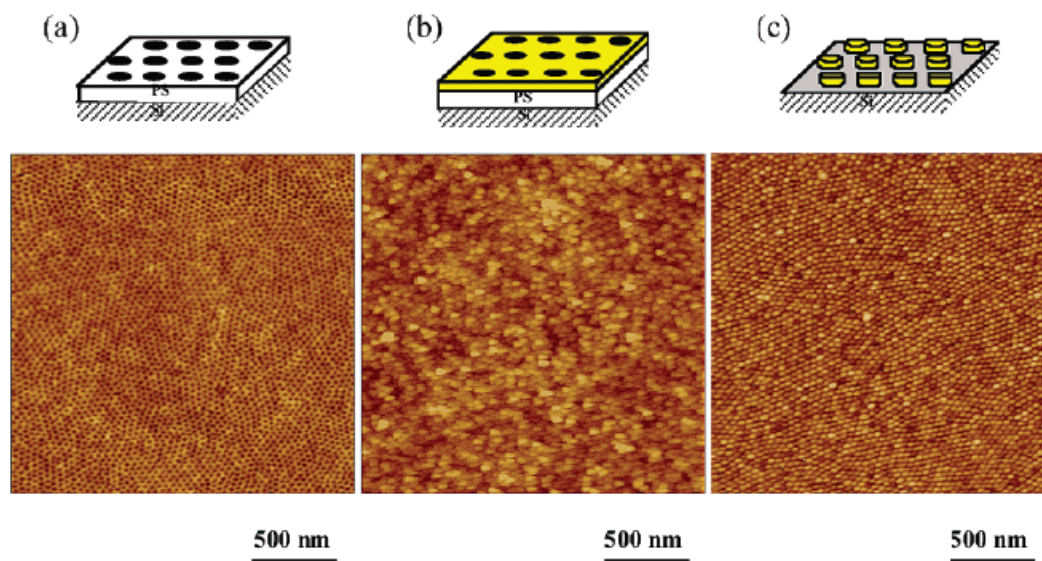


**Figure A9.** Schematic diagram of the fabrication process for Cr dot arrays (upper pictures) and height images of tapping mode atomic force microscope (AFM) of each

step (lower pictures): (a) nanoscopic holes in cross-linked PS matrix, (b) evaporated Cr onto the PS template, and (c) Cr nanodot arrays. Reprinted in part with permission from *Nano Letters* 2002, 2, 933-936, Copyright 2002 American Chemical Society.

As an example, Russell and coworkers fabricated high density arrays of metal dots and nanoholes in metal films. Poly(styrene-*b*-methyl methacrylate)s, synthesized by living anionic polymerization, were used to prepare templates on a silicon wafer (Figure A9). Spin-coated onto a pretreated silicon wafer and followed with annealing, the diblock copolymer can self-assemble into highly ordered cylindrical microdomains which were normal to the substrate. Nanoporous films of PS or nanoscopic posts of PS could be produced by selective removing PMMA from the parent block copolymers. Thus, a template, either comprising an array of hexagonally packed pores in a PS matrix or PS posts, was fabricated. Evaporation of Cr and Au onto the template, followed by sonication and UV degradation of the PS, left Cr or Au/Cr nanodots or a nanoporous metallic film.<sup>52</sup>

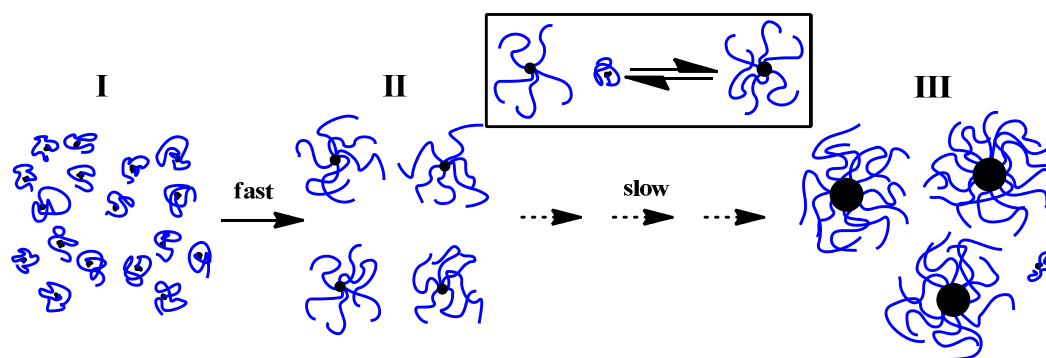
### **A.3.2 Block Copolymer Micelles**

Block copolymers, like low molecular weight surfactants, undergo self-assembly to form micelles in solvents selective for one of the blocks. The insoluble block forms the core of micelles, whereas the soluble block forms the corona which is also called a shell. Solvent

selectivity and, hence, copolymer self-assembly, have been observed for a variety of block copolymers in water, polar, nonpolar organic solvents and even supercritical fluids. It is possible to tune the aggregate properties by varying the size and/or ratio of the constituting blocks. The concentration at which micelles first appear is defined as the critical micelle concentration (cmc). When a concentration of a given block copolymer is lower than the critical micelle concentration with respect to the block selective solvent used, the copolymer chains are in an unassociated state. The insoluble block has a collapsed conformation and is protected from the unfavorable environment of the selective solvent by the soluble block.

A complete understanding of the physical mechanisms of the self-assembly of block copolymer into micelles is still lacking. Some theories favor the classical Aniansson-Wall mechanism, a step-by-step insertion mechanism of single molecules (unimers), while others emphasize the role of fragmentation or recombination mechanisms, i.e., fusion and fission of individual micellar entities. Recently a direct observation was reported by Lund and coworkers.<sup>53</sup> Micellization of a well defined amphiphilic poly(ethylene-*alt*-propylene)-block-poly(ethylene oxide) (PEP-*b*-PEO) (**A31**) in a mixture of water and DMF was studied. In the DMF solution, only unimers were present in the stock solution, and micellization was induced spontaneously by rapidly mixing the stock solution with a mixture of water and DMF. The micellization process thereafter was monitored by means of synchrotron x-ray scattering with millisecond time resolution. As a result shown in

Scheme A16, upon a quick change of the solvent quality the initial free unimers are transformed rapidly into metastable micelles with a process resembling nucleation (region I). Growth of micelles (region II) below the cmc level can only occur when some of the metastable micelles are dissolved to release their constituting unimers which in turn insert to the other micelles.



**Scheme A16.** Growth mechanism of a well defined amphiphilic diblock copolymer, poly(ethylene-*alt*-propylene)-block-poly(ethylene oxide) (**A31**), in a mixture of water and DMF.

The requirement for decreasing excess free energy at the core–shell interface apparently drives the block copolymer micelles to increase in association number, allowing the relative surface area of the interface to be lowered. However, in turn, the increase in the association number leads to an increased core radius, resulting in the stretching of the core-forming segments because their junctions with shell-forming segments should align

at the core-shell interface in order to avoid thermodynamically unfavorable mixing of the two phases. Furthermore, the increased density of the shell upon block copolymer association causes the shell-forming segment to assume a more stretched conformation. Stretching of both the core and shell forming segments, with an increased association, apparently decreases the conformational entropy, which should compensate for the decreased interface free energy upon micellization. It is this balance between interfacial energy and conformational entropy of the polymer strands that uniquely determines the thermodynamically stable size of the micelles (Figure A10).<sup>54</sup>

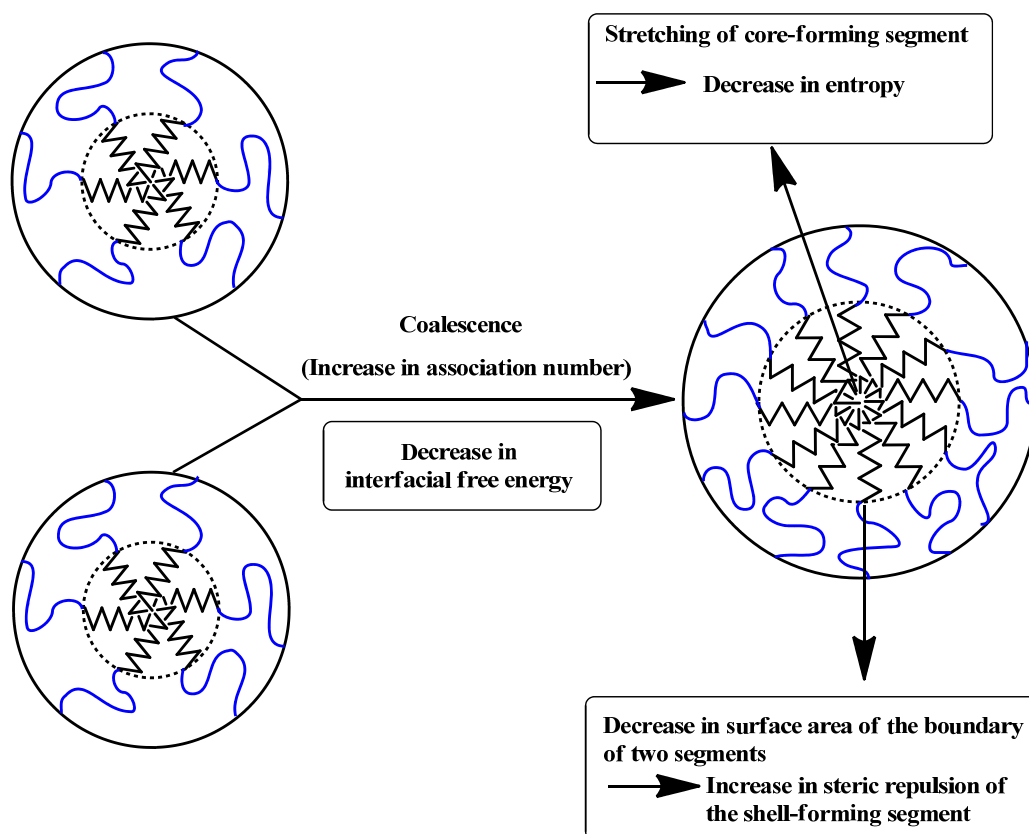


**Figure A10.** Determining factors for the size of polymeric micelles from block copolymers.

## **A.4 Boron Containing Block Copolymers**

### **A.4.1 Introduction of Organoboron Chemistry**

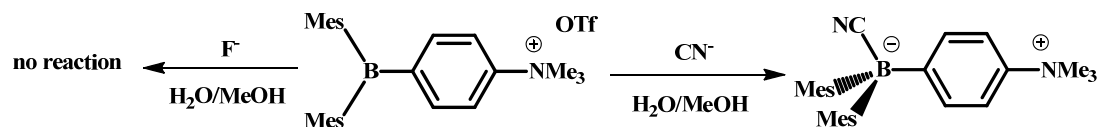
#### **A.4.1.1 Applications in Organic Chemistry**

Organoborane compounds have been playing important roles in organic chemistry. The well-known hydroboration reaction is an anti-Markovnikov reaction, i.e. hydroboranes such as 9-borabicyclo[3.3.1]nonane (9-BBN) can react rapidly with alkenes with the borane groups attaching to the less-substituted carbon, which has been useful in preparing terminal alcohols, aldehydes and amines and so on by subsequent transformation reactions. Organoboronic acids have been important reagents to facilitate the carbon-carbon bond formation in the widely used Suzuki coupling reactions.

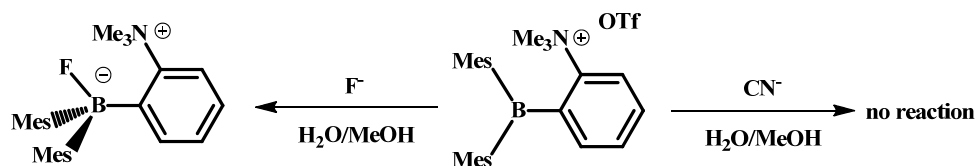
#### **A.4.1.2 Applications of Lewis Acidity**

While organoboron compounds exist as critical reagents and intermediates in organic synthesis reactions, attention has been increasingly paid to their attractive Lewis acid characters for applications in catalysis and as chemosensors. In the past two decades, tris(perfluorophenyl) borane and its derivatives have been extensively used as very efficient activators in olefin polymerization reactions when combined with group 4 metallocene alkyls.<sup>55</sup> Their ability to form weakly coordinating anions by abstraction of alkyl groups such as methyl and benzyl groups from a metal center has led to reactive cationic metal catalysts that exhibit high polymerization activities.<sup>56</sup>

The empty p orbital at the boron center of an organoborane can also overlap with neighboring  $\pi$  systems leading to extended conjugation. Upon binding of a nucleophile to the boron center, the photophysical properties can be drastically altered due to the interruption of the extended conjugation between the  $\pi$ -conjugated substituents and boron itself.<sup>57</sup> Bulky aromatic substituents such as mesityl groups have been frequently employed to protect the highly Lewis acidic boron center. This improves the stability and at the same time leads to high selectivity for small anions including fluoride, cyanide, hydroxide and azide. Cationic water soluble fluoride and cyanide selective borane sensors can be obtained, for example, upon placement of a tetramethylammonium moiety in the ortho or para position of the phenylborane moiety.<sup>58</sup> As shown in Scheme A17, compound **A32** has an ammonium group in the para position and binds to cyanide more strongly than fluoride. On the other hand, compound **A33** has an ammonium group in the meta position and shows good selectivity for fluoride binding. The electronic effect of the cationic substituent increases the Lewis acidity and, meanwhile, the increased steric crowding of the boron center can prevent the coordination of the larger cyanide. Two bulky mesityl substituents on boron afford good stability to the borane functionality so that both of the borane anion sensors show good stability in aqueous environment.



A32



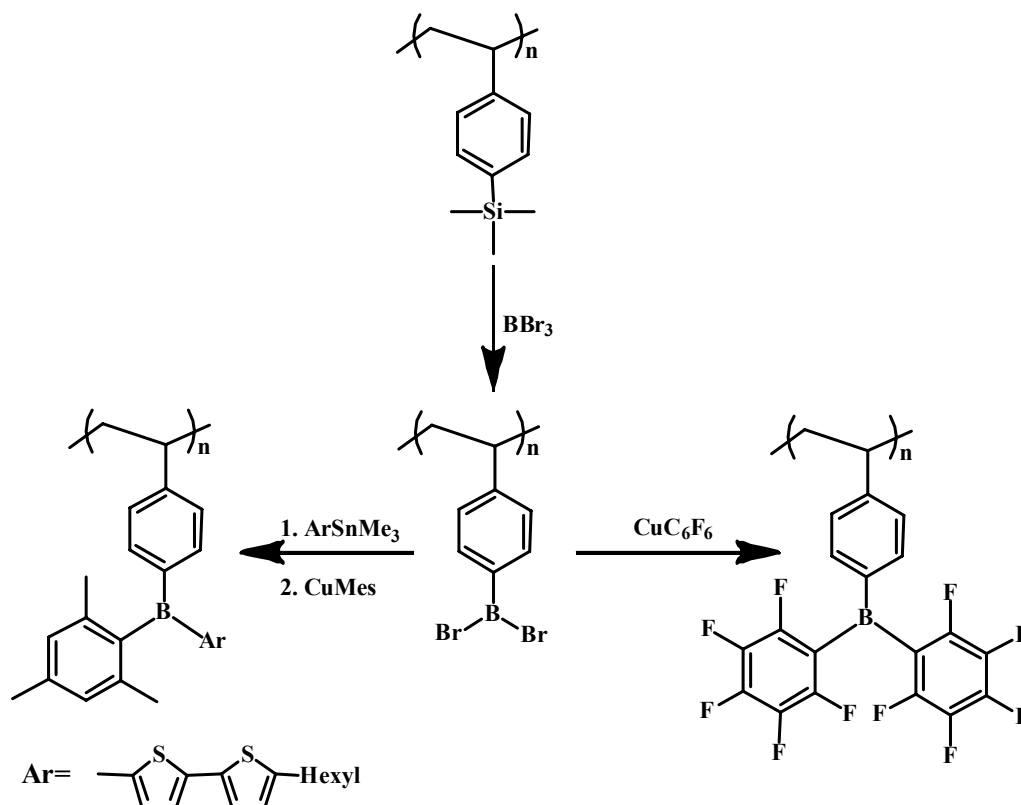
A33

**Scheme A17.** Mechanism of the selective sensing of fluoride or cyanide with water soluble borane sensors.

#### A.4.2 Building Blocks of Polymeric Materials

The introduction of inorganic elements such as boron to organic polymers can be of tremendous benefit as a means to impart additional functionality.<sup>59,60</sup> Boron containing polymers and especially block copolymers are becoming increasingly important for their interesting properties and promising applications. Recently, new and more selective strategies have been developed for the synthesis of boron containing polymers. Among these are efficient new polymer modification procedures. Poly(4-trimethylsilylstyrene)s synthesized via ATRP of silylated styrene monomer were modified through a quantitative borylation reaction into highly Lewis acidic polymer intermediates enabling subsequent versatile post-polymerization modifications (Scheme A18).<sup>61</sup> This synthetic route has the advantage that even highly Lewis acidic polymers can be prepared, for which the very

reactive monomers are either inaccessible or hard to be polymerized in a controlled manner. Many other boron functionalized polymers with versatile functionalities can be synthesized through this route.



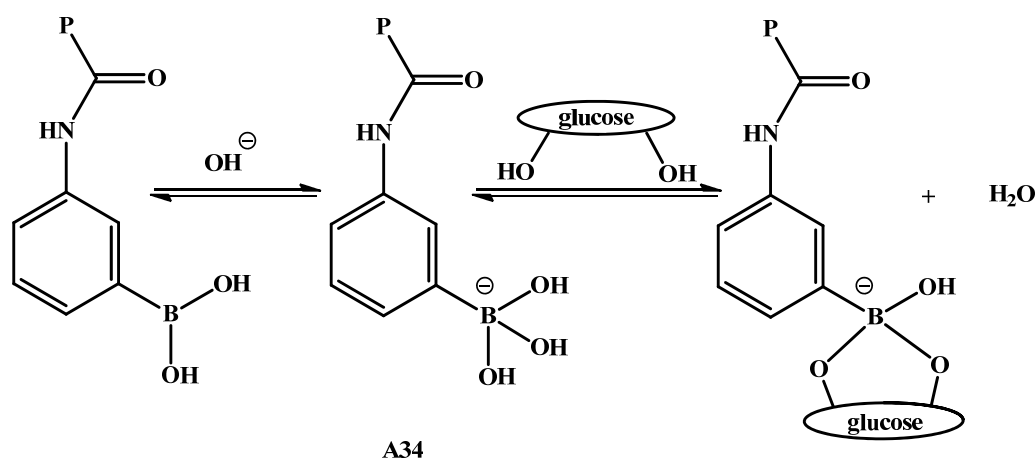
**Scheme A18.** Examples of the synthesis of highly Lewis acidic organoboron polymers via post-polymerization modification.

Excellent control over the molecular weight and distribution has been achieved for the polymerization of 4-trimethylsilylstyrene by ATRP, which therefore opens up opportunities to synthesize new block copolymers.<sup>62</sup> Controlled polymerization of

trimethylsilylstyrene and subsequent chain extension with styrene was shown to readily produce a block copolymer, poly(4-trimethylsilylstyrene)-b-polystyrene, which can be converted to organoboron block copolymers by highly selective boron-silicon exchange with  $\text{BBr}_3$ . The resulting  $-\text{BBr}_2$  functional groups can then be further elaborated, for example, into a less Lewis acidic alkoxyborane diblock copolymer by reaction with  $\text{MeOSiMe}_3$ . The alkoxyborane diblock copolymer was converted into a poly(styrylboronic acid) diblock copolymer by hydrolysis and into a boronic ester derivative, poly(4-pinacolatoborylstyrene)-b-polystyrene, by reaction with pinacol.

Boronic acid functionalized polymers have attracted a lot of interest due to their ability to reversibly bind biologically active diol species. In one example, random copolymers were prepared from 3-(acrylamido)phenylboronic acid (AAPBA) and other acrylamido monomers through conventional radical polymerization.<sup>63</sup> These polymers display a lower critical solution temperature (LCST) due to the constituting N-isopropylacrylamide (NIPAM).<sup>64</sup> Upon addition of a small amount of glucose, a large change in the LCST was observed between pH 8.8 and 9.1, which is close to the  $\text{pK}_a$  of phenylboronates. At higher pH, boronates (**A34**) formed by ionization of boronic acids can bind strongly to monosaccharides through the formation of reversible covalent bonds (Scheme A19). The thermal precipitation temperature is shifted to higher temperature upon formation of a complex between the phenyl boronic acid groups of the copolymer and glucose due to the increased hydrophilicity of the complexed copolymer.<sup>63a</sup> At physiological pH of 7.4, the

presence of a very low content of ionic boronate and a large amount of hydrophobic phenylboronic acid groups results in a low LCST of the copolymer. However, the sensitivity to glucose is still appreciably high which can be rationalized by the strong complexation between phenylboronic acid groups and glucose driving the equilibrium toward the formation of the ionic boronate **A34**.<sup>63b</sup>



**Scheme A19.** The equilibrium of the complexation between a phenylboronic acid polymer and glucose.

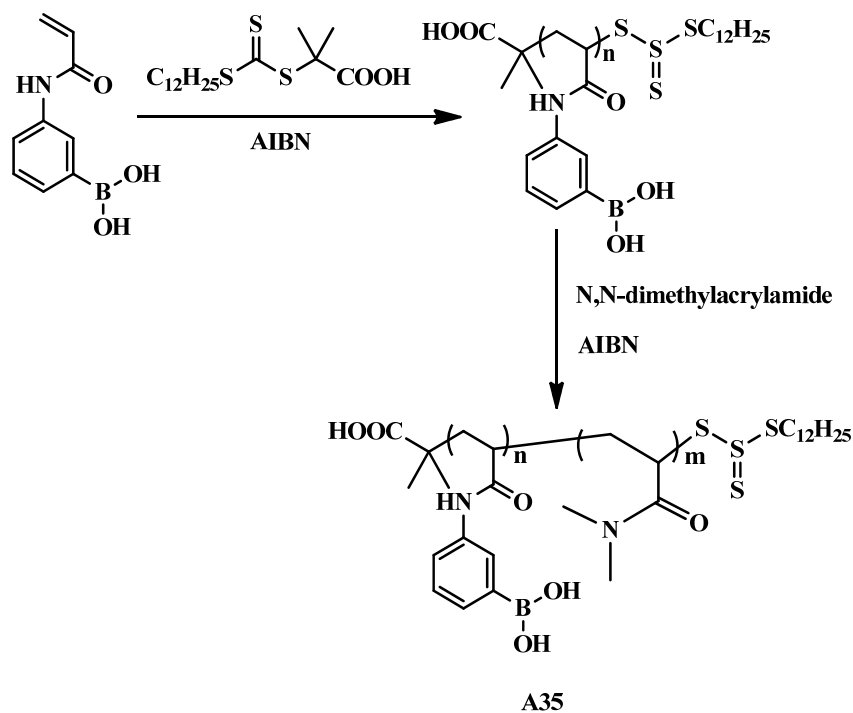
Boronic acid-containing acrylamido block copolymers have been successfully prepared by Sumerlin and coworkers via RAFT of 4-pinacolatoborylstyrene and subsequent chain extension with N, N- dimethylacrylamide.<sup>65</sup> Efficient removal of the pinacol protecting groups was achieved by a transesterification process using an insoluble support with an excess immobilized boronic acid. It was the first time a block copolymer containing both

boronic acid and acrylamido segments has been prepared. ATRP was used by Jäkle and coworkers to directly polymerize 4-pinacolatoborylstyrene, and the resulting boron containing polymer was used as a macroinitiator in the chain extension with styrene to prepare poly(4-pinacolatoborylstyrene)-b-polystyrene.<sup>62</sup>

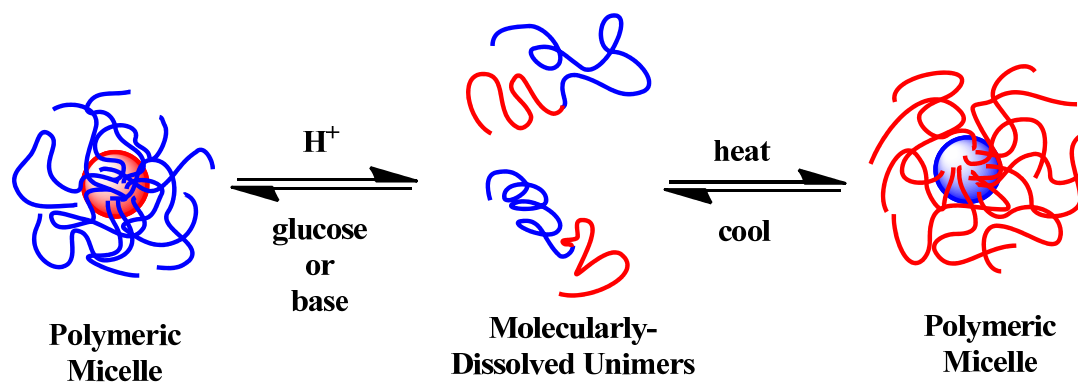
Later, Sumerlin and coworkers showed that the free boronic acid monomer 3-(acrylamido)phenylboronic acid (AAPBA) can be directly polymerized by RAFT with good control over the molecular weight distribution (PDI =1.13) and end group fidelity, allowing further chain extension with *N,N*-dimethylacrylamide (DMAA) to obtain diblock copolymers, PAAPBA-b-PDMAA (**A35**) (Scheme A20). Self-assembly and stimuli-triggered disassembly were studied by dynamic light scattering.<sup>66</sup> A block copolymer unimer solution at high pH was prepared and then dialyzed against deionized water to trigger the formation of micelles at reduced pH. The micelles were assumed to consist of a hydrophilic PDMAA corona and a hydrophobic PAAPBA core. Glucose and pH sensitive micelle disassembly to unimer was demonstrated by dynamic light scattering. Besides sugar sensing applications, these reverse micelles with boronic acid function groups inside the core should be of promise for drug delivery applications.

Triply-responsive boronic acid block copolymers were also reported by Sumerlin and coworkers.<sup>67</sup> *N*-isopropylacrylamide (NIPAM) was used in the chain extension step to give a second block that is temperature-responsive. While the block copolymer forms unimers at room temperature, at elevated temperature regular micelles formed. These

regular micelles consist of hydrophilic boronate corona and a poly(NIPAM) core with thermally induced hydrophobicity (Scheme A21).

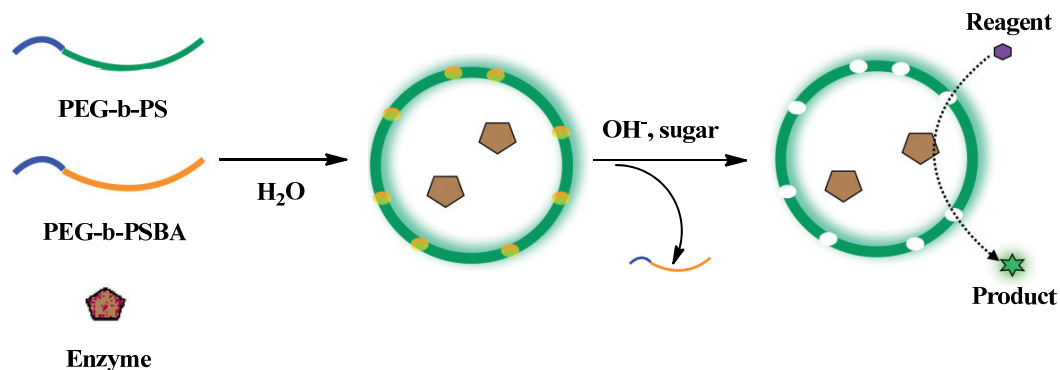


**Scheme A20.** Preparation of diblock copolymer **A35** through RAFT.



**Scheme A21.** The triply- responsive boronic acid block copolymers can undergo reversible micellizations triggered by heat, base or glucose.

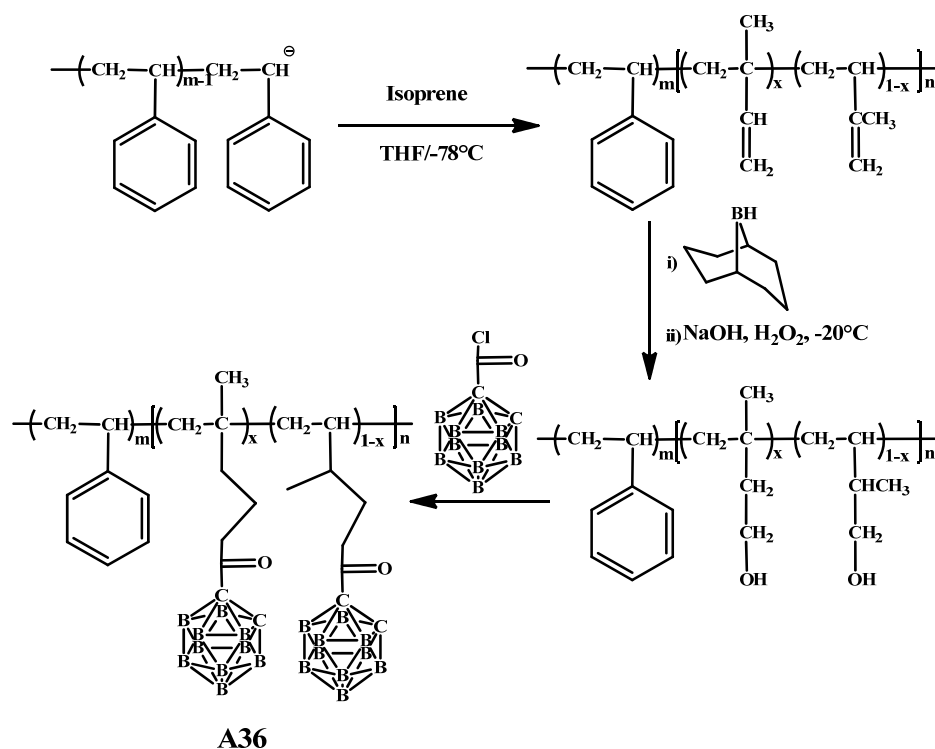
van Hest and coworkers used ATRP of 4-pinacolatoborylstyrene with a poly(ethylene glycol) macroinitiator, followed by removal of the pinacol groups to synthesize boronic acid diblock copolymers, poly(ethylene glycol)-b-poly(styrene boronic acid) (PEG-b-PSBA).<sup>68</sup> The diblock copolymers were creatively used for the preparation of polymersome nanoreactors with controllable permeability (Scheme A22). PEG-b-PSBA and poly(ethylene glycol)-b-polystyrene (PEG-b-PS) were dissolved in THF and subsequently gently dripped into water. Within a range of ratios of the two component block copolymers, the phase-segregated PSBA domains would be assumed to be dispersed throughout the PS matrix. The resulting vesicles were then treated with a concentrated D-fructose solution in a buffer of pH 9.4, such that the PEG-b-PSBA diblock copolymer in the vesicle membrane can be selectively dissolved into solution without changing the structural integrity of the vesicles themselves. The size of the resulting holes in the membrane after removal of the PEG-b-PSBA was found to be dependent on the ratio of the block copolymers so that the permeability of these vesicles can be properly adjusted. The vesicles were used to encapsulate an enzyme to form bioreactors which have voids in their membranes permitting only transmembrane diffusion of molecular reagents and products. (Scheme A22)



**Scheme A22.** Encapsulation of an enzyme in vesicles with controllable permeability to form bioreactors. Reprinted in part with permission from *Adv. Mater.*, 2009, 21, 2787-2791, Copyright 2009 Wiley-VCH Verlag GmbH&Co. KGaA.

Several examples of carborane-functionalized block copolymers have also been reported. Because of their remarkable stability, icosahedral carboranes have been viewed as ideal candidates for chemical and thermal strengthening of polymers. Ober and coworkers found that incorporation of a small amount of boron can significantly enhance oxygen etch resistance of photoresist polymers in lithography.<sup>69</sup> Block copolymers, polystyrene-*b*-polyisoprene, were polymerized through sequential living anionic polymerization (Scheme A23). The pendent vinyl groups of isoprene block were subsequently converted into hydroxyl groups which were used to introduce icosahedral (1-carboxyl chloride) carborane through a simple etherification mechanism. The degree of functionalization with the carborane was controlled anywhere from 0% to 100% by changing the feed ratio. The diblock copolymer (**A36**) with 7.6 mol% carborane units

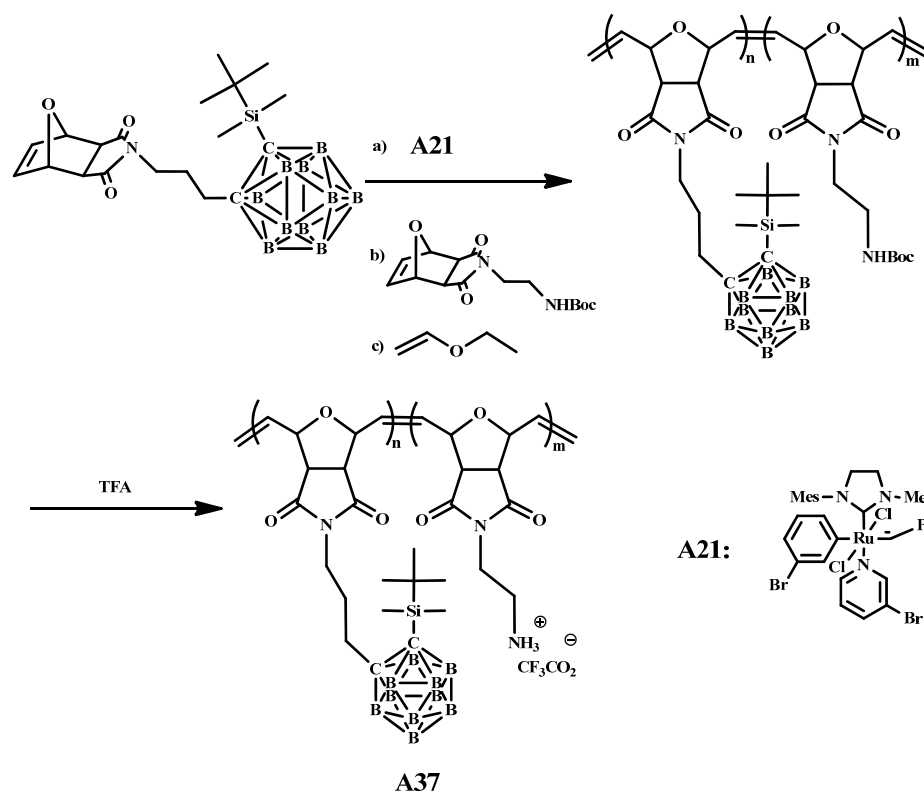
showed remarkably higher oxygen etch resistance than a random carborane copolymer consisting of 20 mol% carborane.



**Scheme A23.** Preparation of the diblock copolymer (**A36**) containing carborane units.

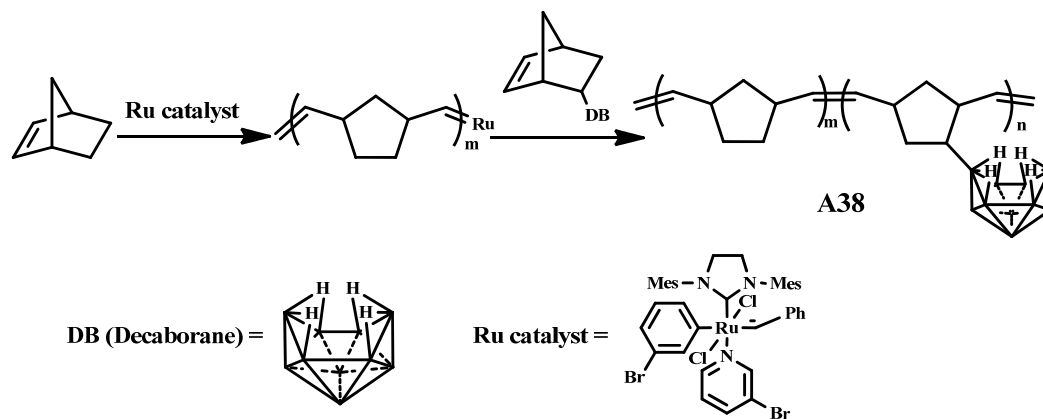
Carborane – macromolecule conjugates are also attractive for selective boron delivery to brain tumor for boron neutron capture therapy (BNCT).<sup>70</sup> Using one of the 3<sup>rd</sup> generation of Grubbs catalysts, **A21**, Coughlin and coworkers synthesized diblock copolymers<sup>71</sup> by sequential ring opening metathesis polymerization of two *exo*-7-oxonorbornene imide derivatives, silyl-protected oxonorbornene imide carborane (SONIC) and boc-protected oxonorbornene imide amine, respectively (Scheme A24). The diblock copolymers can be

transformed into amphiphilic copolymers (**A37**) through post-polymerization cleavage of the *t*Boc protecting groups in the second block with trifluoroacetic acid (TFA). Micellization in water was confirmed by dynamic light scattering; the resulting micelles presumably have the hydrophobic carborane containing block in the core and the charged hydrophilic block in the corona. Amphiphilic diblock copolymers of this kind are expected to have potential applications in the delivery of high boron content micelles for BNCT.



**Scheme A24.** Preparation of amphiphilic diblock copolymers (**A37**) functionalized with carborane groups through ROMP.

Malenfant and coworkers used the 3<sup>rd</sup> generation of Grubbs catalyst, **A21**, to prepare a boron containing diblock copolymer (**A38**) as a precursor of nano-structured ceramics.<sup>72</sup> Having a norbornene block (PNB) and decaborane functionalized norbornene block (PDNB), the copolymers were synthesized by sequential polymerization of the two monomers with 30 mol% PDNB block particularly (Scheme A25). The volume ratio for the PNB and PDNB is close to 1:1 so that, as predicted by the classical block copolymer phase diagram, a lamellar morphology was obtained when cast in a non-selective solvent such as chloroform. A cylindrical morphology was obtained from THF solutions as THF preferentially solvates the PDNB block. Elemental mapping by electron energy loss spectroscopy confirmed that the PNB block forms a cylindrical phase and the boron-containing PDNB forms the matrix. (Figure A11). Nano-structured boron nitride with hexagonally packed cylindrical mesoporous structure was prepared by pyrolysis of the diblock copolymer cast from THF at 1000°C in ammonia. Upon pyrolysis in nitrogen at 1000°C, the block copolymer cast from chloroform was transformed into boron carbonitride with a lamellar nano-structure.



**Scheme A25.** Preparation of a diblock copolymer having a norbornene block and decaborane functionalized norbornene block through ROMP.

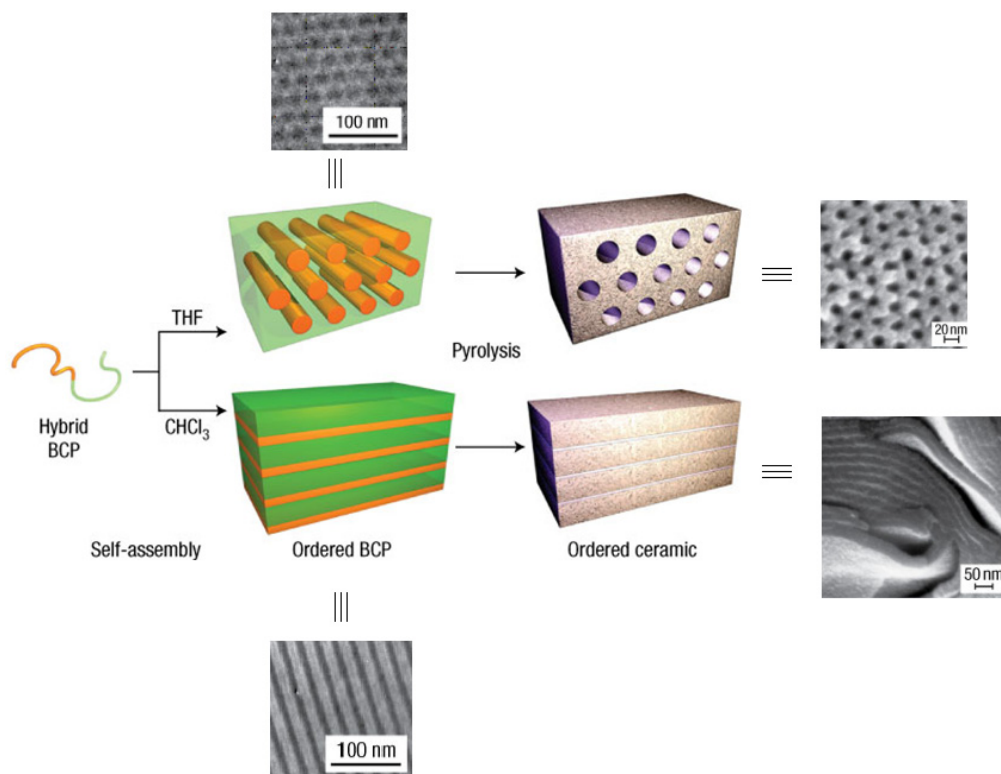
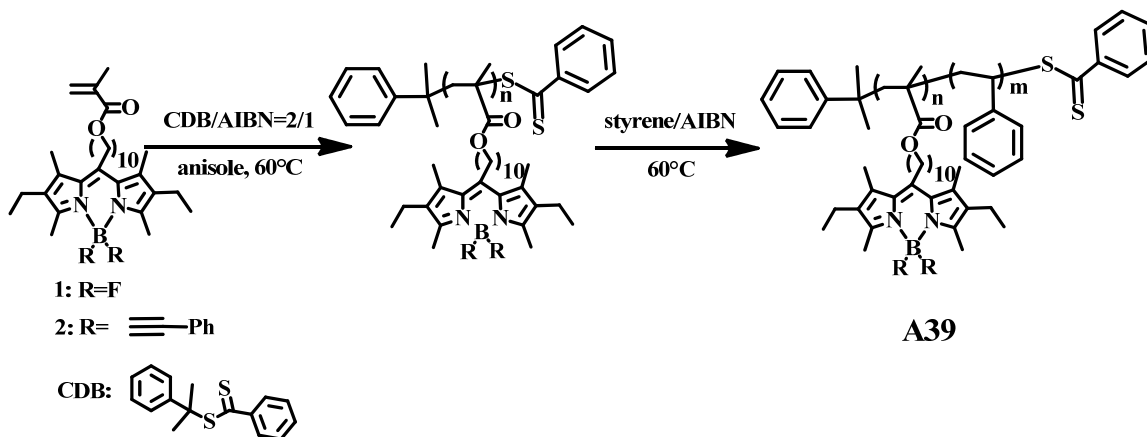


**Figure A11.** Preparation of different nanostructured ceramic materials through pyrolysis of the same diblock copolymer (A38) cast from different solvents. Reprinted in part with

permission from *Nature Nanotechnol.* 2007, 2, 43-46, Copyright 2007 Nature Publishing Group.

Luminescent boron-containing nano structures are of interest for imaging applications. Chujo and coworkers synthesized highly fluorescent boron polymers by incorporating the BODIPY (boron-dipyrromethene) dye into a  $\pi$  conjugated polymer, i.e. poly(p-phenylene-ethynylene), via Sonogashira-Hagihara coupling reaction.<sup>73</sup> The red shift of the absorption maxima and increase of molar absorption coefficients were ascribed to extension of  $\pi$ -conjugation along the polymer main chain. Interestingly, the strong  $\pi$ - $\pi$  stacking interaction facilitated the aggregation of these homopolymers in solutions. Recently, block copolymers with BODIPY dyes in their side chain were successfully synthesized by RAFT polymerization (Scheme A26). Methyl methacrylate monomers functionalized with different BODIPY dyes were polymerized in a control manner. Narrow molecular weight distributions (PDI<1.2) were achieved with a relatively low ratio (such as 50:2) of monomer to RAFT agent. Used as macroinitiators, these BODIPY functional homopolymers were adopted in the sequential polymerization of styrene. Very long polystyrene blocks with, for example, 685 repeating units, were obtained. The PDIs of the final diblock copolymers (**A39**) were about 1.4, which is a little higher than those of the macroinitiators. The  $\pi$ - $\pi$  stacking of the BODIPY dyes on the short poly(methyl methacrylate) block was suggested to work as the only driving force

for the self-assembly of the diblock copolymers in THF solution. Spherical micelles obtained from THF solution were observed by SEM and fluorescence microscopy and they were claimed as the first reported luminescent polystyrene ‘nano’particles (of dimensions bigger than 100 nm) obtained through controlled synthesis.

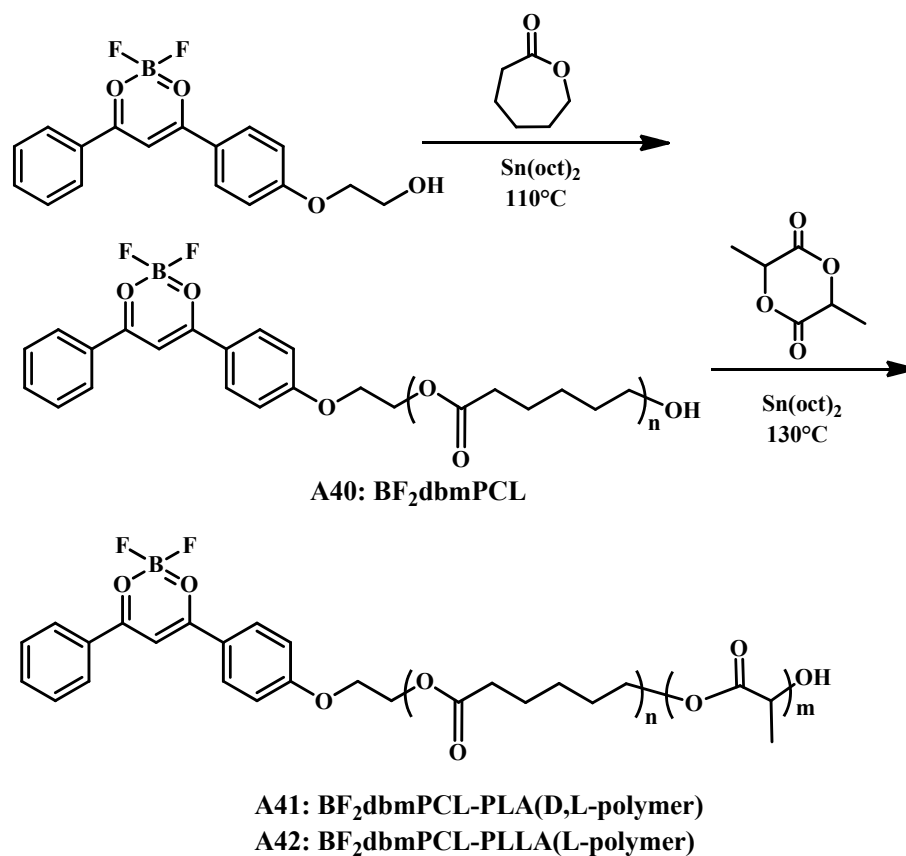


**Scheme A26.** Preparation of a diblock copolymer block copolymers (**A39**) with BODIPY dyes in their side chain through RAFT.

Fraser and coworkers reported monotelechelic diblock copolymers with another boron dye, difluoroboron dibenzoylmethane ( $\text{BF}_2\text{dbm}$ ), as the head group.  $\text{BF}_2\text{dbm}$ -polylactide (PCL) (**A40**) was synthesized by tin catalyzed ( $(\text{Sn}(\text{oct})_2$ , i.e., tin(II) 2-ethylhexanoate) ring-opening polymerization (ROP) and employed as a macroinitiator in combination with D, L- and L-lactide for the preparation of  $\text{BF}_2\text{dbmPCL-PLA}$  (**A41**) and  $\text{BF}_2\text{dbmPCL-PLLA}$  (**A42**) block copolymers, respectively (Scheme A27). Well-defined materials with low PDIs were obtained in good yield.<sup>74</sup>

Nearly identical intense blue fluorescence in solution was observed for all of these boron dye end group-functionalized polymers, however the photophysical properties were different in the solid state. The polymer **A40** did not show room temperature phosphorescence (RTP) as noted for BF<sub>2</sub>dbm-PLA in prior work by Fraser. Normally, RTP of BF<sub>2</sub>dbm dye should be enhanced in rigid matrices because of restricted degrees of freedom and thus fewer thermal decay pathways for its excited states. It was suggested that, in the semicrystalline **A40** the dye chain ends are excluded from polymer crystalline regions and concentrated in the amorphous regions, where there are microcavities of greater free volume, providing more degrees of freedom for the dye. When PLA or PLLA segments are grown from **A40** macroinitiators, however, the RTP is restored for the resulting block copolymers. Both RTP intensities and lifetimes increase with longer PLA or PLLA segments. Interestingly, as a semicrystalline material, PLLA segments can considerably enhance RTP of the block copolymer. With a T<sub>g</sub> (60°C) higher than room temperature, the chains of PLLA in the amorphous region are still “frozen” below T<sub>g</sub> and the volume of microcavities is quite small. The copolymer **A41** showed stronger RTP because the PLA segments are purely amorphous. These findings point to the utility of difluoroboron diketonate dyes as probes of polymer properties and microdomains. Their fluorescence, as described in the literature, is sensitive to the polarity of the surrounding medium, both solvent and polymer compositions as well as dye-dye interactions (i.e., dye concentration or polymer MW effects). Meanwhile, their phosphorescence is sensitive to

the polymer microstructure. This family of stimuli-responsive boron biomaterials (biodegradable) can also be utilized as imaging agents and oxygen sensors in cells and for tissues.



**Scheme A27.** Synthesis of diblock copolymers of boron dye head group, BF<sub>2</sub>dbm.

## A.5 References

1. Hadjichristidis, N.; Pispas, S.; Floudas, G., *Block Copolymers: Synthetic Strategies, Physical Properties, and Applications*. Wiley Interscience: New York, 2003.
2. Matyjaszewski, K.; Müller, A. H. E., *Prog. Polym. Sci.* **2006**, *31* 1039-1040.
3. (a) Szwarc, M.; Levy, M.; Milkovich, R., *Journal of the American Chemical Society* **1956**, *78*, 2656-2657, (b) Szwarc, M., *Nature* **1956**, *178*, 1168-1169.

4. Quirk, R. P., Anionic Polymerization In *Encyclopedia of Polymer Science and Technology*, 3rd ed.; Kroschwitz, J. I., Ed.; Wiley-Interscience: New York, 2003; Vol. 5, p 111.
5. Smid, J., *Journal of Polymer Science Part A: Polymer Chemistry* **2002**, *40*, 2101-2107.
6. Odian, G., *Principles of Polymerization*. 4th ed.; John Wiley & Sons, Inc.: Hoboken, New Jersey, 2004.
7. Yu, J. M.; Dubois, P.; Teyssie, P.; Jerome, R., *Macromolecules* **1996**, *29*, 6090-6099.
8. Yu, J. M.; Yu, Y.; Dubois, P.; Teyssié, P.; Jérôme, R., *Polymer* **1997**, *38*, 3091-3101.
9. Higashihara, T.; Ueda, M., *Macromolecules* **2009**, ASAP.
10. Sawamoto, M., *Progress in Polymer Science* **1991**, *16*, 111-172.
11. Kennedy, J. P.; Iván, B., *Designed Polymers by Carbocationic Macromolecular Engineering: Theory and Practice*. Carl Hanser Verlag: Munich, 1992.
12. Kennedy, J. P.; Marechal, E., *Carbocationic Polymerization*. Wiley-Interscience: New York, 1982.
13. Kamigaito, M.; Sawamoto, M.; Higashimura, T., *Macromolecules* **1992**, *25*, 2587-2591.
14. (a) Novak, B. M.; Risse, W.; Grubbs, R. H., *Adv. Polym. Sci.* **1992**, *102* 47-72, (b) K. J. Ivin; J. C. Mol, *Olefin Metathesis and Metathesis Polymerization* Academic Press San Diego, CA, 1997, (c) Grubbs, R. H.; Khosravi, E., *Mater. Sci. Technol.* **1999**, *20*, 65-104, (d) Buchmeiser, M. R., *Chemical Reviews* **2000**, *100*, 1565-1604, (e) Frenzel, U.; Nuyken, O., *Journal of Polymer Science Part A: Polymer Chemistry* **2002**, *40*, 2895-2916.
15. Hérisson, P. J.-L.; Chauvin, Y., *Die Makromolekulare Chemie* **1971**, *141*, 161-176.
16. Cannizzo, L. F.; Grubbs, R. H., *Macromolecules* **1988**, *21*, 1961-1967.
17. (a) Schaverien, C. J.; Dewan, J. C.; Schrock, R. R., *Journal of the American Chemical Society* **1986**, *108*, 2771-2773, (b) Kress, J.; Osborn, J. A.; Greene, R. M. E.; Ivin, K. J.; Rooney, J. J., *J. Chem. Soc., Chem. Commun.* **1985**, 874 - 876, (c) F. Quignard, M. L., J.-M. Basset, *J. Chem. Soc. Chem. Commun.* **1985**, 1816-1817, (d) Katz, T. J.; Lee, S. J.; Shippey, M. A., *J. Mol. Catal.* **1980**, *8*, 219-226.
18. Schrock, R. R.; Feldman, J.; Cannizzo, L. F.; Grubbs, R. H., *Macromolecules* **1987**, *20*, 1169-1172.
19. Schrock, R. R., *Accounts of Chemical Research* **1990**, *23*, 158-165.
20. Murdzek, J. S.; Schrock, R. R., *Macromolecules* **1987**, *20*, 2640-2642.
21. Bielawski, C. W.; Grubbs, R. H., *Prog. Polym. Sci.* **2007**, *32*, 1-29.
22. Trzaska, S. T.; Lee, L.-B. W.; Register, R. A., *Macromolecules* **2000**, *33*, 9215-9221.
23. Nguyen, S. T.; Johnson, L. K.; Grubbs, R. H.; Ziller, J. W., *Journal of the American Chemical Society* **1992**, *114*, 3974-3975.
24. Bielawski, C. W.; Benitez, D.; Morita, T.; Grubbs, R. H., *Macromolecules* **2001**, *34*, 8610-8618.

25. Schwab, P.; Grubbs, R. H.; Ziller, J. W., *Journal of the American Chemical Society* **1996**, *118*, 100-110.
26. Ulman, M.; Grubbs, R. H., *The Journal of Organic Chemistry* **1999**, *64*, 7202-7207.
27. (a) Herrmann, W. A.; Köcher, C., *Angewandte Chemie International Edition in English* **1997**, *36*, 2162-2187, (b) Weskamp, T.; Schattenmann, W. C.; Spiegler, M.; Herrmann, W. A., *Angewandte Chemie International Edition* **1998**, *37*, 2490-2493, (c) Arduengo, A. J., *Accounts of Chemical Research* **1999**, *32*, 913-921, (d) Huang, J.; Schanz, H.-J.; Stevens, E. D.; Nolan, S. P., *Organometallics* **1999**, *18*, 5375-5380, (e) Bourissou, D.; Guerret, O.; Gabbai, F. P.; Bertrand, G., *Chemical Reviews* **2000**, *100*, 39-92.
28. (a) Choi, T.-L.; Grubbs, R. H., *Angewandte Chemie International Edition* **2003**, *42*, 1743-1746, (b) Sanford, M. S.; Love, J. A.; Grubbs, R. H., *Journal of the American Chemical Society* **2001**, *123*, 6543-6554, (c) Love, J. A.; Morgan, J. P.; Trnka, T. M.; Grubbs, R. H., *Angewandte Chemie International Edition* **2002**, *41*, 4035-4037.
29. Sanford, M. S.; Ulman, M.; Grubbs, R. H., *Journal of the American Chemical Society* **2001**, *123*, 749-750.
30. Moad, G.; Rizzardo, E.; Solomon, D. H., *Polymer Bulletin* **1982**, *6*, 589-593.
31. Georges, M. K.; Veregin, R. P. N.; Kazmaier, P. M.; Hamer, G. K., *Macromolecules* **1993**, *26*, 2987-2988.
32. Cunningham, M. F., *Comptes Rendus Chimie* **6**, 1351-1374.
33. Benoit, D.; Chaplinski, V.; Braslau, R.; Hawker, C. J., *Journal of the American Chemical Society* **1999**, *121*, 3904-3920.
34. Kuo, W. F.; Tong, S. N.; Pearce, E. M.; Kwei, T. K., *Journal of Applied Polymer Science* **1993**, *48*, 1297-1301.
35. Benoit, D.; Grimaldi, S.; Robin, S.; Finet, J.-P.; Tordo, P.; Gnanou, Y., *Journal of the American Chemical Society* **2000**, *122*, 5929-5939.
36. (a) Wang, J.-S.; Matyjaszewski, K., *Journal of the American Chemical Society* **1995**, *117*, 5614-5615, (b) Wang, J.-S.; Matyjaszewski, K., *Macromolecules* **1995**, *28*, 7901-7910.
37. Kato, M.; Kamigaito, M.; Sawamoto, M.; Higashimura, T., *Macromolecules* **1995**, *28*, 1721-1723.
38. Matyjaszewski, K.; Xia, J., *Chem. Rev.* **2001**, *101*, 2921-2990.
39. (a) Shipp, D. A.; Wang, J.-L.; Matyjaszewski, K., *Macromolecules* **1998**, *31*, 8005-8008, (b) Zhang, X.; Matyjaszewski, K., *Macromolecules* **1999**, *32*, 1763-1766.
40. Tang, W.; Matyjaszewski, K., *Macromolecules* **2006**, *39*, 4953-4959.
41. Vana, P.; Davis, T. P.; Barner-Kowollik, C., *Macromolecular Theory and Simulations* **2002**, *11*, 823-835.
42. Barner-Kowollik, C., *Handbook of RAFT Polymerization*. Wiley-VCH Verlag GmbH & Co. KGaA: Weinheim, 2008

- 43.Chong, Y. K.; Krstina, J.; Le, T. P. T.; Moad, G.; Postma, A.; Rizzardo, E.; Thang, S. H., *Macromolecules* **2003**, *36*, 2256-2272.
- 44.Zhang, L.; Chen, Y., *Polymer* **2006**, *47*, 5259-5266.
- 45.Matyjaszewski, K.; Davis, K. A., Statistical, Gradient, Block and Graft Copolymers by Controlled/Living Radical Polymerizations, In *Advances in Polymer Science*, Springer-Verlag: Berlin Heidelberg,2002; Vol. 159, p 169.
- 46.Bates, F. S.; Fredrickson, G. H., *Physics Today* **1999**, *52*, 32-38.
- 47.Painter, P. C.; Coleman, M. M., *Essentials of Polymer Science and Engineering*. DEStech Publications, Inc. : Lancaster, PA, 2008.
- 48.Sun, S.-S.; Sariciftci, N. S., *Organic photovoltaics: mechanism, materials, and devices*. Taylor & Francis Group: Boca Raton, FL, 2005.
- 49.Matsen, M. W.; Bates, F. S., *Macromolecules* **1996**, *29*, 1091-1098.
- 50.Matsen, M. W.; Schick, M., *Physical Review Letters* **1994**, *72*, 2660-2663.
- 51.Hamley, I. W., *Nanotechnology* **2003**, *14*, R39-R54.
- 52.Shin, K.; Leach, K. A.; Goldbach, J. T.; Kim, D. H.; Jho, J. Y.; Tuominen, M.; Hawker, C. J.; Russell, T. P., *Nano Letters* **2002**, *2*, 933-936.
- 53.Lund, R.; Willner, L.; Monkenbusch, M.; Panine, P.; Narayanan, T.; Colmenero, J.; Richter, D., *Physical Review Letters* **2009**, *102*, 188301-188304.
- 54.Kataoka, K.; Harada, A.; Nagasaki, Y., *Advanced Drug Delivery Reviews* **2001**, *47*, 113-131.
- 55.(a)Ewen, J. A.; Edler, M. J.; (Fina Technology, Inc., United State), Application: EP 0427697, 1991, (b)Ewen, J. A.; Edler, M. J.; (Fina Technology, Inc., United State), Application: US 5561092, 1996, (c)Yang, X.; Stern, C. L.; Marks, T. J., *Journal of the American Chemical Society* **2002**, *113*, 3623-3625, (d)Yang, X.; Stern, C. L.; Marks, T. J., *Journal of the American Chemical Society* **1991**, *113*, 3623-3625, (e)Yang, X. M.; Stern, C. L.; Marks, T. J., *J. Am. Chem. Soc.* **1994**, *116*, 10015-10031.
- 56.Piers, W. E.; Chivers, T., *Chem. Soc. Rev.* **1997**, *26*, 345-354.
- 57.Yamaguchi, S.; Akiyama, S.; Tamao, K., *J. Am. Chem. Soc.* **2001**, *123*, 11372-11375.
- 58.Hudnall, T. W.; Gabbai, F. P., *J. Am. Chem. Soc.* **2007**, *129*, 11978-11986.
- 59.Mark, J. E.; Allcock, H. R.; West, R., *Inorganic Polymers*. Oxford University Press: Oxford, 2004.
- 60.Manners, I., *Angew. Chem. Int. Ed.* **1996**, *35*, 1602-1621.
- 61.(a)Qin, Y.; Cheng, G.; Sundararaman, A.; Jäkle, F., *J. Am. Chem. Soc.* **2002**, *124*, 12672-12673, (b)Qin, Y.; Cheng, G.; Parab, K.; Achara, O.; Jäkle, F., *Macromolecules* **2004**, *37*, 7123-7131.
- 62.Qin, Y.; Sukul, V.; Pagakos, D.; Cui, C.; Jäkle, F., *Macromolecules* **2005**, *38*, 8987-8990.
- 63.(a)Shiomori, K.; Ivanov, A. E.; Galaev, I. Y.; Kawano, Y.; Mattiasson, B., *Macromol. Chem. Phys.* **2004**, *205*, 27-34, (b)Kataoka, K.; Miyazaki, H.; Okano, T.; Sakurai, Y.,

- Macromolecules* **1994**, *27*, 1061-2, (c)Kikuchi, A.; Suzuki, K.; Okabayashi, O.; Hoshino, H.; Kataoka, K.; Sakurai, Y.; Okano, T., *Analytical Chemistry* **1996**, *68*, 823-8.
- 64.(a)Kanazawa, H.; Kashiwase, Y.; Yamamoto, K.; Matsushima, Y.; Kikuchi, A.; Sakurai, Y.; Okano, T., *Analytical Chemistry* **1997**, *69*, 823-830, (b)Yakushiji, T.; Sakai, K.; Kikuchi, A.; Aoyagi, T.; Sakurai, Y.; Okano, T., *Analytical Chemistry* **1999**, *71*, 1125-1130.
- 65.Cambre, J. N.; Roy, D.; Gondi, S. R.; Sumerlin, B. S., *J. Am. Chem. Soc.* **2007**, *129*, 10348-10349.
- 66.Roy, D.; Cambre, J. N.; Sumerlin, B. S., *Chem. Commun.* **2008**, 2477-2479.
- 67.Roy, D.; Cambre, J. N.; Sumerlin, B. S., *Chem. Commun.* **2009**, 2106-2108.
- 68.Kim, K. T.; Cornelissen, J. J. L. M.; Nolte, R. J. M.; van Hest, J. C. M., *Adv. Mater.* **2009**, *21*, 2787-2791.
- 69.(a)Dai, J.; Ober, C. K.; Wang, L.; Cerrina, F.; Nealey, P. F. Proceedings of the SPIE, Fedynyshyn, T. H., Ed. 4690, 1193-1202,2002, (b)Dai, J.; Ober, C. K. Proceedings of the SPIE, Sturtevant, J. L., Ed. 5376, 508-516,2004.
- 70.Chen, W.; Mehta, S. C.; Lu, D. R., *Advanced Drug Delivery Reviews* **1997**, *26*, 231-247.
- 71.Simon, Y. C.; Ohm, C.; Zimny, M. J.; Coughlin, E. B., *Macromolecules* **2007**, *40*, 5628-5630.
- 72.Malenfant, P. R. L.; Wan, J. L.; Taylor, S. T.; Manoharan, M., *Nature Nanotechnol.* **2007**, *2*, 43-46.
- 73.Nagai, A.; Miyake, J.; Kokado, K.; Nagata, Y.; Chujo, Y., *Journal of the American Chemical Society* **2008**, *130*, 15276-15278.
- 74.Zhang, G.; Fiore, G. L.; St. Clair, T. L.; Fraser, C. L., *Macromolecules* **2009**, *42*, 3162-3169.

# Chapter B. Synthesis of Organoboronium-functionalized Polystyrene Homopolymers and Amphiphilic Block Copolymers

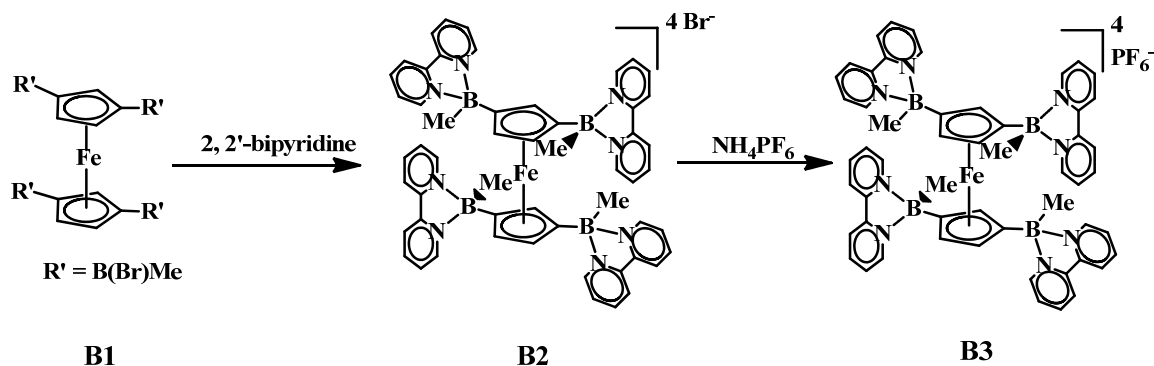
## B.1 Introduction

Organoboron cations, as outlined in a recent review by Piers,<sup>75</sup> are a promising class of compounds that are receiving increasing interest due to their potential use, for example, as alternatives to ionic liquids based on quaternary ammonium salts (pyridinium, imidazolium, etc.),<sup>76</sup> as multi-step redox-active materials,<sup>77</sup> and as disinfectants.<sup>78</sup> While different synthetic routes for their preparation are available, a straightforward approach is the reaction of diorganoboron halides  $R_2BX$  with chelating ligands such as 2,2'-bipyridine. These effectively replace the halide substituent on boron thereby giving rise to the desired cations  $[R_2B(\text{bipy})]X$ , in which boron is tetracoordinate and thus electronically saturate<sup>77a, 77c, d, 79</sup> The products usually enjoy exceptionally high stability if chelating ligands are employed and they are soluble in common polar organic solvents and even in protic media.<sup>79d</sup>

Several aspects of the chemistry of boronium cations could prove highly beneficial for the preparation of functional polymeric materials. First, cation formation occurs under very mild conditions (RT) and the products are typically formed in essentially quantitative yields. In this respect, the formation of boronium cations resembles the

broadly applied “click chemistry,”<sup>80</sup> without the need for any catalyst. Secondly, many derivatives of 2,2'-bipyridine and related chelate ligands<sup>81</sup> are commercially available and a plethora of methods allow for further functionalization. Similarly, the organic substituents on boron can easily be varied, thereby providing for additional tunability.

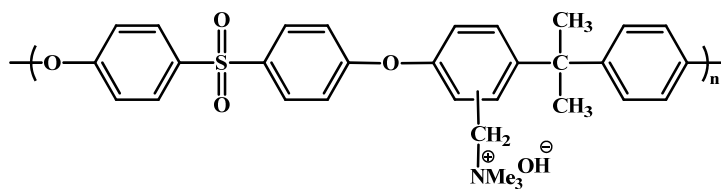
For example, Wagner and coworkers have synthesized a variety of mono- and multiply boronium substituted ferrocene compounds with exceptional multistep redox processes. One representative synthesis of these compounds is exemplified in Scheme B1. A ferrocene derivative (**B2**) with four boronium functional groups was synthesized by reaction of 1,1',3,3'-Fe[C<sub>5</sub>H<sub>3</sub>(BMeBr)<sub>2</sub>][C<sub>5</sub>H<sub>4</sub>(BMeBr)] (**B1**) with 2,2'-bipyridine (bipy). The bromide salt (**B2**) was in-situ converted to the PF<sub>6</sub> salt (**B3**) by ion exchange upon treatment with NH<sub>4</sub>PF<sub>6</sub>.



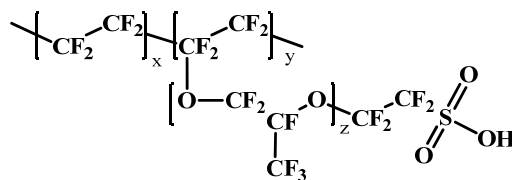
**Scheme B1.** Synthesis of ferrocenylboronium salts **B2** and **B3**.

Compound **B3** showed an intense purple color. UV/Vis analysis and ESR spectroscopy indicated that the observed color is primarily due to charge transfer (CT) interactions between the ferrocene unit and the electron-poor B(Me)bipy substituents. Additionally, electrochemical studies performed on compound **B3** revealed the formation of three step redox systems capable of storing up to nine electrons.

Among polymers with cationic functionalities, ammonium-functionalized polymers have been widely studied. For example, to avoid expensive noble metal catalysts such as platinum predominantly employed in the current fuel cells using Nafion as the membrane, Zhuang<sup>82</sup> and coworkers recently reported a polymeric alkaline electrolyte as membrane material in fuel cells employing a quaternary ammonium polysulphone (QAPS) polymer (**B4**) (Figure B1). **B4** is hydroxide ion conductive and able to work in the absence of a strongly acidic environment which is critical for the widely used Nafion (**B5**) membrane, such that nonprecious metals can be used as the catalysts. Other recent applications include their use in nanofiltration membranes,<sup>83</sup> smart surfaces with switchable wettability,<sup>84</sup> and antimicrobial surfaces,<sup>85</sup> just to name a few.

**B4**

a)

**B5**

b)

**Figure B1.** a) The quaternary ammonium polysulphone (QAPS) polymer (**B4**) is hydroxide ion conductive; b) the Nafion polymer (**B5**) is proton conductive requiring low pH environment.

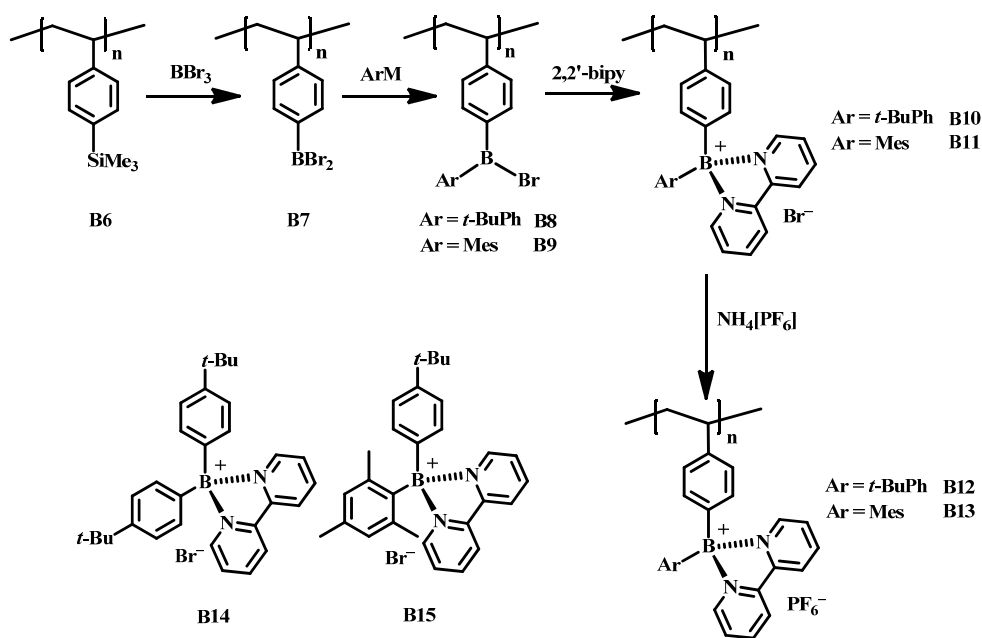
However, other polycations are comparatively rare. The development of boronium-functionalized polymers is expected to lead to new materials with useful properties such as antibacterial activity<sup>78, 85</sup> or neutron shielding behavior based on the well-known large neutron cross section of the <sup>10</sup>B nucleus.<sup>86</sup>

## B.2 Organoboronium-Functionalized Polystyrenes

Note: This section is adapted from a published paper.<sup>87</sup>

### B.2.1 Synthesis of Organoboronium-Functionalized Polystyrenes

The attachment of dipyridylboronium moieties to a polymeric framework can ultimately be achieved either by treatment of a suitable bipy-functionalized polymer with an organoboron halide or by reaction of an organoboron-functionalized polymer with bipy derivatives. Demonstrated here is the facile formation of boronium-cation functionalized polymeric materials from boron polymer precursors.



**Scheme B2.** Synthesis of "boronium-type" polyelectrolytes (**B10-B13**) and molecular model systems (**B14** & **B15**).  $\text{ArM} = (t\text{-BuPh})\text{SnMe}_3$ ,  $\text{MesCu}$ ;  $\text{Mes} = 2,4,6\text{-trimethylphenyl}$ ,  $2,2'\text{-bipy} = 2,2'\text{-bipyridine}$ ,  $t\text{-BuPh} = 4\text{-}t\text{-butylphenyl}$ .

The trimethylsilyl groups of poly(4-trimethylsilylstyrene) (**B6**) were exchanged with boron tribromide resulting in quantitative formation of the boron-functionalized

polymer PSBBr<sub>2</sub> (**B7**). Using highly selective organometallic transformations, one of the bromine substituents of each boryl group was replaced with an organic group as illustrated in Scheme B2. Treatment of **B7** with one equivalent of *t*-butylphenyl trimethyltin produces the polymer **B8** containing reactive -BBr(*t*-BuPh) pendant groups. Similarly, reaction with mesityl copper<sup>88</sup> produces a polymer, **B9**, that is decorated with -B(Br)Mes (mesityl = 2,4,6-trimethylphenyl) functional groups. These polymers are obtained with excellent selectivity for the mono-substitution product as shown by multinuclear NMR spectroscopy and further confirmed by comparison with the results for the respective molecular system based on *t*-BuC<sub>6</sub>H<sub>4</sub>BBr<sub>2</sub>. In a second step, the remaining B-Br functionalities were then replaced with 2,2'-bipyridine, giving rise to the cationic polymers, **B10** and **B11** (Ar = *t*-BuPh, Mes), which precipitated from the reaction solution in CH<sub>2</sub>Cl<sub>2</sub>. The products were conveniently purified by dialysis in methanol and isolated as light yellow powdery materials by precipitation into ether.

### B.2.2 Characterization of Organoboronium-Functionalized Polystyrenes

Successful preparation of the boronium salts is evident from a distinct upfield shift in the <sup>11</sup>B NMR spectra as a result of conversion of the tricoordinate borane to tetracoordinate boronium moieties. The <sup>11</sup>B NMR spectra of **B10** and **B11** show one single peak at ca. 4 ppm, which is similar to the chemical shift of 8 ppm for the

molecular models **B14** and **B15** (Figure B3). The slight upfield shift and sharpening of the signal of the polymer may indicate somewhat stronger binding of bipy, but other factors may also contribute and, indeed, similar shielding effects have been previously observed for tricoordinate organoboron polymers.<sup>89</sup> In the  $^1\text{H}$  NMR spectra in DMSO- $d_6$ , several broad resonances are observed in the range from 8.0 to 9.2 ppm, which can be confidently assigned to the boron-bound bipyridyl moieties by comparison to the molecular compounds (Figure B2). Specifically, the signal at ca. 9.2 ppm is characteristic of the 3,3'-protons of the complexed bipy moieties in DMSO- $d_6$ .<sup>3</sup> Integration of the aromatic region relative to the aliphatic resonances ( $t\text{-Bu}$ , Me groups) is consistent with a 1:1 ratio of bipy: $t\text{-buylphenyl/mesityl}$ , confirming quantitative attachment of bipy to the boron sites.

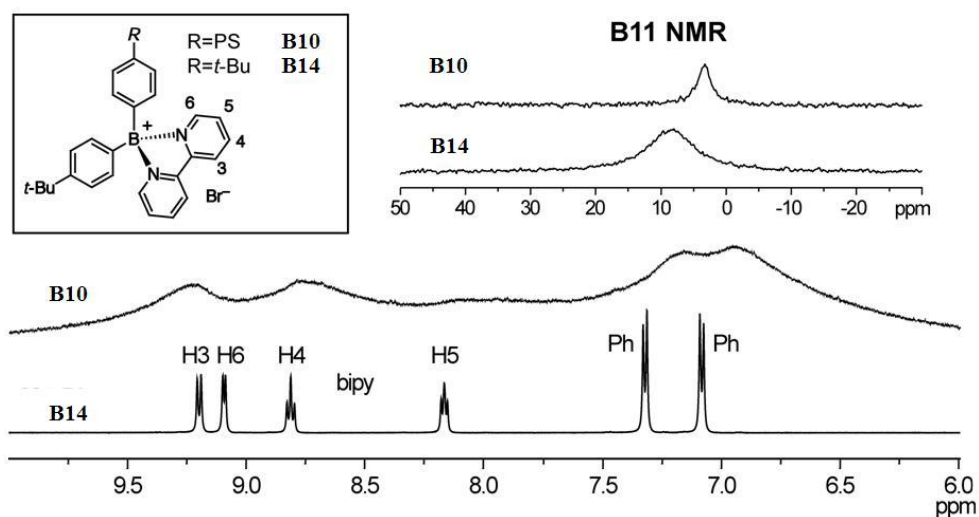


**Figure B2.** Comparison of the  $^1\text{H}$  and  $^{11}\text{B}$  NMR spectra of **B10** with those of the molecular species **B14** in DMSO- $d_6$  ( $\text{Br}^-$  counterion).

The new boronium polyelectrolytes were further studied by gel permeation chromatography (GPC) in DMF containing 20 mM  $\text{NH}_4[\text{PF}_6]$ . Both polymers eluted quite well from the columns under these conditions, and the traces showed monomodal profiles with only a slight broadening at higher elution times, which is likely due to a small extent of column interactions (Figure B3). Analysis relative to narrow PS standards gave considerably higher molecular weights in comparison to the silylated precursor polymer **B6** and the calculated degree of polymerization ( $DP_n$ ) was found to be in the expected range (Table B1).

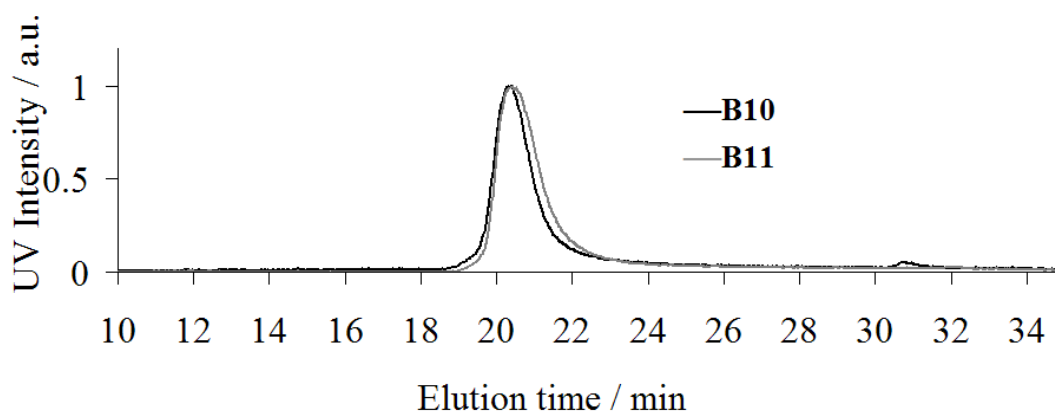


**Figure B3.** Representative GPC-UV traces for the boronium-functionalized polymers (recorded in DMF/20mM  $\text{NH}_4[\text{PF}_6]$  at 60 °C).

**Table B1.** GPC-UV results and yields for organoboronium polymers (DMF/20mM NH<sub>4</sub>[PF<sub>6</sub>] at 60 °C, polystyrene standards)

	$M_n (\times 10^3)^a$	$M_w (\times 10^3)^a$	$PDI^a$	$DP_n$	$Yield (\%)^b$
<b>B6</b>	15.4	17.7	1.15	87	
<b>B10</b>	43.7	56.1	1.28	80	79
<b>B11</b>	42.2	51.5	1.22	79	71

[a] Based on GPC-UV detection (*vs* PS) in DMF/20mM NH<sub>4</sub>[PF<sub>6</sub>] at 60 °C and for the silylated precursor polymer **B6** in THF at 35 °C using styragel columns (Polymer Laboratories)<sup>61a</sup>; the [PF<sub>6</sub>]<sup>-</sup> counterions are included in the calculations. [b] Isolated yield of bromide salt.

These data confirm that the polymer substitution reactions occur with excellent selectivity for the boronium cation formation and without any sign of crosslinking or degradation processes.

The product composition was also examined by elemental analysis of the [PF<sub>6</sub>]<sup>-</sup> derivatives, which were obtained by precipitation of the boronium polymers into an aqueous NH<sub>4</sub>[PF<sub>6</sub>] solution. For both polymers elemental analyses are consistent with the proposed structure.

### B.3 Synthesis and Characterization of Organoboronium Amphiphilic Block

#### Copolymers

Note: this section is adapted from a published paper.<sup>90</sup>

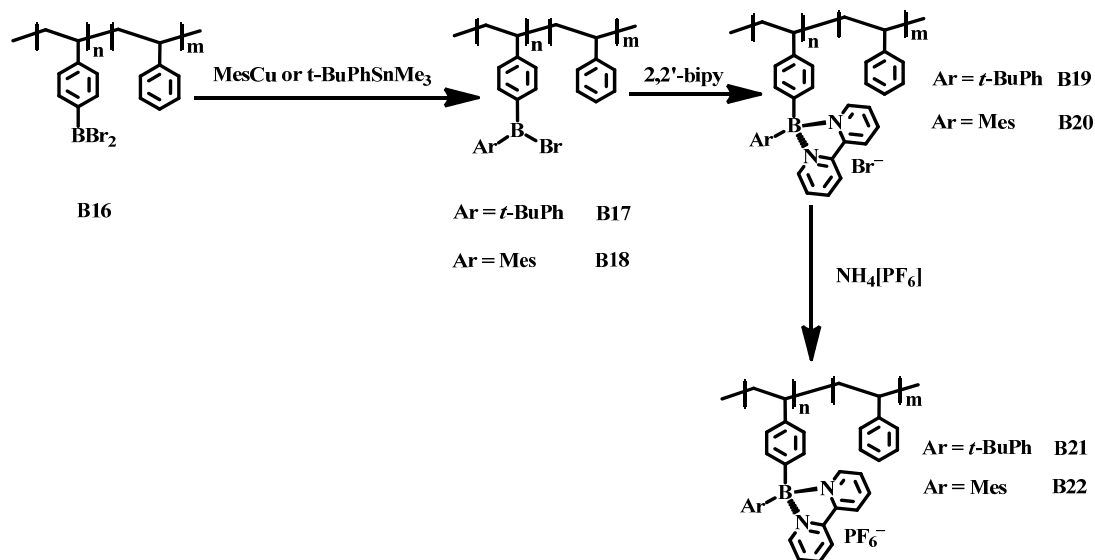
The development of amphiphilic block-copolymers,<sup>91</sup> which are well-known to form unusual self-assembled structures in solution and in bulk, with organoboronium moieties could offer a facile entry to boron-based nanomaterials.<sup>62, 65, 71-72, 92</sup>

As shown above, organoboronium polyelectrolytes enjoy good stability and are well soluble in common polar organic solvents such as alcohols, DMF, DMSO, acetonitrile, etc.<sup>79d</sup> We decided to take advantage of this facile change in polarity of the organoboron polymer upon boronium cation formation for the developed of a new class of amphiphilic organometallic block copolymers.<sup>93</sup> We demonstrate here the formation of the first boronium-cation functionalized block copolymers from organoborane-substituted precursors. Studies on the self-assembly of these novel amphiphilic block copolymers in solvents that selectively dissolve one of the constituent copolymer components are also presented.

### **B.3.1 Synthesis of Organoboronium Amphiphilic Block Copolymers**

The block copolymer poly(4-dibromoborylstyrene)-*block*-polystyrene (**B16**) was prepared by ATRP<sup>38</sup> of 4-trimethylsilylstyrene, followed by chain extension with styrene and subsequent exchange of the trimethylsilyl groups with BBr<sub>3</sub> as reported previously.<sup>61-62</sup> Using highly selective organometallic transformations, we then replaced one of the bromine substituents of each boryl group with an organic group (Scheme B3). Treatment of **B16** with one equivalent of *t*-butylphenyl trimethyltin (4-*t*-BuC<sub>6</sub>H<sub>4</sub>SnMe<sub>3</sub>)

produces the polymer **B17** containing reactive  $-B(t\text{-BuPh})\text{Br}$  pendant groups. Similarly, reaction with mesityl copper produces a polymer, **B18**, that features  $-B(\text{Mes})\text{Br}$  (mesityl = 2,4,6-trimethylphenyl) functional groups. The remaining B-Br functionalities were then replaced with 2,2'-bipyridine to give the cationic block copolymers **B19** and **B20**, respectively, which precipitated from the reaction solution in  $\text{CH}_2\text{Cl}_2$ . The products were conveniently purified by dialysis in methanol and isolated as light yellow powdery materials by precipitation into ether or hexanes. Exchange of the bromide counterion for  $\text{PF}_6^-$  was achieved by addition of  $\text{NH}_4[\text{PF}_6]$  to a solution of the polymer in a mixture of MeOH and acetone, followed by precipitation of the  $\text{PF}_6^-$  salts, **B21** and **B22**, by addition of distilled water.



**Scheme B3.** Synthesis of Boronium-Functionalized Amphiphilic Block Copolymers;

Mes = 2,4,6-trimethylphenyl,  $t\text{-BuPh}$  = 4- $t$ -butylphenyl, 2,2'-bipy = 2,2'-bipyridine.

### B.3.2 Characterization of Organoboronium Amphiphilic Block Copolymers

Successful attachment of the boronium groups was evident from a distinct upfield shift in the  $^{11}\text{B}$  NMR spectra as a result of conversion of the tricoordinate borane to tetracoordinate boronium moieties. The  $^{11}\text{B}$  NMR spectra of **B19** and **B20** show one single peak at ca. 4 ppm, which is similar to the chemical shift of the respective homopolymers **B10** and **B11**<sup>87</sup> (Figure B4).

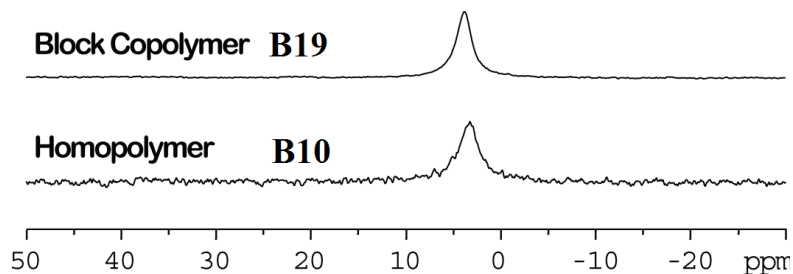


**Figure B4.**  $^{11}\text{B}$  NMR spectra of block copolymer **B19** and homopolymer **B10**.

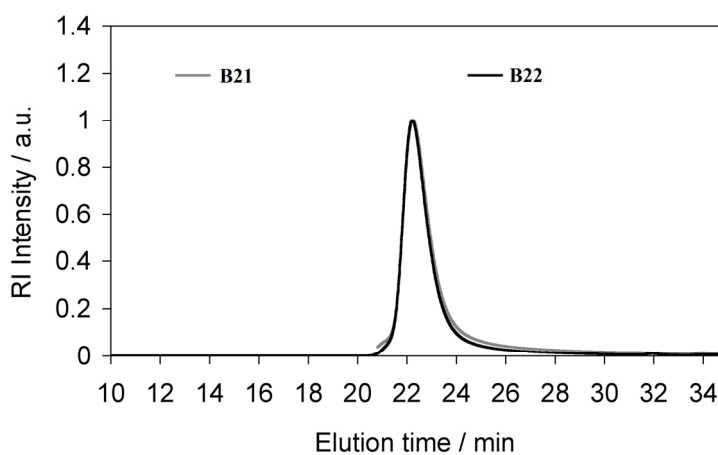


**Figure B5.** GPC traces for boronium-functionalized block copolymers **B21** and **B22**

(recorded in DMF/20mM  $\text{NH}_4[\text{PF}_6]$  at 60 °C).

The molecular weight was determined by GPC in DMF, which serves as a common solvent for both blocks (Figure B5, Table B2). With DMF containing 20 mM  $\text{NH}_4[\text{PF}_6]$ , both polymers eluted well from the columns and, as expected, monomodal distributions were observed with appreciably higher MWs than for the silylated precursor block copolymer relative to PS standards. The observation that the MW changes only moderately is consistent with the short functional boron block employed (styrene:4-trimethylsilylstyrene = 120:33). The product composition was also examined by elemental analysis of the  $\text{PF}_6^-$  derivatives, which were obtained as light yellow solid materials upon addition of water to a mixture of the boronium polymer and  $\text{NH}_4[\text{PF}_6]$ . For both block copolymers elemental analyses were in reasonably good agreement with the proposed polymer structure.

**Table B2.** GPC-RI results and yields for organoboronium polymers **B21** and **B22** (DMF/20mM  $\text{NH}_4[\text{PF}_6]$  at 60 °C, PS standards).

	$M_n$ ( $\times 10^3$ ) <sup>a</sup>	$M_w$ ( $\times 10^3$ ) <sup>a</sup>	$PDI$ <sup>a</sup>	$DP_n$	$Yield$ (%) <sup>b</sup>
PSSiMe <sub>3</sub> - <i>b</i> -PS ( <b>B23</b> )	18.3	19.5	1.07	33/120	
<b>B21</b>	20.2	24.3	1.21	17/120 <sup>c</sup>	64
<b>B22</b>	21.1	25.6	1.21	17/120 <sup>c</sup>	67

[a] Based on GPC-RI detection (vs PS) of the  $\text{PF}_6^-$  salts in DMF/20mM  $\text{NH}_4[\text{PF}_6]$  at 60 °C and the silylated precursor polymers in THF at 35 °C; the  $\text{PF}_6^-$  counterions are

included in the calculations. [b] Isolated yield of the bromide derivative. [c] Calculated assuming that the MW of the PS block remained constant.

### **B.3.3 Micellizations in Selective Solvents**

The new organometallic amphiphilic block copolymers were found to readily assemble into micellar structures in solution as shown by  $^1\text{H}$  NMR spectroscopy, DLS and transmission electron microscopy (TEM). The  $^1\text{H}$  NMR spectra of **B19** in different common and block-selective solvents are shown in Figure B6. In  $\text{CDCl}_3$  as a selective solvent for the polystyrene and in methanol- $d_4$  as a selective solvent for the boronium block, respectively, only the resonances for the individual blocks are observed. This indicates that larger aggregates are formed in both weakly and highly polar solvents, consistent with formation of regular and reverse micelles. In contrast, in a mixture of  $\text{CDCl}_3$  and methanol- $d_4$  signals of both constituent blocks are observed in the expected ratio based on the lengths of the two blocks.

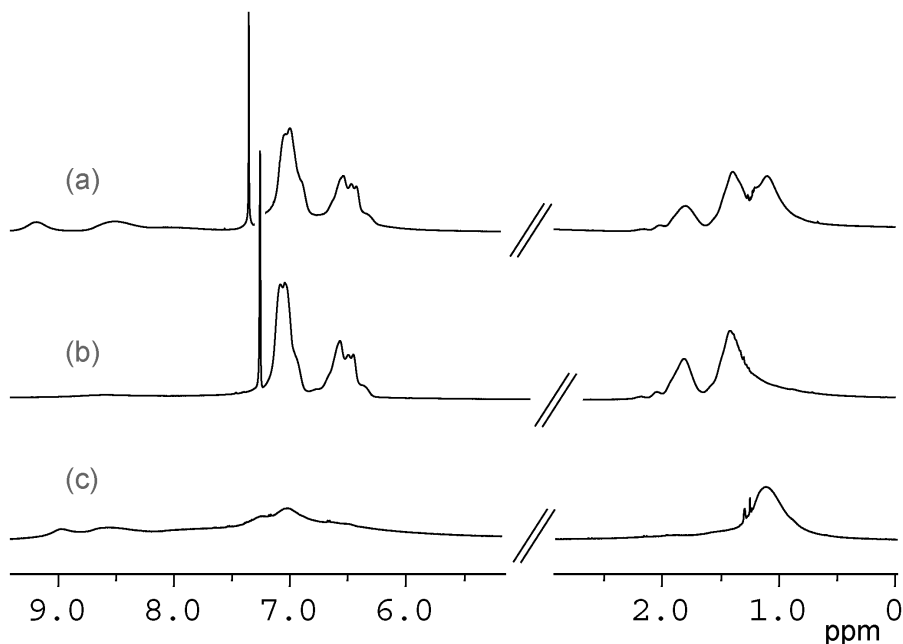
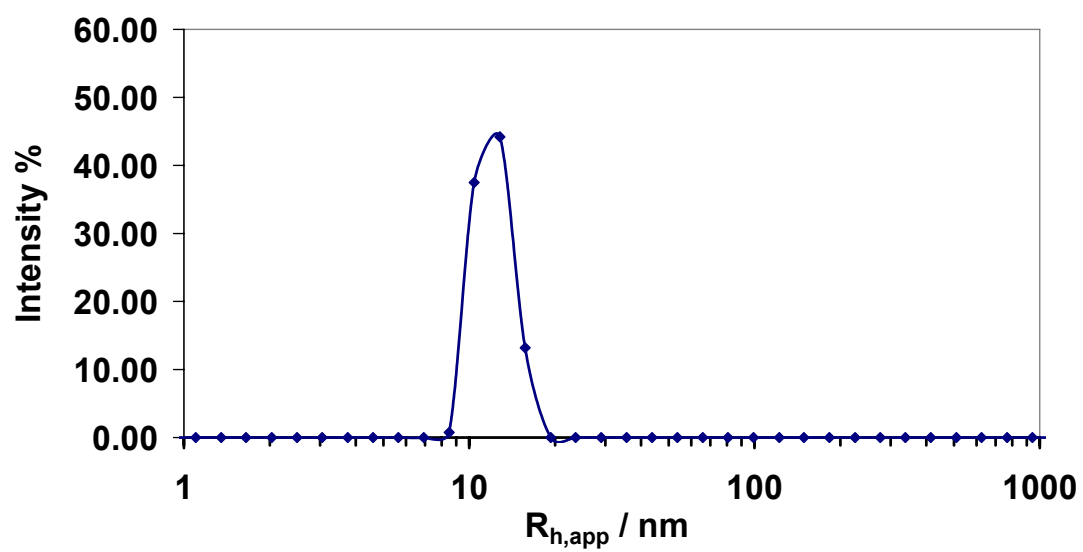


**Figure B6.** Comparison of the NMR spectra of **B19** in different solvents, (a)  $\text{CDCl}_3:\text{CD}_3\text{OD}=5:1$ ; (b)  $\text{CDCl}_3$  (PS selective solvent); (c)  $\text{CD}_3\text{OD}$  (boronium-selective solvent).

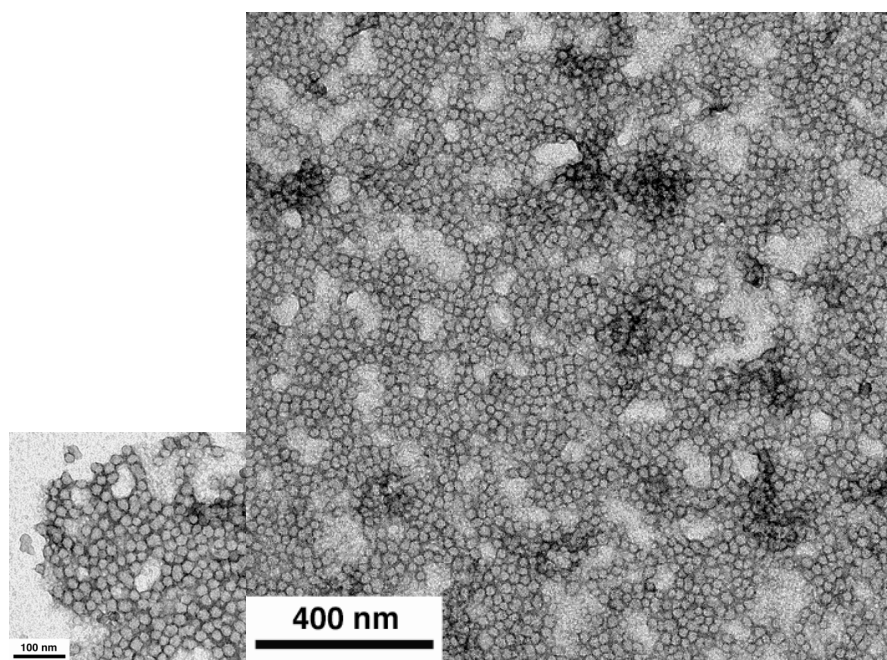
Formation of micellar aggregates in MeOH was further confirmed by DLS studies on **B19** and **B20**. The polymer solutions were prepared by direct dissolution in warm MeOH and filtered through a  $0.45\ \mu\text{m}$  filter before analysis of dynamic light scattering and TEM. The results from regularization analysis (DYNALS algorithm) suggest the presence of aggregates with an apparent average hydrodynamic radius ( $R_{h, \text{app}}$ ) of ca.  $12.2\pm 1.9\ \text{nm}$  (Figure B7(a)) for **B20**.

The same MeOH solution of **B20** was also subjected to transmission electron microscopy (TEM) (Figure B7(b)). One drop of the sample was deposited on a copper grid, which

was coated with a formvar film (30-60 nm) covered with a layer of carbon (5-10 nm). Excess solution was removed with a piece of filter paper. The samples were stained by deposition of a drop of aqueous uranyl acetate solution (1% w/w), and excess uranyl acetate solution was removed with a piece of filter paper after 2-3 minutes. The samples were kept to dry for 24 hours and subjected to TEM analysis without further treatment. The TEM data reveal the formation of very regular spherical micelles. The average diameter of  $22.8 \pm 2.9$  nm is in the same range as that determined from DLS and it is reasonable to assume that in MeOH as the solvent the PS block forms the core of these micellar structures as also suggested by the  $^1\text{H}$  NMR studies. The slightly smaller diameter by TEM may be due to drying effects, which are well documented in the literature. When micellization performed using toluene as a selective solvent for the polystyrene block, formation of reverse micelles was evident from DLS, which has shown mono-dispersed aggregations of slightly larger  $R_{h, \text{app}}$ . Reverse micelles were prepared by dissolution of the block copolymer in a mixture of methanol and toluene (1:1 in volume). The methanol was removed on a rotary evaporator and toluene was then added up to the original volume. The sample solution was filtered through a 0.45  $\mu\text{m}$  filter before studied by DLS.



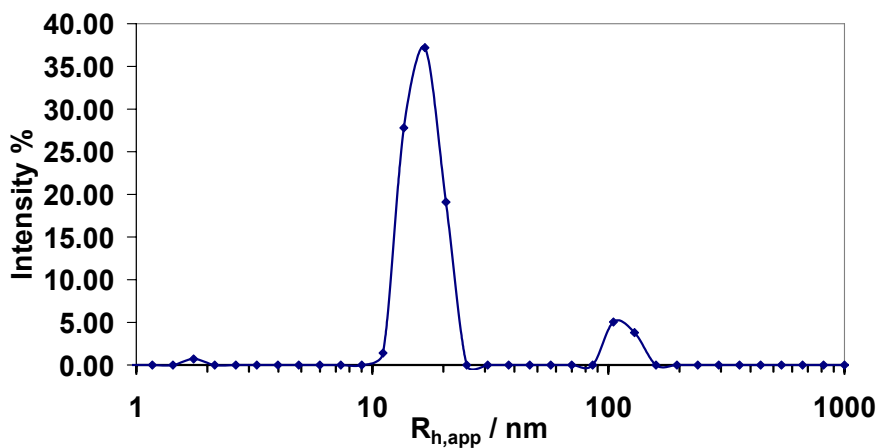
(a)



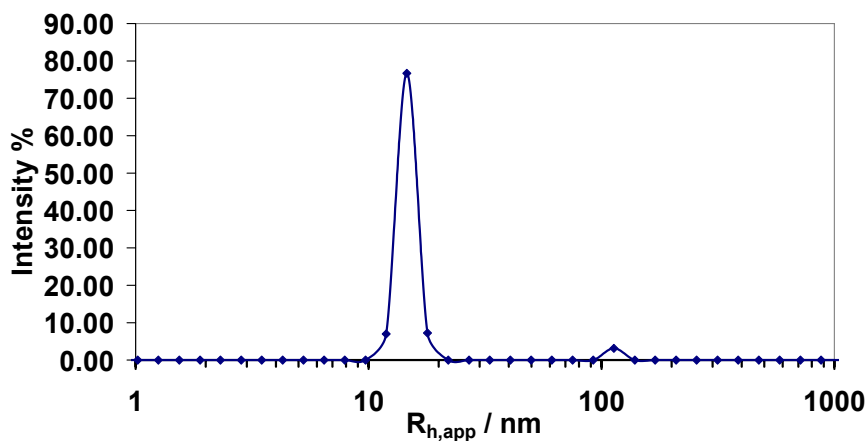
(b)

**Figure B7.** a) Size distribution histogram of a solution of **B20** in MeOH ( $1.4 \text{ mg mL}^{-1}$ ;  $n = 33$ ,  $m = 120$ ). b) TEM images of **B20** (micellization in MeOH; negative staining with uranyl acetate).

Similar results were obtained for the block copolymer **B19** except that a small fraction of larger aggregates was detected in the DLS analysis of its micellar solutions in methanol and toluene (Figure B8). The origin of these larger aggregates is still under investigation.



(a)



(b)

**Figure B8.** a) Size distribution histograms of a solution of **B19** in MeOH ( $0.2 \text{ mg mL}^{-1}$ ;  $n = 33$ ,  $m = 120$ ). b) Size distribution histogram of a solution of **B19** in toluene ( $0.5 \text{ mg mL}^{-1}$ ;  $n = 33$ ,  $m = 120$ ).

#### **B.4 Thermal Properties of Boronium Homo- and Diblock Copolymers**

A representative study of the thermal properties of the diblock copolymer **B19** and the homopolymer **B10** was performed by thermogravimetric analysis (TGA) under air (Figure B9). For **B19**, the first onset of degradation at 254.7 °C was assigned to the thermal decomposition of the boronium block according to the comparison to the homopolymer and the second one at 349.4 °C was assigned to the polystyrene block according to the literature.<sup>94</sup> There was another onset at 482.7 °C. Because this step was also observed for **B10**, it was reasonably ascribed to thermolysis of the boronium block. In both, the homopolymer and diblock copolymer samples, about 5.0% solvents consisting mainly of water as shown by NMR was fully removed at ca. 170 °C, a lower temperature than the first onset temperature. The particular batch of boronium bromide polymer used for TGA analysis was not fully dried. Taking this into account, the weight percentage of **B19** residue at the third onset temperature is 7.5% which is about half of the residue of the homopolymer **B10** which is measured to be 15.5% weight percent for the homopolymer **B10** at 468.8°C as its second onset temperature. Accordingly, **B19** consists of 48% weight percent of boronium block from TGA analysis which is roughly consistent with the composition of **B19** calculated from its formula (56% weight percentage of the boronium block).

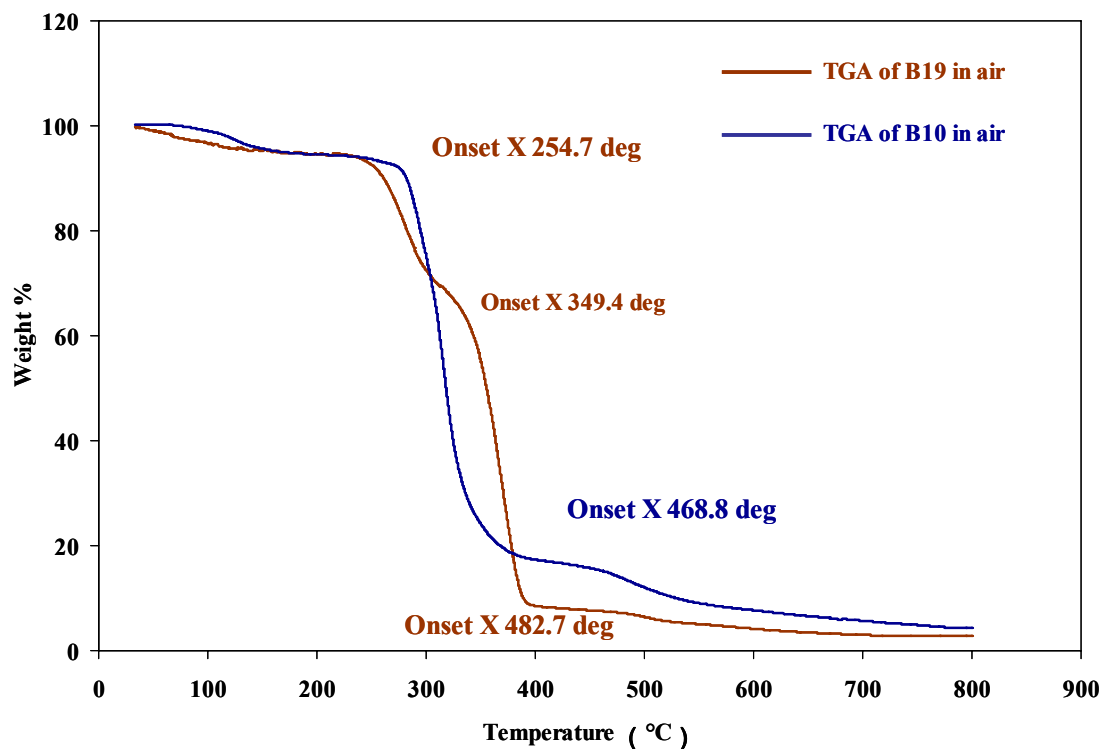


**Figure B9.** TGA results of **B10** and **B19** in air.

## B.5 Conclusions

We have developed a new class of cationic polyelectrolytes, in which the commonly used quaternary ammonium functionality was formally replaced with isoelectronic boronium moieties. The reactive poly(4-dibromoboryl)styrene (**B7**) was successfully used as a precursor, in which just one bromine substituent on each boryl group was selectively exchanged by reaction with mild organometallic aryl transfer reagents. The resulting  $-B(Ar)Br$  functional groups spontaneously reacted with 2,2'-bipyridine leading to cationic boronium moieties. Highly selective attachment to the PS backbone was confirmed by multinuclear NMR, elemental analysis, and molecular

weight determination by GPC in DMF/NH<sub>4</sub>[PF<sub>6</sub>] mixtures. Potential applications as antimicrobial coatings and possibly as neutron protection materials are anticipated for these organoboronium polyelectrolytes.

The reactive well-defined block copolymer poly(4-dibromoboryl)styrene-*block*-polystyrene (**B16**) has been successfully used as a precursor for the development of a novel class of organometallic block copolymers. Formation of the targeted amphiphilic block copolymers was confirmed by NMR and GPC analysis. The self-assembly into very regular micellar structures provides access to new boron-containing nano-structured materials.

## **B.6 Experimental Section**

### **B.6.1 Materials and General Methods**

The compounds 2,2'-bipyridine (bipy), NH<sub>4</sub>[PF<sub>6</sub>], and BBr<sub>3</sub> were purchased from Acros. Trimethyltin chloride was purchased from Strem Chemicals. All chemicals were used as received without further purification. Poly(4-trimethylsilylstyrene),<sup>61</sup> 4-*t*-butylphenyltrimethyl stannane,<sup>95</sup> and (CuMes)<sub>n</sub><sup>88,96</sup> were prepared according to literature procedures. Reactions and manipulations involving reactive boron species were carried out under an atmosphere of prepurified nitrogen using either Schlenk techniques or an inert-atmosphere glove box (Innovative Technologies). Ether solvents were distilled from

Na/benzophenone prior to use. Hydrocarbon and chlorinated solvents were purified using a solvent purification system (Innovative Technologies; alumina/copper columns for hydrocarbon solvents); chlorinated solvents and acetonitrile were distilled from CaH<sub>2</sub> and degassed via several freeze-pump-thaw cycles.

The 499.9 MHz <sup>1</sup>H, 125.7 MHz <sup>13</sup>C, 470.4 MHz <sup>19</sup>F, and 202.4 MHz <sup>31</sup>P NMR spectra were recorded on a Varian INOVA 500 MHz spectrometer. The 160.4 MHz <sup>11</sup>B NMR spectra were recorded with a boron-free probe using boron-free quartz NMR tubes. <sup>1</sup>H and <sup>13</sup>C NMR spectra were referenced internally to the solvent peaks, <sup>19</sup>F NMR spectra were referenced externally to  $\alpha,\alpha',\alpha''$ -trifluorotoluene (0.05% in C<sub>6</sub>D<sub>6</sub>;  $\delta = -63.73$ ), and the <sup>11</sup>B NMR spectra externally to BF<sub>3</sub>•Et<sub>2</sub>O ( $\delta = 0$ ) in C<sub>6</sub>D<sub>6</sub>. MALDI-TOF measurements were performed on an Applied Biosystems 4800 Proteomics Analyzer in reflectron (+)-mode with delayed extraction. Benzo[a]pyrene was used as the matrix (20 mg/mL in toluene) and the samples were dissolved in MeOH (10 mg/mL), mixed with the matrix in a 1:10 ratio, and then spotted on the wells of a sample plate. Peptides were used for calibration (Des-Arg-Bradykinin (904.4681), Angiotensin I (1296.6853), Glu-Fibrinopeptide B (1570.6774), ACTH (clip 1-17) (2093.0867), ACTH (clip 18-39) (2465.1989), ACTH (clip 7-38) (3657.9294) with  $\alpha$ -hydroxy-4-cyanocinnamic acid as the matrix. Elemental analyses were performed by Quantitative Technologies Inc. Whitehouse, NJ.

GPC analyses were performed in DMF / 20 mM  $\text{NH}_4[\text{PF}_6]$  (0.5 mL/min) using a Waters Breeze system equipped with a 717 plus auto sampler, a 1525 binary HPLC pump, a 2487 dual  $\lambda$  absorbance detector, and a 2414 refractive index detector. A series of Shodex Asahipak columns (GF-510 HQ, GF-310 HQ), which were kept in a column heater at 60 °C, were used for separation. The columns were calibrated with PS standards (Polymer Laboratories). Dynamic light scattering (DLS) studies were performed using the Wyatt Dawn EOS modified with a Wyatt QELS attachment. Data were collected using an avalanche photodiode and an optical fiber and processed with the Wyatt QELS software (regularization analysis with DYNALS algorithm, intensity-weighted average hydrodynamic radius). Transmission electron microscopy (TEM) studies were performed on a FEI Tecnai 12 electron microscope operated at 80 kV and images were collected using a GATAN 890 cooled-CCD with 4k by 4k chip. TGA measurements were performed on a Perkin Elmer Pyris 1 Thermogravimetric Analyzer at a scan rate of 20 °C / min and up to 800 °C.

**Caution!**  $\text{BBr}_3$  is toxic and corrosive and should be handled appropriately with great care. Fluorinated grease was used for ground glass joints in reactions involving boron tribromide.

## B.6.2 Synthesis of Organoboronium Polymers and Block Copolymers

### Synthesis of Poly(dipyridyl(*t*-butylphenyl)styrylboronium bromide) (B10)

A solution of poly(4-trimethylsilylstyrene) (**B6**) (0.50 g, 2.84 mmol SiMe<sub>3</sub>, M<sub>n</sub> = 15390, M<sub>w</sub> = 17680, PDI = 1.15) in CH<sub>2</sub>Cl<sub>2</sub> (10 mL) was added to a solution of BBr<sub>3</sub> (0.85 g, 3.39 mmol) in CH<sub>2</sub>Cl<sub>2</sub> (10 mL) in a glove box. The reaction mixture was stirred at room temperature for 12 h. A solution of 1-trimethylstannyl-4-*t*-butylbenzene (1.30 g, 4.38 mmol) in CH<sub>2</sub>Cl<sub>2</sub> (30 mL) was slowly added. The reaction mixture was stirred for 4 h, and then all volatile components were removed under high vacuum. The white residue was redissolved in CH<sub>2</sub>Cl<sub>2</sub> (50 mL), and a solution of 2,2'-bipyridine (2.00 g, 12.8 mmol) in CH<sub>2</sub>Cl<sub>2</sub> (20 mL) was added dropwise. After stirring for 5 h, the mixture was dried under vacuum, redissolved in methanol (35 mL), dialyzed against methanol (regenerated cellulose membrane with 6000 to 8000 Dalton molecular weight cut-off), concentrated and precipitated into ether. The product was dried under high vacuum at 60 °C to give a light yellow solid. Yield: 1.08 g (79%). <sup>1</sup>H NMR (499.890 MHz, DMSO-d<sub>6</sub>) δ = 9.2, 8.7, 8.0 (v br, 8H, bipy-H), 7.1, 6.9 (br, 8H, styryl-H, Ph-H), 1.0 (br, 9H, *t*-Bu), backbone n.r.. <sup>11</sup>B NMR (160.385 MHz, DMSO-d<sub>6</sub>) δ = 3.4 (w<sub>1/2</sub> = 210 Hz).

### Conversion to Poly[dipyridyl(*t*-butylphenyl)styrylboronium hexafluorophosphate] (B12)

Poly(dipyridyl(*t*-butylphenyl)styrylboronium bromide) (**B10**) (0.30 g, 0.62 mmol boronium groups) in methanol (5 mL) was added to a solution of  $\text{NH}_4[\text{PF}_6]$  (0.30 g, 1.84 mmol) in  $\text{H}_2\text{O}$  (100 mL). The resulting suspension was stirred for 1 h at RT. A white solid was collected on a filter paper and then washed extensively with water. The product was dried under high vacuum at 60 °C. Yield: 0.27 g (80%).  $^1\text{H}$  NMR (499.890 MHz, acetonitrile- $d_3$ )  $\delta$  = 8.6, 8.1, 7.2, 6.9 (v br, 16H, aromatic H), 1.0 (br, 9H, *t*-Bu), backbone H n.r..  $^{13}\text{C}$  NMR (125.697 MHz, acetonitrile- $d_3$ )  $\delta$  = 152.7, 146.6, 144.2, 140, 133.8, 129 (v br), 126.6, 124.8 (aromatic C), 46-38 (backbone C), 35.2 ( $\text{Me}_3\text{C}$ ), 31.6 ( $\text{Me}_3\text{C}$ ).  $^{11}\text{B}$  NMR (160.385 MHz,  $\text{CD}_3\text{CN}$ )  $\delta$  = 3.6 (w1/2 = 210 Hz).  $^{19}\text{F}$  NMR (470.367 MHz,  $\text{CD}_3\text{CN}$ )  $\delta$  = -72.4 (d, 1JPF = 709 Hz,  $[\text{PF}_6]^-$ ).  $^{31}\text{P}$  NMR (202.394 MHz,  $\text{CD}_3\text{CN}$ )  $\delta$  = -144.7 (sept, 1JPF = 709 Hz,  $[\text{PF}_6]^-$ ). Elemental analysis for  $\{\text{C}_{28}\text{H}_{28}\text{BF}_6\text{N}_2\text{P}\}_n$ : calcd C 61.33, H 5.15, N 5.11; found C 61.70, H 5.33, N 4.98%.

### Synthesis of Poly(dipyridylmesitylstyrylboronium bromide) (**B11**)

A solution of poly(4-trimethylsilylstyrene) (**B6**) (1.00 g, 5.67 mmol  $\text{SiMe}_3$ ,  $M_n$  = 15390,  $M_w$  = 17680,  $PDI$  = 1.15 based on GPC-UV) in  $\text{CH}_2\text{Cl}_2$  (30 mL) was added to a solution of  $\text{BBr}_3$  (1.71 g, 6.83 mmol) in  $\text{CH}_2\text{Cl}_2$  (20 mL) in a glove box. The reaction mixture was stirred at room temperature for 24 h. Copper mesityl (1.60 g, 8.76 mmol) in  $\text{CH}_2\text{Cl}_2$  (20 mL) was added, and the mixture was kept stirring for 12 h. A yellow-orange precipitate

formed, which was removed by filtration through celite on a medium fritted funnel. A solution of 2,2'-dipyridyl (4.00 g, 25.6 mmol) in CH<sub>2</sub>Cl<sub>2</sub> (20 mL) was added drop-wise leading to a brownish suspension. After stirring for 12 h, the reaction mixture was poured into acetone (250 mL). The mixture was filtered to give an off-white solid, which was redissolved in methanol and dialyzed against methanol (Fisherbrand regenerated cellulose membrane with 6000 to 8000 Dalton molecular weight cut-off). The resulting solution was concentrated and precipitated into ether. The precipitate was collected on a filter paper and dried under high vacuum at 60 °C for 12 h to give the product as a light yellow solid. Yield: 1.88 g (71%). <sup>1</sup>H NMR (499.884 MHz, DMSO-d<sub>6</sub>) δ = 9.1, 8.8, 8.2 (very br, 8H, bipy-H), 7.0-6.0 (very br, 6H, styryl-H, Mes-H<sub>3,5</sub>), 2.4-0.8 (br, 12H, *p*-Me, *o*-Me, backbone H). <sup>13</sup>C NMR (125.699 MHz, DMSO-d<sub>6</sub>) δ = 144.6, 137.3, 133, 130.4, 126.7 (br, aromatic C), 26.1, 22.0, 20.5 (*p*-Me, *o*-Me), backbone C n.r.. <sup>11</sup>B NMR (160.386 MHz, methanol-d<sub>4</sub>) δ = 3.6 (w<sub>1/2</sub> = 300 Hz).

### **Conversion to Poly(dipyridylmesitylstyrylboronium hexafluorophosphate) (B13)**

Poly(dipyridylmesitylstyrylboronium bromide) (**B11**) (0.35 g, 0.75 mmol boronium groups) in methanol (5 mL) was added into NH<sub>4</sub>[PF<sub>6</sub>] (0.36 g, 2.2 mmol) in H<sub>2</sub>O (100 mL). The resulting suspension was stirred for 1 h at room temperature. A white solid was collected on a filter paper and then washed extensively with water followed by hexanes. The product was dried under high vacuum at 60 °C. Yield: 0.31 g (77%). <sup>1</sup>H NMR

(499.890 MHz, acetonitrile-d<sub>3</sub>)  $\delta$  = 8.6, 7.9, 7.3, 6.7, 5.9 (v br, aromatic H), 2.2-1.0 (br, *p*-Me, *o*-Me, backbone). <sup>13</sup>C NMR (125.697 MHz, acetonitrile-d<sub>3</sub>)  $\delta$  = 146.1, 144.9, 139.6, 134.2, 131.8, 130.5, 129.9, 125.0 (br, aromatic C), 46-40 (backbone C), 28-20 (v br, *p*-Me, *o*-Me). <sup>11</sup>B NMR (160.384 MHz, acetonitrile-d<sub>3</sub>)  $\delta$  = 4.7 ( $w_{1/2}$  = 520 Hz). <sup>19</sup>F NMR (470.367 MHz, acetonitrile-d<sub>3</sub>)  $\delta$  = -72.6 (d, <sup>1</sup>J<sub>PF</sub> = 708 Hz, [PF<sub>6</sub>]<sup>-</sup>). <sup>31</sup>P NMR (202.394 MHz, DMSO-d<sub>6</sub>)  $\delta$  = -144.2 (sept, <sup>1</sup>J<sub>PF</sub> = 709 Hz, [PF<sub>6</sub>]<sup>-</sup>). Elemental analysis for {C<sub>27</sub>H<sub>26</sub>BF<sub>6</sub>N<sub>2</sub>P}<sub>n</sub>: calcd C 60.70, H 4.90, N 5.24; found C 61.40, H 4.89, N 5.30%.

### **Synthesis of Poly[dipyridyl(*t*-butylphenyl)styrylboronium bromide] -*block*-polystyrene (B19)**

A solution of poly(4-trimethylsilylstyrene)-*block*-polystyrene (**B23**) ( $M_n$  = 18270,  $M_w$  = 19480, PDI = 1.07, block ratio = 1:3.7; 0.50 g, 0.89 mmol SiMe<sub>3</sub>) in CH<sub>2</sub>Cl<sub>2</sub> (10 mL) was added to a solution of BBr<sub>3</sub> (0.27 g, 1.08 mmol) in CH<sub>2</sub>Cl<sub>2</sub> (10 mL). The reaction mixture was stirred at room temperature for 12 h. A solution of 1-trimethylstannyl-4-*t*-butylbenzene (0.23 g, 1.47 mmol) in CH<sub>2</sub>Cl<sub>2</sub> (15 mL) was slowly added into the reaction solution. The reaction solution was stirred for 3 h. The mixture was then kept under high vacuum to remove all volatile components. The white residue was redissolved in a mixture of CH<sub>2</sub>Cl<sub>2</sub> and CH<sub>3</sub>CN (1:1, 50 mL). A solution of 2,2'-bipyridine (1.0 g, 6.4 mmol) in CH<sub>3</sub>CN (20 mL) was added into the reaction solution drop-wise, and the resulting white suspension was stirred for 12 h. The suspension was treated with

methanol to give a clear yellow solution, which was then dialyzed against a mixture of methanol and acetone (1:1, 3 × 500 mL). The resulting solution was filtered through celite on a fritted funnel, concentrated and then precipitated into ether. The product was collected by filtration and dried under high vacuum at 70 °C to give a light yellow solid. Yield: 0.52 g (67%). <sup>1</sup>H NMR (499.884 MHz, DMSO-d<sub>6</sub>) δ = 9.2, 8.7, 7.9 (very br, bipy-H), 6.99, 6.59 (styryl-H, Ph-H), 2.5-1.2 (br, backbone H), 1.06 (br, *t*-Bu). <sup>11</sup>B NMR (160.386 MHz, methanol-d<sub>4</sub>:CDCl<sub>3</sub> 1:1) δ = 4 (*w*<sub>1/2</sub> = 530 Hz). DLS (MeOH): *R*<sub>h, app</sub> = 16.4±2.8 nm and minor component at 116±13.7 nm; cumulant analysis: *R*<sub>h, app</sub> = 17.0 (0.03) nm.

**Conversion to Poly[dipyridyl(*t*-butylphenyl)styrylboronium hexafluorophosphate]-*block*-polystyrene (B21)**

**B19** (block ratio = 1:3.7; 110 mg, 0.13 mmol dipyridyl(*t*-butylphenyl)styryl boronium bromide) was converted to the PF<sub>6</sub><sup>-</sup> salt in analogy to the procedure for the mesityl derivative to give a light yellow solid. Yield for **B21**: 75 mg (65%). <sup>1</sup>H NMR (499.976 MHz, DMSO/acetone-d<sub>6</sub> = 1:1) δ = 9.1, 8.7, 8.0 (v br, bipy-H), 7.1, 6.6 (styryl-H), 2.4-1.0 (br, m, backbone H), 1.0 (br, *t*-Bu). <sup>13</sup>C NMR (125.719 MHz, DMSO/acetone-d<sub>6</sub> = 1:1) δ = 151.3, 143.5 (br), 140.0 (br), 133.0, 129.0 (br, overlapping with styryl C), 125.6 (overlapping with styryl C), 124.5 (boronium aromatic), 145.8, 128.5, 127.9, 126.2 (styryl), 48-36 (backbone C), 34.6 (Me<sub>3</sub>C), 31.3 (Me<sub>3</sub>C). <sup>11</sup>B NMR (160.385 MHz,

acetone-d6/DMSO-d6 = 1:1)  $\delta = 4.2$  ( $w_{1/2} = 470$  Hz).  $^{19}\text{F}$  NMR (470.367 MHz, acetone-d6/DMSO-d6 = 1:1)  $\delta = -71.5$  (d,  $^1J_{\text{FP}} = 711$  Hz,  $\text{PF}_6^-$ ). GPC-RI (DMF / 20 mM  $\text{NH}_4[\text{PF}_6]$ , 60 °C):  $M_n = 21150$ ,  $M_w = 25560$ ,  $PDI = 1.21$ . Elemental analysis for the  $\{\text{C}_{28}\text{H}_{28}\text{BF}_6\text{N}_2\text{P}\}_{33}\{\text{C}_8\text{H}_8\}_{120}$ : calcd C 73.97, H 6.21, N 3.02; found C 73.47, H 6.26, N 2.92%.

### Synthesis of Poly(dipyridylmesitylstyrylboronium)-*block*-polystyrene (B20)

A solution of poly(4-trimethylsilylstyrene)-*block*-polystyrene (**B23**) ( $M_n = 18270$ ,  $M_w = 19480$ ,  $PDI = 1.07$ , block ratio = 1:3.7; 0.50 g, 0.89 mmol  $\text{SiMe}_3$ ) in  $\text{CH}_2\text{Cl}_2$  (10 mL) was added to a solution of  $\text{BBr}_3$  (0.27 g, 1.08 mmol) in  $\text{CH}_2\text{Cl}_2$  (10 mL). The reaction mixture was stirred at room temperature for 12 h. Copper mesityl (0.24 g, 1.31 mmol) in  $\text{CH}_2\text{Cl}_2$  (5 mL) was added, and the mixture was kept stirring for 12 h. A yellow-orange precipitate formed, which was removed by filtration through celite on a medium fritted funnel. Acetonitrile (5 mL) was slowly added to the filtrate, followed by addition of 2,2'-bipyridine (0.50 g, 3.20 mmol) in acetonitrile (10 mL). A brown suspension formed, which was stirred for 3 h. A small amount of methanol was added to fully dissolve the mixture, which was then dialyzed against methanol. The resulting light yellow solution was precipitated into hexanes to give a white powder, which was washed with a small amount of methanol and recovered by centrifugation. The product was dried under high vacuum at 60 °C. Yield: 0.43 g (64%).  $^1\text{H}$  NMR (499.884 MHz, DMSO-d6)  $\delta$

= 9.2, 8.8, 8.2 (v br, bipy-H), 7.0, 6.6 (v br, PS block, B-styryl, Mes-H3,5), 2.2-1.0 (br, backbone H, *o*-Me, *p*-Me).  $^{11}\text{B}$  NMR (160.383 MHz, DMSO- $d_6$ )  $\delta = 3.8$  ( $w_{1/2} = 260$  Hz).

DLS (MeOH):  $R_{h, \text{app}} = 12.2 \pm 1.9$  nm; cumulant analysis:  $R_{h, \text{app}} = 12.3$  (0.01) nm.

### **Conversion to Poly(dipyridylmesitylstyrylboronium hexafluorophosphate)-block-polystyrene (B22)**

**B22** (block ratio =1:3.7; 98 mg, 0.12 mmol dipyridylmesitylstyryl boronium bromide) was dissolved in a mixture of methanol (15 mL) and acetone (15 mL), and a solution of  $\text{NH}_4[\text{PF}_6]$  (0.20 g, 1.2 mmol) in acetone (10 mL) was added. The mixture was stirred for 1 h at room temperature and subsequently 50 mL of distilled water were added. A white solid was isolated from the resulting suspension by centrifugation. The solid was re-suspended in distilled water (50 mL) and kept stirring for 30 min. The final product was again isolated by centrifugation and dried under high vacuum at 50 °C for 24 h to give a very light yellow solid. Yield: 62 mg (59%).  $^1\text{H}$  NMR (499.884 MHz, acetone- $d_6$ )  $\delta = 8.9, 8.1$  (v br, bipy-H), 7.1, 6.7 (v br, PS block, B-styryl, Mes-H3,5), 1.96, 1.60, 1.45 (br, backbone H, *o*-Me, *p*-Me).  $^{13}\text{C}$  NMR (125.696 MHz, acetone- $d_6$ )  $\delta = 145.1, 139.0, 135.8$  (br), 134.5 (br), 131.8, 130.5, 125.0 (v br, bipy block), 146.2, 129.0, 128.6, 126.7 (PS block), 48-38 (backbone C), 34-20 (*o*-Me), 21.0 (*p*-Me).  $^{11}\text{B}$  NMR (160.383 MHz, acetone- $d_6$ )  $\delta = 3.8$  ( $w_{1/2} = 1000$  Hz).  $^{19}\text{F}$  NMR (470.367 MHz, acetone- $d_6$ )  $\delta = -72.0$  (d,  $^1J_{\text{FP}} = 709$  Hz,  $\text{PF}_6^-$ ). GPC-RI (DMF / 20 mM  $\text{NH}_4[\text{PF}_6]$ , 60 °C):  $M_n = 20160$ ,  $M_w =$

24300,  $PDI = 1.21$ . Elemental analysis for the  $\{C_{27}H_{26}BF_6N_2P\}_{33}\{C_8H_{81}20\}$ : calcd C 73.79, H 6.08, N 3.07; found C 74.94, H 6.11, N 2.42%.

### B.6.3 Synthesis of Model Compounds

#### Synthesis of Di(*t*-butylphenyl)dipyridylboronium Bromide (B12)

Under nitrogen protection, a solution of 1-trimethylstannyl-4-*t*-butylbenzene (0.26 g, 0.88 mmol) in  $CH_2Cl_2$  (30 mL) was slowly added to a solution of 4-dibromoboryl-1-*t*-butylbenzene (0.25 g, 0.82 mmol) in  $CH_2Cl_2$  (30 mL). The reaction mixture was stirred for 2 h. The mixture was dried under high vacuum at room temperature. The white residue was redissolved in  $CH_3CN$  (20 mL) and the resulting solution was added dropwise into a solution of 2,2'-dipyridyl (0.25 g, 1.60 mmol) in  $CH_3CN$  (20 mL). A white precipitate formed immediately. After stirring for 1 h, the supernatant was removed and the white crystalline residue was washed three times with cold acetonitrile (2 mL). A second crop of product was obtained from the supernatant and acetonitrile extracts upon concentration and precipitation into ether. The white solids were dried under high vacuum at 60 °C. Yield: 0.41 g (97%).  $^1H$  NMR (499.895 MHz, DMSO- $d_6$ )  $\delta = 9.20$  (d,  $^3J = 8.0$  Hz, 2H, bipy-H3,3'), 9.09 (d,  $^3J = 5.5$  Hz, 2H, bipy-H6,6'), 8.79 (pst,  $^3J = 7.7$  Hz, 2H, bipy-H4,4'), 8.17 (pst,  $^3J = 6.7$  Hz, 2H, bipy-H5,5'), 7.32 (d,  $^3J = 8.0$  Hz, 4H, tBuPh-H2,6 / tBuPh-H3,5), 7.08 (d,  $^3J = 8.0$  Hz, 4H, tBuPh-H2,6 / tBuPh-H3,5), 1.24 (s, 18H, *t*-Bu).  $^{13}C$  NMR (125.689 MHz,

DMSO-d<sub>6</sub>)  $\delta$  = 150.4 (tBuPh-C4), 145.5 (bipy-C2,2'), 145.0, 144.1 (bipy-C4,4',6,6'), 139.2 (tBuPh-C1), 132.4 (tBuPh-C2,6), 129.1 (bipy-C5,5'), 124.9 (Ph-C3,5), 123.7 (bipy-C3,3'), 34.2 (Me<sub>3</sub>C), 31.0 (Me<sub>3</sub>C). <sup>11</sup>B NMR (160.386 MHz, DMSO-d<sub>6</sub>)  $\delta$  = 8 ( $w_{1/2}$  = 1280 Hz). MALDI-TOF MS (+ reflectron mode): m/z (Da) = 433.2740 (calcd for [C<sub>30</sub>H<sub>34</sub>BN<sub>2</sub>]<sup>+</sup> 433.2815).

### Synthesis of Dipyridyl(*t*-butylphenyl)(mesityl)boronium Bromide (B13)

In a glove box, 4-dibromoboryl-1-*t*-butylbenzene (0.25 g, 0.82 mmol) in CH<sub>2</sub>Cl<sub>2</sub> (20 mL) was added to a solution of copper mesityl (1.66 g, 0.91 mmol) in CH<sub>2</sub>Cl<sub>2</sub> (20 mL), and the reaction mixture was stirred at room temperature for 1 h. An orange precipitate formed and the volume was reduced to ca. 2 mL. Hexanes (40 mL) were added and the mixture was stirred for 1 h. The solid was filtered off, and a colorless oil was obtained after evaporation of hexanes. The residue was redissolved in CH<sub>2</sub>Cl<sub>2</sub> (30 mL) and a solution of 2,2'-dipyridyl (0.32 g, 2.05 mmol) in CH<sub>2</sub>Cl<sub>2</sub> (10 mL) was added to give a clear yellow solution. After stirring for 1 h, the reaction mixture was concentrated and precipitated into hexanes to give a light yellow solid that was dried under high vacuum. Yield: 0.35 g (87%). <sup>1</sup>H NMR (499.896 MHz, DMSO-d<sub>6</sub>)  $\delta$  = 9.30 (d, <sup>3</sup>J = 8.0 Hz, 2H, bipy-H3,3'), 9.20 (d, <sup>3</sup>J = 6.0 Hz, 2H, bipy-H6,6'), 8.86 (pst, <sup>3</sup>J = 8.0 Hz, 4H, bipy-H4,4'), 8.25 (pst, <sup>3</sup>J = 7.5 Hz, 2H, bipy-H5,5'), 7.20, 6.90 (2 x d, <sup>3</sup>J = 8.5 Hz, 2 x 2H, tBuPh-H2,6 and tBuPh-H3,5), 6.77 (br s, 2H, mesityl-H3,5), 2.17 (s, 3H, *p*-Me),

1.48 (br s, 6H, *o*-Me), 1.17 (s, 9H, *t*-Bu).  $^{13}\text{C}$  NMR (125.707 MHz, DMSO- $d_6$ )  $\delta$  = 149.4 (tBuPh-C4), 145.1 (bipy-C4,4'), 144.9 (bipy-C2,2'), 144.3 (bipy-C6,6'), 144.1 (br, tBuPh-C1), 143.2 (br, Mes-C2,6), 137.3 (Mes-C4), 133.7 (br, Mes-C1), 130.4 (Mes-C3,5), 129.6 (bipy-C5,5'), 129.3, 125.1 (tBuPh-C2,6 / tBuPh-C3,5), 124.2 (bipy-3,3'), 34.0 ( $\text{Me}_3\text{C}$ ), 31.0 ( $\text{Me}_3\text{C}$ ), 24.1 (br, *o*-Me), 20.3 (*p*-Me).  $^{11}\text{B}$  NMR (160.386 MHz, DMSO- $d_6$ )  $\delta$  = 8 ( $w_{1/2}$  = 1520 Hz). MALDI-TOF MS (+ reflectron mode):  $m/z$  (Da) = 419.2555 (calcd for  $[\text{C}_{29}\text{H}_{32}\text{BN}_2]^+$  419.2658).

## B.7 References

1. Piers, W. E.; Bourke, S. C.; Conroy, K. D., *Angew. Chem. Int. Ed.* **2005**, *44*, 5016-5036.
2. Fox, P. A.; Griffin, S. T.; Reichert, W. M.; Salter, E. A.; Smith, A. B.; Tickell, M. D.; Wicker, B. F.; Cioffi, E. A.; Davis, J. H.; Rogers, R. D.; Wierzbicki, A., *Chem. Commun.* **2005**, 3679-3681.
3. (a) Biani, F. F. d.; Gmeinwieser, T.; Herdtweck, E.; Jäkle, F.; Laschi, F.; Wagner, M.; Zanello, P., *Organometallics* **1997**, *16*, 4776-4787, (b) Tonzola, C. J.; Alam, M. M.; Jenekhe, S. A., *Advanced Materials* **2002**, *14*, 1086-1090, (c) Ding, L.; Ma, K.; Dürner, G.; Bolte, M.; de Biani, F. F.; Zanello, P.; Wagner, M., *J. Chem. Soc., Dalton Trans.* **2002**, 1566-1573, (d) Scheibitz, M.; Heilmann, J. B.; Winter, R. F.; Bolte, M.; Bats, J. W.; Wagner, M., *Dalton Trans.* **2005**, 159-170.
4. Skvortsova, E. K.; Putyatina, T. I.; Mikhailov, B. M.; Dorokhov, V. A.; Shchegoleva, T. I.; Kamennov, N. A.; Limanov, V. E.; Starkov, A. V., *Trudy Tsentral'nogo Nauchno-Issledovatel'skogo Dezinfektsionnogo Instituta* **1967**, *18*, 154-156.
5. (a) Tonzola, C. J.; Alam, M. M.; Jenekhe, S. A., *Advanced Materials (Weinheim, Germany)* **2002**, *14*, 1086-1090, (b) Braunschweig, H.; Radacki, K.; Seeler, F.; Whittell, G. R., *Organometallics* **2006**, *25*, 4605-4610, (c) Hartmann, H., *Z. Naturforsch. B - Chem. Sci.* **2006**, *61*, 360-372, (d) Davis, L. H.; Madura, L. D., *Tetrahedron Lett.* **1996**, *37*, 2729-2730, (e) Jutzi, P.; Krato, B.; Hursthouse, M.; Howes, A. J., *Chem. Ber.* **1987**, *120*, 1091-8, (f) Braunschweig, H.; Kaupp, M.; Lambert, C.; Nowak, D.; Radacki, K.; Schinzel, S.; Uttinger, K., *Inorg. Chem.* **2008**, *47*, 7456-7458.

- 6.(a)Li, J.; Duan, M.; Zhang, L. H.; Jiang, X. H., *Prog. Chem.* **2007**, *19*, 1754-1760, (b)Nandivada, H.; Jiang, X. W.; Lahann, J., *Adv. Mater.* **2007**, *19*, 2197-2208, (c)Moses, J. E.; Moorhouse, A. D., *Chem. Soc. Rev.* **2007**, *36*, 1249-1262, (d)Gil, M. V.; Arevalo, M. J.; Lopez, O., *Synthesis-Stuttgart* **2007**, 1589-1620, (e)Binder, W. H.; Sachsenhofer, R., *Macromol. Rap. Comm.* **2007**, *28*, 15-54.
- 7.(a)Miyazaki, T.; Sugawara, M.; Danjo, H.; Imamoto, T., *Tetrahedron Lett.* **2004**, *45*, 9341-9344, (b)Yamamoto, Y.; Koizumi, T.; Katagiri, K.; Furuya, Y.; Danjo, H.; Imamoto, T.; Yamaguchi, K., *Org. Lett.* **2006**, *8*, 6103-6106, (c)Mlodzianowska, A.; Latos-Grayzyski, L.; Szterenber, L.; Stepien, M., *Inorg. Chem.* **2007**, *46*, 6950-6957, (d)Hodgkins, T. G.; Powell, D. R., *Inorg. Chem.* **1996**, *35*, 2140-2148.
- 8.Lu, S.; Pan, J.; Huang, A.; Zhuang, L.; Lu, J., *Proc. Natl. Acad. Sci. U. S. A.* **2008**, *105*, 20611-20614.
- 9.Li, X.; De Feyter, S.; Chen, D.; Aldea, S.; Vandezande, P.; Du Prez, F.; Vankelecom, I. F. J., *Chem. Mater.* **2008**, *20*, 3876-3883.
- 10.Lim, H. S.; Lee, S. G.; Lee, D. H.; Lee, D. Y.; Lee, S.; Cho, K., *Adv. Mater.* **2008**, *20*, 4438-4441.
- 11.Zhang, Z.; Cheng, G.; Carr, L. R.; Vaisocherova, H.; Chen, S.; Jiang, S., *Biomaterials* **2008**, *29*, 4719-4725.
- 12.(a)Sakurai, Y.; Sasaki, A.; Kobayashi, T., *Nuclear Instruments & Methods in Physics Research, Section A: Accelerators, Spectrometers, Detectors, and Associated Equipment* **2004**, *522*, 455-461, (b)Simon, Y. C.; Peterson, J. J.; Mangold, C.; Carter, K. R.; Coughlin, E. B., *Macromolecules* **2009**, *42*, 512-516.
- 13.Cui, C.; Jäkle, F., *Chem. Commun.* **2009**, 2744-2746
- 14.(a)Eriksson, H.; Håkansson, M., *Organometallics* **1997**, *16*, 4243-4244, (b)Sundaraman, A.; Jäkle, F., *J. Organomet. Chem.* **2003**, *681*, 134-142.
- 15.Parab, K.; Venkatasubbaiah, K.; Jäkle, F., *J. Am. Chem. Soc.* **2006**, *128*, 12879-12885.
- 16.Qin, Y.; Cheng, G.; Sundaraman, A.; Jäkle, F., *J. Am. Chem. Soc.* **2002**, *124*, 12672-12673.
- 17.Cui, C.; Bonder, E. M.; Jäkle, F., *Journal of Polymer Science Part A: Polymer Chemistry* **2009**, *47*, 6612-6618.
- 18.(a)Eisenberg, A.; Kim, J.-S., *Introduction to Ionomers*. Wiley Interscience: New York, 1998, (b)Bates, F. S., *Science* **1991**, *251*, 898-905, (c)Förster, S.; Antonietti, M., *Adv. Mater.* **1998**, *10*, 195-217.
- 19.(a)Iyengar, D. R.; Perutz, S. M.; Dai, C.-A.; Ober, C. K.; Kramer, E. J., *Macromolecules* **1996**, *29*, 1229-1234, (b)Dai, J.; Ober, C. K., *Proc. SPIE-Int. Soc. Opt. Eng.* **2004**, *5376 (Pt. 1, Advances in Resist Technology and Processing XXI)*, 508-516, (c)Qin, Y.; Sukul, V.; Pagakos, D.; Cui, C.; Jäkle, F., *Polym. Prepr.* **2005**, *46(2)*, 351-352, (d)Qin, Y.; Sukul, V.; Pagakos, D.; Cui, C.; Jäkle, F., *Macromolecules* **2005**, *38*, 8987-8990, (e)Cambre, J. N.; Roy, D.; Gondi, S. R.; Sumerlin, B. S., *J. Am. Chem.*

- Soc.* **2007**, *129*, 10348-10349, (f)Wei, X. L.; Carroll, P. J.; Sneddon, L. G., *Chem. Mater.* **2006**, *18*, 1113-1123, (g)Malenfant, P. R. L.; Wan, J. L.; Taylor, S. T.; Manoharan, M., *Nature Nanotechnol.* **2007**, *2*, 43-46, (h)Simon, Y. C.; Ohm, C.; Zimny, M. J.; Coughlin, E. B., *Macromolecules* **2007**, *40*, 5628-5630.
- 20.(a)Manners, I., *Angew. Chem., Int. Ed.* **2007**, *46*, 1565-1568, (b)Avgeropoulos, A.; Chan, V. A.-H.; Lee, V. Y.; Ngo, D.; Miller, R. D.; Hadjichristidis, N.; Thomas, E. L., *Chem. Mater.* **1998**, *10*, 2109-1225, (c)Kulbaba, K.; Manners, I., *Macromol. Rap. Comm.* **2001**, *22*, 711-724, (d)Cohen, S.; Bano, M. C.; Visscher, K. B.; Chow, M.; Allcock, H. R.; Langer, R., *J. Am. Chem. Soc.* **1990**, *112*, 7832-7833, (e)Seki, T.; Tohnai, A.; Tanigaki, N.; Yase, K.; Tamaki, T.; Kaito, A., *Macromolecules* **1997**, *30*, 1768-1775, (f)Power-Billard, K. N.; Manners, I., *Macromol. Rap. Comm.* **2002**, *23*, 607-611, (g)Chen, B. Z.; Sleiman, H. F., *Macromolecules* **2004**, *37*, 5866-5872, (h)Allcock, H. R.; Powell, E. S.; Chang, Y.; Kim, C., *Macromolecules* **2004**, *37*, 7163-7167, (i)Miinea, L. A.; Sessions, L. B.; Ericson, K. D.; Glueck, D. S.; Grubbs, R. B., *Macromolecules* **2004**, *37*, 8967-8972, (j)Chang, Y.; Powell, E. S.; Allcock, H. R., *J. Polym. Sci. A: Polym. Chem.* **2005**, *43*, 2912-2920, (k)Cheng, K. W.; Chan, W. K., *Langmuir* **2005**, *21*, 5247-5250, (l)Tse, C. W.; Lam, L. S. M.; Man, K. Y. K.; Wong, W. T.; Chan, W. K., *J. Polym. Sci., Part A: Polym. Chem.* **2005**, *43*, 1292-1308, (m)Nair, K. P.; Pollino, J. M.; Weck, M., *Macromolecules* **2006**, *39*, 931-940, (n)South, C. R.; Higley, M. N.; Leung, K. C. F.; Lanari, D.; Nelson, A.; Grubbs, R. H.; Stoddart, J. F.; Weck, M., *Chem.--Eur. J.* **2006**, *12*, 3789-3797, (o)Noonan, K. J. T.; Gates, D. P., *Angew. Chem., Int. Ed.* **2006**, *45*, 7271-7274, (p)Rider, D. A.; Winnik, M. A.; Manners, I., *Chem. Commun.* **2007**, 4483-4485, (q)Aamer, K. A.; Tew, G. N., *J. Polym. Sci., Part A: Polym. Chem.* **2007**, *45*, 1109-1121, (r)Metera, K. L.; Sleiman, H., *Macromolecules* **2007**, *40*, 3733-3738, (s)Aamer, K. A.; de Jeu, W. H.; Tew, G. N., *Macromolecules* **2008**, *41*, 2022-2029, (t)Noonan, K. J. T.; Gillon, B. H.; Cappello, V.; Gates, D. P., *J. Am. Chem. Soc.* **2008**, *130*, 12876-12877, (u)Wang, Y.; Zou, S.; Kim, K. T.; Manners, I.; Winnik, M. A., *Chem.-Eur. J.* **2008**, *14*, 8624-8631.
- 21.Matyjaszewski, K.; Xia, J., *Chem. Rev.* **2001**, *101*, 2921-2990.
- 22.Qin, Y.; Cheng, G.; Parab, K.; Achara, O.; Jäkle, F., *Macromolecules* **2004**, *37*, 7123-7131.
- 23.Beach, M. W.; Rondan, N. G.; Froese, R. D.; Gerhart, B. B.; Green, J. G.; Stobby, B. G.; Shmakov, A. G.; Shvartsberg, V. M.; Korobeinichev, O. P., *Polymer Degradation and Stability* **2008**, *93*, 1664-1673.
- 24.Qin, Y.; Kiburu, I.; Shah, S.; Jakle, F., *Org. Lett.* **2006**, *8*, 5227-5230.
- 25.Tsuda, T.; Yazawa, T.; Watanabe, K.; Fujii, T.; Saegusa, T., *J. Org. Chem.* **1981**, *46*, 192-194.

# **Chapter C. Synthesis of Weakly-Coordinating Organoborate-Functionalized Styrene Homopolymers and Amphiphilic Block Copolymers**

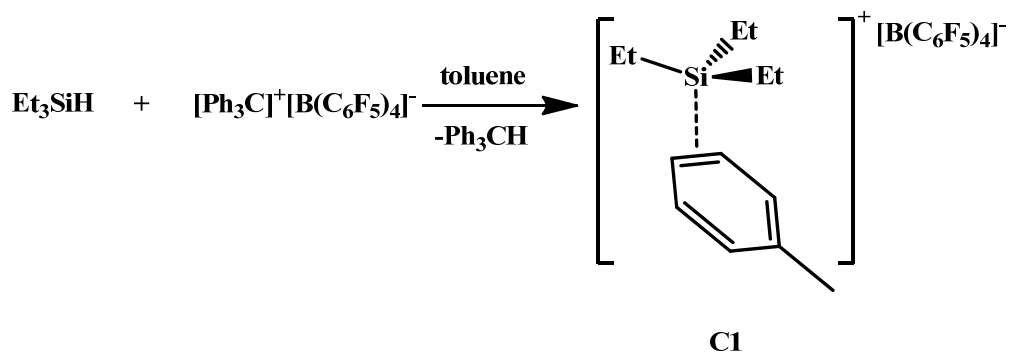
## **C.1 Introduction**

The search for the least coordinating anion has been a long term theme of inorganic chemists. Weakly coordinating anions have been widely used to enhance the chemical reactivities of cationic organometallic complexes. For instance, they have already achieved major commercial importance in olefin polymerization.<sup>97</sup> Ideally, they should have one or two negative charges being delocalized over their atoms so that no individual atom or group of atoms has a high concentration of charge. Therefore, more weakly coordinating properties can be anticipated for anions of large size, highly delocalized charges and most importantly in the absence of basic sites on their peripheries.<sup>98</sup> A successful weakly coordinating anion must also be stable enough to prevent dissociation into smaller and more strongly coordinating fragments. Because many highly electrophilic cations are also strong oxidants, oxidation resistance of the weakly coordinating anions should be also considered.

## C.2 Weakly Coordinating Organoborate Anions

One of the most widely used weakly coordinating anions is the tetraphenylborate anion ( $\text{BPh}_4^-$ ) and its derivatives. It has been used as the counterion in soluble Ziegler-Natta olefin polymerization catalysts, in which the catalytically active species is usually a cationic group 4 metallocene complex of a general type,  $\text{M}(\text{Cp})_2\text{R}^+$ . However, the parent tetraphenylborate anion can frequently coordinate to a metal center with one of its phenyl rings through  $\pi$  interactions. Its decomposition is usually associated with phenyl group transfer to the metal center and it is also susceptible to electrochemical and photochemical oxidative decomposition. In order to reduce the coordinating ability and also the reactivity of  $\text{BPh}_4^-$ , several derivatives with fluorine or trifluoromethyl substituents on the phenyl groups, such as  $\text{B}(\text{C}_6\text{F}_5)_4^-$  and  $\text{B}(3,5\text{-C}_6\text{H}_3(\text{CF}_3)_2)_4^-$ , have been explored. The incorporation of electron-withdrawing substituents can suppress  $\pi$ -coordination of the phenyl ring and increase the reduction potential of the borates. The negative charge at the *ipso* carbon atoms also decreases, resulting in a lower tendency for B-Ar cleavage. The tetrakis(pentafluorophenyl)borate anion,  $\text{B}(\text{C}_6\text{F}_5)_4^-$ , is therefore much more weakly coordinating and more stable than  $\text{BPh}_4^-$ . Significantly higher polymerization rates were achieved by using  $\text{B}(\text{C}_6\text{F}_5)_4^-$  as a counterion to stabilize the cationic metallocenes in olefin polymerizations. The  $\text{B}(\text{C}_6\text{F}_5)_4^-$  anion has also allowed to isolate the very reactive three-coordinate silylium cation. For example, an X-ray study

revealed that  $B(C_6F_5)_4^-$  has even less basicity than toluene solvent in the crystal of  $[Et_3Si(toluen)]^+B(C_6F_5)_4^-$  (compound **C1** in Scheme C1).<sup>99</sup>



**Scheme C1.** Synthesis of **C1** containing a very reactive three coordinate silylium cation stabilized with weakly-coordinating  $B(C_6F_5)_4^-$ .

In addition to stabilization of reactive cationic metal complexes, electrochemistry in low-polarity media can be enhanced by using  $B(C_6F_5)_4^-$  as an anion in supporting electrolytes, because of its ability to solubilize metal ions and its inherent tendency to dissociate from metal ions. As an example,  $[NBu_4][B(C_6F_5)_4]$  used as supporting electrolyte has dramatically improved electrochemistry of polyferrocenyl compounds in low-polarity media. Multiply charged species of polyferrocenyl compounds frequently passivate electrode surfaces due to precipitation. However, product precipitation is avoided with a  $B(C_6F_5)_4^-$  containing electrolyte. Due to the reduced ion pairing of  $Fe^{III}$  with the borate anion as the ferrocenyl groups are progressively oxidized, the resistivity

of low polarity solvents containing  $[\text{NBu}_4][\text{B}(\text{C}_6\text{F}_5)_4]$  is decreased. The resulting lowering of ohmic losses allowed voltammograms of greater accuracy to be recorded at conventional electrodes than with the analogous solutions containing traditional anions.<sup>100</sup>

Weakly coordinating anions including organoborates also serve important roles as electrolytes in lithium ion batteries. The weak interactions between the lithium cation and weakly coordinating anions favor a high dissociation of ion pairs, leading to high ion conductivity. However, high ion conductivity does not ensure a high lithium transference number, which is indicative of the selectivity for cation transfer, a critical measure for a lithium ion battery. Ohno and coworkers have reported that immobilization of weakly coordinating borate anions into polymers can be achieved through post polymerization modification of alkylborane polymers using aryllithiums. The lithium cation then serves as a unique mobile charge carrier in the polymeric electrolytes (Figure C1). When phenyl lithium was used, a very high lithium transference number ( $t_{\text{Li}} = 0.82$ ; at 30 °C) was observed. The relatively low ion conductivity was attributed to only partial generation (6.2%) of the borate functionality.<sup>101</sup> The enhanced mechanical properties associated with polymeric electrolytes will usually lower the ion conductivities which depend on the chain flexibility, i.e.  $T_g$ , of the polymer used. However, the important role of borate anions and the associated weakly coordinating property was confirmed in these single ion conductors. When pentafluorophenyllithium was used, the ionic conductivity ( $1.13 \times 10^{-5}$

S/cm) was one order of magnitude higher compared with the use of phenyllithium due to the even more weakly coordinating nature of the borate produced.<sup>102</sup>

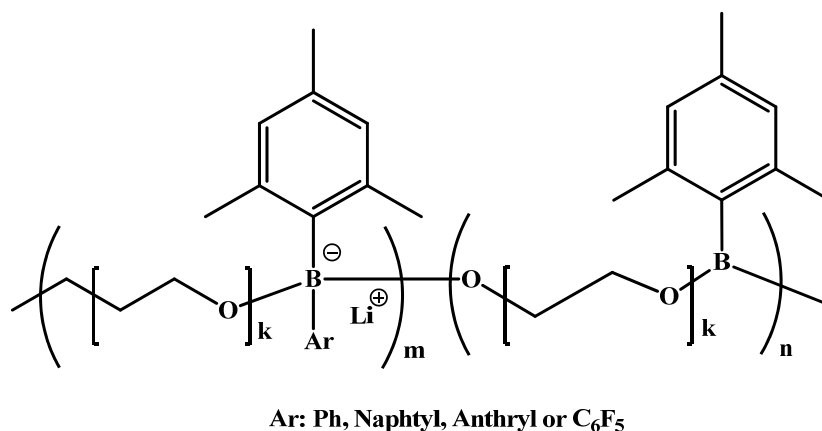


**Figure C1.** Immobilization of weakly coordinating borate anions into polymers gives rise to polymeric electrolytes having the lithium cation as the unique mobile charge carrier.

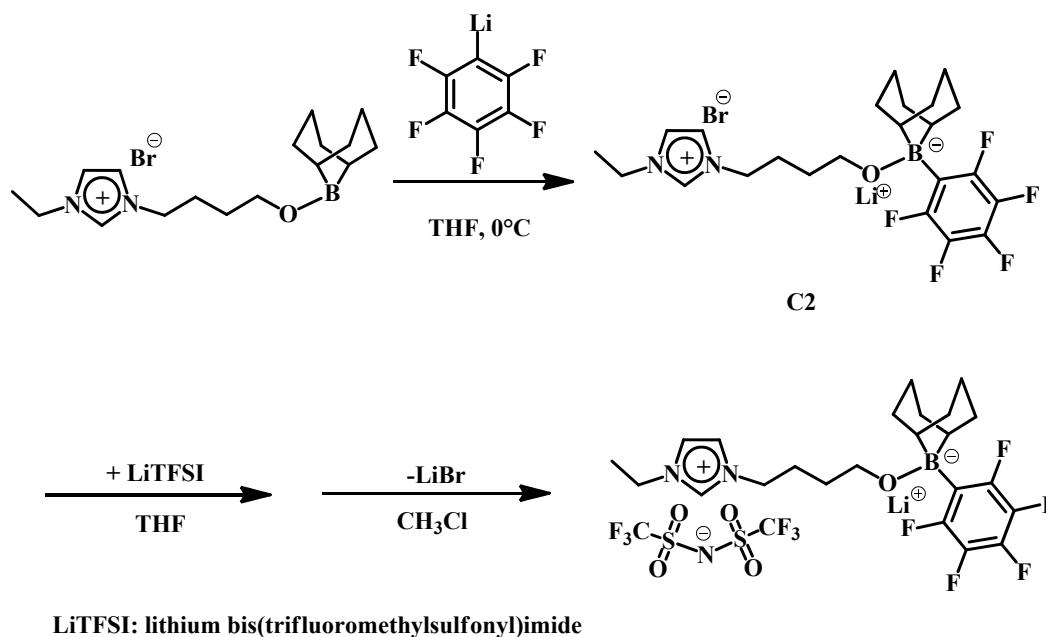
Ionic liquids (ILs) have attracted increasing interest for applications as new media for inorganic reactions, biocatalytic transformations, and separation technologies, and as potential electrolytes in various electrochemical devices. ILs can have many advantages over conventional organic solvents and electrolytes such as nonflammability, nonvolatility, high thermal stability and wide potential window.<sup>103</sup> ILs have also been referred to as “designed solvents” because their physical and chemical properties can be fine tuned by alteration of the cation or anion for specific applications. However, many barriers need to be overcome to allow ILs to replace the conventional solvents or electrolyte. Among them, serious is the inherently high viscosity of ILs. For example, a

high viscosity can be a big obstacle to achieve high ion conductivities of electrolytes according to the empirical rule of Walden.<sup>104</sup> To obtain low viscosity ILs, perfluoroalkyltrifluoroborates  $[R_FBF_3]^-$ , was used as anion in a series of chemically and electrochemically stable ILs consisting of imidazoliums. The low melting points (-42°C to 35°C), low glass transition temperatures (between -87°C and -117°C) and fairly low viscosities (26-77 cP at 25°C) of the resulting ILs have been explained to originate from the relative low symmetry and good charge distribution in  $[R_FBF_3]^-$ .<sup>105</sup>

Even though ILs show great potentials to be used as electrolytes, the addition of salts or acid is usually needed for most ordinary ILs. However, with salts or acid additives, all component ions tend to migrate under a potential gradient, thus causing the carrier cations in the mixtures to have low transference numbers being about 0.2 as reported.<sup>106</sup>

However, Ohno and coworkers solved this problem by design and synthesis of IL in form of zwitterions.<sup>107</sup> An imidazolium bromide molten salt with a N- substituted alkylborane moiety was converted to a zwitterion by reaction with pentafluorophenyl lithium. Lithium bis(trifluoromethylsulfonyl)imide (LiTFSI) was used to exchange the resulting lithium bromide in order to achieve a strong ion pairing interaction between the anion of the lithium salt additive and the imidazolium cation. A high lithium transference number (0.69) was obtained due to the absence of ion migration of the zwitterion and also the low tendency of dissociation of bis(trifluoromethylsulfonyl)imide from its ion pair with imidazolium. Meanwhile, high ion conductivity ( $3.0 \times 10^{-5}$  S/cm) associated with

markedly low  $T_g$  was also achieved which was credited to the weakly coordinating borate anion.

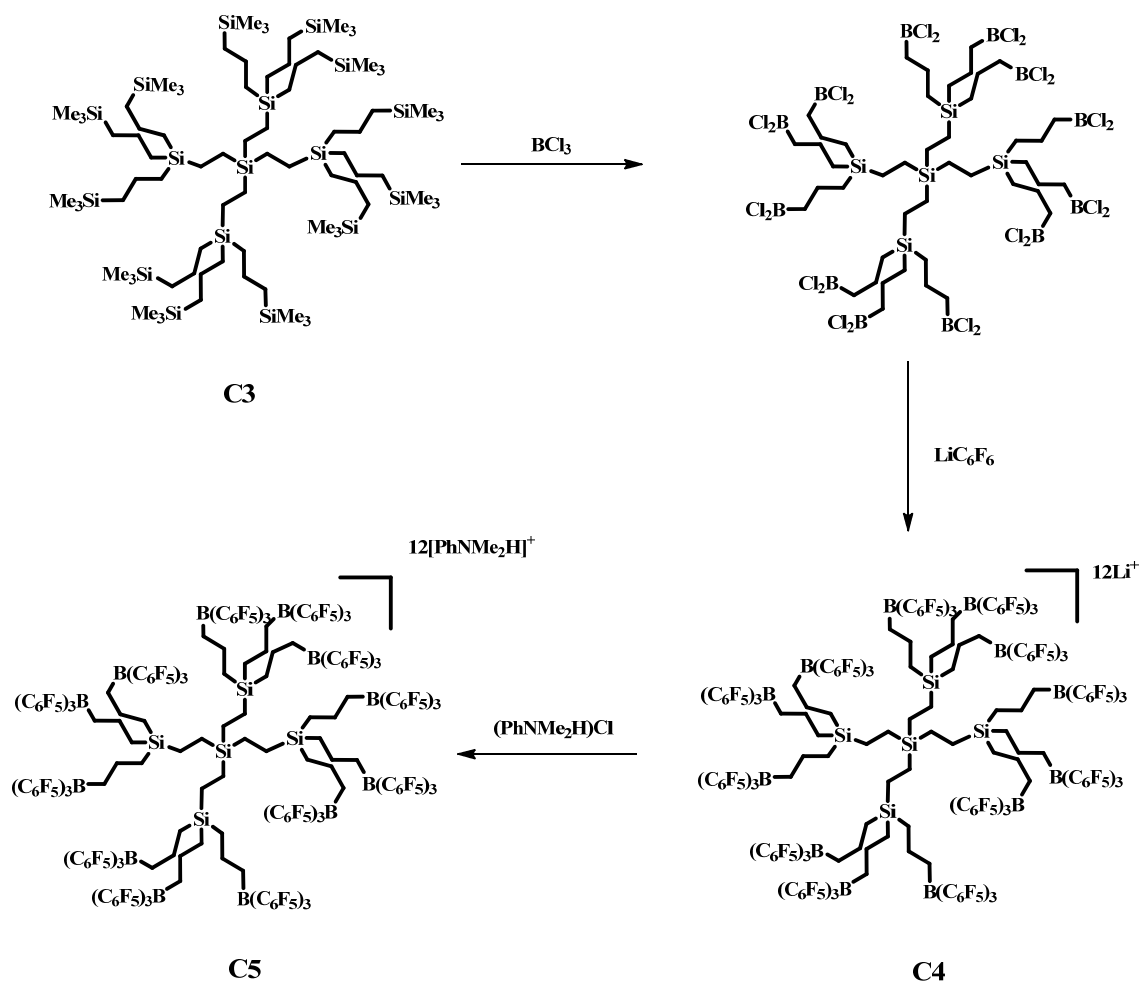


**Scheme C2.** Synthesis of an ionic liquid (**C2**) of a weakly-coordinating borate moiety and an imidazolium cation; the IL can further react with LiTFSI providing anions of strong ion pairing interaction with the imidazolium cations.

### C.3 Immobilization of Organometallic Catalysts onto Ionic Polymers via Electrostatic Interactions

To incorporate weakly coordinating borate ions into polymeric structures is an intriguing premise,<sup>108</sup> because beneficial effects can be expected from the improved processibility and anticipated stabilizing effect of the polymer chain. The preparation of polymers

derived from styryl monomers (e.g.  $\text{CH}_2=\text{CH}-\text{Sp}-\text{B}(\text{C}_6\text{F}_5)_3^-$ ; Sp = aromatic spacer unit) by standard free radical polymerization and their use in olefin polymerization has been claimed in the patent literature.<sup>109</sup> Mecking and coworkers reported the preparation of amphiphilic submicron particles through a ‘Surfactant-free’ emulsion polymerization of styrene in the presence of various amounts of sodium triphenylstyrylborate as a comonomer, divinylbenzene (DVB) as a cross-linker, a p-vinylbenzyl terminated poly(ethylene oxide) macromonomer and a water soluble free radical initiator. The borate comonomer served as surfactant during the polymerization to stabilize the colloidal lattices in the emulsion polymerization. These particles were eventually used to immobilize a rhodium catalyst,  $[\text{Rh}(\text{dppp})(\text{cod})]\text{BF}_4$ , through ion exchange to obtain rhodium catalyst loaded polymer particles. Electrostatic interactions led to immobilization of the cationic homogeneous catalyst.<sup>108</sup> Dendrimers (**C5**) that are decorated with  $\text{RB}(\text{C}_6\text{F}_5)_3^-$  (R = alkyl linker) moieties have been developed for use as polyanionic cocatalysts in zirconocene catalyst systems.<sup>110</sup> By reaction with  $\text{BCl}_3$ , the trimethylsilane groups on the periphery of the carbosilane dendrimers (**C3**) were first replaced with  $-\text{BCl}_2$  borane moieties which were subsequently reacted with pentafluorophenyllithium to give desired borate moieties. The lithium borate moieties were converted to dimethylanilinium borates before use as cocatalysts in zirconocene catalyst systems (Scheme C3).

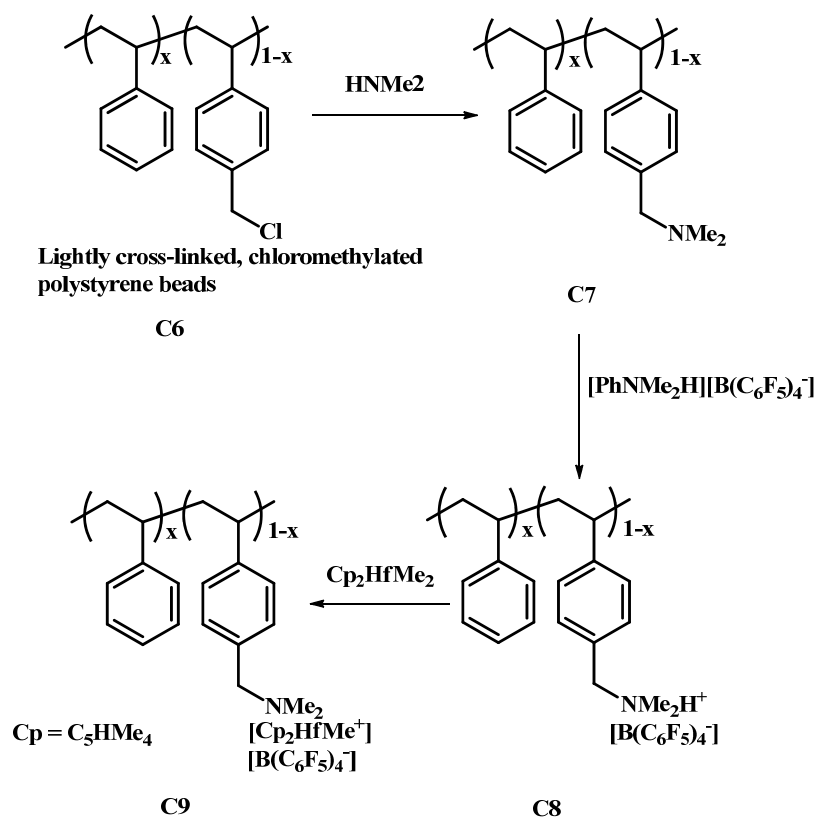


**Scheme C3.** Preparation of dendrimers **C4** and **C5** featuring weakly-coordinating borate anions.

Post polymerization modifications were used by Uozumi and coworkers to prepare random borate polymers and borate functionalized polystyrene beads as polymer supported cocatalysts for metallocene polymerizations.<sup>111</sup> Via a free radical polymerization in the presence of styrene and 4-bromostyrene, a random copolymer with 14.3 mol% 4-bromostyrene units was prepared. Subsequent lithiation of the bromostyrene

units using n-BuLi gave phenyllithium groups on the side chains with approximately 75mol% conversion. Eventually tris(pentafluorophenyl)borane was added resulting in anionic borate functionalities which were further transformed into tritylium borate groups. The polymeric cocatalysts were subjected to ion exchange with zirconium complexes with approximate conversions of 55.4 and 18.5% for two different zirconium complexes used. To functionalize polystyrene beads with borate groups, bromobenzyl groups have also been used and similar post modifications were applied.

The reverse approach of electrostatic attachment of Ziegler-Natta-type catalysts to ammonium borate functionalized polymers (**C8**) has been pursued by Frechet and coworkers (Scheme C4).<sup>112</sup> Commercially available chloromethylated polystyrene-co-divinylbenzene beads (**C6**) were modified with an excess of dimethylamine to yield the basic tertiary amine functionalized polymer (**C7**). Treatment of the polymer-bound amine with a standard activator salt, [PhNMe<sub>2</sub>H][B(C<sub>6</sub>F<sub>5</sub>)<sub>4</sub>], protonates the basic resin and binds the perfluorinated borate anion to the support by ion pairing.



**Scheme C4.** Synthesis of ammonium borate functionalized polymers (C7); Electrostatic attachment of active metallocene catalyst to C7.

The final active metallocene catalyst was generated with variable loadings by treating the borated beads with a toluene solution of a metallocene such as bis(tetramethylcyclopentadienyl) dimethylhafnium.

Mecking and coworkers immobilized a catalytically active rhodium complex with a soluble quaternary ammonium polyelectrolyte by electrostatic interactions between ammonium and a multiple charged phosphine ligand on the rhodium complex (Scheme C5).<sup>113</sup> First, the chloride counterions of the commercially available ammonium



## **C.4 Synthesis and Characterization of Organoborate-Functionalized Homo and Amphiphilic Block Copolymers**

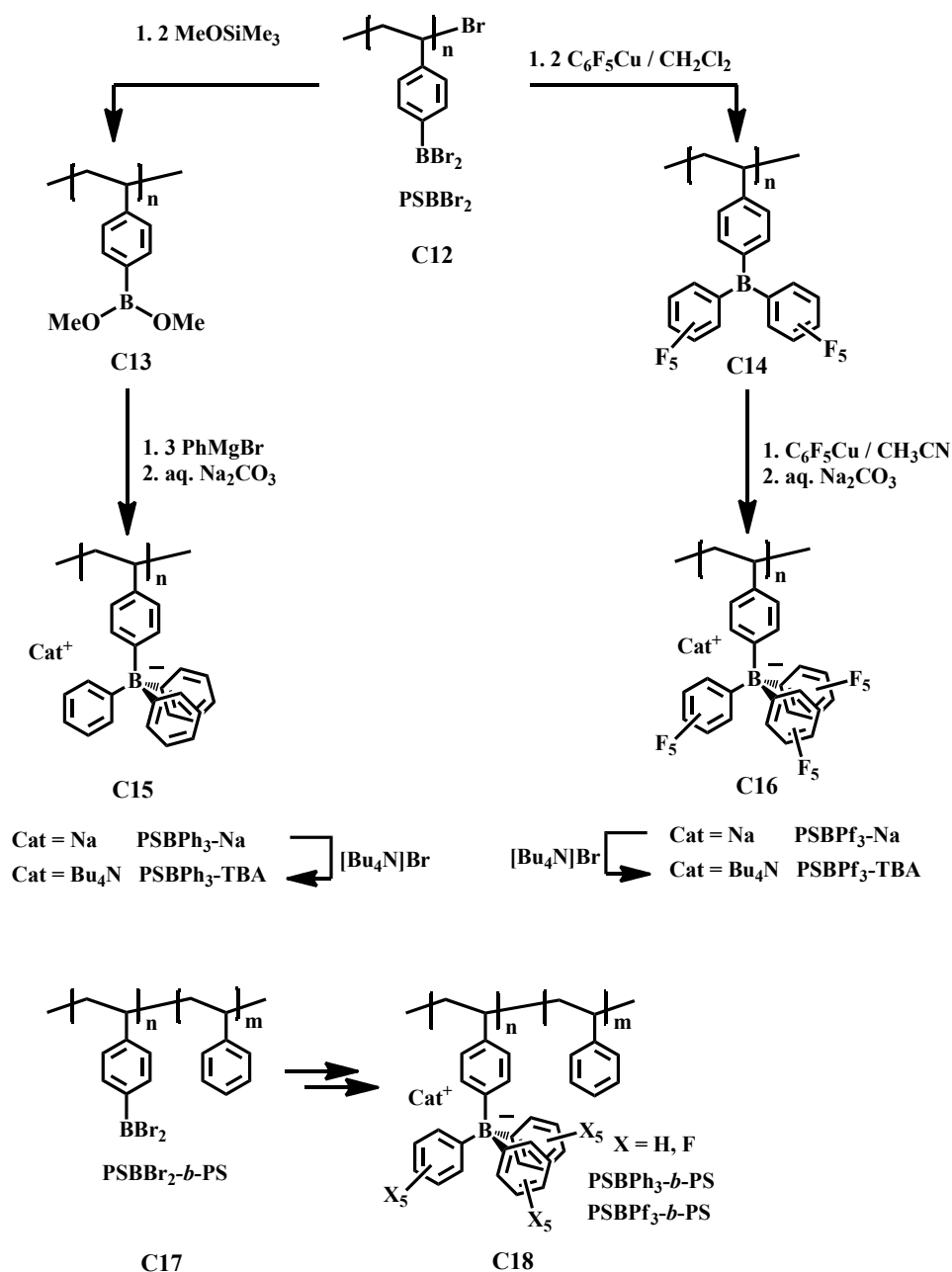
Note: this chapter has been adapted from a submitted paper.<sup>114</sup>

### **C.4.1 Synthesis of Organoborate-Functionalized Polystyrenes**

We became interested in the incorporation of organoborate functionalities into amphiphilic block copolymers<sup>91</sup> for their well-known ability to form interesting micellar aggregates. However, despite the potential advantages in a variety of applications, organoborate block copolymers have to the best of our knowledge not been reported to date and new controlled synthesis routes to these types of materials are in great demand.<sup>71-72, 92b, 92d, 62, 65-66, 115, 116</sup> Described here is a versatile new method for the preparation of organoborate polymers and report the first block copolymers, in which one of the constituent blocks is functionalized with weakly coordinating organoborate moieties, while the other block (polystyrene, PS) is unfunctionalized and thus provides solubility in non-polar solvents. Preliminary studies on the self-assembly of these novel block copolymers in solvents that selectively dissolve one of the constituent copolymer components are also presented.

As described in Chapter B, poly(4-trimethylsilylstyrene) (PSSiMe<sub>3</sub>; n = 93) and the corresponding block copolymers with styrene as a second block (PSSiMe<sub>3</sub>-b-PS; n = 33, m = 120 or n = 29, m = 239) are readily accessible via ATRP according to published procedures.<sup>61, 116</sup> Exchange of the trimethylsilyl groups with BBr<sub>3</sub> results in the selective

formation of the boron-functionalized homo- and block copolymers, PSBBr<sub>2</sub> (C12) and PSBBr<sub>2</sub>-*b*-PS (C17).



**Scheme C6.** Synthesis of organoborate-functionalized homopolymers and block copolymers; Cat<sup>+</sup> = Na<sup>+</sup>, Bu<sub>4</sub>N<sup>+</sup>.

There are several possible approaches for the conversion of these  $\text{BBr}_2$ -functionalized polymers to the desired organoborate polymers. One method that was applied to the triphenylborate-modified polymer (**C15**) is based on the treatment of boronates with an excess of organolithium or Grignard reagents.<sup>117</sup> Hence, we first converted the  $\text{BBr}_2$  groups to  $\text{B}(\text{OMe})_2$  moieties with the mild reagent  $\text{Me}_3\text{SiOMe}$ , and the resulting boronate polymer was then reacted with  $\text{PhMgBr}$  at  $85\text{ }^\circ\text{C}$  in THF for 3 h (Scheme C6). An alternative route involves initial formation of the triorganoborane intermediate which, if it is readily available (the phenyl derivative  $\text{PSBPh}_2$  is not readily accessible from  $\text{PSBBr}_2$ ), can be very selectively and under mild conditions converted to the organoborate. This method was successfully applied to the preparation of **C16**.  $\text{PSBBr}_2$  (**C12**) was first reacted with the organo-copper reagent  $\text{CuC}_6\text{F}_5$  in  $\text{CH}_2\text{Cl}_2$  to give  $\text{PSBPf}_2$  (**C14**), which in turn was converted *in situ* to the desired borate polymer by addition of a third equivalent of  $\text{CuC}_6\text{F}_5$  in acetonitrile. Acetonitrile coordinates to copper, and thereby promotes formation of the  $[\text{Cu}(\text{CH}_3\text{CN})_x]_n[\text{PSBPf}_3]$  polymeric complex. The organoborate polymers were isolated in the form of their sodium derivatives after pouring the reaction mixture into an aqueous sodium carbonate solution, extraction into acetone and subsequent dialysis against acetone. Another possible advantage of this latter route is that mixed-substituted organoborate polymers  $\text{PS}[\text{BR}^1\text{R}^2\text{R}^3]$  could become available through selective stepwise introduction of the organic substituents. While not further explored in this work, such an approach could prove highly useful for the development of

other functional organoborate polymers. The amphiphilic block copolymers PSBAr<sub>3</sub>-*b*-PS (**C18**) were prepared from PSBBr<sub>2</sub>-*b*-PS (**C17**) using similar methods.

The sodium borate homopolymers are water-soluble, while the block copolymers are soluble in either polar (e.g. THF, acetone, MeOH, DMF, DMSO, water) or non-polar (e.g. toluene) solvents. For dissolution in block-selective solvents, such as MeOH, water or toluene, the block copolymers were first taken up in a common solvent such as acetone and then dialyzed. Conversion to the Bu<sub>4</sub>N derivatives was achieved by dissolution in water or and subsequent addition into a solution of [Bu<sub>4</sub>N]Br. The products were obtained as white solids that are readily isolated and well soluble in a range of polar organic solvents.

#### **C.4.2 Characterizations of Amphiphilic Organoborate Block Copolymers**

Formation of the borate polymers was confirmed by multinuclear NMR spectroscopy. The phenylborate homo and block-copolymers show slightly broadened <sup>11</sup>B NMR resonances at ca. -6 ppm ( $w_{1/2} = 30$  Hz), a chemical shift that is identical to that of the related molecular model compound Na[<sup>t</sup>BuC<sub>6</sub>H<sub>4</sub>BPh<sub>3</sub>] ( $w_{1/2} = 10$  Hz). The fluorinated derivatives PSBPf<sub>3</sub> and PSBPf<sub>3</sub>-*b*-PS feature slightly more upfield shifted signals at ca. -13 ppm, again consistent with the chemical shift of the molecular species Na[<sup>t</sup>BuC<sub>6</sub>H<sub>4</sub>B(C<sub>6</sub>F<sub>5</sub>)<sub>3</sub>] (Figure C2). The fluorinated polymers are conveniently analyzed by <sup>19</sup>F NMR; three broad resonances at -129.7, -166.6, and -168.7 ppm are found as

expected for the *ortho*, *para*, and *meta*-fluorines of PSBPf<sub>3</sub> and essentially identical shifts are observed for the respective block copolymer (Figure C3). The absence of any other signals asserts the high selectivity of the borate formation.

While the <sup>1</sup>H NMR data are less informative due to the broad nature of the signals, <sup>13</sup>C NMR spectroscopy proved highly useful, and the downfield region of the spectra that shows the *ipso*-carbon atoms is most instructive. For the molecular model Na[<sup>t</sup>BuC<sub>6</sub>H<sub>4</sub>BPh<sub>3</sub>] a large and a small quartet are found for the boron-bound carbons of the phenyl and *t*-butylphenyl groups, respectively, as a result of coupling to <sup>11</sup>B. The same pattern is found in the spectra for PSBPh<sub>3</sub> and PSBPh<sub>3</sub>-*b*-PS, except that the signals are slightly broadened, thus confirming the selective attachment of the tetraarylborate functionalities to the polymers. For the block copolymer, a second set of resonances that match those of PS is also apparent (Figure C4).

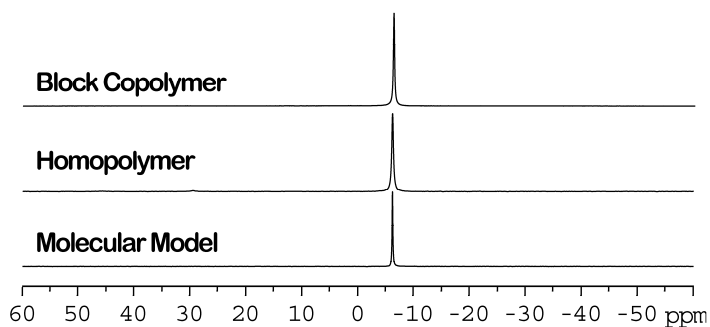


**Figure C2.** Comparison of the <sup>11</sup>B NMR spectrum of the block copolymer PSBPh<sub>3</sub>-*b*-PS with those of the homopolymer PSBPh<sub>3</sub> and the molecular species MBPh<sub>3</sub>. Cation = Na, solvent = acetone-d<sub>6</sub>.

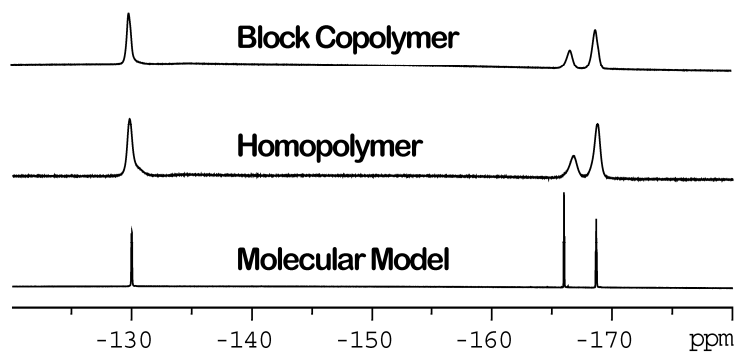


**Figure C3.** Comparison of the  $^{19}\text{F}$  NMR spectra of the block copolymer PSBPf<sub>3</sub>-*b*-PS with those of PSBPf<sub>3</sub> and the molecular species Na[<sup>t</sup>BuC<sub>6</sub>H<sub>4</sub>BPh<sub>3</sub>]; cation = Na<sup>+</sup>, solvent = acetone-d<sub>6</sub>.

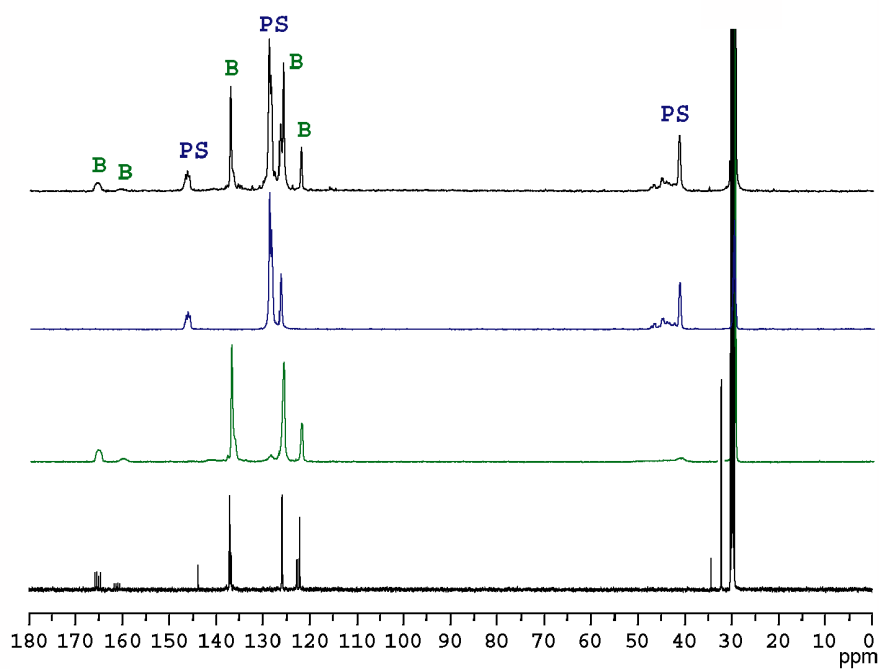


**Figure C4.** Comparison of the  $^{13}\text{C}$  NMR spectrum of the organoborate-functionalized block copolymer PSBPh<sub>3</sub>-*b*-PS with those of the homopolymer PSBPh<sub>3</sub> (green), polystyrene (PS, blue), and the molecular species MBPh<sub>3</sub>; cation = Na<sup>+</sup>, solvent = acetone-d<sub>6</sub>.

The molecular weight of the organoborate homo and block copolymers was estimated by GPC relative to PS standards in DMF using 20 mM LiBr as an additive (Figure C5). For all polymers, well-defined monomodal elution profiles were observed with polydispersities in the range of PDI = 1.14 to 1.20 (Table C1). The bands are only slightly broadened relative to those of the silylated precursor polymers, thereby further confirming the high selectivity of the polymer modification reactions. The molecular weights are generally in the expected range, but those of the fluorinated polymers are similar to or even lower than for the phenylborate polymers. This may be the result of a relatively more compact conformation of the fluorinated polymers in the presence of LiBr (more effective shielding of the charges).

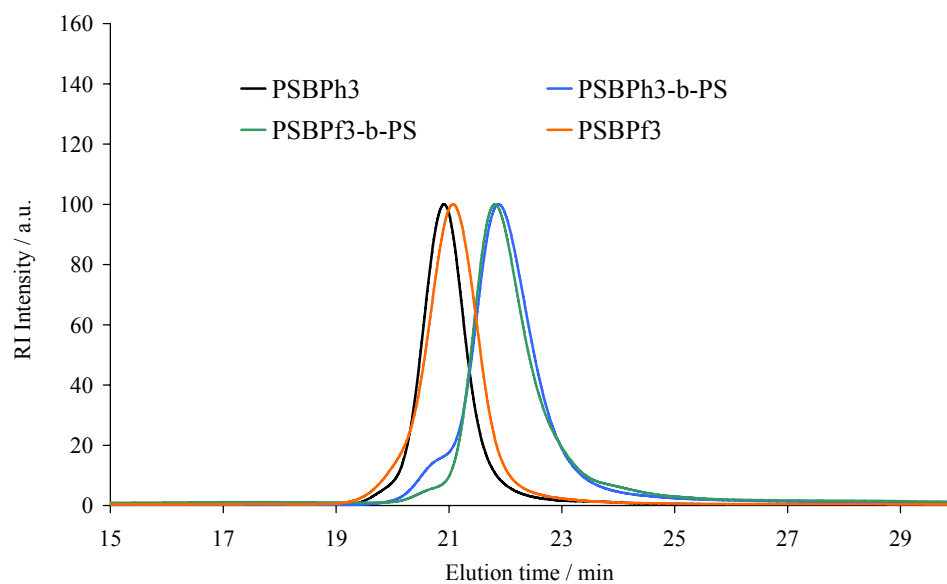


**Figure C5.** GPC traces for the organoborate-functionalized homopolymers and block copolymers (the slight high MW shoulder for the block copolymers was also present for the silylated precursor polymer).

**Table C1.** Results for polymer modification procedures.

	$M_n (\times 10^3)^a$	$M_w (\times 10^3)^a$	$PDI^a$	$DP_n$	$Yield (\%)^b$
PSSiMe <sub>3</sub>	16.4	18.4	1.11	93	
PSBPh <sub>3</sub>	60.1	70.3	1.17	102	54
PSBPf <sub>3</sub>	52.1	59.7	1.14	61	69
PSSiMe <sub>3</sub> - <i>b</i> -PS	18.3	19.5	1.07	33/120	
PSBPh <sub>3</sub> - <i>b</i> -PS	28.9	34.5	1.20	28/120 <sup>c</sup>	70
PSBPf <sub>3</sub> - <i>b</i> -PS	28.2	32.7	1.16	18/120 <sup>c</sup>	66

[a] Based on GPC-RI detection (*vs* PS) of the ammonium salts in DMF/20mM LiBr at 40 °C and the silylated precursor polymers in THF at 35 °C; the Bu<sub>4</sub>N counterions are included in the calculations. [b] Isolated yield of the sodium derivative. [c] Calculated assuming that the MW of the PS block remains constant.

#### C.4.3 Micellization in Selective Solvents

We also carried out studies on the assembly behavior of the organoborate block copolymers in solvents that selectively dissolve one of the constituent blocks. DLS was performed on toluene solutions of the sodium and TBA salts of PSBPh<sub>3</sub>-*b*-PS and PSBPf<sub>3</sub>-*b*-PS (derived from PSSiMe<sub>3</sub>-*b*-PS with  $n = 33$ ;  $m = 120$ ), which were obtained by dialysis from acetone. The results from regularization analysis (DYNALS algorithm) suggest the presence of aggregates with an average apparent hydrodynamic radius ( $R_{h,app}$ ) of ca. 14 to 16 nm, independent of the particular aryl substituents on boron or the counterion employed (Figure C6). It is reasonable to assume that in toluene as the solvent

the PS block forms the corona of the micellar structures (Figure C7). Conversely, when the ammonium borate block copolymer PSBPf<sub>3</sub>-*b*-PS is dissolved in (hot) MeOH, the polystyrene should form the core, leaving the organoborate functionalities exposed to the polar solvent. Slightly larger aggregates with an average apparent hydrodynamic radius of ca. 20 nm and a somewhat broader distribution were observed in this case.

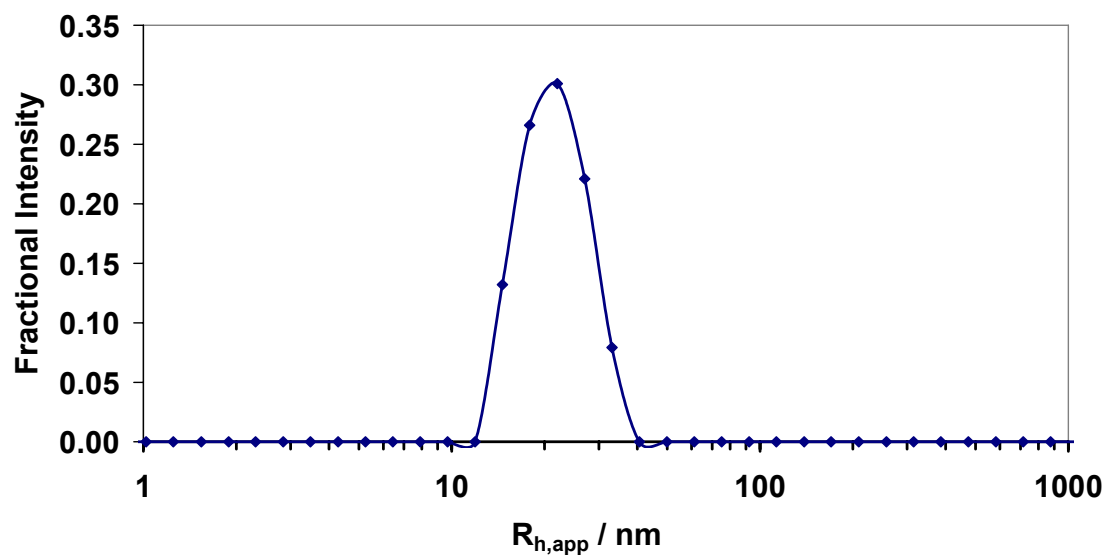


**Figure C6.** Size distribution histogram of a solution of PSBPf<sub>3</sub>-*b*-PS in toluene;  $n = 33$ ,  $m = 120$ .

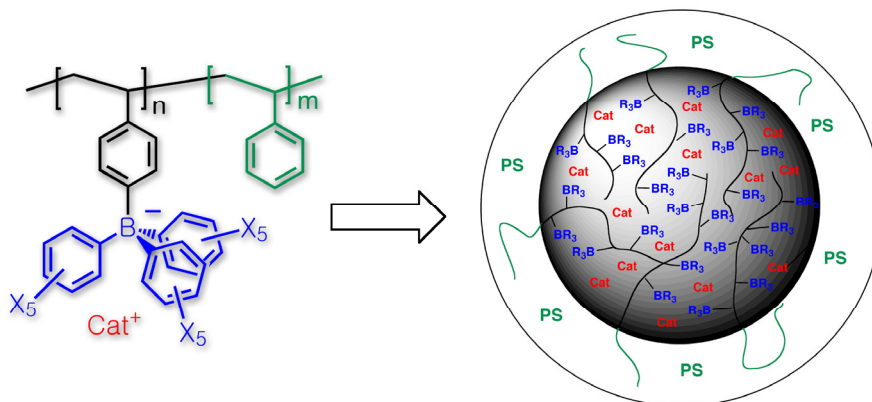
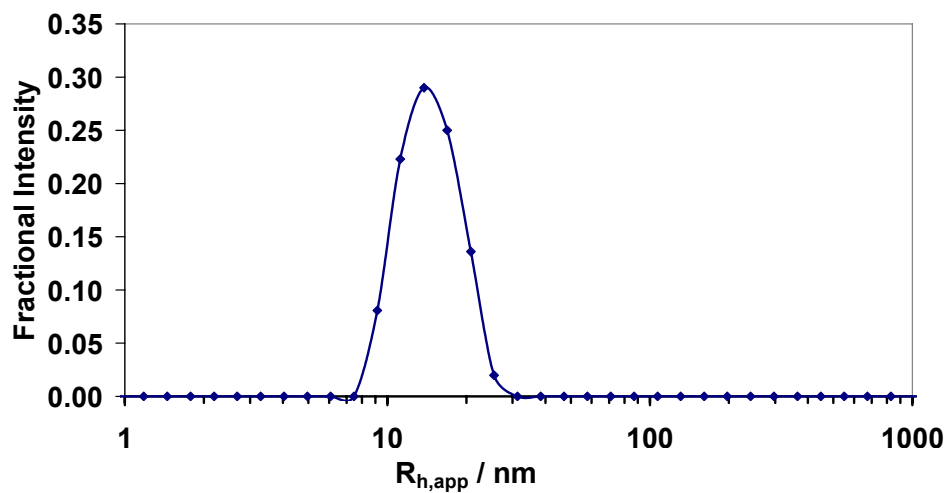


**Figure C7.** Schematic illustration of the block copolymer assembly of PSBR<sub>3</sub>-*b*-PS in toluene (BR<sub>3</sub> = B(C<sub>6</sub>F<sub>5</sub>)<sub>3</sub>, Cat = counterion (Na<sup>+</sup>, Bu<sub>4</sub>N<sup>+</sup>, PS = polystyrene)).

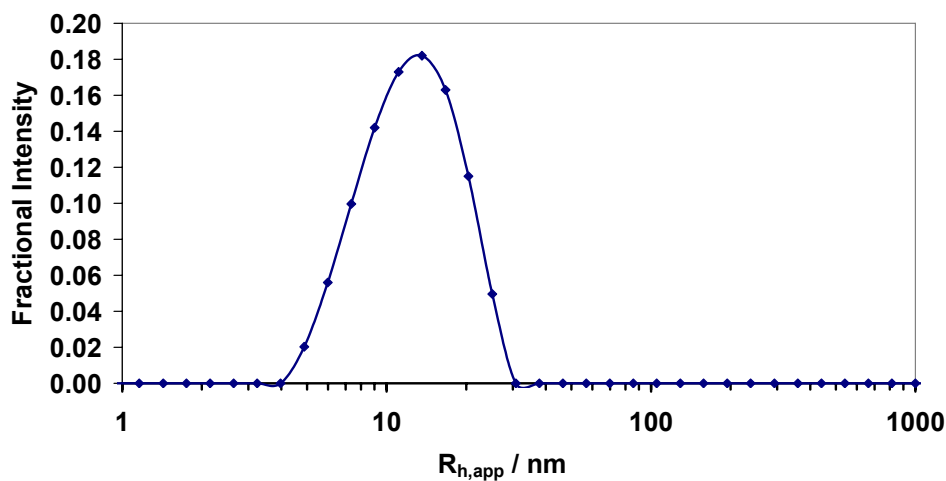
#### C.4.4 Immobilization of a Rhodium Complex

To demonstrate the ability of the reverse micelles to accept cationic transition metal complexes, we treated the sodium salt of the block copolymer PSBPf<sub>3</sub>-*b*-PS with [Rh(cod)(dppb)]<sup>+</sup>(OTf)<sup>-</sup>.<sup>118</sup> By <sup>1</sup>H NMR integration, the degree of loading was estimated to be ca. 37%. Micellization was then induced by (a) addition of MeOH as a borate-selective solvent to a solution of the block copolymer in THF as a common solvent and (b) dialysis of the block copolymer in THF to toluene as a PS selective solvent. As expected, formation of regular micelles in MeOH could be confirmed by DLS and TEM analysis (Figure C8). Interestingly, TEM analysis of the unstained samples prepared in toluene revealed the formation of reverse micelles, which contained dark cores as a result of the rhodium metal loading (Figure C9). The size of these micellar structures was in reasonably good agreement with data derived from DLS ( $R_{h,app}$  ca. 19

nm). This is slightly larger than what we found prior to reaction with the Rh complex, suggesting a modest expansion of the micellar core upon loading with the transition metal complex.



(a)



(b)

**Figure C8.** Size distribution histogram of a solution of PSBPf<sub>3</sub>-*b*-PS loaded with [Rh(cod)(dppb)]<sup>+</sup> (a) after dialysis from THF to toluene (1 mg mL<sup>-1</sup>; n = 33, m = 120) and (b) in THF/ MeOH (1:4) (1 mg mL<sup>-1</sup>; n = 33, m = 120).

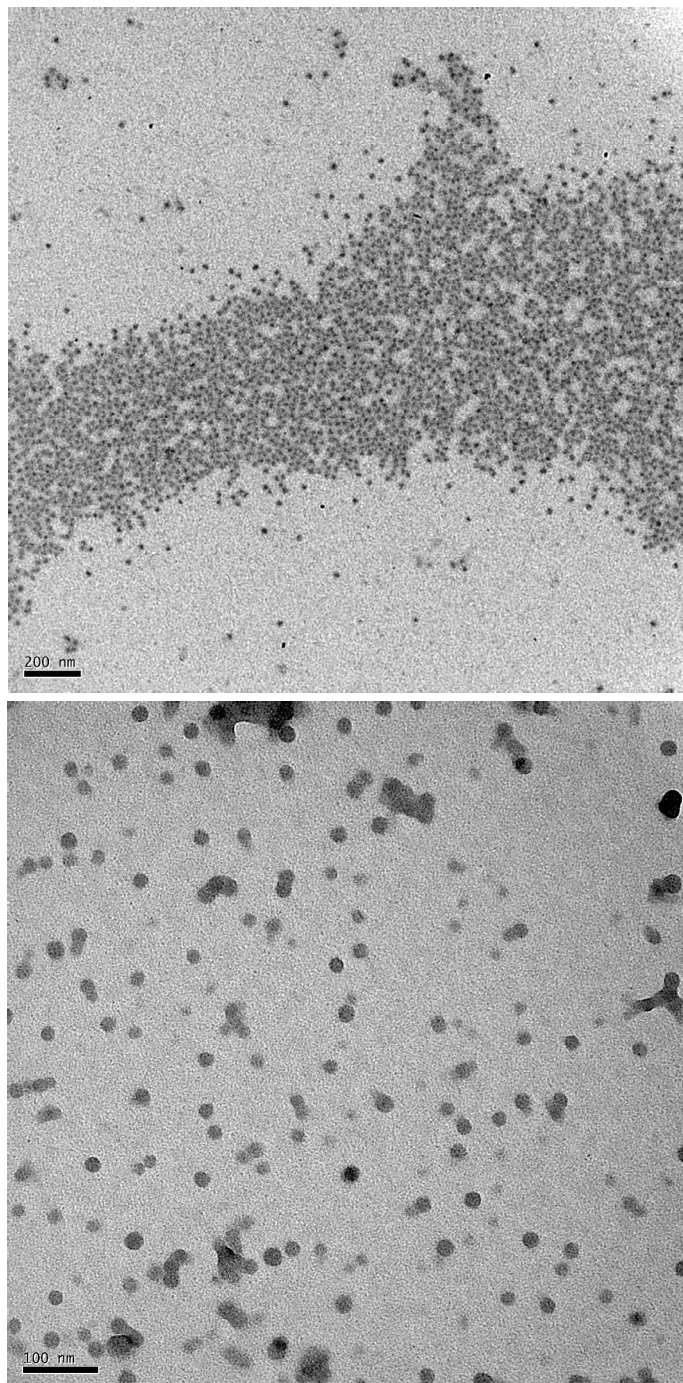


**Figure C9.** TEM image of PSBPf<sub>3</sub>-*b*-PS after loading with [Rh(cod)(dppb)]<sup>+</sup> and subsequent micellization in toluene (top) and MeOH:THF = 4:1 (bottom).

## C.5 Conclusions

In conclusion, a novel method for the preparation of organoborate polymers has been developed. Both, homopolymers and the first examples of organoborate block copolymers are readily accessible through selective post polymerization modification procedures. These weakly coordinating polyanions, and in particular self-assembled block copolymer micelles, are promising candidates as novel supports for reactive cationic metal complexes, where the “inert” PS corona can not only act as a protective layer, but also promote solubility of charged species  $[ML_n]^+[BR_4]^-$  in non-polar solvents. Also interesting is their potential utility as electrolytes in batteries and membranes and possibly as protective coatings based on the large neutron cross-section of  $^{10}B$ .<sup>119</sup>

## C.6 Experimental Part

### C.6.1 Materials and General Methods.

Phenyl magnesium bromide (1.0 M solution in tetrahydrofuran) was purchased from Aldrich and  $Bu_4NBr$  from Acros.  $(CuC_6F_5)_4$ <sup>120</sup> were prepared according to literature procedures. Acetone was used as received from Pharmco.

The MALDI TOF measurements were performed on an Applied Biosystems 4800 Proteomics Analyzer in reflectron (+) or (-)-mode with delayed extraction. For the data acquisition in positive mode benzo[a]pyrene was used as the matrix (20 mg/mL in toluene) and the sample was dissolved in MeOH (10 mg/mL), mixed with the matrix in a

1:10 ratio, and then spotted on the wells of a sample plate. For acquisition in negative mode  $\alpha$ -cyano-4-hydroxycinnamic acid was used as the matrix (50% acetonitrile, 0.1% TFA in deionized water) and the sample was dissolved in MeOH (10 mg/mL), mixed with the matrix in a 1:10 ratio, and then spotted on the wells of a sample plate. Peptides were used for calibration (Des-Arg-Bradykinin (904.4681), Angiotensin I (1296.6853), Glu-Fibrinopeptide B (1570.6774), ACTH (clip 1-17) (2093.0867), ACTH (clip 18-39) (2465.1989), ACTH (clip 7-38) (3657.9294) with  $\alpha$ -hydroxy-4-cyanocinnamic acid as the matrix.

GPC analyses of the borate polymers were performed in DMF / 20 mM LiBr (0.5 mL/min) using a Waters Breeze system equipped with a 717 plus auto sampler, a 1525 binary HPLC pump, a 2487 dual  $\square$  absorbance detector, and a 2414 refractive index detector. A series of Shodex Asahipak columns (GF-510 HQ, GF-310 HQ), which were kept in a column heater at 40 °C, were used for separation. The columns were calibrated with PS standards (Polymer Laboratories).

The samples were dialyzed prior to analysis (Fisherbrand regenerated cellulose dialysis tubing with 6000 to 8000 Dalton molecular weight cut-off, which was extensively washed with distilled water).

In a typical procedure for solution preparation of reverse micelle, a solution of 3 mg of block copolymer in 3 mL of acetone was transferred into the dialysis tubing and dialyzed

first against acetone (300 mL) and then against toluene (300 mL). The dialysate was replaced with fresh toluene after three hours and the procedure was repeated three times.

In the sample preparation for TEM, one drop of the sample under investigation was deposited on a copper grid, which was coated with carbon (< 10 nm). Excess solution was removed with a filter paper. The samples were kept to dry for 24 hours and subjected to TEM analysis without further treatment.

### **C.6.2 Synthesis of Organoborate Polymers and Block Copolymers**

#### **Synthesis of Poly(sodium triphenyl(styryl)borate).**

In a glove box, a solution of PSSiMe<sub>3</sub> (0.50 g, 2.84 mmol SiMe<sub>3</sub>,  $M_n = 16400$ ,  $M_w = 18400$ ,  $PDI = 1.11$ ) in CH<sub>2</sub>Cl<sub>2</sub> (20 mL) was added to a solution of BBr<sub>3</sub> (0.854 g, 3.41 mmol) in CH<sub>2</sub>Cl<sub>2</sub> (10 mL). The reaction mixture was stirred at room temperature for 24 h. Me<sub>3</sub>SiOMe (1.8 mL, 13 mmol) was added into the reaction solution and the mixture was stirred for 3 h. All volatile components were removed under high vacuum and the white residue was redissolved in THF (50 mL). A solution of PhMgBr (18 mL, 1M in THF, 18 mmol) was added and the reaction mixture was slowly heated to reflux and kept stirring for 3 h. The mixture was then allowed to cool down to RT and poured into a saturated aqueous Na<sub>2</sub>CO<sub>3</sub> solution (100 mL). The resulting suspension was first filtered and then extracted with acetone (3 × 80 mL). The solvents were removed from the combined organic layers under vacuum. The residue was dialyzed first with water and

then acetone (Fisherbrand regenerated cellulose membrane with 6000 to 8000 Dalton molecular weight cut-off). The resulting solution was filtered, concentrated and then precipitated into hexanes to give a white solid, which was dried under high vacuum at RT for 24 h. Yield: 0.74 g (54%; the product contains ca. 25% water).  $^1\text{H}$  NMR (499.896 MHz, acetone- $d_6$ )  $\delta$  = 7.37 (br, 6H, Ph-H<sub>2,6</sub>), 6.90 (br, 6H, Ph-H<sub>3,5</sub>), 6.73 (br, 3H, Ph-H<sub>4</sub>), 7.4-6.4 (not resolved, 4H, styryl-H), 2.7-1.0 (br, 3H, CHCH<sub>2</sub>).  $^{13}\text{C}$  NMR (125.699 MHz, acetone- $d_6$ )  $\delta$  = 165.6 (Ph-C<sub>1</sub>), 160.2 (br, styryl-C<sub>1</sub>), 141.6 (br, styryl-C<sub>4</sub>), 137.0 (Ph-C<sub>2,6</sub>), 136.4 (styryl-C<sub>2,6</sub>), 128.7 (br, styryl-C<sub>3,5</sub>), 126.0 (Ph-C<sub>3,5</sub>), 122.1 (Ph-C<sub>4</sub>), 52.0-39.0 (br m, CHCH<sub>2</sub>).  $^{11}\text{B}$  NMR (160.386 MHz, acetone- $d_6$ )  $\delta$  = -6.2 ( $w_{1/2}$  = 30 Hz).

#### **Conversion to Poly(tetrabutylammonium triphenyl(styryl)borate).**

An aqueous solution (20 mL) of poly(sodium triphenyl(styryl)borate) (0.16 g, water content ca. 25%, 0.33 mmol borate) was added into a solution of Bu<sub>4</sub>NBr (0.50 g, 1.6 mmol) in H<sub>2</sub>O (50 mL). After stirring for 1 h, the white precipitate was collected by centrifugation. The solid was washed extensively first with water and then with hexanes, and dried under high vacuum at 60 °C. Yield: 0.14 g (73%).  $^1\text{H}$  NMR (499.896 MHz, acetone- $d_6$ )  $\delta$  = 7.35 (br, 6H, Ph-H<sub>2,6</sub>), 6.94 (br, 6H, Ph-H<sub>3,5</sub>), 6.78 (br, 3H, Ph-H<sub>4</sub>), 7.4-6.4 (n.r., 4H, styryl-H), 2.69, 1.31, 1.14, 0.81 (br, 36H, NBu<sub>4</sub>), backbone Hs not resolved.  $^{13}\text{C}$  NMR (125.699 MHz, acetone- $d_6$ )  $\delta$  = 165.8 (Ph-C<sub>1</sub>), 159 (br, styryl-C<sub>1</sub>),

142 (br, styryl-C4), 137.4 (Ph-C2,6), 136.7 (styryl-C2,6), 129 (br, styryl-C3,5), 126.1 (Ph-C3,5), 122.2 (Ph-C4), 59.1 (NBu<sub>4</sub>), 52-38 (br m, CHCH<sub>2</sub>), 24.4, 20.3, 14.3 (NBu<sub>4</sub>). <sup>11</sup>B NMR (160.386 MHz, acetone-d<sub>6</sub>)  $\delta = -6.2$  ( $w_{1/2} = 30$  Hz). GPC (RI):  $M_n = 60100$ ,  $M_w = 70300$ ,  $PDI = 1.17$ .

### **Synthesis of Poly(sodium tris(pentafluorophenyl)(styryl)borate).**

A solution of PSSiMe<sub>3</sub> (0.50 g, 2.84 mmol SiMe<sub>3</sub>,  $M_n = 16400$ ,  $M_w = 18200$ ,  $PDI = 1.11$ ) in CH<sub>2</sub>Cl<sub>2</sub> (15 mL) was added to a solution of BBr<sub>3</sub> (0.854 g, 3.41 mmol) in CH<sub>2</sub>Cl<sub>2</sub> (10 mL) inside a glove box. The reaction mixture was stirred at room temperature for 24 h. A solution of pentafluorophenylcopper (2.62 g, 11.3 mmol) in CH<sub>2</sub>Cl<sub>2</sub> (10 mL) was added and the mixture was stirred for 2 h. Then, a solution of pentafluorophenylcopper (1.08 g, 4.68 mmol) in acetonitrile (50 mL) was added. The mixture was first stirred for 10 h at RT, then heated to a gentle reflux for 1 h, and finally allowed to cool to room temperature under nitrogen. The resulting suspension was poured into a saturated solution of aqueous Na<sub>2</sub>CO<sub>3</sub> (100 mL). The slurry was extracted with acetone (3 × 200 mL) and the combined organic layers were evaporated to dryness under high vacuum. The residue was redissolved in acetone, the solution filtered, and the filtrate dialyzed against acetone (Fisherbrand regenerated cellulose membrane with 6000 to 8000 Dalton molecular weight cut-off). The acetone solution was filtered once again, concentrated, and then precipitated into hexanes. The product was isolated as a white solid that was dried at 65

°C under high vacuum for 24 h. Yield: 1.25 g (69%).  $^1\text{H}$  NMR (499.891 MHz, acetone-d<sub>6</sub>)  $\delta$  = 7.45, 7.04, 6.47 (br m, 4H, styryl-H), 2.6-0.6 (br m, 3H, CHCH<sub>2</sub>).  $^{13}\text{C}$  NMR (125.697 MHz, acetone-d<sub>6</sub>)  $\delta$  = 150 (br, styryl(borate)-C1, overlapped with one of the doublets of Pf-C2,6), 149.0 (d,  $^1J_{\text{CF}}$  = 240 Hz, Pf-C2,6), 138.5 (d,  $^1J_{\text{CF}}$  = 242 Hz, Pf-C4), 137.2 (d,  $^1J_{\text{CF}}$  = 245 Hz, Pf-C3,5), 133.4 (styryl-C2,6), 128.8 (Pf-C1), 126.2 (styryl-C3,5), n.r. (styryl-C4), 52-38 (br m, CHCH<sub>2</sub>).  $^{11}\text{B}$  NMR (160.386 MHz, acetone-d<sub>6</sub>),  $\delta$  = -12.9 ( $w_{1/2}$  = 70 Hz).  $^{19}\text{F}$  NMR (470.365 MHz, acetone-d<sub>6</sub>)  $\delta$  = -129.7 (6F, ortho-F), -166.7 (3F, para-F), -168.7 (6F, meta-F).

#### **Conversion to Poly(tetrabutylammonium tris(pentafluorophenyl)(styryl)borate).**

To a solution of poly(sodium tris(pentafluorophenyl)(styryl)borate) (0.50 g, 0.78 mmol borate) in 30 mL of acetone was added [Bu<sub>4</sub>N]Br (0.50 g, 1.6 mmol) and the reaction mixture was stirred for 20 min. After filtration, a clear solution was obtained, which was added into water (300 mL). The resulting suspension was kept under vacuum to remove some of the acetone and induce precipitation of the product. The product was collected as a white solid, washed extensively with water and dried under high vacuum at 75 °C for 24 h. Yield: 0.49 g (73%).  $^1\text{H}$  NMR (499.891 MHz, methanol-d<sub>4</sub>)  $\delta$  = 7.48, 7.02, 6.52 (br m, styryl-H), 2.1-1.2 (br, 3H, CHCH<sub>2</sub>), 3.29, 1.70, 1.43, 0.87 (br, 36H, NBu<sub>4</sub>).  $^{13}\text{C}$  NMR (125.697 MHz, acetone-d<sub>6</sub>)  $\delta$  = 150 (br, styryl(borate)-C1, overlapped with one of the doublets of Pf-C2,6), 149.0 (d,  $^1J_{\text{CF}}$  = 241 Hz, Pf-C2,6), 138.4 (d,  $^1J_{\text{CF}}$  = 248 Hz, Pf-C4),

137.2 (d,  $^1J_{CF} = 248$  Hz, Pf-C3,5), 133.4 (styryl-C2,6), 128.9 (Pf-C1), 126.1 (styryl-C3,5), n.r. (styryl-C4), 52-38 (br m, CHCH<sub>2</sub>), 59.5, 24.4, 20.4, 13.8 (NBu<sub>4</sub>).  $^{11}\text{B}$  NMR (160.386 MHz, acetone-d<sub>6</sub>)  $\delta = -12.6$  ( $w_{1/2} = 90$  Hz).  $^{19}\text{F}$  NMR (470.362 MHz, acetone-d<sub>6</sub>)  $\delta = -129.5$  (6F, ortho-F),  $-166.4$  (3F, para-F),  $-168.6$  (6F, meta-F). GPC (RI):  $M_n = 52100$ ,  $M_w = 59700$ ,  $PDI = 1.14$ .

### **Synthesis of Poly(sodium triphenyl(styryl)borate)-*block*-polystyrene.**

A solution of PSSiMe<sub>3</sub>-*block*-PS (0.50 g, PSSiMe<sub>3</sub>:PS = 1:3.7,  $M_n = 18270$ ,  $M_w = 19480$ ,  $PDI = 1.07$ ; 0.89 mmol SiMe<sub>3</sub>) in CH<sub>2</sub>Cl<sub>2</sub> (10 mL) was added to a solution of BBr<sub>3</sub> (0.27 g, 1.08 mmol) in CH<sub>2</sub>Cl<sub>2</sub> (10 mL) in a glove box. The reaction mixture was stirred at room temperature for 24 h. Neat Me<sub>3</sub>SiOMe (0.5 mL, 3.6 mmol) was added into the reaction solution. After stirring for 3 h, all volatile compounds were removed under high vacuum. The white residue was redissolved in THF (30 mL), and a solution of PhMgBr (10 mL, 1M in THF, 10 mmol) was slowly added. The reaction mixture was then stirred at 85 °C for 3 h, allowed to cool down to room temperature, and poured into aqueous Na<sub>2</sub>CO<sub>3</sub> solution. The organic layer was separated and the aqueous layer was extracted three times with acetone (80 mL). The organic layers were combined, filtered, and the solvents were then evaporated under vacuum. The residue was dialyzed first against water and then against acetone (Fisherbrand regenerated cellulose membrane with 6000 to 8000 Dalton molecular weight cut-off). The resulting solution was filtered,

concentrated and then precipitated into hexanes to give an off-white solid, which was dried under high vacuum at 50 °C for 24 h. Yield: 0.47 g (70%).  $^1\text{H}$  NMR (499.891 MHz, acetone- $d_6$ )  $\delta$  = 7.33 (br, Ph(borate)-H2,6), 6.85 (br, Ph(borate)-H3,5), 6.7 (br, Ph(borate)-H4), 7.09 (br, styryl-H3,4,5), 6.68 (br, styryl-H2,6), styryl(borate) n.r., 2.6-1.0 (br, CHCH<sub>2</sub>),  $^{13}\text{C}$  NMR (125.697 MHz, acetone- $d_6$ )  $\delta$  = 165.6 (Ph(borate)-C1), 160.6 (br, styryl(borate)-C1), 146.5 (m, styrene), 140.4 (br, styryl(borate)-C4), 137.2 (Ph(borate)-C2,6), 136.7 (styryl(borate)-C2,6), 129.0 (styrene), 128.6 (styrene), 127.7 (styryl(borate)-C3,5), 126.6 (styrene), 126.0 (Ph(borate)-C3,5), 122.1 (Ph(borate)-C4), 48-39 (br m, CHCH<sub>2</sub>).  $^{11}\text{B}$  NMR (160.386 MHz, acetone- $d_6$ ) = -6.3 ( $w_{1/2}$  = 30 Hz). DLS (acetone):  $R_{h, \text{app}}$  = 1.5 nm; DLS (toluene):  $R_{h, \text{app}}$  = 15.7±5.21 nm.

**Conversion to Poly(tetrabutylammonium triphenyl(styryl)borate)-block-polystyrene.**

A solution of poly(sodium triphenyl(styryl)borate)-*block*-polystyrene prepared as described above (0.15 g, PSBPh<sub>3</sub>:PS = 1:3.7, 0.20 mmol borate) in acetone (3 mL) was slowly added into a solution of Bu<sub>4</sub>NBr (0.20 g, 0.62 mmol) in H<sub>2</sub>O (50 mL). A white precipitate formed after stirring for 1 h and evaporation of some of the acetone under vacuum. The solid was collected by filtration and washed extensively first with water and then hexanes, and dried under high vacuum at 50 °C for 12 h. Yield: 0.16 g (83%).  $^1\text{H}$  NMR (499.891 MHz, acetone- $d_6$ ) = 7.35 (br, Ph(borate)-H2,6), 6.96 (br,

Ph(borate)-H3,5), 6.8 (br, Ph(borate)-H4), 7.09 (br, styryl-H3,4,5), 6.78 (br, styryl-H2,6), styryl(borate) n.r., 2.4-1.0 (br, CHCH<sub>2</sub>), 2.71, 1.32, 1.15, 0.82 (br, 36H, NBu<sub>4</sub>). <sup>13</sup>C NMR (125.697 MHz, acetone-d<sub>6</sub>) = 165.9 (Ph(borate)-C1), 159.4 (br, styryl(borate)-C1), 146.4 (m, styrene), 141.1 (br, styryl(borate)-C4), 137.3 (Ph(borate)-C2,6), 136.7 (styryl(borate)-C2,6), 129.0 (styrene), 128.6 (m, styrene), 126.7 (styrene), 126.1 (Ph(borate)-C3,5), 122.3 (Ph(borate)-C4), 48-39 (br m, CHCH<sub>2</sub>), 59.1, 24.4, 20.3, 14.2 (br, NBu<sub>4</sub>). <sup>11</sup>B NMR (160.386 MHz, acetone-d<sub>6</sub>) = -6.2 (w<sub>1/2</sub> = 30 Hz). GPC (RI): M<sub>n</sub> = 28900, M<sub>w</sub> = 34500, PDI = 1.20. DLS (toluene): R<sub>h, app</sub> = 15.0±3.96 nm.

### **Synthesis of Poly(sodium tris(pentafluorophenyl)(styryl)borate)-*block*-polystyrene.**

The organoborate block copolymer was obtained in analogy to the procedure for the homopolymer from PSSiMe<sub>3</sub>-*block*-PS (1.00 g, PSSiMe<sub>3</sub>:PS = 1:3.7, M<sub>n</sub> = 18300, M<sub>w</sub> = 19500, PDI = 1.07; 1.78 mmol SiMe<sub>3</sub>) in CH<sub>2</sub>Cl<sub>2</sub> (10 mL), BBr<sub>3</sub> (0.54 g, 2.15 mmol) in CH<sub>2</sub>Cl<sub>2</sub> (10 mL), pentafluorophenylcopper (1.64 g, 7.12 mmol) in CH<sub>2</sub>Cl<sub>2</sub> (10 mL), and a solution of pentafluorophenylcopper (0.82 g, 3.56 mmol) in acetonitrile (25 mL). Yield: 1.20 g (66%). A similar procedure was used to prepare a block copolymer with a block ratio of 1:8.2. <sup>1</sup>H NMR (499.891 MHz, acetone-d<sub>6</sub>) δ = 7.10, 6.69 6.58 (br m, styryl-H), 2.5-1.4 (br m, CHCH<sub>2</sub>). <sup>13</sup>C NMR (125.719 MHz, acetone-d<sub>6</sub>) δ = 150 (br, styryl(borate)-C1, overlapped with one of the doublets of Pf-C2,6), 149.0 (d, <sup>1</sup>J<sub>CF</sub> = 237 Hz, Pf-C2,6), 146.5 (m, styrene), 138.4 (d, <sup>1</sup>J<sub>CF</sub> = 242 Hz, Pf-C4), 137.1 (d, <sup>1</sup>J<sub>CF</sub> = 246

Hz, Pf-C3,5), 133.4 (br, styryl(borate)-C2,6), 129.0 (styrene), 129 (br, Pf-C1, overlapped with styrene peak), 128.6 (m, styrene), 126.7 (styrene), 126.2 (br, styryl(borate)-C3,5), n.r. (styryl(borate)-C1), 49-38 (br m, CHCH<sub>2</sub>). <sup>11</sup>B NMR (160.386 MHz, acetone-d<sub>6</sub>)  $\delta$  = -13.1 ( $w_{1/2}$  = 120 Hz). <sup>19</sup>F NMR (470.365 MHz, acetone-d<sub>6</sub>)  $\delta$  = -129.7 (6F, ortho-F), -166.5 (3F, para-F), -168.6 (6F, meta-F). DLS (toluene, for block copolymer with 1:3.7 block copolymer):  $R_{h, app}$  = 14.8±3.9 nm.

**Conversion to Poly(tetrabutylammonium tris(pentafluorophenyl)(styryl)borate)-*block*-polystyrene.**

The product was obtained from poly(sodium tris(pentafluorophenyl)(styryl)borate)-*block*-polystyrene (0.50 g, PSBPf<sub>3</sub>:PS = 1:3.7, 0.49 mmol borate) and [Bu<sub>4</sub>N]Br (0.29 g, 0.90 mmol) using a procedure similar to that for the homopolymer. To remove any traces of [Bu<sub>4</sub>N]Br, a second precipitation from acetone into water was performed, and the white solid product obtained upon concentration under vacuum was collected by centrifugation and then dried at 75 °C under high vacuum for 24 h. Yield: 0.51 g (84%). A similar procedure was used to prepare a block copolymer with a block ratio of 1:8.2 and used for elemental analysis. <sup>1</sup>H NMR (499.891 MHz, acetone-d<sub>6</sub>)  $\delta$  = 7.09, 6.68, 6.57 (br m, styryl-H), 3.25, 1.67, 1.29, 0.84 (br, 36H, NBu<sub>4</sub>), 2.5-1.4 (br m, 3H, CHCH<sub>2</sub>). <sup>11</sup>B NMR (160.386 MHz, acetone-d<sub>6</sub>)  $\delta$  = -13.2 ( $w_{1/2}$  = 90 Hz). <sup>19</sup>F NMR (470.365 MHz, acetone-d<sub>6</sub>)  $\delta$  = -129.6 (6F, ortho-F), -166.9 (3F, para-F), -168.8 (6F, meta-F). GPC (RI,

for block copolymer with 1:3.7 block ratio):  $M_n = 28200$ ,  $M_w = 32700$ ,  $PDI = 1.16$ . DLS (toluene, for block copolymer with 1:3.7 block ratio):  $R_{h, app} = 14.8 \pm 1.7$  nm). DLS (MeOH, for block copolymer with 1:3.7 block ratio):  $R_{h, app} = 19.7 \pm 9.57$  nm. Elemental analysis for  $\{C_{42}H_{43}BF_{15}N\}_{29}\{C_8H_8\}_{239}$ : calcd C 75.51, H 6.40, N 0.82; found C 75.77, H 6.12, N 0.81%.

**Conversion to Poly[(1,5-cyclooctadiene)(1,4-bis(diphenylphosphino)butane)rhodium(I) tris(pentafluorophenyl)(styryl)borate]-*block*-polystyrene.**

To a slurry of (1,5-cyclooctadiene)(1,4-bis(diphenylphosphino)butane)rhodium(I) trifluoromethanesulfonate (0.10 g, 0.13 mmol) in tetrahydrofuran (5 mL), a solution of poly(sodium tris(pentafluorophenyl)(styryl)borate)-*block*-polystyrene (block ratio = 1:3.7; 0.10 g, 0.10 mmol borate) in tetrahydrofuran (5 mL) was added slowly. The reaction solution was kept stirring for 1 h, concentrated and then precipitated into a 1:1 mixture of hexanes and methanol (50 mL). The mixture was shaken vigorously and a light yellow solid was isolated by filtration and dried under high vacuum. Yield: 0.12 g (73%); degree of loading based on  $^1H$  NMR integration (cod vs. Ph signals): 37%.  $^1H$  NMR (499.976 MHz, DMSO- $d_6$ )  $\delta = 7.6$  (v br, styryl-H), 7.59 (br, PPh<sub>o</sub>), 7.51 (br, PPh<sub>m,p</sub>), 7.0 (v br, styryl-H), 6.55 (br, styryl-H), 4.36 (br, -CH=CH-), 2.47, 2.31, 2.15, 1.60 (4  $\times$  br, -CH<sub>2</sub>-), 2.2-1.0 (v br, backbone).  $^{11}B$  NMR (160.411 MHz, CDCl<sub>3</sub>)  $\delta = -13.3$  ( $w_{1/2} = 70$  Hz).  $^{19}F$  NMR (470.445 MHz, CDCl<sub>3</sub>)  $\delta = -128.2$  (br, 6F, ortho-F),

-163.8 (br, 3F, para-F), -166.4 (br, 6F, meta-F). DLS (toluene, for block copolymer with 1:3.7 block ratio):  $R_{h, app} = 21.9 \pm 5.4$  nm. DLS (MeOH/THF (4:1), for block copolymer with 1:3.7 block ratio):  $R_{h, app} = 13.1 \pm 5.2$  nm.

### **C.6.3 Micellization Experiments of Organoborate Polymers**

#### **Micellization in Toluene.**

A dialysis tube was rinsed with distilled water for 30 min and then charged with a solution of rhodium diblock copolymer (1 mg/mL, 10 mL) in tetrahydrofuran. Excess water from the rinsing process was removed by dialysis against tetrahydrofuran (150 mL). Then, the tetrahydrofuran solution of the diblock copolymer was dialyzed against toluene (3×150 mL). The resulting micellar solution was diluted with toluene to 0.5 mg/mL and filtered through a 0.45  $\mu$ m filter. This stock solution was further diluted with toluene for analysis by DLS (1 mg/mL) and TEM (0.05 mg/mL).

#### **Micellization of Organoborate Polymers in a Mixture of THF and Methanol.**

The rhodium diblock copolymer (10 mg) was dissolved in 2 mL of THF. Under vigorous stirring 8 mL of methanol were added dropwise. The final solution (1 mg/mL) was filtered through a 0.45  $\mu$ m filter prior to analysis by DLS. For TEM analysis, the polymer solution was diluted with methanol to a final concentration of 0.1 mg/mL.

## C.6.4 Synthesis of Model Compounds

### Synthesis of Sodium Triphenyl(*t*-butylphenyl)borate.

Under nitrogen protection, a solution of 4-dimethoxyboryl-*t*-butylbenzene (0.50 g, 2.43 mmol) in THF (20 mL) was added to a solution of PhMgBr in THF (8.5 mL, 1.0M, 8.5 mmol). The reaction mixture was stirred at 60 °C for 5 h and then poured into an aqueous Na<sub>2</sub>CO<sub>3</sub> solution. THF (50 mL) was added, the organic layer was separated, and the aqueous layer was washed twice with THF (30 mL). The organic layers were combined and a yellow oil was obtained after rotary evaporation. The residue was redissolved in ether (50 mL) and dried over Na<sub>2</sub>SO<sub>4</sub>. Addition of toluene (150 mL) followed by concentration to ca. 130 mL led to formation of a white precipitate, which was collected on a filter paper and washed with toluene and then hexanes. The white solid was dried under high vacuum for 10 h at 50 °C. Yield: 0.78 g (81%). <sup>1</sup>H NMR (499.896 MHz, acetone-d<sub>6</sub>) δ = 7.36 (m, 6H, Ph-H<sub>2,6</sub>), 7.29 (m, 2H, tPh-H<sub>2,6</sub>), 7.00 (d, <sup>3</sup>J = 8.0 Hz, 2H, tPh-H<sub>3,5</sub>), 6.93 (pst, <sup>3</sup>J = 7.5Hz, 6H, Ph-H<sub>3,5</sub>), 6.77 (t, <sup>3</sup>J = 7.5Hz, 3H, Ph-H<sub>4</sub>), 1.25 (s, 9H, *t*-Bu). <sup>13</sup>C NMR (125.698 MHz, acetone-d<sub>6</sub>) δ = 165.3 (quartet, <sup>1</sup>J<sub>CB</sub> = 49 Hz, Ph-C1), 161.2 (quartet, <sup>1</sup>J<sub>CB</sub> = 50 Hz, tPh-C1), 143.8 (tPh-C4), 137.1 (Ph-C<sub>2,6</sub>), 136.8 (tPh-C<sub>2,6</sub>), 126.0 (Ph-C<sub>3,5</sub>), 122.8 (tPh-C<sub>3,5</sub>), 122.2 (Ph-C4), 34.4 (Me<sub>3</sub>C), 32.2 (Me<sub>3</sub>C). <sup>11</sup>B NMR (160.386 MHz, acetone-d<sub>6</sub>) δ = -6.4 (w<sub>1/2</sub> = 10 Hz). High res MALDI-TOF MS (+ reflectron mode): m/z (Da) = 421.2076 (calcd for [Na<sub>2</sub>{(tBuPh)BPh<sub>3</sub>}]<sup>+</sup> 421.2079).

### Conversion to Tetrabutylammonium Triphenyl(*t*-butylphenyl)borate.

An aqueous solution of sodium triphenyl(*t*-butylphenyl)borate (0.20 g, 0.50 mmol) was added to an aqueous solution of [Bu<sub>4</sub>N]Br (0.65 g, 2.5 mmol). A very fine white suspension formed, which was stirred for 1 h. The reaction mixture was kept at 0 °C for 10 h, and then allowed to warm to room temperature. The chunky solid that formed was collected by filtration, washed first with H<sub>2</sub>O and then hexanes, and dried under high vacuum. Yield: 0.26 g (84%). <sup>1</sup>H NMR (499.891 MHz, acetone-d<sub>6</sub>) δ = 7.35 (br m, 6H, Ph-H<sub>2,6</sub>), 7.28 (m, 2H, *t*Ph-<sub>2,6</sub>), 6.99 (d, <sup>3</sup>J = 8.0 Hz, 2H, *t*Ph-H<sub>3,5</sub>), 6.92 (pst, <sup>3</sup>J = 7.5 Hz, 6H, Ph-H<sub>3,5</sub>), 6.77 (t, <sup>3</sup>J = 7.5 Hz, 3H Ph-<sub>4</sub>), 3.42 (t, <sup>3</sup>J = 8.5 Hz, 8H, CH<sub>2</sub>CH<sub>2</sub>CH<sub>2</sub>CH<sub>3</sub>), 1.81 (m, 8H, CH<sub>2</sub>CH<sub>2</sub>CH<sub>2</sub>CH<sub>3</sub>), 1.42 (m, 8H, CH<sub>2</sub>CH<sub>2</sub>CH<sub>2</sub>CH<sub>3</sub>), 1.24 (s, 9H, *t*-Bu), 0.98 (t, <sup>3</sup>J = 7.5 Hz, 12H, CH<sub>2</sub>CH<sub>2</sub>CH<sub>2</sub>CH<sub>3</sub>). <sup>13</sup>C NMR (125.698 MHz, acetone-d<sub>6</sub>) δ = 165.3 (quartet, <sup>1</sup>J<sub>CB</sub> = 49 Hz, Ph-C<sub>1</sub>), 161.0 (quartet, <sup>1</sup>J<sub>CB</sub> = 49 Hz, *t*Ph-C<sub>1</sub>), 143.9 (*t*Ph-C<sub>4</sub>), 137.1 (Ph-C<sub>2,6</sub>), 136.8 (*t*Ph-C<sub>2,6</sub>), 126.0 (Ph-C<sub>3,5</sub>), 122.8 (*t*Ph-C<sub>3,5</sub>), 122.2 (Ph-C<sub>4</sub>), 59.1 (NBu<sub>4</sub>), 34.4 (Me<sub>3</sub>C), 32.2 (Me<sub>3</sub>C), 24.4, 20.4, 13.9 (NBu<sub>4</sub>). <sup>11</sup>B NMR (160.386 MHz, acetone-d<sub>6</sub>) δ = -6.2 (w<sub>1/2</sub> = 10 Hz).

### Synthesis of Sodium Tris(pentafluorophenyl)(*t*-butylphenyl)borate.

A solution of pentafluorophenyl copper (0.84 g, 3.6 mmol) in CH<sub>2</sub>Cl<sub>2</sub> (15 mL) was added to a solution of 4-dibromoboryl-*t*-butylbenzene (0.50 g, 1.7 mmol) in CH<sub>2</sub>Cl<sub>2</sub> (10 mL). The reaction mixture was heated to 60 °C and stirred for 1 h. A solution of

pentafluorophenyl copper (0.42 g, 1.8 mmol) in acetonitrile (25 mL) was then added. The reaction mixture was heated to reflux for 1 h, cooled to room temperature and subsequently poured into an aqueous sodium carbonate solution (100 mL). The product was extracted with diethyl ether (3 × 100 mL). The organic layers were combined and dried over sodium sulfate. The volatile compounds were removed under vacuum leaving behind an oil, which was washed with hexanes. The remaining solid was redissolved with ether and recrystallized by slow solvent evaporation. The white crystalline product as washed with hexanes and then dried under high vacuum at 50 °C. Yield: 0.90 g (78 %).

$^1\text{H}$  NMR (499.884 MHz, acetone- $d_6$ )  $\delta$  = 7.20 (br d, 2H, tPh-H2,6), 7.02 (d,  $^3J$  = 8.5 Hz, 2H, tPh-H3,5), 1.23 (s, 9H, *t*-Bu).  $^{13}\text{C}$  NMR (125.696 MHz, acetone- $d_6$ )  $\delta$  = 150.9 (br, tPh-C1), 149.0 (d,  $^1J_{\text{CF}}$  = 246 Hz, Pf-C2,6), 145.8 (tPh-C4), 138.6 (d,  $^1J_{\text{CF}}$  = 243 Hz, Pf-C4), 137.2 (d,  $^1J_{\text{CF}}$  = 245 Hz, Pf-C3,5), 133.4 (tPh-C2,6), 128.5 (Pf-C1), 123.3 (tPh-C3,5), 34.6 ( $\text{Me}_3\text{C}$ ), 32.0 ( $\text{Me}_3\text{C}$ ).  $^{11}\text{B}$  NMR (160.386 MHz, acetone- $d_6$ )  $\delta$  = -12.3 ( $w_{1/2}$  = 30 Hz).  $^{19}\text{F}$  NMR (470.365 MHz, acetone- $d_6$ )  $\delta$  = -129.9 (d,  $^3J_{\text{FF}}$  = 20 Hz, 6F, ortho-F), -165.9 (t,  $^3J_{\text{FF}}$  = 20 Hz, 3F, para-F), -168.6 (pst,  $^3J_{\text{FF}}$  = 19 Hz, 6F, meta-F). High res MALDI-TOF MS (- reflectron mode):  $m/z$  (Da) = 645.1257 (calcd for  $[(\text{tBuPh})\text{B}(\text{C}_6\text{F}_5)_3]^-$  645.0870).

**Conversion to Tetrabutylammonium Tris(pentafluorophenyl)(*t*-butylphenyl)borate.**

An aqueous solution (10 mL) of sodium tris(pentafluorophenyl)(*t*-butylphenyl)borate (0.30 g, 0.43 mmol) was added to an aqueous solution (20 mL) of [Bu<sub>4</sub>N]Br (0.21 g, 0.64 mmol). After stirring for 1 h, a white precipitate was collected by centrifugation, washed extensively with water and then with hexanes. The white solid was dried at 50 °C under high vacuum. Yield: 0.29 g (73%). <sup>1</sup>H NMR (499.894 MHz, acetone-d<sub>6</sub>) δ = 7.20 (br d, <sup>3</sup>J = 7.0 Hz, 2H, *t*Ph-H<sub>2,6</sub>), 7.02 (d, <sup>3</sup>J = 8.0 Hz, 2H, *t*Ph-H<sub>3,5</sub>), 3.48 (t, <sup>3</sup>J = 8.5 Hz, 8H, CH<sub>2</sub>CH<sub>2</sub>CH<sub>2</sub>CH<sub>3</sub>), 1.84 (m, 8H, CH<sub>2</sub>CH<sub>2</sub>CH<sub>2</sub>CH<sub>3</sub>), 1.44 (m, 8H, CH<sub>2</sub>CH<sub>2</sub>CH<sub>2</sub>CH<sub>3</sub>), 1.23 (s, 9H, *t*-Bu), 0.98 (t, <sup>3</sup>J = 7.5 Hz, 12H, CH<sub>2</sub>CH<sub>2</sub>CH<sub>2</sub>CH<sub>3</sub>). <sup>13</sup>C NMR (125.697 MHz, acetone-d<sub>6</sub>) δ = 150.3 (br, *t*Ph-C<sub>1</sub>), 148.6 (d, <sup>1</sup>J<sub>CF</sub> = 240 Hz, Pf-C<sub>2,6</sub>), 145.8 (*t*Ph-C<sub>4</sub>), 138.2 (d, <sup>1</sup>J<sub>CF</sub> = 244 Hz, Pf-C<sub>4</sub>), 136.9 (d, <sup>1</sup>J<sub>CF</sub> = 245 Hz, Pf-C<sub>3,5</sub>), 132.9 (*t*Ph-C<sub>2,6</sub>), 128.2 (b, Pf-C<sub>1</sub>), 123.0 (*t*Ph-C<sub>3,5</sub>), 59.0 (Bu<sub>4</sub>N), 34.2 (Me<sub>3</sub>C), 31.6 (Me<sub>3</sub>C), 24.0, 20.0, 13.6 (Bu<sub>4</sub>N). <sup>11</sup>B NMR (160.386 MHz, acetone-d<sub>6</sub>) δ = -12.7 (w<sub>1/2</sub> = 50 Hz). <sup>19</sup>F NMR (470.365 MHz, acetone-d<sub>6</sub>) δ = -130.3 (d, <sup>3</sup>J<sub>FF</sub> = 20 Hz, 6F, *ortho*-F), -165.9 (t, <sup>3</sup>J<sub>FF</sub> = 20 Hz, 3F, *para*-F), -168.7 (pst, <sup>3</sup>J<sub>FF</sub> = 19 Hz, 6F, *meta*-F).

**Synthesis of (1,5-Cyclooctadiene)(1,4-bis(diphenylphosphino)butane)rhodium(I) trifluoromethanesulfonate.**

To a solution of bis(1,5-cyclooctadiene)rhodium(I) trifluoromethanesulfonate (0.65 g, 1.39 mmol) in tetrahydrofuran (50 mL), a solution of 1,4-bis(diphenylphosphino)butane

(0.59 g, 1.38 mmol) in tetrahydrofuran (50 mL) was slowly added. The reaction solution was kept stirring for 5 h and then concentrated to ca. 20 mL. An orange solid was isolated from the resulting slurry by filtration and washed with aliquots of tetrahydrofuran (3×10 mL). The product was obtained as a yellow solid and dried under high vacuum for 6 h. Yield: 0.93 g (86%). <sup>1</sup>H NMR (499.973 MHz, CDCl<sub>3</sub>) δ = 7.65 (br m, 8H, PPh<sub>o</sub>), 7.57 (br m, 12H, PPh<sub>m,p</sub>), 4.50 (br s, 4H, -CH=CH-), 2.49, 2.38, 2.22, 1.69 (4 × br m, 16H, -CH<sub>2</sub>-).

**Conversion to (1,5-Cyclooctadiene)(1,4-bis(diphenylphosphino) butane)rhodium(I) tris(pentafluorophenyl)(t-butylphenyl)borate.<sup>118c</sup>**

To a slurry of (1,5-cyclooctadiene)(1,4-bis(diphenylphosphino)butane)rhodium(I) trifluoromethanesulfonate (0.10 g, 0.13 mmol) in tetrahydrofuran (5 mL), a solution of sodium tris(pentafluorophenyl)(t-butylphenyl)borate (0.077 g, 0.12 mmol) in tetrahydrofuran (5 mL) was added slowly to give a yellow orange solution. After stirring for 1 h, the solvent was removed on a rotary evaporator. The residue redissolved in ethyl acetate and then passed through a silica gel with solvent gradients being varied from hexanes to ethyl acetate. A yellow solid was obtained after solvent evaporation under high vacuum. Yield: 0.12 g (78%). <sup>1</sup>H NMR (499.973 MHz, CDCl<sub>3</sub>) δ = 7.56 (m, 12H, PPh<sub>m,p</sub>), 7.49 (m, 8H, PPh<sub>o</sub>), 7.25 (d, <sup>3</sup>J = 7.5 Hz, 2H, tPh<sub>o</sub>), 7.03 (d, <sup>3</sup>J = 8.0 Hz, 2H, tPh<sub>m</sub>), 4.44 (br s, 4H, -CH=CH-), 2.44, 2.29, 2.22, 1.64 (4 × br m, 16H, -CH<sub>2</sub>-). <sup>11</sup>B NMR

(160.411 MHz, CDCl<sub>3</sub>)  $\delta = -12.9$  ( $w_{1/2} = 60$  Hz). <sup>19</sup>F NMR (470.445 MHz, CDCl<sub>3</sub>)  $\delta = -129.6$  (d, <sup>3</sup>J<sub>FF</sub> = 20.7, 6F, ortho-F),  $-164.5$  (t, <sup>3</sup>J<sub>FF</sub> = 20.0, 3F, para-F),  $-166.9$  (pst, <sup>3</sup>J<sub>FF</sub> = 20.0, 6F, meta-F).

## C.7 References

1. Hadjichristidis, N.; Pispas, S.; Floudas, G., *Block Copolymers: Synthetic Strategies, Physical Properties, and Applications*. Wiley Interscience: New York, 2003.
2. Matyjaszewski, K.; Müller, A. H. E., *Prog. Polym. Sci.* **2006**, *31* 1039-1040.
- 3.(a) Szwarc, M.; Levy, M.; Milkovich, R., *Journal of the American Chemical Society* **1956**, *78*, 2656-2657, (b) Szwarc, M., *Nature* **1956**, *178*, 1168-1169.
4. Quirk, R. P., Anionic Polymerization In *Encyclopedia of Polymer Science and Technology*, 3rd ed.; Kroschwitz, J. I., Ed.; Wiley-Interscience: New York, 2003; Vol. 5, p 111.
5. Smid, J., *Journal of Polymer Science Part A: Polymer Chemistry* **2002**, *40*, 2101-2107.
6. Odian, G., *Principles of Polymerization*. 4th ed.; John Wiley & Sons, Inc.: Hoboken, New Jersey, 2004.
7. Yu, J. M.; Dubois, P.; Teyssie, P.; Jerome, R., *Macromolecules* **1996**, *29*, 6090-6099.
8. Yu, J. M.; Yu, Y.; Dubois, P.; Teyssié, P.; Jérôme, R., *Polymer* **1997**, *38*, 3091-3101.
9. Higashihara, T.; Ueda, M., *Macromolecules* **2009**, ASAP.
10. Sawamoto, M., *Progress in Polymer Science* **1991**, *16*, 111-172.
11. Kennedy, J. P.; Iván, B., *Designed Polymers by Carbocationic Macromolecular Engineering: Theory and Practice*. Carl Hanser Verlag: Munich, 1992.
12. Kennedy, J. P.; Marechal, E., *Carbocationic Polymerization*. Wiley-Interscience: New York, 1982.
13. Kamigaito, M.; Sawamoto, M.; Higashimura, T., *Macromolecules* **1992**, *25*, 2587-2591.
- 14.(a) Novak, B. M.; Risse, W.; Grubbs, R. H., *Adv. Polym. Sci.* **1992**, *102* 47-72, (b) K. J. Ivin; J. C. Mol, *Olefin Metathesis and Metathesis Polymerization* Academic Press San Diego, CA, 1997, (c) Grubbs, R. H.; Khosravi, E., *Mater. Sci. Technol.* **1999**, *20*, 65-104, (d) Buchmeiser, M. R., *Chemical Reviews* **2000**, *100*, 1565-1604, (e) Frenzel, U.; Nuyken, O., *Journal of Polymer Science Part A: Polymer Chemistry* **2002**, *40*, 2895-2916.
15. Hérisson, P. J.-L.; Chauvin, Y., *Die Makromolekulare Chemie* **1971**, *141*, 161-176.
16. Cannizzo, L. F.; Grubbs, R. H., *Macromolecules* **1988**, *21*, 1961-1967.

- 17.(a)Schaverien, C. J.; Dewan, J. C.; Schrock, R. R., *Journal of the American Chemical Society* **1986**, *108*, 2771-2773, (b)Kress, J.; Osborn, J. A.; Greene, R. M. E.; Ivin, K. J.; Rooney, J. J., *J. Chem. Soc., Chem. Commun.* **1985**, 874 - 876, (c)F. Quignard, M. L., J.-M. Basset, *J. Chem. Soc. Chem. Commun.* **1985**, 1816-1817, (d)Katz, T. J.; Lee, S. J.; Shippey, M. A., *J. Mol. Catal.* **1980**, *8*, 219-226.
- 18.Schrock, R. R.; Feldman, J.; Cannizzo, L. F.; Grubbs, R. H., *Macromolecules* **1987**, *20*, 1169-1172.
- 19.Schrock, R. R., *Accounts of Chemical Research* **1990**, *23*, 158-165.
- 20.Murdzek, J. S.; Schrock, R. R., *Macromolecules* **1987**, *20*, 2640-2642.
- 21.Bielawski, C. W.; Grubbs, R. H., *Prog. Polym. Sci.* **2007**, *32*, 1-29.
- 22.Trzaska, S. T.; Lee, L.-B. W.; Register, R. A., *Macromolecules* **2000**, *33*, 9215-9221.
- 23.Nguyen, S. T.; Johnson, L. K.; Grubbs, R. H.; Ziller, J. W., *Journal of the American Chemical Society* **1992**, *114*, 3974-3975.
- 24.Bielawski, C. W.; Benitez, D.; Morita, T.; Grubbs, R. H., *Macromolecules* **2001**, *34*, 8610-8618.
- 25.Schwab, P.; Grubbs, R. H.; Ziller, J. W., *Journal of the American Chemical Society* **1996**, *118*, 100-110.
- 26.Ulman, M.; Grubbs, R. H., *The Journal of Organic Chemistry* **1999**, *64*, 7202-7207.
- 27.(a)Herrmann, W. A.; Köcher, C., *Angewandte Chemie International Edition in English* **1997**, *36*, 2162-2187, (b)Weskamp, T.; Schattenmann, W. C.; Spiegler, M.; Herrmann, W. A., *Angewandte Chemie International Edition* **1998**, *37*, 2490-2493, (c)Arduengo, A. J., *Accounts of Chemical Research* **1999**, *32*, 913-921, (d)Huang, J.; Schanz, H.-J.; Stevens, E. D.; Nolan, S. P., *Organometallics* **1999**, *18*, 5375-5380, (e)Bourissou, D.; Guerret, O.; Gabbai, F. P.; Bertrand, G., *Chemical Reviews* **2000**, *100*, 39-92.
- 28.(a)Choi, T.-L.; Grubbs, R. H., *Angewandte Chemie International Edition* **2003**, *42*, 1743-1746, (b)Sanford, M. S.; Love, J. A.; Grubbs, R. H., *Journal of the American Chemical Society* **2001**, *123*, 6543-6554, (c)Love, J. A.; Morgan, J. P.; Trnka, T. M.; Grubbs, R. H., *Angewandte Chemie International Edition* **2002**, *41*, 4035-4037.
- 29.Sanford, M. S.; Ulman, M.; Grubbs, R. H., *Journal of the American Chemical Society* **2001**, *123*, 749-750.
- 30.Moad, G.; Rizzardo, E.; Solomon, D. H., *Polymer Bulletin* **1982**, *6*, 589-593.
- 31.Georges, M. K.; Veregin, R. P. N.; Kazmaier, P. M.; Hamer, G. K., *Macromolecules* **1993**, *26*, 2987-2988.
- 32.Cunningham, M. F., *Comptes Rendus Chimie* **6**, 1351-1374.
- 33.Benoit, D.; Chaplinski, V.; Braslau, R.; Hawker, C. J., *Journal of the American Chemical Society* **1999**, *121*, 3904-3920.
- 34.Kuo, W. F.; Tong, S. N.; Pearce, E. M.; Kwei, T. K., *Journal of Applied Polymer Science* **1993**, *48*, 1297-1301.

35. Benoit, D.; Grimaldi, S.; Robin, S.; Finet, J.-P.; Tordo, P.; Gnanou, Y., *Journal of the American Chemical Society* **2000**, *122*, 5929-5939.
36. (a) Wang, J.-S.; Matyjaszewski, K., *Journal of the American Chemical Society* **1995**, *117*, 5614-5615, (b) Wang, J.-S.; Matyjaszewski, K., *Macromolecules* **1995**, *28*, 7901-7910.
37. Kato, M.; Kamigaito, M.; Sawamoto, M.; Higashimura, T., *Macromolecules* **1995**, *28*, 1721-1723.
38. Matyjaszewski, K.; Xia, J., *Chem. Rev.* **2001**, *101*, 2921-2990.
39. (a) Shipp, D. A.; Wang, J.-L.; Matyjaszewski, K., *Macromolecules* **1998**, *31*, 8005-8008, (b) Zhang, X.; Matyjaszewski, K., *Macromolecules* **1999**, *32*, 1763-1766.
40. Tang, W.; Matyjaszewski, K., *Macromolecules* **2006**, *39*, 4953-4959.
41. Vana, P.; Davis, T. P.; Barner-Kowollik, C., *Macromolecular Theory and Simulations* **2002**, *11*, 823-835.
42. Barner-Kowollik, C., *Handbook of RAFT Polymerization*. Wiley-VCH Verlag GmbH & Co. KGaA: Weinheim, 2008
43. Chong, Y. K.; Krstina, J.; Le, T. P. T.; Moad, G.; Postma, A.; Rizzardo, E.; Thang, S. H., *Macromolecules* **2003**, *36*, 2256-2272.
44. Zhang, L.; Chen, Y., *Polymer* **2006**, *47*, 5259-5266.
45. Matyjaszewski, K.; Davis, K. A., Statistical, Gradient, Block and Graft Copolymers by Controlled/Living Radical Polymerizations, In *Advances in Polymer Science*, Springer-Verlag: Berlin Heidelberg, 2002; Vol. 159, p 169.
46. Bates, F. S.; Fredrickson, G. H., *Physics Today* **1999**, *52*, 32-38.
47. Painter, P. C.; Coleman, M. M., *Essentials of Polymer Science and Engineering*. DEStech Publications, Inc. : Lancaster, PA, 2008.
48. Sun, S.-S.; Sariciftci, N. S., *Organic photovoltaics: mechanism, materials, and devices*. Taylor & Francis Group: Boca Raton, FL, 2005.
49. Matsen, M. W.; Bates, F. S., *Macromolecules* **1996**, *29*, 1091-1098.
50. Matsen, M. W.; Schick, M., *Physical Review Letters* **1994**, *72*, 2660-2663.
51. Hamley, I. W., *Nanotechnology* **2003**, *14*, R39-R54.
52. Shin, K.; Leach, K. A.; Goldbach, J. T.; Kim, D. H.; Jho, J. Y.; Tuominen, M.; Hawker, C. J.; Russell, T. P., *Nano Letters* **2002**, *2*, 933-936.
53. Lund, R.; Willner, L.; Monkenbusch, M.; Panine, P.; Narayanan, T.; Colmenero, J.; Richter, D., *Physical Review Letters* **2009**, *102*, 188301-188304.
54. Kataoka, K.; Harada, A.; Nagasaki, Y., *Advanced Drug Delivery Reviews* **2001**, *47*, 113-131.
55. (a) Ewen, J. A.; Edler, M. J.; (Fina Technology, Inc., United State), Application: EP 0427697, 1991, (b) Ewen, J. A.; Edler, M. J.; (Fina Technology, Inc., United State), Application: US 5561092, 1996, (c) Yang, X.; Stern, C. L.; Marks, T. J., *Journal of the American Chemical Society* **2002**, *113*, 3623-3625, (d) Yang, X.; Stern, C. L.; Marks, T.

- J., *Journal of the American Chemical Society* **1991**, *113*, 3623-3625, (e)Yang, X. M.; Stern, C. L.; Marks, T. J., *J. Am. Chem. Soc.* **1994**, *116*, 10015-10031.
- 56.Piers, W. E.; Chivers, T., *Chem. Soc. Rev.* **1997**, *26*, 345-354.
- 57.Yamaguchi, S.; Akiyama, S.; Tamao, K., *J. Am. Chem. Soc.* **2001**, *123*, 11372-11375.
- 58.Hudnall, T. W.; Gabbai, F. P., *J. Am. Chem. Soc.* **2007**, *129*, 11978-11986.
- 59.Mark, J. E.; Allcock, H. R.; West, R., *Inorganic Polymers*. Oxford University Press: Oxford, 2004.
- 60.Manners, I., *Angew. Chem. Int. Ed.* **1996**, *35*, 1602-1621.
- 61.(a)Qin, Y.; Cheng, G.; Sundararaman, A.; Jäkle, F., *J. Am. Chem. Soc.* **2002**, *124*, 12672-12673, (b)Qin, Y.; Cheng, G.; Parab, K.; Achara, O.; Jäkle, F., *Macromolecules* **2004**, *37*, 7123-7131.
- 62.Qin, Y.; Sukul, V.; Pagakos, D.; Cui, C.; Jäkle, F., *Macromolecules* **2005**, *38*, 8987-8990.
- 63.(a)Shiomori, K.; Ivanov, A. E.; Galaev, I. Y.; Kawano, Y.; Mattiasson, B., *Macromol. Chem. Phys.* **2004**, *205*, 27-34, (b)Kataoka, K.; Miyazaki, H.; Okano, T.; Sakurai, Y., *Macromolecules* **1994**, *27*, 1061-2, (c)Kikuchi, A.; Suzuki, K.; Okabayashi, O.; Hoshino, H.; Kataoka, K.; Sakurai, Y.; Okano, T., *Analytical Chemistry* **1996**, *68*, 823-8.
- 64.(a)Kanazawa, H.; Kashiwase, Y.; Yamamoto, K.; Matsushima, Y.; Kikuchi, A.; Sakurai, Y.; Okano, T., *Analytical Chemistry* **1997**, *69*, 823-830, (b)Yakushiji, T.; Sakai, K.; Kikuchi, A.; Aoyagi, T.; Sakurai, Y.; Okano, T., *Analytical Chemistry* **1999**, *71*, 1125-1130.
- 65.Cambre, J. N.; Roy, D.; Gondi, S. R.; Sumerlin, B. S., *J. Am. Chem. Soc.* **2007**, *129*, 10348-10349.
- 66.Roy, D.; Cambre, J. N.; Sumerlin, B. S., *Chem. Commun.* **2008**, 2477-2479.
- 67.Roy, D.; Cambre, J. N.; Sumerlin, B. S., *Chem. Commun.* **2009**, 2106-2108.
- 68.Kim, K. T.; Cornelissen, J. J. L. M.; Nolte, R. J. M.; van Hest, J. C. M., *Adv. Mater.* **2009**, *21*, 2787-2791.
- 69.(a)Dai, J.; Ober, C. K.; Wang, L.; Cerrina, F.; Nealey, P. F. Proceedings of the SPIE, Fedynyshyn, T. H., Ed. 4690, 1193-1202,2002, (b)Dai, J.; Ober, C. K. Proceedings of the SPIE, Sturtevant, J. L., Ed. 5376, 508-516,2004.
- 70.Chen, W.; Mehta, S. C.; Lu, D. R., *Advanced Drug Delivery Reviews* **1997**, *26*, 231-247.
- 71.Simon, Y. C.; Ohm, C.; Zimny, M. J.; Coughlin, E. B., *Macromolecules* **2007**, *40*, 5628-5630.
- 72.Malenfant, P. R. L.; Wan, J. L.; Taylor, S. T.; Manoharan, M., *Nature Nanotechnol.* **2007**, *2*, 43-46.
- 73.Nagai, A.; Miyake, J.; Kokado, K.; Nagata, Y.; Chujo, Y., *Journal of the American Chemical Society* **2008**, *130*, 15276-15278.

- 74.Zhang, G.; Fiore, G. L.; St. Clair, T. L.; Fraser, C. L., *Macromolecules* **2009**, *42*, 3162-3169.
- 75.Piers, W. E.; Bourke, S. C.; Conroy, K. D., *Angew. Chem. Int. Ed.* **2005**, *44*, 5016-5036.
- 76.Fox, P. A.; Griffin, S. T.; Reichert, W. M.; Salter, E. A.; Smith, A. B.; Tickell, M. D.; Wicker, B. F.; Cioffi, E. A.; Davis, J. H.; Rogers, R. D.; Wierzbicki, A., *Chem. Commun.* **2005**, 3679-3681.
- 77.(a)Biani, F. F. d.; Gmeinwieser, T.; Herdtweck, E.; Jäkle, F.; Laschi, F.; Wagner, M.; Zanello, P., *Organometallics* **1997**, *16*, 4776-4787, (b)Tonzola, C. J.; Alam, M. M.; Jenekhe, S. A., *Advanced Materials* **2002**, *14*, 1086-1090, (c)Ding, L.; Ma, K.; Dürner, G.; Bolte, M.; de Biani, F. F.; Zanello, P.; Wagner, M., *J. Chem. Soc., Dalton Trans.* **2002**, 1566-1573, (d)Scheibitz, M.; Heilmann, J. B.; Winter, R. F.; Bolte, M.; Bats, J. W.; Wagner, M., *Dalton Trans.* **2005**, 159-170.
- 78.Skvortsova, E. K.; Putyatina, T. I.; Mikhailov, B. M.; Dorokhov, V. A.; Shchegoleva, T. I.; Kamennov, N. A.; Limanov, V. E.; Starkov, A. V., *Trudy Tsentral'nogo Nauchno-Issledovatel'skogo Dezinfeksionnogo Instituta* **1967**, *18*, 154-156.
- 79.(a)Tonzola, C. J.; Alam, M. M.; Jenekhe, S. A., *Advanced Materials (Weinheim, Germany)* **2002**, *14*, 1086-1090, (b)Braunschweig, H.; Radacki, K.; Seeler, F.; Whittell, G. R., *Organometallics* **2006**, *25*, 4605-4610, (c)Hartmann, H., *Z. Naturforsch. B - Chem. Sci.* **2006**, *61*, 360-372, (d)Davis, L. H.; Madura, L. D., *Tetrahedron Lett.* **1996**, *37*, 2729-2730, (e)Jutzi, P.; Krato, B.; Hursthouse, M.; Howes, A. J., *Chem. Ber.* **1987**, *120*, 1091-8, (f)Braunschweig, H.; Kaupp, M.; Lambert, C.; Nowak, D.; Radacki, K.; Schinzel, S.; Uttinger, K., *Inorg. Chem.* **2008**, *47*, 7456-7458.
- 80.(a)Li, J.; Duan, M.; Zhang, L. H.; Jiang, X. H., *Prog. Chem.* **2007**, *19*, 1754-1760, (b)Nandivada, H.; Jiang, X. W.; Lahann, J., *Adv. Mater.* **2007**, *19*, 2197-2208, (c)Moses, J. E.; Moorhouse, A. D., *Chem. Soc. Rev.* **2007**, *36*, 1249-1262, (d)Gil, M. V.; Arevalo, M. J.; Lopez, O., *Synthesis-Stuttgart* **2007**, 1589-1620, (e)Binder, W. H.; Sachsenhofer, R., *Macromol. Rap. Comm.* **2007**, *28*, 15-54.
- 81.(a)Miyazaki, T.; Sugawara, M.; Danjo, H.; Imamoto, T., *Tetrahedron Lett.* **2004**, *45*, 9341-9344, (b)Yamamoto, Y.; Koizumi, T.; Katagiri, K.; Furuya, Y.; Danjo, H.; Imamoto, T.; Yamaguchi, K., *Org. Lett.* **2006**, *8*, 6103-6106, (c)Mlodzianowska, A.; Latos-Grayzynski, L.; Szterenber, L.; Stepien, M., *Inorg. Chem.* **2007**, *46*, 6950-6957, (d)Hodgkins, T. G.; Powell, D. R., *Inorg. Chem.* **1996**, *35*, 2140-2148.
- 82.Lu, S.; Pan, J.; Huang, A.; Zhuang, L.; Lu, J., *Proc. Natl. Acad. Sci. U. S. A.* **2008**, *105*, 20611-20614.
- 83.Li, X.; De Feyter, S.; Chen, D.; Aldea, S.; Vandezande, P.; Du Prez, F.; Vankelecom, I. F. J., *Chem. Mater.* **2008**, *20*, 3876-3883.
- 84.Lim, H. S.; Lee, S. G.; Lee, D. H.; Lee, D. Y.; Lee, S.; Cho, K., *Adv. Mater.* **2008**, *20*, 4438-4441.

85. Zhang, Z.; Cheng, G.; Carr, L. R.; Vaisocherova, H.; Chen, S.; Jiang, S., *Biomaterials* **2008**, *29*, 4719-4725.
- 86.(a) Sakurai, Y.; Sasaki, A.; Kobayashi, T., *Nuclear Instruments & Methods in Physics Research, Section A: Accelerators, Spectrometers, Detectors, and Associated Equipment* **2004**, *522*, 455-461, (b) Simon, Y. C.; Peterson, J. J.; Mangold, C.; Carter, K. R.; Coughlin, E. B., *Macromolecules* **2009**, *42*, 512-516.
87. Cui, C.; Jäkle, F., *Chem. Commun.* **2009**, 2744-2746
- 88.(a) Eriksson, H.; Håkansson, M., *Organometallics* **1997**, *16*, 4243-4244, (b) Sundararaman, A.; Jäkle, F., *J. Organomet. Chem.* **2003**, *681*, 134-142.
89. Parab, K.; Venkatasubbaiah, K.; Jäkle, F., *J. Am. Chem. Soc.* **2006**, *128*, 12879-12885.
90. Cui, C.; Bonder, E. M.; Jäkle, F., *Journal of Polymer Science Part A: Polymer Chemistry* **2009**, *47*, 6612-6618.
- 91.(a) Eisenberg, A.; Kim, J.-S., *Introduction to Ionomers*. Wiley Interscience: New York, 1998, (b) Bates, F. S., *Science* **1991**, *251*, 898-905, (c) Förster, S.; Antonietti, M., *Adv. Mater.* **1998**, *10*, 195-217.
- 92.(a) Iyengar, D. R.; Perutz, S. M.; Dai, C.-A.; Ober, C. K.; Kramer, E. J., *Macromolecules* **1996**, *29*, 1229-1234, (b) Dai, J.; Ober, C. K., *Proc. SPIE-Int. Soc. Opt. Eng.* **2004**, *5376 (Pt. 1, Advances in Resist Technology and Processing XXI)*, 508-516, (c) Qin, Y.; Sukul, V.; Pagakos, D.; Cui, C.; Jäkle, F., *Polym. Prepr.* **2005**, *46(2)*, 351-352, (d) Wei, X. L.; Carroll, P. J.; Sneddon, L. G., *Chem. Mater.* **2006**, *18*, 1113-1123.
- 93.(a) Manners, I., *Angew. Chem., Int. Ed.* **2007**, *46*, 1565-1568, (b) Avgeropoulos, A.; Chan, V. A.-H.; Lee, V. Y.; Ngo, D.; Miller, R. D.; Hadjichristidis, N.; Thomas, E. L., *Chem. Mater.* **1998**, *10*, 2109-1225, (c) Kulbaba, K.; Manners, I., *Macromol. Rap. Comm.* **2001**, *22*, 711-724, (d) Cohen, S.; Bano, M. C.; Visscher, K. B.; Chow, M.; Allcock, H. R.; Langer, R., *J. Am. Chem. Soc.* **1990**, *112*, 7832-7833, (e) Seki, T.; Tohnai, A.; Tanigaki, N.; Yase, K.; Tamaki, T.; Kaito, A., *Macromolecules* **1997**, *30*, 1768-1775, (f) Power-Billard, K. N.; Manners, I., *Macromol. Rap. Comm.* **2002**, *23*, 607-611, (g) Chen, B. Z.; Sleiman, H. F., *Macromolecules* **2004**, *37*, 5866-5872, (h) Allcock, H. R.; Powell, E. S.; Chang, Y.; Kim, C., *Macromolecules* **2004**, *37*, 7163-7167, (i) Miinea, L. A.; Sessions, L. B.; Ericson, K. D.; Glueck, D. S.; Grubbs, R. B., *Macromolecules* **2004**, *37*, 8967-8972, (j) Chang, Y.; Powell, E. S.; Allcock, H. R., *J. Polym. Sci. A: Polym. Chem.* **2005**, *43*, 2912-2920, (k) Cheng, K. W.; Chan, W. K., *Langmuir* **2005**, *21*, 5247-5250, (l) Tse, C. W.; Lam, L. S. M.; Man, K. Y. K.; Wong, W. T.; Chan, W. K., *J. Polym. Sci., Part A: Polym. Chem.* **2005**, *43*, 1292-1308, (m) Nair, K. P.; Pollino, J. M.; Weck, M., *Macromolecules* **2006**, *39*, 931-940, (n) South, C. R.; Higley, M. N.; Leung, K. C. F.; Lanari, D.; Nelson, A.; Grubbs, R. H.; Stoddart, J. F.; Weck, M., *Chem.--Eur. J.* **2006**, *12*, 3789-3797, (o) Noonan, K. J. T.; Gates, D. P., *Angew. Chem., Int. Ed.* **2006**, *45*, 7271-7274, (p) Rider, D. A.; Winnik, M. A.; Manners, I., *Chem. Commun.* **2007**,

- 4483-4485, (q)Aamer, K. A.; Tew, G. N., *J. Polym. Sci., Part A: Polym. Chem.* **2007**, *45*, 1109-1121, (r)Metera, K. L.; Sleiman, H., *Macromolecules* **2007**, *40*, 3733-3738, (s)Aamer, K. A.; de Jeu, W. H.; Tew, G. N., *Macromolecules* **2008**, *41*, 2022-2029, (t)Noonan, K. J. T.; Gillon, B. H.; Cappello, V.; Gates, D. P., *J. Am. Chem. Soc.* **2008**, *130*, 12876-12877, (u)Wang, Y.; Zou, S.; Kim, K. T.; Manners, I.; Winnik, M. A., *Chem.-Eur. J.* **2008**, *14*, 8624-8631.
- 94.Beach, M. W.; Rondan, N. G.; Froese, R. D.; Gerhart, B. B.; Green, J. G.; Stobby, B. G.; Shmakov, A. G.; Shvartsberg, V. M.; Korobeinichev, O. P., *Polymer Degradation and Stability* **2008**, *93*, 1664-1673.
- 95.Qin, Y.; Kiburu, I.; Shah, S.; Jakle, F., *Org. Lett.* **2006**, *8*, 5227-5230.
- 96.Tsuda, T.; Yazawa, T.; Watanabe, K.; Fujii, T.; Saegusa, T., *J. Org. Chem.* **1981**, *46*, 192-194.
- 97.Thayer, A. M., *Chem. Eng. News* **1995**, *73*, 15-20.
- 98.Strauss, S. H., *Chem. Rev.* **1993**, *93*, 927.
- 99.Lambert, J. B.; Zhang, S.; Stern, C. L.; Huffman, J. C., *Science* **1993**, *260*, 1917-1918.
- 100.LeSuer, R. J.; Geiger, W. E., *Angew. Chem., Int. Ed.* **2000**, *39*, 248-250.
- 101.Matsumi, N.; Sugai, K.; Ohno, H., *Macromolecules* **2002**, *35*, 5731-5732.
- 102.Abd-El-Aziz, A. S.; Carraher Jr., C. E.; Pittman Jr., C. U.; Zeldin, M., *Macromolecules Containing Metal and Metal-Like Elements, Volume 8, Boron-Containing Polymers*. John Wiley & Sons: Hoboken, 2007.
- 103.Ohno, H., *Electrochemical Aspects of Ionic Liquids*. Wiley-Interscience: New York,, 2005.
- 104.Walden, P., *Z. Phys. Chem.* **1911**, *78*, 257-283.
- 105.Zhou, Z.-B. H.; Matsumoto, H.; Tatsumi, K., *Chem. Eur. J.* **2004**, *10*, 6581-6591.
- 106.Shin, J.-H.; Henderson, W. A.; Passerini, S., *Electrochem. Commun.* **2003**, *5*, 1016-1020.
- 107.Narita, A.; Shibayama, W.; Sakamoto, K.; Mizumo, T.; Matsumi, N.; Ohno, H., *Chem. Commun.* **2006**, 1926-1928.
- 108.Sablong, R.; van der Vlugt, J. I.; Thomann, R.; Mecking, S.; Vogt, D., *Advanced Synthesis & Catalysis* **2005**, *347*, 633-636.
- 109.(a)Ono, M.; Hinokuma, S.; Miyake, S.; Inazawa, S.; (Japanes Polyolefin Co., Ltd., Japan), Application: EP 0710663A1, 1996, (b)Kanamaru, M.; Fujikawa, S.; Okamoto, T.; (Idemitsu Petrochemical Co., Ltd., Japan), Application: JP 11286491, 1999, (c)Kanamaru, M.; Okamoto, T.; Okuda, F.; Kamisawa, M.; (Idemitsu Petrochemical Co., Ltd. Japan), Application: JP 2000212225, 2000, (d)Sivak, A. J.; Zambelli, A.; (Sunoco, Inc. (R&M), USA). Application: US 6465385, 2002.
- 110.Mager, M.; Becke, S.; Windisch, H.; Denninger, U., *Angew. Chem. Int. Ed.* **2001**, *40*, 1898-1902.

111. Kishi, N.; Ahn, C. H.; Jin, J.; Uozumi, T.; Sano, T.; Soga, K., *Polymer* **2000**, *41*, 4005-4012.
112. Roscoe, S. B.; Fréchet, J. M. J.; Walzer, J. F.; Dias, A. J., *Science* **1998**, *280*, 270-273.
113. Schwab, E.; Mecking, S., *Organometallics* **2001**, *20*, 5504-5506.
114. Cui, C.; Bonder, E. M.; Jäkle, F., *Weakly-Coordinating Amphiphilic Organoborate Block Copolymers*, Rutgers University in Newark, NJ, 2009
115. Roy, D.; Cambre, J. N.; Sumerlin, B. S., *Chem. Commun.* **2009**, 2106-2108.
116. Qin, Y.; Sukul, V.; Pagakos, S.; Cui, C.; Jäkle, F., *Macromolecules* **2005**, *38*, 8987-8990.
117. Muetterties, E. L., *The Chemistry of Boron and Its Compounds*. John Wiley & Sons, Inc.: New York, London, Sydney, 1967.
118. (a) Zhou, Z.; Facey, G.; James, B. R.; Alper, H., *Organometallics* **1996**, *15*, 2496-2503, (b) Guzel, B.; Omary, M. A.; Fackler, J. P.; Akgerman, A., *Inorg. Chim. Acta* **2001**, *325*, 45-50, (c) van den Broeke, J.; de Wolf, E.; Deelman, B. J.; van Koten, G., *Adv. Synth. Catal.* **2003**, *345*, 625-635.
119. Herzog, A.; Maderna, A.; Harakas, G. N.; Knobler, C. B.; Hawthorne, M. F., *Chem.-Eur. J.* **1999**, *5*, 1212-1217.
120. (a) Cairncross, A.; Sheppard, W. A.; Wonchoba, E.; Guildford, W. J.; House, C. B.; Coates, R. M., *Org. Synth.* **1980**, *59*, 122-131, (b) Sundararaman, A.; Lalancette, R. A.; Zakharov, L. N.; Rheingold, A. L.; Jäkle, F., *Organometallics* **2003**, *22*, 3526-3532.
121. (a) Trofimenko, S., *J. Am. Chem. Soc.* **1966**, *88*, 1842-1844, (b) Trofimenko, S., *J. Coord. Chem.* **1972**, *2*, 75-77.
122. (a) Trofimenko, S., *Chem. Rev.* **2002**, *93*, 943-980, (b) Marques, N.; Sella, A.; Takats, J., *Chem. Rev.* **2002**, *102*, 2137-2160, (c) Dias, H. V. R.; Lovely, C. J., *Chem. Rev.* **2008**, *108*, 3223-3238, (d) Trofimenko, S., *Polyhedron* **2004**, *23*, 197-203.
123. Pettinari, C., *Inorg. Chim. Acta* **2009**, *362*, 4273-4275.
124. Trofimenko, S., *Scorpionates: Polypyrazolylborate Ligands and Their Coordination Chemistry*. Imperial College Press: London, 1999.
125. Trofimenko, S., *Chem. Rev.* **1993**, *93*, 943-980.
126. Sohrin, Y.; Kokusen, H.; Matsui, M., *Inorg. Chem.* **2002**, *34*, 3928-3934.
127. Oliver, J. D.; Mullica, D. F.; Hutchinson, B. B.; Milligan, W. O., *Inorg. Chem.* **1980**, *19*, 165-169.
128. Trofimenko, S.; Calabrese, J. C.; Domaille, P. J.; Thompson, J. S., *Inorg. Chem.* **2002**, *28*, 1091-1101.
129. Szczipura, L. F.; Witham, L. M.; Takeuchi, K. J., *Coord. Chem. Rev.* **1998**, *174*, 5-32.
130. Garcia, F.; Hopkins, A. D.; Humphrey, S. M.; McPartlin, M.; Rogers, M. C.; Wright, D. S., *Dalton Transactions* **2004**, 361-362.

131. Garcia, F.; Hopkins, A. D.; Kowenicki, R. A.; McPartlin, M.; Rogers, M. C.; Wright, D. S., *Organometallics* **2004**, *23*, 3884-3890.
132. Beswick, M. A.; Belle, C. J.; Davies, M. K.; Halcrow, M. A.; Raithby, P. R.; Steiner, A.; Wright, D. S., *Dalton Trans.* **2004**, 361 - 362.
133. Garcia, F.; Hopkins, A. D.; Kowenicki, R. A.; McPartlin, M.; Rogers, M. C.; Silvia, J. S.; Wright, D. S., *Organometallics* **2006**, *25*, 2561-2568.
134. Beswick, M. A.; Davies, M. K.; Raithby, P. R.; Steiner, A.; Wright, D. S., *Organometallics* **1997**, *16*, 1109-1110.
135. López-Linares, F.; Fuentes, A.; Tenia, R.; Martinez, M.; Karam, A., *Reaction Kinetics and Catalysis Letters* **2007**, *92*, 285-292.
136. Garcia, F.; Hopkins, A. D.; Kowenicki, R. A.; McPartlin, M.; Silvia, J. S.; Rawson, J. M.; Rogers, M. C.; Wright, D. S., *Chem. Commun.* **2007**, 586-588.
137. Khaskin, E.; Zavalij, P. Y.; Vedernikov, A. N., *J. Am. Chem. Soc.* **2006**, *128*, 13054-13055.
- 138.(a) Bullock, T. H.; Chan, W. T. K.; Wright, D. S., *Dalton Transactions* **2009**, 6709-6711, (b) Bullock, T. H.; Chan, W. T. K.; Eisler, D. J.; Streib, M.; Wright, D. S., *Dalton Transactions* **2009**, 1046-1054.
139. Alvarez, C. S.; García, F.; Humphrey, S. M.; Hopkins, A. D.; Kowenicki, R. A.; McPartlin, M.; Layfield, R. A.; Raja, R.; Rogers, M. C.; Woods, A. D.; Wright, D. S., *Chem. Commun.* **2005**, 198 - 200.
140. Fox, J. D.; Rowan, S. J., *Macromolecules* **2009**, *42*, 6823-6835.
141. Bergbreiter, D. E., *Chem. Rev.* **2002**, *102*, 3345-3384.
- 142.(a) Hofmeier, H.; Schubert, U. S., *Chem. Soc. Rev.* **2004**, *33*, 373-399, (b) Schubert Ulrich, S.; Eschbaumer, C., *Angew. Chem. Int. Ed.* **2002**, *41*, 2892-2926.
- 143.(a) Dobrawa, R.; Lysetska, M.; Ballester, P.; Gruene, M.; Wuerthner, F., *Macromolecules* **2005**, *38*, 1315-1325, (b) Gohy, J. F.; Lohmeijer, B. G. G.; Varshney, S. K.; Schubert, U. S., *Macromolecules* **2002**, *35*, 7427-7435.
144. Gohy, J.-F.; Lohmeijer, B. G. G.; Alexeev, A.; Wang, X.-S.; Manners, I.; Winnik, M. A.; Schubert, U. S., *Chem. Eur. J.* **2004**, *10*, 4315-4323.
145. Balzani, V.; Juris, A.; Venturi, M.; Campagna, S.; Serroni, S., *Chem. Rev.* **1996**, *96*, 759-834.
146. Shunmugam, R.; Tew, G. N., *J. Polym. Sci., Part A: Polym. Chem.* **2005**, *43*, 5831-5843.
147. Shunmugam, R.; Tew, G. N., *Polym. Adv. Technol.* **2008**, *19*, 596-601.
148. Heller, M.; Schubert, U. S., *Macromol. Rapid Comm.* **2002**, *23*, 411-415.
- 149.(a) F. F. de Biani; Jäkle, F.; Spiegler, M.; Wagner, M.; Zanello, P., *Inorg. Chem.* **1997**, *36*, 2103-2111, (b) Guo, S. L.; Peters, F.; de Biani, F. F.; Bats, J. W.; Herdtweck, E.; Zanello, P.; Wagner, M., *Inorg. Chem.* **2001**, *40*, 4928-4936.
150. Qin, Y.; Cui, C.; Jäkle, F., *Macromolecules* **2008**, *41*, 2972-2974.

- 151.(a)Trécourt, F.; Breton, G.; Bonnet, V.; Mongin, F.; Marsais, F.; Quéguiner, G., *Tetrahedron Lett.* **1999**, *40*, 4339-4342, (b)Martin, G. J.; Mechin, B.; Leroux, Y.; Paulmier, C.; Meunier, J. C., *Journal of Organometallic Chemistry* **1974**, *67*, 327-339, (c)Krasovskiy, A.; Knochel, P., *Angewandte Chemie International Edition* **2004**, *43*, 3333-3336.
- 152.Churakov, A. V.; Krut'ko, D. P.; Borzov, M. V.; Kirsanov, R. S.; Belov, S. A.; Howard, J. A. K., *Acta Cryst. E* **2006**, *62*, m1094-m1096.
- 153.Anderson, P. A.; Astley, T.; Hitchman, M. A.; Keene, F. R.; Moubaraki, B.; Murray, K. S.; Skelton, B. W.; Tiekink, E. R. T.; Toftlund, H.; White, A. H., *J. Chem. Soc., Dalton Transactions* **2000**, 3505-3512.
- 154.Moore, E. A.; Abel, E. W.; Janes, R., *Metal-Ligand Bonding*. The Open University: Milton Keynes, United Kingdom, 2004; p 104.
- 155.Sohrin, Y.; Kokusen, H.; Matsui, M., *Inorg. Chem.* **1995**, *34*, 3928-3934.

## Chapter D. Synthesis of Polymerizable Tris(2-pyridyl)borate Ligands and Their Metal Complexes

### D.1 Introduction

#### D.1.1 Pyrazolylborate and Pyridylborate Ligands

Since Trofimenko synthesized the first tris(pyrazolyl)borate ligands,<sup>121</sup> these materials have given rise to a tremendous amount of chemistry with an amazing diversity and have been considered some of the most useful ligands in modern coordination chemistry.<sup>122</sup> The great advantage of pyrazolylborate ligands is their versatility derived from the different steric and electronic effects that are readily attained by varying the nature, number and position of the substituents in the pyrazole rings. Thus, fine-tuning of the reactivity at the metal center in the complex can be achieved by choosing different pyrazolylborate ligands. Complexes with all the metals or metalloids in the periodic table have been prepared over the years.<sup>123</sup> The tris(pyrazolyl)borates have been named as scorpionate ligands<sup>124</sup> by Trofimenko for their coordination geometry and also potency of their complexation with metals. The tris(pyrazolyl)borates, being uninegative tri-coordinated six-electron donors, have also been considered as analogs of cyclopentadienyls<sup>125</sup> and have found applications in diverse fields ranging from homogeneous catalysis and metallocene polymerization to bioinorganic chemistry.

Complexes with one or multiple tris(pyrazolyl)borate ligands are readily prepared. The physical properties of these complexes can be fine tuned by varying either the substituents on the pyrazole ring or the fourth substituent on the boron atom. For example, Matsui and coworkers compared X-ray structures of different tris(pyrazolyl)borate Fe(II) complexes and found that the ligand field strength can be varied through intra- and interligand contacts.<sup>126</sup> Trigonal distorted octahedral geometries about the Fe atom in Fe(II) complex (**D1**) are observed (Figure D1). As the fourth substituent on the boron atom, the phenyl group in  $[\text{PhB}(\text{pz})_3]_2\text{Fe}$  enforces a narrow arrangement on the tripod resulting in low-spin complex formation. In the absence of a bulky group on boron, in  $[\text{HB}(3,5\text{-Me}_2\text{pz})_3]_2\text{Fe}$  (**D2**),<sup>127</sup> the methyl group in the 3-position of the pyrazolyl ring brings about a significant interligand contact with the metal ion prohibiting low-spin complex formation.

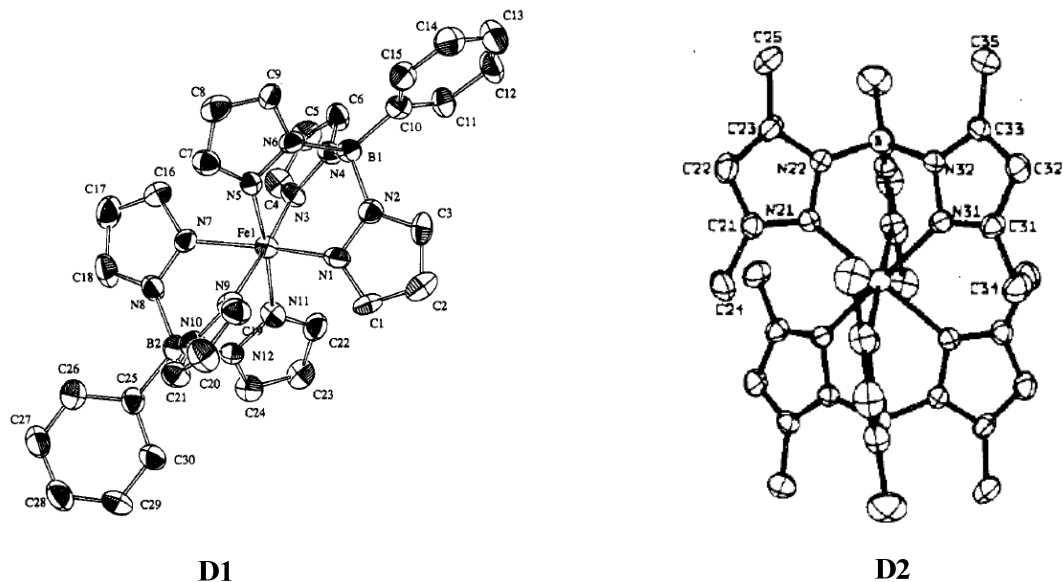


**Figure D1.** A) X-ray structure of  $[\text{PhB}(\text{pz})_3]\text{Fe}$  (**D1**); B) X-ray structure of  $[\text{HB}(3,5\text{-Me}_2\text{pz})_3]_2\text{Fe}$  (**D2**); (**D1**) Reprinted in part with permission from *Inorg. Chem.* 2002, 34, 3928-3934, Copyright 2002 American Chemical Society; (**D2**) Reprinted in part with permission from *Inorg. Chem.* 1980, 19, 165-169, Copyright 1980 American Chemical Society.

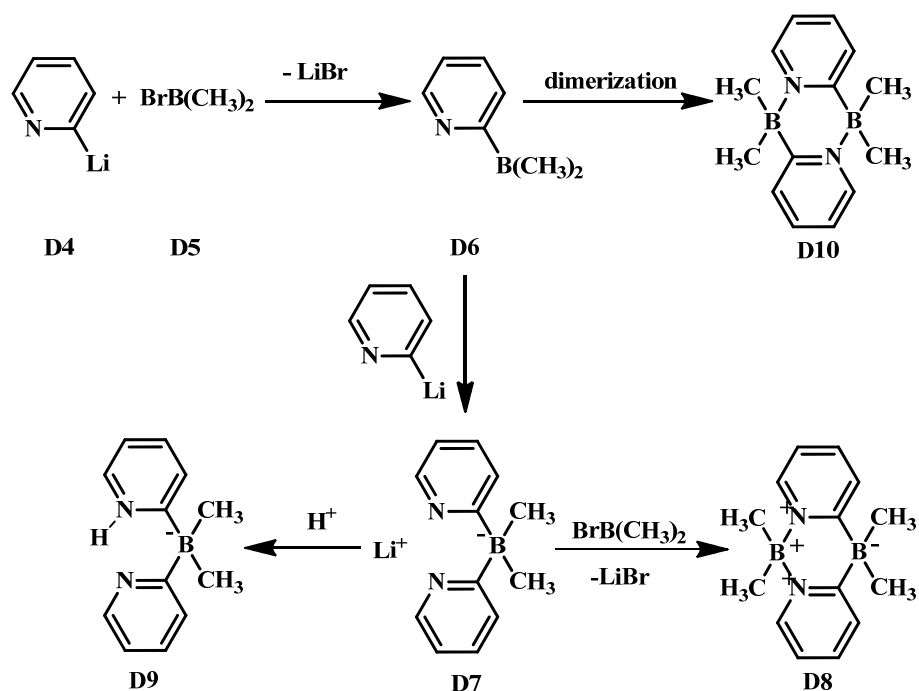
While the pyrazolylborate ligands offer advantages in terms of their ease of synthesis and variation, the stability of the B-N bonds has at times been a concern. Ligand rearrangement reactions illustrate the relatively unstable nature of the B-N bond in tris(pyrazolyl)borate ligands. As an example, the poly(pyrazolyl)borate ligand  $\text{HB}(3\text{-}i\text{-Prpz})_3$  (**D3**) containing a 3-isopropyl group on the pyrazole ring was used to form complexes  $\text{L}_2\text{M}$  with cobalt (II); the ligand was found to undergo a 1,2-borotropic shift in one of its pyrazolyl substituents to yield a 5-isopropylpyrazolyl isomer.<sup>128</sup> The

rearrangement originating from the steric effect can be avoided by placing substituents on both the 3- and 5-positions. Moreover, decomposition with formation of the parent pyrazoles is quite common and can be catalyzed by Lewis acids or Brønsted acids. On the contrary, boron forms strong and less polar bonds to carbon, which has enabled organoboron chemistry as an important field in modern synthesis.

A possible alternative is therefore to place 2-pyridyl groups on boron to form tris(2-pyridyl)borate ligands. So far tris(2-pyridyl) tripod ligands have been synthesized with a variety of different bridge atoms including C, N, P, As, <sup>129</sup> Si, <sup>130</sup> Al, <sup>131</sup> Sn, <sup>132</sup> In <sup>133</sup> and Pb<sup>134</sup>. However, tris(2-pyridyl)borate ligands have not been reported to date. In addition to an enhanced stability, there are significant other differences to be expected between tris(pyrazolyl)borate and tris(2-pyridyl)borate ligands. Most importantly, pyridine is a better  $\sigma$  donor than pyrazole,<sup>135</sup> which should greatly affect the complexation behavior.

The fact that boron is closely surrounded by C, N and Al in periodic table, all of which have been employed as bridge atoms in tris(2-pyridyl) tripod ligands, strongly suggests the possibility of successfully synthesizing tris(2-pyridyl)borate ligands. However, so far only bis(2-pyridyl)borate ligands are available.<sup>81d</sup> Hodgkins and coworkers prepared the first dimethylbis(2-pyridyl)borate ligand (**D9**) in 1996 (Scheme D1). Dimethylbromoborane (**D5**) in diethyl ether was added into a solution of two equivalents of 2-pyridyllithium (**D4**) in a mixture of hexanes and diethyl ether. Formation of the

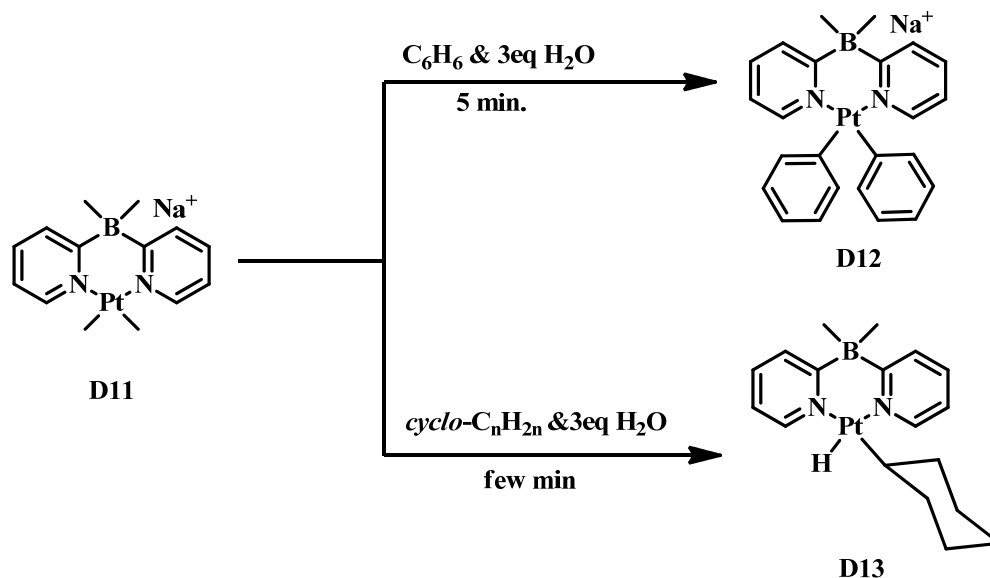
lithium borate **D7** was accompanied with by-products including a dimeric adduct (**D10**) from Lewis acid and base coordination and a zwitterion (**D8**) from chelation between the **D7** and the starting material **D5**.<sup>136</sup> Selective extraction into acidic aqueous solution and recovery by precipitation at elevated pH gave rise to the pure dimethylbis(2-pyridyl)borate ligand (**D9**) as colorless crystals in 46% yield following recrystallization.



**Scheme D1.** Preparation of dimethylbis(2-pyridyl)borate ligand (**D9**) from pyridyllithium (**D4**) reagent.

The dimethylbis(2-pyridyl)borate ligands (**D9**) didn't attract much attention at the time until Vedernikov and coworkers started to employ them as ubiquitous anionic bidentate

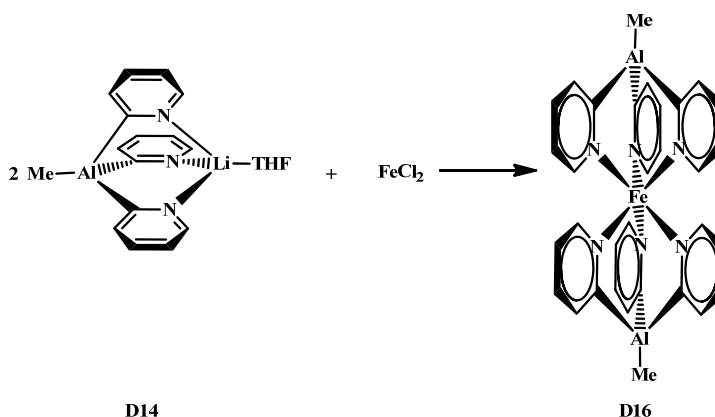
pyridine ligands to organoplatinum complexes (**D11**) for the purpose of C-H activation reactions (Scheme D2).<sup>137</sup>



**Scheme D2.** Application of the dimethylbis(2-pyridyl)borate platinum complex (**D11**) in C-H activation reactions.

The successful synthesis of bis(2-pyridylborate) ligands suggests that tris(2-pyridyl)borate ligands could be synthesized if a di-bromo substituted borane was used. However, the higher Lewis acidity and reactivity of dibromoalkylboranes in comparison to bromodialkylboranes may pose a synthetic challenge. Moreover, diethyl ether solvent can readily react with dibromoalkylboranes to give dialkoxy substituted boranes, which in turn may not be reactive enough to form the desired tris(2-pyridyl) borate species.

Being in the same group as boron, aluminum has already been used as the bridging atom of the corresponding tris(2-pyridyl) tripod ligands. Wright and coworkers have synthesized lithium tris(2-pyridyl)aluminate<sup>131, 138</sup> (**D14**) using a 1:3 stoichiometric reaction between MeAlCl<sub>2</sub> (**D15**) and 2-pyridyllithium (**D4**) in THF at -78 °C. MeAlCl<sub>2</sub> does not undergo ring opening reaction with THF so that the reaction proceeds as anticipated to give lithium tris(2-pyridyl)aluminate. Bis-coordinated complexes of Fe(II) (**D16**) and Mn(II) (**D17**) with this lithium tris(2-pyridyl)aluminate (**D14**) were also investigated (Scheme D3). These complexes can be compared with classical tris(pyrazolyl)borate complexes, such as the Fe(II) complex [{HB(pz)<sub>3</sub>]<sub>2</sub>Fe] (**D18**).<sup>139</sup> The bis-coordinated complex of Fe(II) has also been proven to be one of the best catalysts for selective epoxidation of styrene under mild conditions, with just air as the oxidant, rather than stronger oxidants like H<sub>2</sub>O<sub>2</sub> used in other catalytic systems.



**Scheme D3.** Preparation of Fe(II) complex (**D16**) with lithium methyltris(2-pyridyl)aluminate (**D14**).

### D.1.2 Pyrazolylborates and Polypyridyl Ligands in Supramolecular Chemistry and Polymer Science

The successful preparation of tris(2-pyridyl)borate is not only expected to be of interest for catalytic applications, but could also prove highly versatile as a building block for the preparation of functional inorganic polymers. Conjugated nitrogen-based tridentate ligands possessing a planar conformation have been extensively employed and had a dramatic impact on supramolecular chemistry and polymer chemistry.<sup>140</sup> Many different coordination polymers have been synthesized through metal-ligand complexation. Moreover, significant attention has been also paid to chelate-ligand functionalized polymers for recovering precious organometallic catalysts.<sup>141</sup>

Among the most well-known conjugated nitrogen-based tridentate ligands are terpyridine and its derivatives. One particularly useful property of terpyridine ligands is the formation of highly stable bis-coordinated complexes with a variety of metal ions. Appropriate design of building blocks with terpyridyl functional groups has indeed been a fruitful strategy to prepare a plethora of metal containing materials.<sup>142</sup> And a range of metal ions can be used to connect these building blocks through complexation with the terpyridine substituents<sup>143</sup> leading to metal coordination polymers, metal-containing dendrimers and even metal-containing macrocycles (**D19**) (Figure D2).<sup>142b</sup>

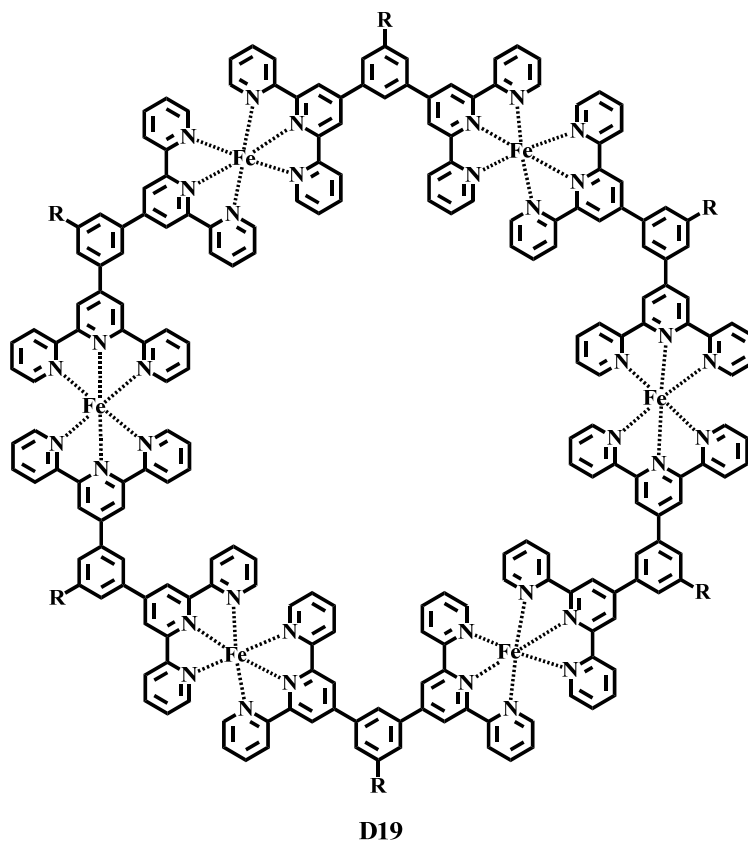
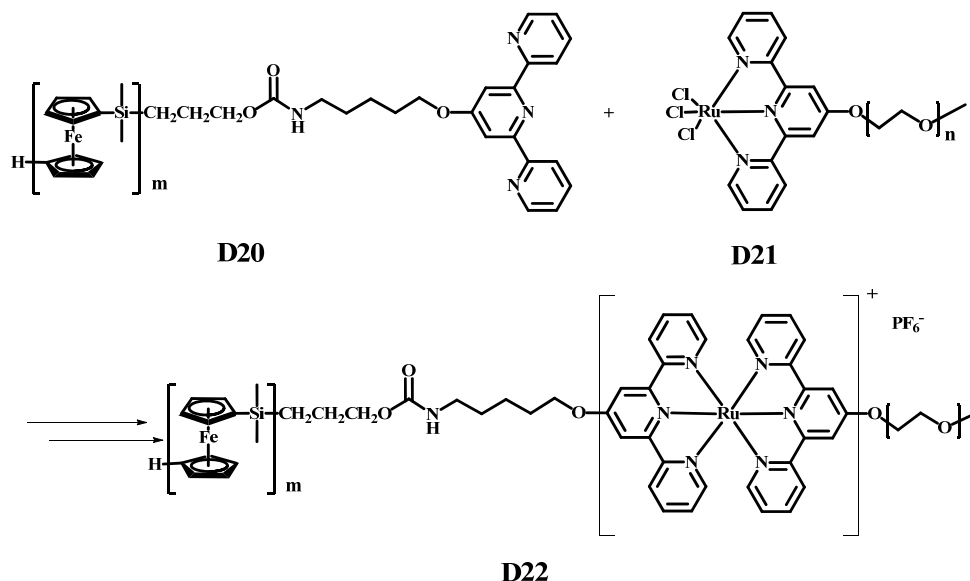


**Figure D2.** A metal-containing macrocycle (**D19**) prepared through complexation of a terpyridine ligand and Fe (II) ion.

Block copolymers can also be made by connecting two different homopolymers via the strong complexation between terpyridines and metal ions.<sup>143b,142b,144</sup> For example, Schubert and coworkers used a terpyridine ruthenium complex as a linker in the preparation of diblock copolymers, (PFS-*block*-PEO) (**D22**), which consist of a poly(ferrocenylsilane) (PFS) and a poly(ethylene oxide) (PEO) block (Scheme D4).<sup>144</sup>



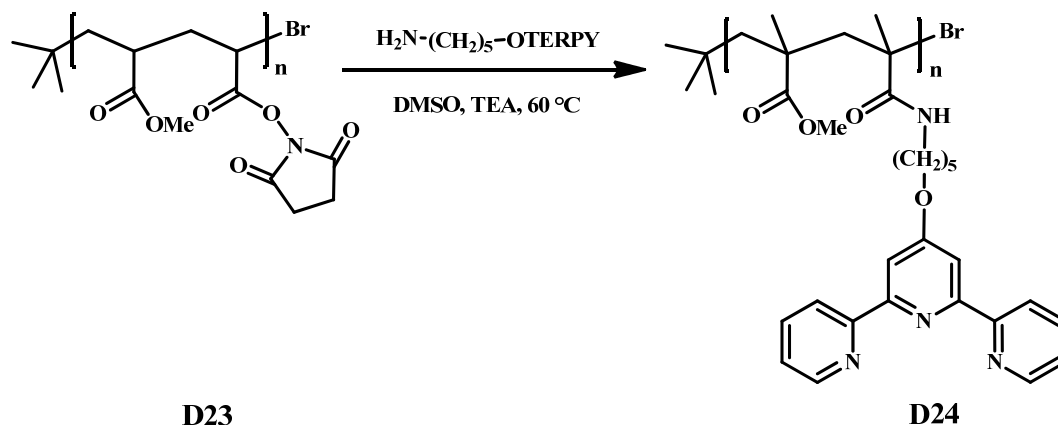
**Scheme D4.** Preparation of a diblock copolymer (PFS-*block*-PEO) (**D22**) through the strong metal complexation of the end terpyridine ligand group.

Exclusive formation of the diblock copolymer (**D22**) was achieved. These types of diblock copolymers have been used to prepare cylindrical micelles in aqueous solution.

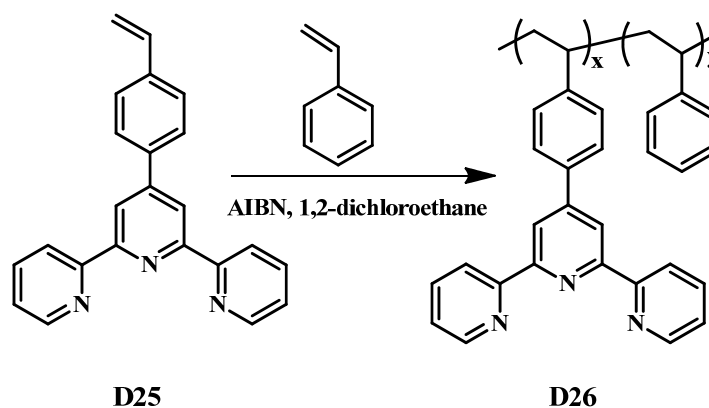
The crystalline PFS cylinder cores were anticipated to be useful for charge transfer and as precursors for ferromagnetic nanostructures.

Since complexation of terpyridine ligands with metal ions can also impart interesting properties like luminescence, electro- and photo-chemistry, magnetism, and thermochromism,<sup>145</sup> Tew and coworkers have been pursuing attachment of terpyridine ligands or their metal complexes to the side chain of polyolefins (**D24**) through a post-polymerization modification procedure as shown in scheme D5.<sup>146</sup> One such polymer with terpyridine functionalized side chains has been employed to complex

with transition metal ions in the preparation of electroluminescent materials for light emitting devices.<sup>147</sup>



**Scheme D5.** Synthesis of a terpyridine functionalized polymer (**D24**) through post-polymerization modification.



**Scheme D6.** Free radical polymerization of a terpyridine functionalized styrene (**D26**).

Direct polymerization has also been applied for the preparation of terpyridyl-functionalized polymers (**D26**). As an example, Schubert and coworkers

synthesized a random copolymer with styrene and terpyridine-functionalized styrene by free radical polymerization (Scheme D6).<sup>148</sup>

However, although magnificent achievements have been attained in the employment of the terpyridyl ligands as linkers in supramolecular and polymer chemistry, relatively little attention has so far been paid to other tripod ligands. Wagner and coworkers synthesized ferrocene-based tris(pyrazolyl)borate ligands (**D27**). A variety of divalent metal ions were employed to form bis-coordinate metal complexes (**D28**) (Figure D3). Communication between the two ferrocene centers was found when Cu(II) was used.<sup>149</sup> The potential of making coordination polymers with these tris(pyrazolyl)borate ligands has also been discussed.

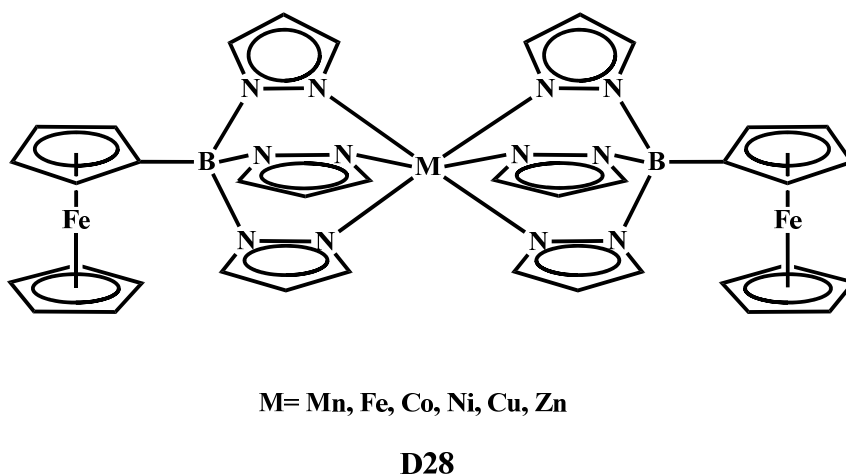
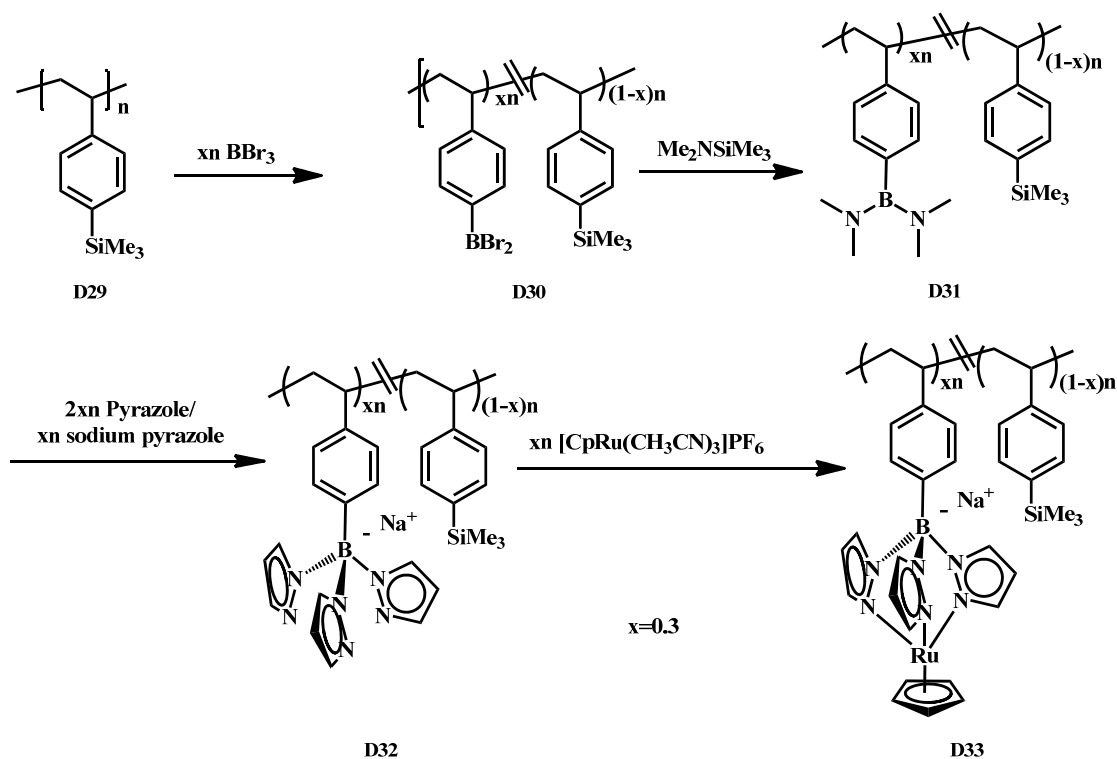


**Figure D3.** Metal complexes (**D28**) formed by complexation between a ferrocene-based tris(pyrazolyl)borate ligand (**D27**) and divalent metal ions.

Jäkle and coworkers have elaborated on attachment of tris(pyrazolyl)borate ligands to well-defined styrenic polymers<sup>150</sup> (**D32**) for applications as scaffolds for catalysts and the preparation of new supramolecular materials (Scheme D7).



**Scheme D7.** Tris(pyrazolyl)borate ligands are attached to a styrenic polymer via a post modification procedure (**D32**); and the ligand functionalized polymer can be further complexed with organotransition metals, such as CpRu (**D33**).

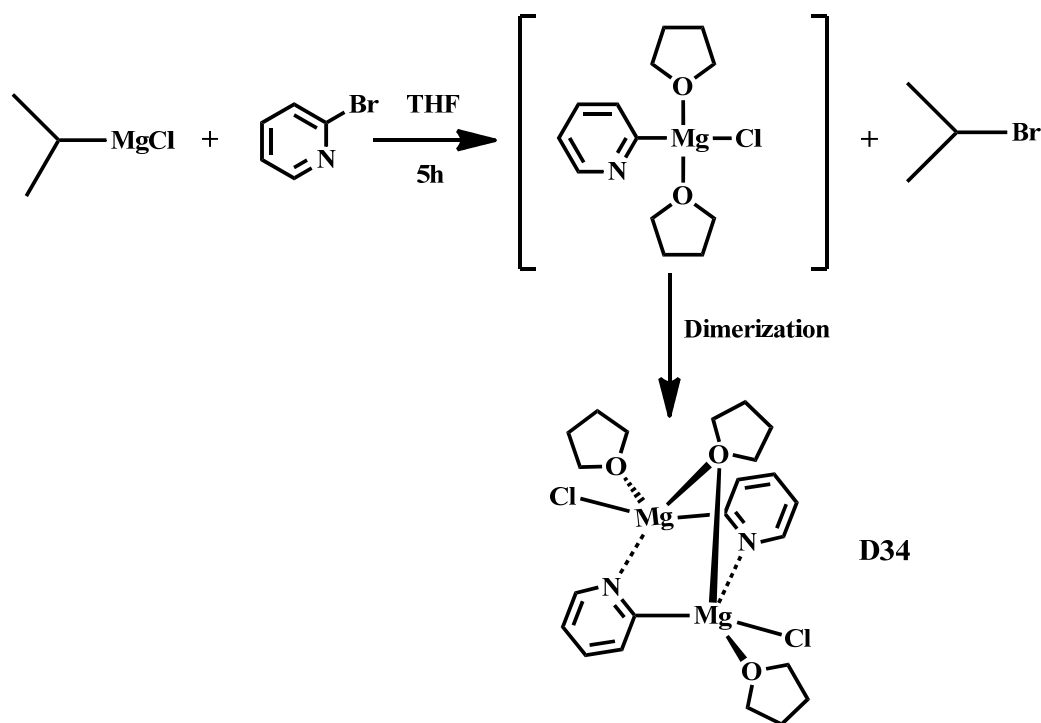
## D.2 Synthesis and Characterization of Polypyridylborate Ligands and Their Metal Complexes

The synthesis of tris(2-pyridyl)borate ligands and di(2-pyridyl)borate ligands is described in the following. The major synthetic breakthrough was the adoption of a 2-pyridyl Grignard reagent instead of 2-pyridyllithium previously used in the preparation of di(2-pyridyl)dimethylborate (**D9**) as described by Hodgkins and coworkers.<sup>81d</sup>

### D.2.1 Synthesis of 2-Pyridyl Grignard Reagent

As described in the literature,<sup>151</sup> the 2-pyridylmagnesium chloride (**D34**) was prepared by reaction between isopropyl magnesium chloride and 2-bromopyridine. At room temperature, one equivalent of neat 2-bromopyridine was introduced to a freshly prepared solution of isopropyl magnesium chloride in THF. The THF solvent was partially removed by evaporation under high vacuum. Sudden formation of a yellow slurry was observed, and the product was isolated as a white solid by filtration and subsequent washing with THF (Scheme D8). <sup>1</sup>H NMR in CD<sub>2</sub>Cl<sub>2</sub> showed four broad peaks in the phenyl region and two additional relatively broad peaks, which were assigned to the protons of THF. While being moderately stable in dichloromethane solution with only a gradual color change from light yellow to greenish, the white solid reacted immediately with chloroform resulting in formation of a white precipitate. The Grignard product has low solubility in THF and a purple THF solution was obtained under heating. Colorless

crystals formed at room temperature from this solution. Single crystal X-ray analysis revealed a dimeric structure similar (Figure D4) to that reported by Churakov and coworkers<sup>152</sup> who used a slightly different procedure starting from using isopropyl magnesium bromide instead of isopropyl magnesium chloride.<sup>151a</sup>



**Scheme D8.** Synthesis of dimeric 2-pyridylmagnesium chloride (**D34**).

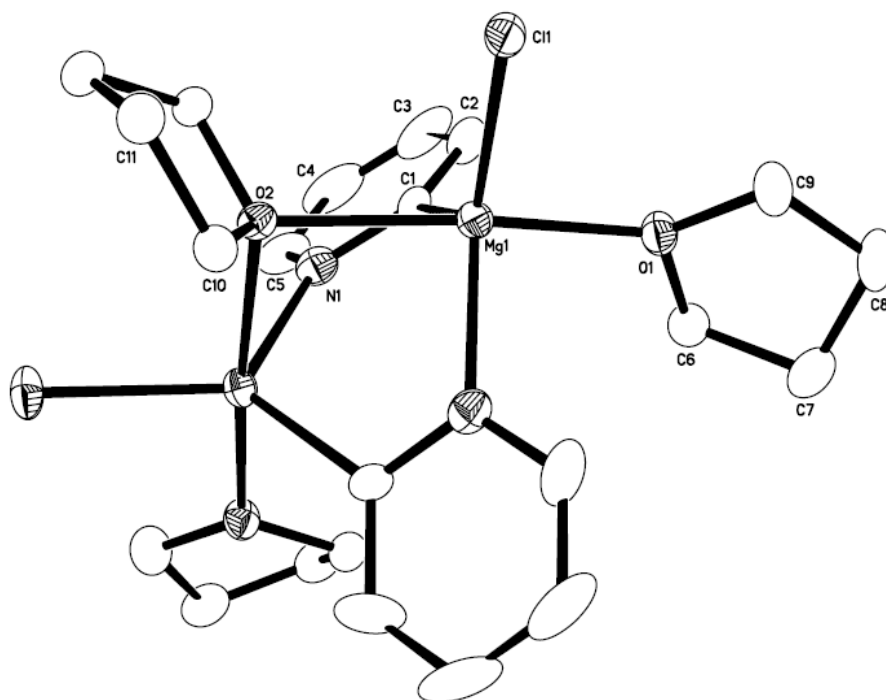


**Figure D4.** Tentative view from “diamond” of the dimeric structure of 2-PyMgCl (**D34**) with three coordinating THF (0.5 equivalent disordered THF is omitted for clarity). (50% probability)

In both cases, the magnesium atoms are coordinated by pyridyl nitrogens to form a dimeric structure. At the same time, each magnesium atom is coordinated by one THF molecule and a bridging THF is also found to coordinate with both magnesium atoms. There are a few differences between the two dimeric structures of the pyridyl Grignard reagent. The unit cell of 2-PyMgCl is about 4% smaller than that of 2-PyMgBr. The angle between the pyridyl rings in the dimeric structure of 2-PyMgCl is  $42.22^\circ$ , which is slightly larger than that of  $40.61^\circ$  for 2-PyMgBr. The crystals of 2-PyMgCl also contain

disordered solvent THF molecules which are inside the cell rather than on a fourfold axis as found for 2-PyMgBr.

The Grignard reagent 2-PyMgCl was not further purified by recrystallization due to its poor solubility in THF; instead, it was washed with a large amount of THF giving rise to a white solid product in good yield. This white solid was dried under vacuum at 60°C.  $\text{Mg}_2\text{Cl}_2(\text{C}_5\text{H}_4\text{N})_2(\text{C}_4\text{H}_8\text{O})_{3.5}$  was used as an empirical formula for all further reactions.

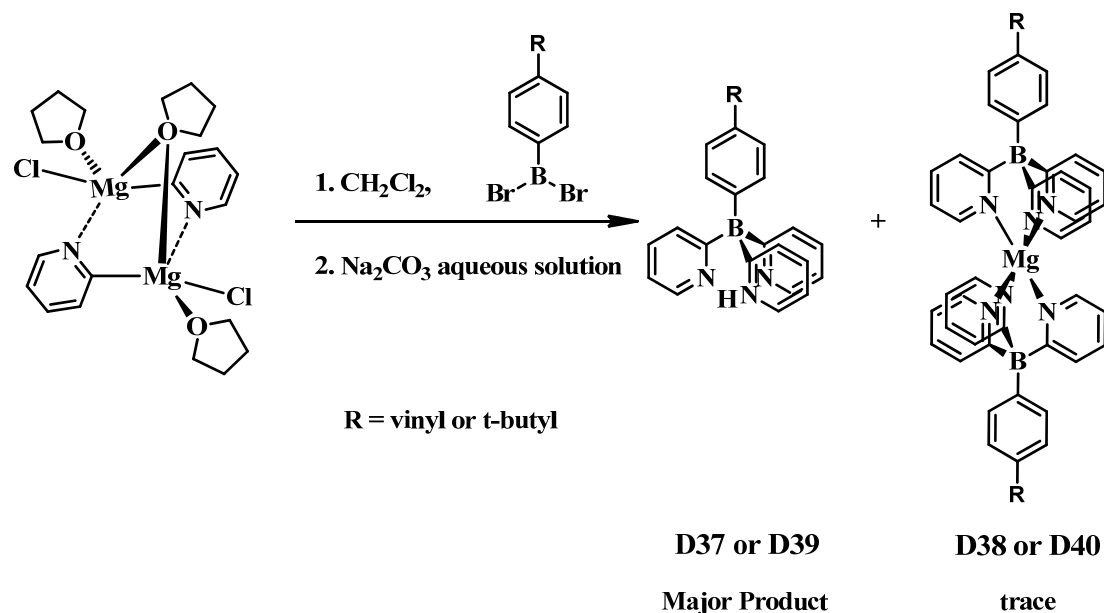
## **D.2.2 Tris(2-pyridyl)borate Ligands and Their Magnesium Complexes**

### **D.2.2.1 Synthesis of Polypyridylborate Ligands and Magnesium Complexes**

*t*-Butylphenyldibromoborane (**D35**) was used as dibromoarylborane and prepared as previously reported. *t*-Butylphenyltrimethylsilane was reacted with boron tribromide in dichloromethane and the colorless product was collected by distillation under high vacuum. Similarly, styryldibromoborane (**D36**) was prepared from reaction between 4-trimethylsilylstyrene and boron tribromide. The reaction solution was concentrated to a viscous oil followed by sublimation under high vacuum at a moderate temperature. The product was isolated as white solid.

The synthesis of the tris(2-pyridyl)borate ligands was achieved by addition of a dichloromethane solution of *t*-butylphenyldibromoborane or styryldibromoborane to a dichloromethane solution of 2-PyMgCl (Scheme D9). Addition of the dibromoborane to the Grignard solution is critical to maintain an excess amount of Grignard reagent

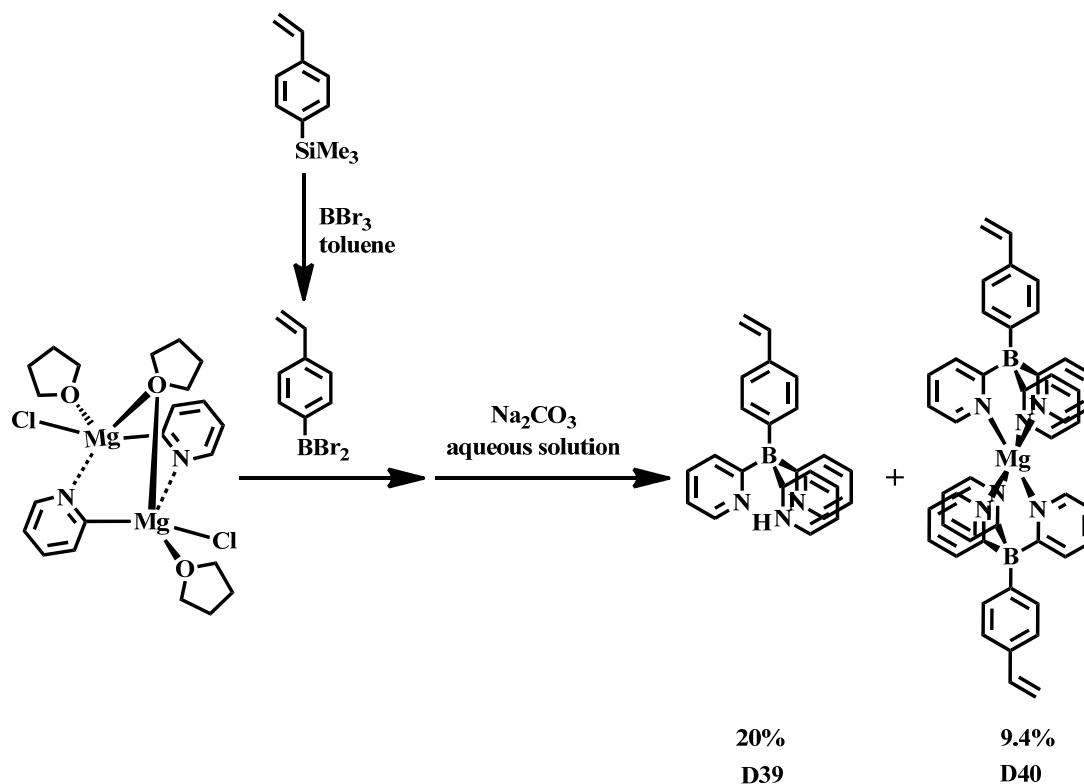
throughout the reaction, which was found to help reduce the side reactions between dibromoborane and THF. An aqueous solution of  $\text{Na}_2\text{CO}_3$  was then used to quench the reaction and the product was extracted into dichloromethane. The dichloromethane solution was brought to dryness under vacuum and the product was extracted into acetone. A white crystalline product with yellow tint can be attained after the acetone solution was brought to dryness. Finally the t-butylphenyltris(2-pyridyl)borate free acid (**D37**) was purified by chromatography on silica. It is worth noting that the small amount of insoluble residue remaining after acetone extraction was found to contain another borate species, which showed a characteristic sharp peak in the  $^{11}\text{B}$  NMR spectrum. Extraction with dichloromethane and recrystallization from toluene afforded colorless crystals, which were identified by single crystal X-ray diffraction to be a bis-coordinated t-butylphenyltris(2-pyridyl)magnesium complex (**D38**). This bis-coordinated magnesium complex was also present in the reaction solution (about 5%) as the only boron containing impurity. The absence of other  $^{11}\text{B}$ -NMR active species suggests that side reactions between the dibromoborane and THF were suppressed to a negligible level.



**Scheme D9.** Synthesis of (2-pyridyl)borate free acids (**D37** and **D39**) in  $\text{CH}_2\text{Cl}_2$ ; The magnesium complexes were found to be the only side product in trace amount.

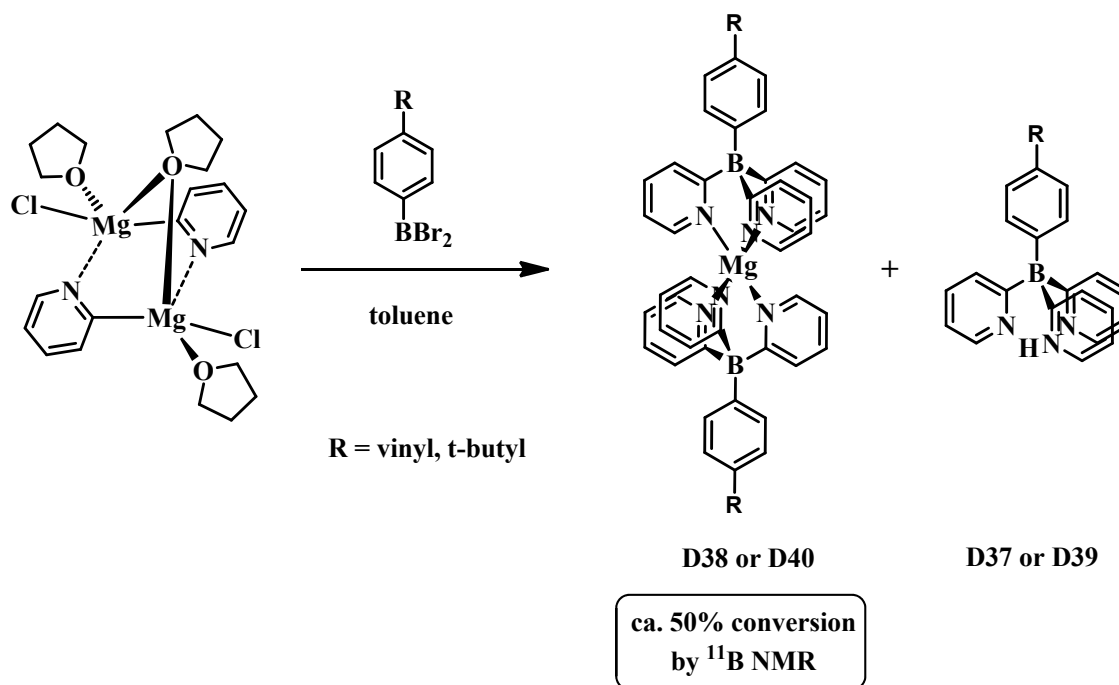
When a similar reaction was performed in toluene, the reaction solution also showed two borate species; however, more bis-coordinated magnesium complex was generated in this case (ca. 50% estimated from  $^{11}\text{B}$  NMR). Therefore a different procedure for quenching the reaction mixture was applied: the toluene solvent was removed completely and methanol was subsequently introduced to extract the white solid residue. Both the pyridylborate free acid and the magnesium salts were extracted into methanol solution leaving behind the bis-coordinated magnesium complex in high purity. This method allowed for isolation of the Mg complexes in 35% yield.

A similar procedure was also successfully applied for the preparation of styryltris(2-pyridyl)borate free acid (**D39**) monomer. However, a one-pot synthesis procedure was desirable to minimize spontaneous polymerization during work up. The reaction solution of styryldibromoborane was directly transferred into a toluene solution of 2-pyridylmagnesium chloride. The reaction mixture was then quenched by addition of an aqueous solution of  $\text{Na}_2\text{CO}_3$ , and dichloromethane was used to extract the pyridylborate species (Scheme D10). The dark greenish dichloromethane solution was directly passed through a silica column. Bis(styryltris(2-pyridyl)borate) magnesium (**D40**) first eluted with dichloromethane, followed by styryltris(2-pyridyl)borate free acid with acetone as a second eluent. Solid products were obtained after solvent evaporation under vacuum. The ligand free acid was subjected to additional chromatography on silica to achieve sufficiently high purity for radical polymerizations. Chromatography of the bis-coordinated magnesium complex was also attempted on silica to remove a trace amount of free ligand, however, when dichloromethane was used as an eluent along with 1% triethylamine, the magnesium complex was found to dissociate completely with formation of the free acid.



**Scheme D10.** One pot synthesis of styryltris(2-pyridyl)borate free acid monomer (**D39**) in toluene; using toluene as solvent, the magnesium complex (**D40**) was generated in moderate yield (9.4% isolated yield).

To obtain a higher yield for bis(styryltris(2-pyridyl)borate) magnesium (**D40**), an analogous procedure as for the preparation of bis[*t*-butylphenyltris(2-pyridyl)borate] magnesium was employed (Scheme D11). Toluene was used again to maximize the yield of the magnesium complex and methanol extraction was used for efficient purification.



**Scheme D11.** Toluene was used to achieve in high conversion to the magnesium complexes (D38 and D40).

#### D.2.2.2 NMR Characterizations

NMR analysis was used to identify the polypyridylborate ligands. The assignments of the protons in the pyridine rings are depicted in Figure D5. Furthermore, 2D NMR data using Correlation Spectroscopy (COSY) and Heteronuclear Multiple Quantum Correlation (HMQC) techniques were acquired to further confirm the NMR assignment for t-butylphenyltris(2-pyridyl)borate free acid.

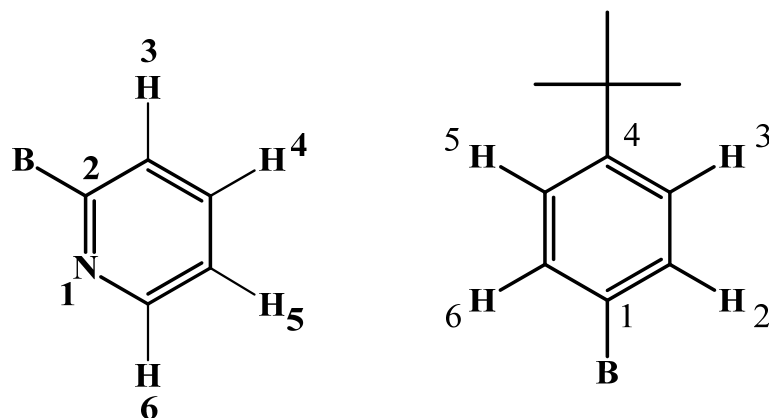


**Figure D5.** Numbering scheme of the protons in the pyridine and t-butylphenyl rings.

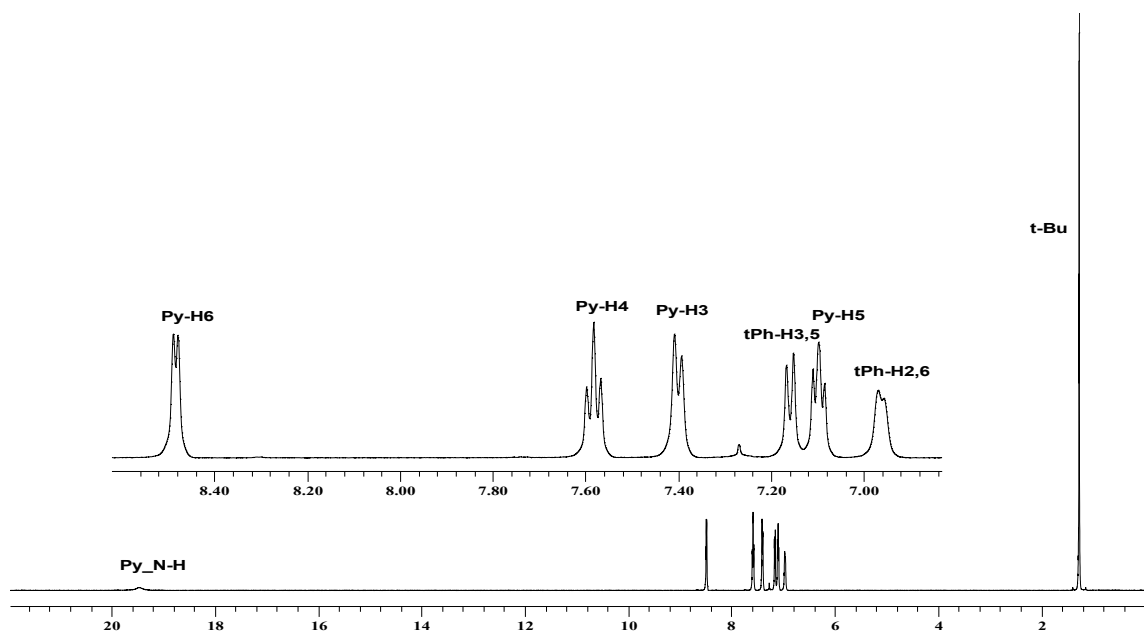


**Figure D6.** <sup>1</sup>H NMR spectrum of t-butylphenyltris(2-pyridyl)borate free acid (**D37**) in CDCl<sub>3</sub>.

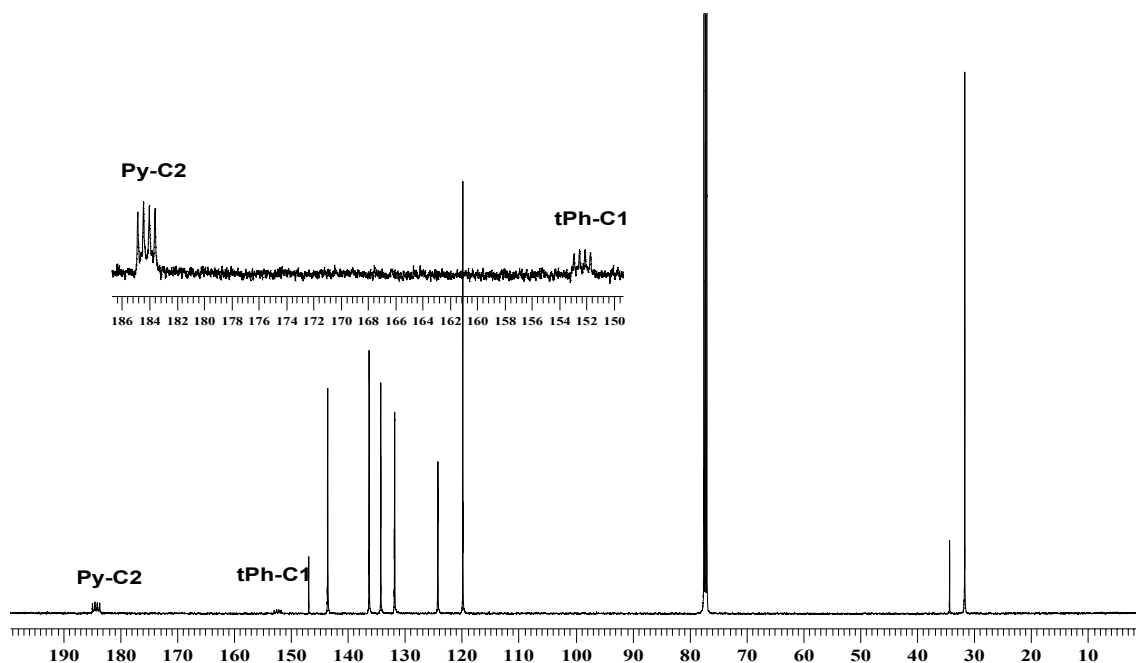


**Figure D7.**  $^{13}\text{C}$  NMR of t-butylphenyltris(2-pyridyl)borate free acid (**D37**) in  $\text{CDCl}_3$ .

The  $^1\text{H}$  NMR spectra of both t-butylphenyltris(2-pyridyl)borate free acid (**D37**) (Figure D6) and styryltris(2-pyridyl)borate free acid in  $\text{CDCl}_3$  feature the expected patterns for pyridyl and phenyl rings (Figure D6). A double doublet at 6.69 ppm and two upfield doublets with coupling constants of 17.5 Hz and 11.0 Hz, respectively, confirm the presence of the vinyl group of styryltris(2-pyridyl)borate free acid whereas a singlet at 1.27 ppm could be assigned to t-butyl group of t-butylphenyltris(2-pyridyl)borate free acid. A singlet was found at 19.5 ppm and 17.3 ppm for the nitrogen-bonded proton. The chemical shift of the nitrogen-bonded proton was found to be strongly dependent on the presence of moisture and the data reported here are for  $^1\text{H}$  NMR analysis of dry samples in dry  $\text{CDCl}_3$ . The  $^{11}\text{B}$  NMR spectra of both compounds showed a sharp singlet near -11

ppm, which is downfield shifted compared with the dimethyldi(2-pyridyl)borate ligand reported previously (-18.4 ppm).<sup>81d</sup> The  $^{13}\text{C}$  NMR spectra exhibited quartets near 185 ppm and 155 ppm with similar coupling constants of ca. 50 Hz (Figure D7). Of higher intensity, the peak near 180 ppm was assigned to the boron-bound pyridyl carbon atoms, therefore, the other quartet near 150 was assigned to the boron-bonded phenyl carbon atoms. The number and positions of the remaining peaks in the  $^{13}\text{C}$  NMR spectra are all consistent with their assignment.

When going to the magnesium complexes, the pattern of the pyridyl rings changed drastically. Large upfield shifts of 0.9 ppm for the t-butylphenyl and 1.1 ppm for the styryl derivative were observed for the pyridyl proton 3 which is adjacent to the boron-carbon bond. The two doublets assigned to protons 3 and 6, respectively, even changed positions. At the same time, the phenyl protons in ortho position to boron also experienced appreciable downfield shifts of ca. 1.0 ppm for both magnesium complexes. A detailed comparison of the  $^1\text{H}$  NMR data is provided in Table D1 in section 4.2.4.

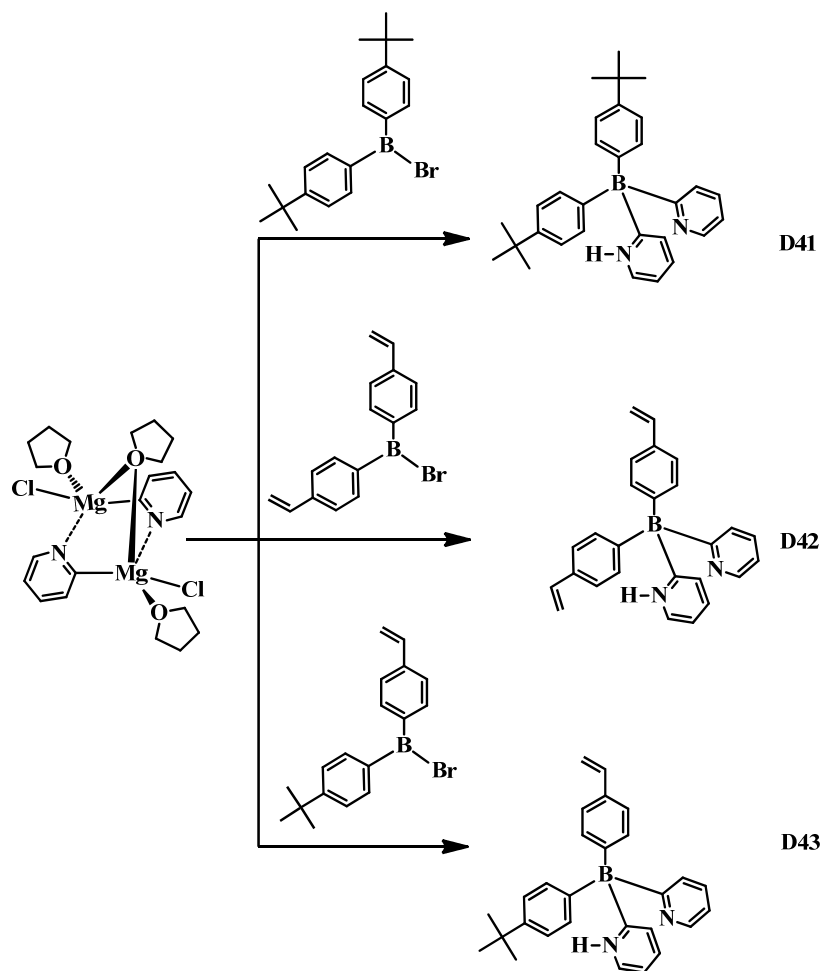
### **D.2.3 Synthesis of Bis(2-pyridyl)borate Ligands**

To prepare diarylbis(2-pyridyl)borate ligands, one of the bromo substituents of dibromoarylboranes can be replaced with another aryl substituents through selective transmetallation procedures. The resulting diarylbromoboranes were used to react with  $\text{PyMgCl}$  in the preparation of di(t-butylphenyl)bis(2-pyridyl)borate (**D41**),

distyrylbis(2-pyridyl)borate (**D42**) and styryl(*t*-butylphenyl)bis(2-pyridyl)borate free acids (**D43**) (Scheme D12).

4-Trimethylstannylstyrene (**D44**) was synthesized in a similar procedure as the one reported for the synthesis of 4-trimethylsilylstyrene.<sup>61a</sup> Instead of trimethylsilyl chloride, trimethyltin chloride was used to react with styrylmagnesium chloride in THF. Except for the preparation of distyrylbis(2-pyridyl)borate free acid, all the transmetallations were performed by addition of a dichloromethane solution of the organotin reagent to a dichloromethane solution of the dibromoborane. In the preparation of distyrylbis(2-pyridyl)borate, a dichloromethane solution of styryldibromoborane (**D36**) was added into a dichloromethane solution of styryltrimethyltin to prevent methyl transfer side reactions. The reaction solutions of the respective diarylbromoboranes were then added to a dichloromethane solution of pyridylmagnesium chloride so that the Grignard reagent was always in excess. In each case, multiple boron species in each reaction solution were found by <sup>11</sup>B NMR analysis. The impurities were assumed to be due to dimerization through the coordination between Lewis acidic boron center and Lewis basic pyridine nitrogen and chelation between the diarylbis(2-pyridyl)borate ligands and the diarylbromoborane starting materials. The reaction solutions were subjected to work-up with an aqueous solution of Na<sub>2</sub>CO<sub>3</sub> followed by extraction with dichloromethane. White solid products were obtained after column chromatography on

silica with solvent mixtures of hexanes to acetone of 1%(v/v) triethylamine as eluent. The isolated yields were moderate varying from 34% to 42%.



**Scheme D12.** Synthesis of bis(2-pyridyl)borate ligands: **D41**, **D42** and **D43**.

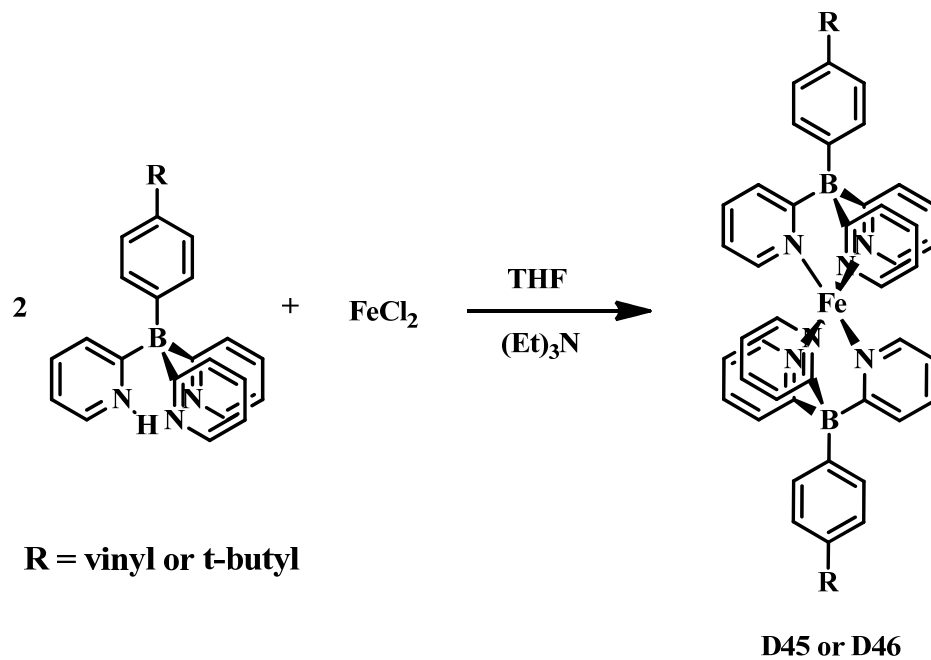
The  $^1\text{H}$  NMR patterns of the pyridine and phenyl rings were similar to those of the tris(2-pyridyl)borate free acids with relatively lower intensities from the proton signals of the pyridine rings. The characteristic patterns for the vinyl group in the styryl derivatives

were observed. All diarylbis(2-pyridyl)borate free acids showed downfield signals at ca. 20.0 ppm. The  $^{11}\text{B}$  NMR spectra all showed a signal at -11 ppm, which is similar to that of the tris(2-pyridyl)borate free acids, but significantly downfield shifted compared with that of dimethylbis(2-pyridyl)borate free acid (-18.4 ppm) reported previously.<sup>81d</sup>

#### **D.2.4 Synthesis and Characterization of Fe(II) Complexes with Tris(2-pyridyl)borate Ligands**

The tris(2-pyridyl)borate ligands were used to complex with Fe(II). The respective free acid was reacted with  $\text{FeCl}_2$  in THF in the presence of triethylamine (Scheme D13). The reaction solution was then brought to dryness giving rise to a red solid, which was extracted with toluene. The toluene solution was passed through a short plug of silica gel with hexanes as the eluent. The red solid products were studied by  $^1\text{H}$  NMR analysis. As observed for the Mg complexes, the pyridyl proton 6 exhibited a large upfield shift. An overlay of  $^1\text{H}$  NMR spectra between the t-butylphenyltris(2-pyridyl)borate ligand and its Fe (II) complex is shown in Figure D8, which displays large chemical shifts of the aromatic protons upon metal complexation. The characteristic patterns for the vinyl group in the Fe (II) complex (**D45**) with styryltris(2-pyridyl)borate ligand was also observed. A detailed comparison of the  $^1\text{H}$  NMR data is provided in Table D1. 2D NMR experiments including Correlation Spectroscopy (COSY) and Heteronuclear Multiple Quantum

Correlation (HMQC) were performed to further confirm the NMR assignment for the Fe(II) complex (**D46**) with t-butylphenyltris(2-pyridyl)borate ligand.



**Scheme D13.** Synthesis of Fe(II) complexes: **D45** and **D46**.

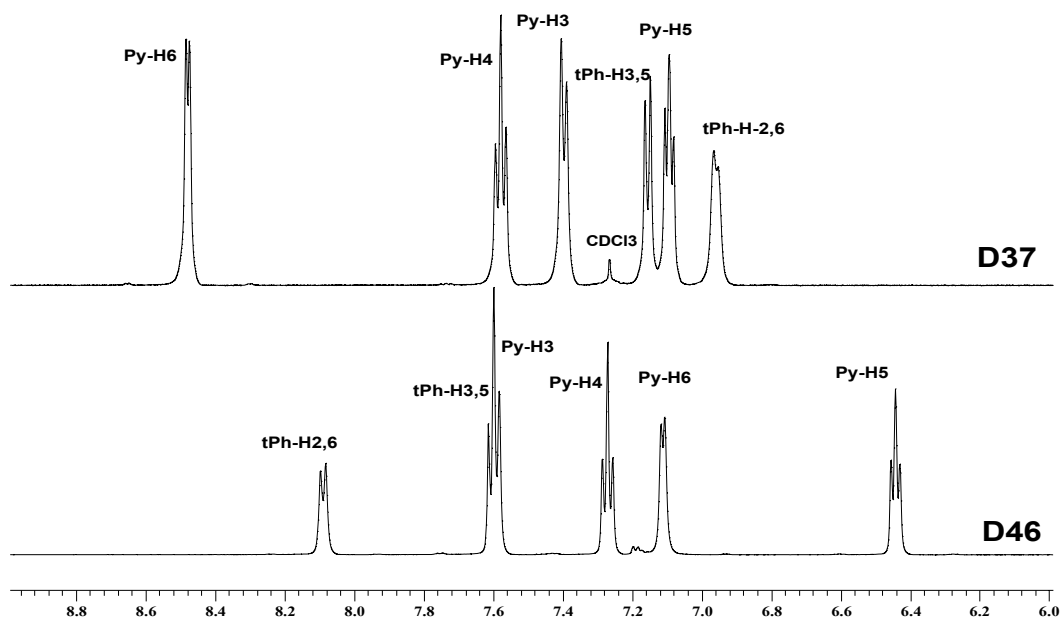


**Figure D8.** An overlaid  $^1\text{H}$  NMR spectra of t-butylphenyltris(2-pyridyl)borate ligand (**D37**) and its Fe(II) complex (**D46**).

**Table D1.**  $^1\text{H}$  NMR assignments of polypyridylborate ligands and metal complexes.

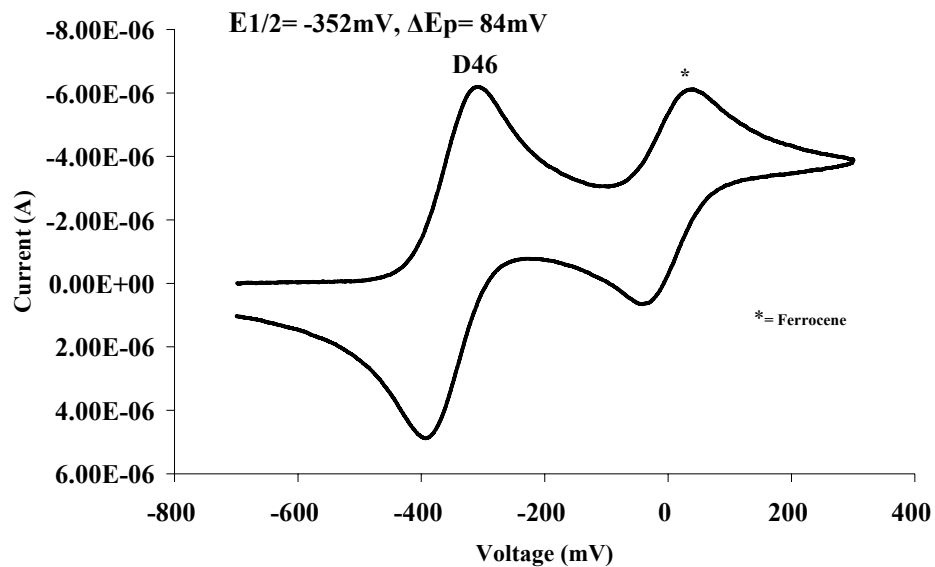
	NH/ Py	H6/ Py	H4/ Py	H3/ Py	H5/ Py	H3,5/ Ph	H2,6/ Ph	tBu/ Ph	Vinyl/ styryl (dd/d/d)
<b>D37</b>	19.5	8.49	7.58	7.40	7.10	7.16	6.96	1.27	
<b>D38</b>		7.58	7.39	7.70	6.64	7.56	7.97	1.51	
<b>D46</b>		7.11	7.27	7.59	6.44	7.60	8.09	1.52	
<b>D39</b>	17.3	8.68	7.86	7.58	7.41	7.29	7.07		6.69/5.70/5.18
<b>D40</b>		7.58	7.41	7.69	6.66	7.63	8.04		6.94/6.66/5.91
<b>D45</b>		7.16	7.29	7.58	6.46	7.67	8.15		6.94/6.46/5.95
<b>D41</b>	19.9	8.42	7.65	7.58	7.16	7.16	7.01	1.29	
<b>D42</b>	20.0	8.44	7.66	7.57	7.20	7.24	7.11		6.70/5.68/5.12
<b>D43</b>	20.0	8.43	7.67	7.57	7.18	7.17 <sup>tPh</sup> / 7.23 <sup>styr</sup>	7.06 <sup>tPh</sup> / 7.10 <sup>styry</sup>	1.29	6.69/5.66/5.10

Importantly, the NMR data suggest that the Fe(II) complexes are diamagnetic at room temperature in solution, which indicates a low spin configuration. Under air, they tend to get gradually oxidized to an ionic paramagnetic Fe(III) species in chlorinated solvents as evidenced by strong broadening and large shifts of the  $^1\text{H}$  NMR signals. Even though the neutral Fe(II) complexes exhibited much better stability in benzene and toluene even in the presence of oxygen, degassed  $\text{CDCl}_3$  was preferred as the NMR solvent in order to allow for comparison between different tris(2-pyridyl)borate species.

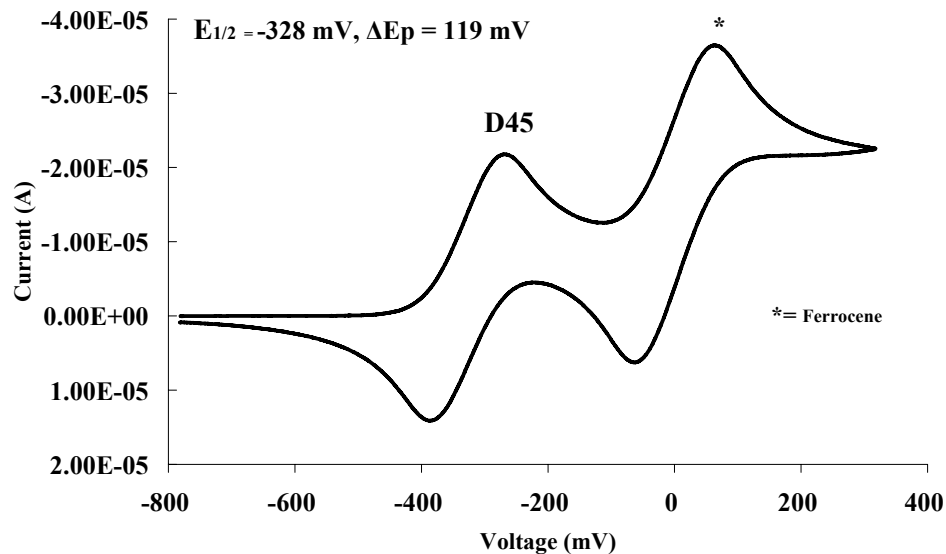
The preparative oxidation of the Fe(II) complex (**D45**) with  $\text{FeCl}_3$  in the presence of *t*-butylphenyltris(2-pyridyl)borate ligand was studied next. In a typical procedure, a solution of the Fe(II) complex was layered with an aqueous solution of  $\text{FeCl}_3$  followed by vigorous shaking. The color of the dichloromethane layer changed quickly from red to deep purple. A dark purple solid was obtained by solvent evaporation and then further purified by repeated precipitation from a dichloromethane solution into diethylether. The  $^1\text{H}$  NMR exhibited significant chemical shifts as compared with the corresponding neutral Fe(II) complex. Proton H6 of the pyridine ring was found to shift from 7.59 ppm for the Fe(II) complex to -79.2 ppm for the Fe(III) complex (**D47**). The smallest chemical shift difference was observed for the *t*-butyl protons that gave a 3.10 ppm downfield shift. These observations are consistent with formation of a paramagnetic Fe(III) complex.

### D.2.5 Cyclic Voltammetry and UV-visible spectroscopy data of Fe(II) complexes

Cyclic voltammetry studies of Fe(II) complexes **D46** and **D45** were carried out in CH<sub>2</sub>Cl<sub>2</sub> (anodic scans) using [Bu<sub>4</sub>N]PF<sub>6</sub> as the electrolyte (Figure D9). Both **D46** and **D45** exhibit a reversible redox process at -352 mV and -328 mV, respectively, which originates from the Fe(II) oxidation. In comparison, the Fe(II) complex of methyltris(2-pyridyl)aluminate (**D16**)<sup>139</sup> showed a quasi-reversible Fe(III)/Fe(II) couple of  $E_{1/2} = -0.08$  V and an irreversible Fe(II)/Fe(I) couple of  $E_{1/2} = -1.130$  V (relative to Ag/Ag<sup>+</sup>). The Fe(III)/Fe(II) couples here are calibrated by referencing the Fe(III)/Fe(II) couple of ferrocene as zero. Apparently, these tris(2-pyridyl)borate Fe(II) complexes appear to be more easily oxidized than ferrocene.



(a)



(b)

**Figure D9.** Cyclic voltammograms of Fe(II) complexes: (a) **D46** ( $1 \times 10^{-3} \text{ M}$ ) and (b) **D45** ( $1 \times 10^{-3} \text{ M}$ ) with  $0.1 \text{ M}$   $[\text{Bu}_4\text{N}]\text{PF}_6$  in  $\text{CH}_2\text{Cl}_2$  as the supporting electrolyte for anionic scans (scan rate  $100 \text{ mV/s}$ ; Fe(III)/Fe(II) couple of ferrocene was used as reference and set as zero).

UV-vis measurements of solutions of Fe(II) complexes **D46** and **D45** in  $\text{CH}_2\text{Cl}_2$  were performed, and similar maximum absorption wavelengths were observed for both complexes at ca. 425 nm and 480 nm (Figure D10). These are significantly longer than the bands at 366 nm and 430 nm for the Fe(II) complex of methyltris(2-pyridyl)aluminate (**D16**) in THF solution. Indeed, Fe(II) complexes,  $[\text{Fe}\{(\text{py})_3\text{CH}\}_2][\text{NO}_3]_2$  and  $[\text{Fe}\{(\text{py})_3\text{PO}\}_2][\text{NO}_3]_2$ , showed similar shapes of the bands in their UV-vis spectra and both of them showed absorption at lower energy. Similarly, the two absorption bands of **D46** can be assigned to M→L Charge Transfer (CT). Moreover, the counter anion seems to play an important role in the CT process of these Fe(II) complexes with neutral ligands; for example, a significant high energy shift was found when the  $\text{NO}_3^-$  of  $[\text{Fe}\{(\text{py})_3\text{CH}\}_2][\text{NO}_3]_2$  was replaced by  $\text{ClO}_4^-$ . A solution of Fe(III) complex **D47** in  $\text{CH}_2\text{Cl}_2$  was also studied by UV-vis spectroscopy; drastical high energy shifts of the UV-vis absorption bands were found with a new absorption band at 340 nm; and this absorption band is at significantly shorter wavelength than the ones at 466 nm and 560 nm reported for the Fe(III) complex,  $[\text{Fe}\{(\text{pz})_3\text{CH}\}_2][\text{ClO}_4]_3$ . A low energy shift from  $[\text{Fe}\{(\text{pz})_3\text{CH}\}_2][\text{ClO}_4]_2$  to  $[\text{Fe}\{(\text{pz})_3\text{CH}\}_2][\text{ClO}_4]_3$  was found in the UV-vis spectra, which is the opposite of what was found for Fe(II) complex **D46** as it was converted to the higher oxidation state Fe(III).<sup>153</sup>

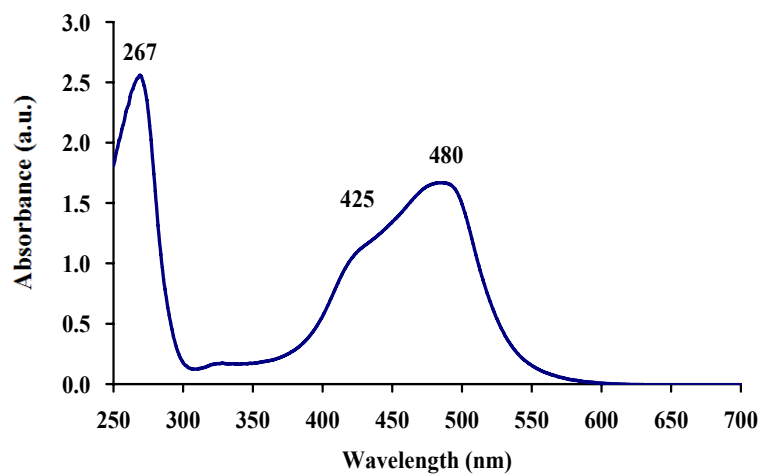


**Figure D10.** UV-vis spectrum of Fe(II) complex D46.

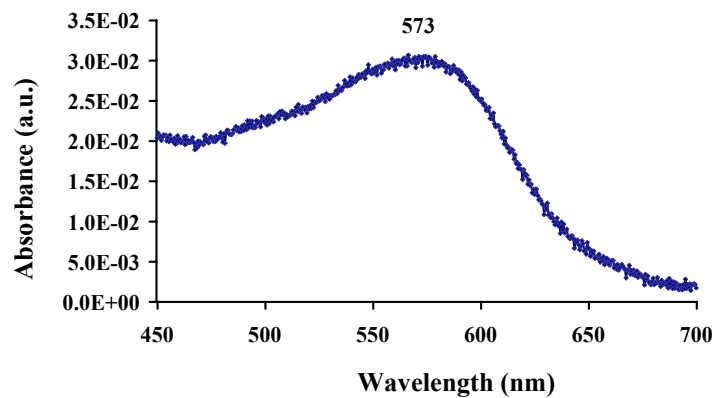
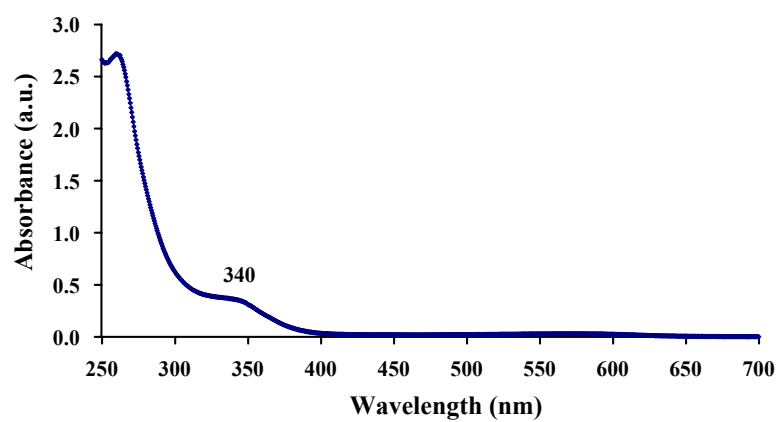


**Figure D11.** UV-vis spectra of Fe(III) complex D47.

### D.2.6 Single Crystal X-ray Diffraction Analysis of the Pyridylborate Ligands

Single crystal X-ray diffraction has been used as an important tool for identification of the pyridyl borate species and to study their structures in the solid state. Single crystals of the multidentate ligands and Mg(II) and Fe(II) complexes were obtained by slow solvent evaporation of a toluene solution.

Two crystallographically independent molecules were found in the unit cell of t-butylphenyltris(2-pyridyl)borate free acid (**D37**). Selected crystal data are listed in Table D2 and one of the two independent molecules is displayed in Figure D12. For each molecule, two pyridyl rings are almost in a coplanar arrangement with a small dihedral angle of  $18.95^\circ$  or  $21.19^\circ$  due to a hydrogen bonding interaction between the pyridyl bound proton of one of the pyridyl rings and the nitrogen of the other. In comparison, the two hydrogen-bonded pyridine rings in the dimethylbis(2-pyridyl)borate free acid were reported to be in the same plane.<sup>81d</sup> The C-B-C angles involving the hydrogen-bonded pyridine rings are  $113.0^\circ$  and  $112.2^\circ$ , respectively, which are very close to  $112.7^\circ$  reported for the corresponding bond angle of dimethylbis(2-pyridyl)borate free acid.

The structure of styryltris(2-pyridyl)borate free acid was also determined by single crystal X-ray (Figure D13). A relatively large dihedral angle between two hydrogen-bonded pyridine rings was found ( $34.98^\circ$ ) and the C-B-C bond angle between the two hydrogen-bonded pyridine rings was found to be slightly smaller with  $109.65^\circ$ . Selected bond lengths and angles are listed in Table D2.

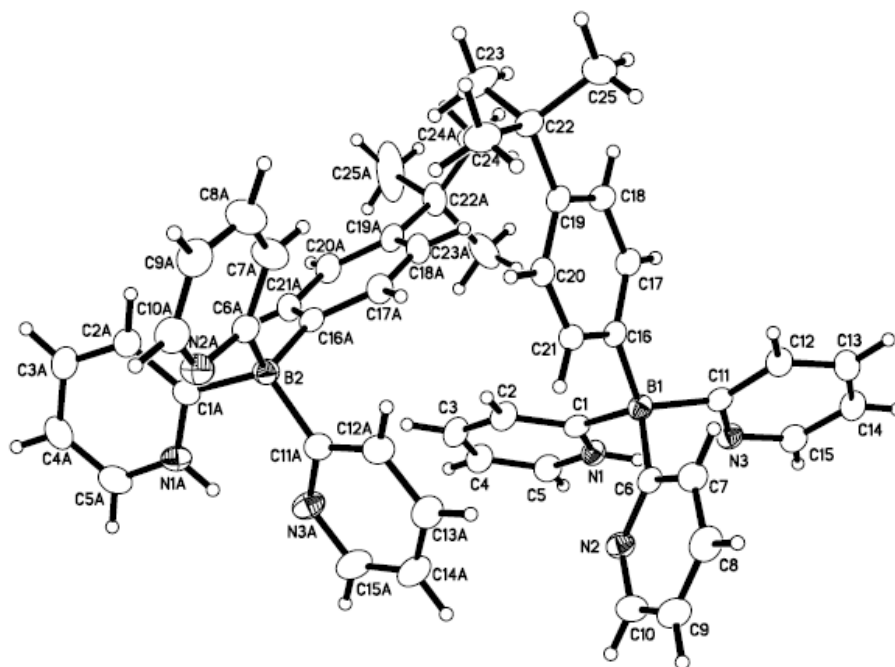


**Figure D12.** ORTEP view of the independent molecules of t-butylphenyltris(2-pyridyl) borate free acid (**D37**) (50% probability).

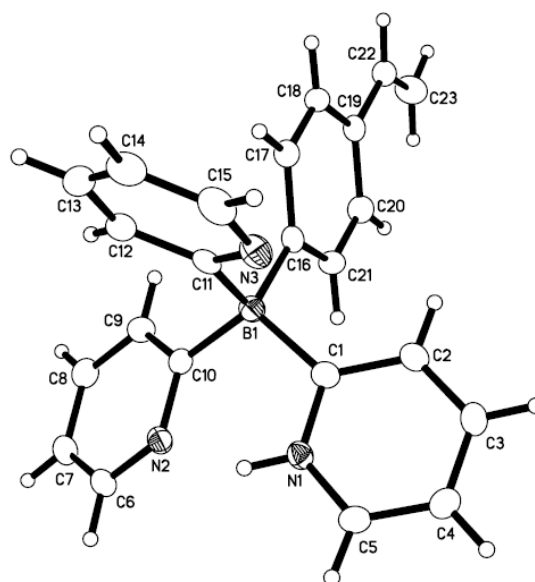


**Figure D13.** ORTEP view of styryltris(2-pyridyl) borate free acid (**D39**) (50% probability).

**Table D2.** Selected bond lengths (Å) and angles (deg) for **D37** and **D39**.

		<b>D37</b>		<b>D39</b>	
		<b>Molecule 1</b>	<b>Molecule 2</b>		
B(1)-C(16)	1.628(2)	B(2)-C(16A)	1.6384(19)	B(1)-C(16)	1.6352(18)
B(1)-C(11)	1.6380(19)	B(2)-C(11A)	1.643(2)	B(1)-C(11)	1.6336(17)
B(1)-C(1)	1.6407(19)	B(2)-C(1A)	1.635(2)	B(1)-C(10)	1.6448(17)
B(1)-C(6)	1.6410(19)	B(2)-C(6A)	1.642(2)	B(1)-C(11)	1.6411(17)
N(1)-C(1)	1.3491(18)	N(1A)-C(1A)	1.3402(19)	N(1)-C(1)	1.3508(16)
N(3)-C(11)	1.3539(18)	N(3A)-C(11A)	1.354(2)	N(2)-C(10)	1.3564(16)
N(2)-C(6)	1.3490(19)	N(2A)-C(6A)	1.3563(18)	N(3)-C(11)	1.3606(16)
C(11)-B(1)-C(16)	113.47(11)	C(16A)-B(2)-C(11A)	106.44(11)	C(10)-B(1)-C(16)	110.08(10)
C(6)-B(1)-C(11)	103.93(10)	C(6A)-B(2)-C(11A)	110.38(11)	C(10)-B(1)-C(11)	109.26(10)
C(6)-B(1)-C(16)	111.13(11)	C(16A)-B(2)-C(6A)	113.53(12)	C(11)-B(1)-C(16)	110.08(10)
C(1)-B(1)-C(6)	107.42(11)	C(1A)-B(2)-C(6A)	106.20(11)	C(1)-B(1)-C(11)	106.54(9)
C(1)-B(1)-C(11)	112.97(11)	C(1A)-B(2)-C(11A)	112.23(12)	C(1)-B(1)-C(10)	109.65(10)
C(1)-B(1)-C(16)	107.77(10)	C(1A)-B(2)-C(16A)	108.15(11)	C(1)-B(1)-C(16)	111.16(10)

For the styryltris(2-pyridyl)borate magnesium complex (**D40**) (Figure D15), one main molecule and one toluene solvent molecule were found in the unit cell, while the t-butylphenyltris(2-pyridyl)borate magnesium complex (**D38**) (Figure D14) crystallized without any solvent. The tris(2-pyridyl)borate moieties act as tridentate ligands in the bis-coordinated magnesium complexes which show an inversion center about the Mg. The geometry about magnesium can be described as tetragonally distorted octahedral.<sup>154</sup>

In complex **D38** (Table D3), two Mg-N bonds were of similar length (2.195(2) and 2.191(2) Å), whereas the other Mg-N bond was found to be much shorter with a length of 2.132(2) Å. On the contrary, in the styryl derivative **D40**, two Mg-N bond lengths (2.1528(13) Å and 2.1656(13) Å) were found to be shorter than the other bond length of 2.2047(13) Å. However, the average of Mg-N bond lengths was found to be ca. 2.17 Å for both complexes. Similar bond lengths were found for the B-C bond to the three pyridine rings of each complex, ranging from 1.640(3) Å to 1.656(3) Å. The largest differences in the N-Mg-N were 7.98° and 8.92°, respectively for **D38** and **D40**. The pyridine nitrogens in each ligand describe two different planes that are coplanar with similar distances of 2.659 Å and 2.666 Å for two complexes respectively. The two phenyl ring of the t-butylphenyltris(2-pyridyl)borate magnesium complex were also found to form two planes that are coplanar with a distance of 1.059 Å. In contrast, the two phenyl rings in the styryltris(2-pyridyl)borate magnesium complex are almost within the same plane (distance of 0.034 Å).

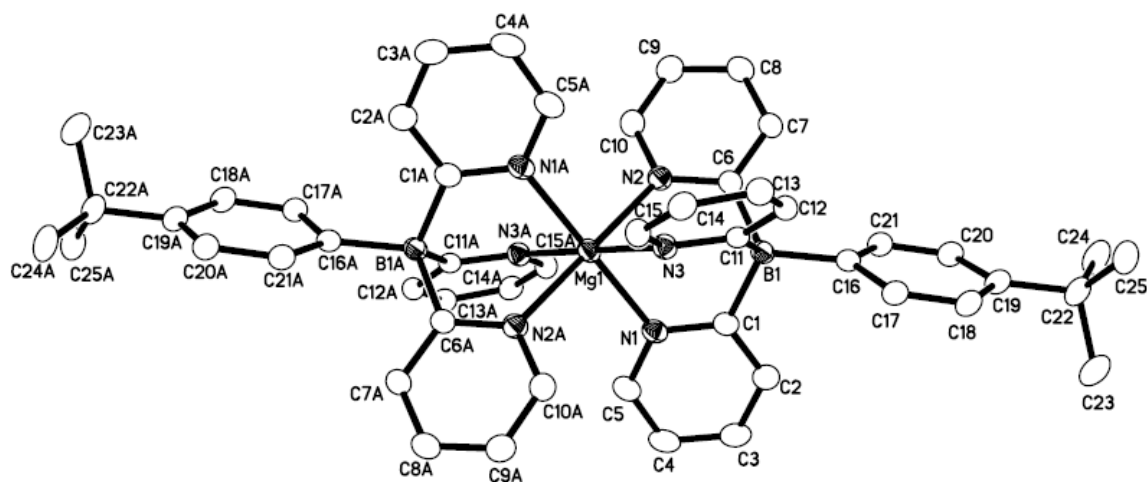


**Figure D14.** ORTEP view of Mg(II) complex (**D38**) (50% probability).

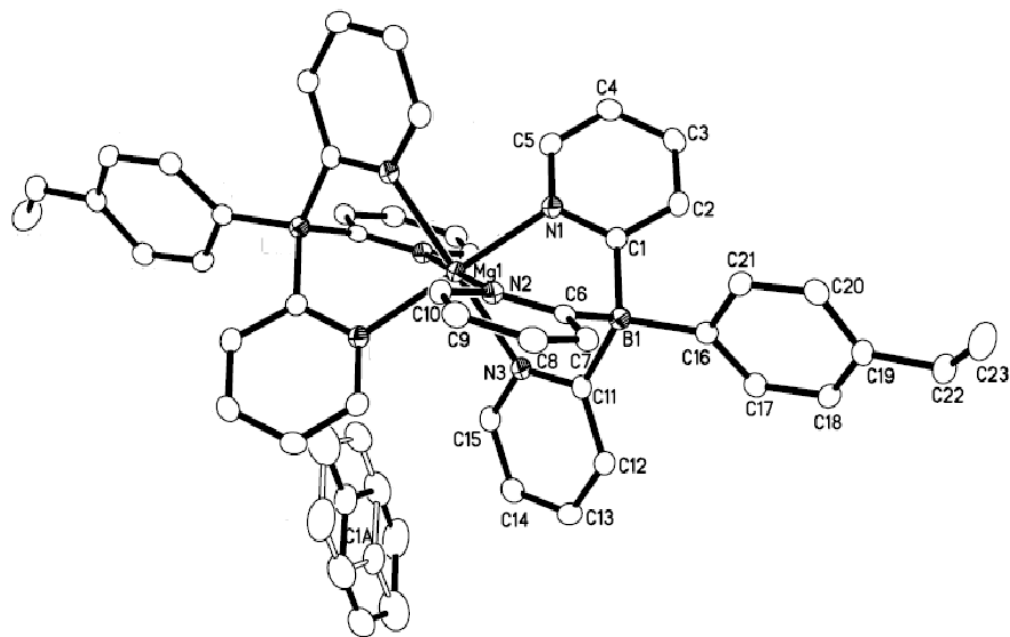


**Figure D15.** ORTEP view of Mg(II) complex (**D40**) (50% probability).

**Table D3.** Selected bond lengths (Å) and angles (deg) for the magnesium complexes **D38** and **D40**.

<b>D38</b>		<b>D40</b>	
Mg(1)-N(1)	2.1322(16)	Mg(1)-N(1)	2.1528(13)
Mg(1)-N(2)	2.1945(16)	Mg(1)-N(2)	2.1656(13)
Mg(1)-N(3)	2.1909(16)	Mg(1)-N(3)	2.2047(13)
B(1)-C(16)	1.632(3)	B(1)-C(16)	1.639(2)
B(1)-C(1)	1.656(3)	B(1)-C(1)	1.655(2)
B(1)-C(6)	1.646(3)	B(1)-C(6)	1.655(2)
B(1)-C(11)	1.640(3)	B(1)-C(11)	1.644(2)
N(1)-Mg(1)-N(1)#1	180	N(1)#1-Mg(1)-N(1)	179.998(1)
N(2)-Mg(1)-N(2)#1	180.00(7)	N(2)-Mg(1)-N(2)#1	180.00(7)
N(3)#1-Mg(1)-N(3)	180.00(8)	N(3)#1-Mg(1)-N(3)	180.0
N(1)-Mg(1)-N(2)	86.29(6)	N(1)-Mg(1)-N(2)	86.18(5)
N(1)#1-Mg(1)-N(2)	93.72(6)	N(1)#1-Mg(1)-N(2)	93.82(5)
N(1)-Mg(1)-N(3)	86.01(6)	N(1)-Mg(1)-N(3)	85.54(5)
N(1)-Mg(1)-N(3)#1	93.99(6)	N(1)-Mg(1)-N(3)#1	94.46(5)
N(2)-Mg(1)-N(3)	87.06(6)	N(2)-Mg(1)-N(3)	87.25(5)
N(2)#1-Mg(1)-N(3)	92.95(6)	N(2)#1-Mg(1)-N(3)	92.75(5)
C(1)-B(1)-C(6)	111.21(15)	C(1)-B(1)-C(6)	111.49(12)
C(1)-B(1)-C(11)	111.44(15)	C(1)-B(1)-C(11)	109.57(13)
C(1)-B(1)-C(16)	107.03(15)	C(1)-B(1)-C(16)	107.55(13)
C(6)-B(1)-C(11)	100.44(14)	C(6)-B(1)-C(11)	101.85(12)
C(6)-B(1)-C(16)	113.38(15)	C(6)-B(1)-C(16)	110.13(13)

C(11)-B(1)-C(16)	113.36(16)	C(11)-B(1)-C(16)	116.24(13)
N(1)-C(1)	1.367(2)	N(1)-C(1)	1.361(2)
N(2)-C(6)	1.361(2)	N(2)-C(6)	1.361(2)
N(3)-C(11)	1.363(2)	N(3)-C(11)	1.366(2)

All crystals of the dipyridylborate free acids (**D41-D43**) were found to feature only one independent molecule without cocrystallized solvent (Figure D16). While the two pyridine rings were found to be in the same plane for the dimethylbis(2-pyridyl)borate free acid<sup>81d</sup>, di(t-butylphenyl)bis(2-pyridyl)borate (**D41**), di(styryl)bis(2-pyridyl)borate (**D42**) and styryl(t-butylphenyl)bis(2-pyridyl)borate (**D43**) free acids exhibited different dihedral angles between the pyridine rings. The largest angle of 40.56° was found for **D42** and the smallest one of 6.45° was observed for **D41**. **D43**, which has both styryl and tbutylphenyl groups, was found to have a dihedral angle of 20.51°. Interestingly, this angle is close to the average of the ones in the former two dipyridylborates; however, a correlation with the electronic effect of the vinyl/t-butyl groups is not possible at this point. All other bond lengths and angles were similar to the ones found for dimethylbis(2-pyridyl)borate free acid and **D41** was structurally most similar to the latter. Selected bond lengths and angles are listed in Table D4.

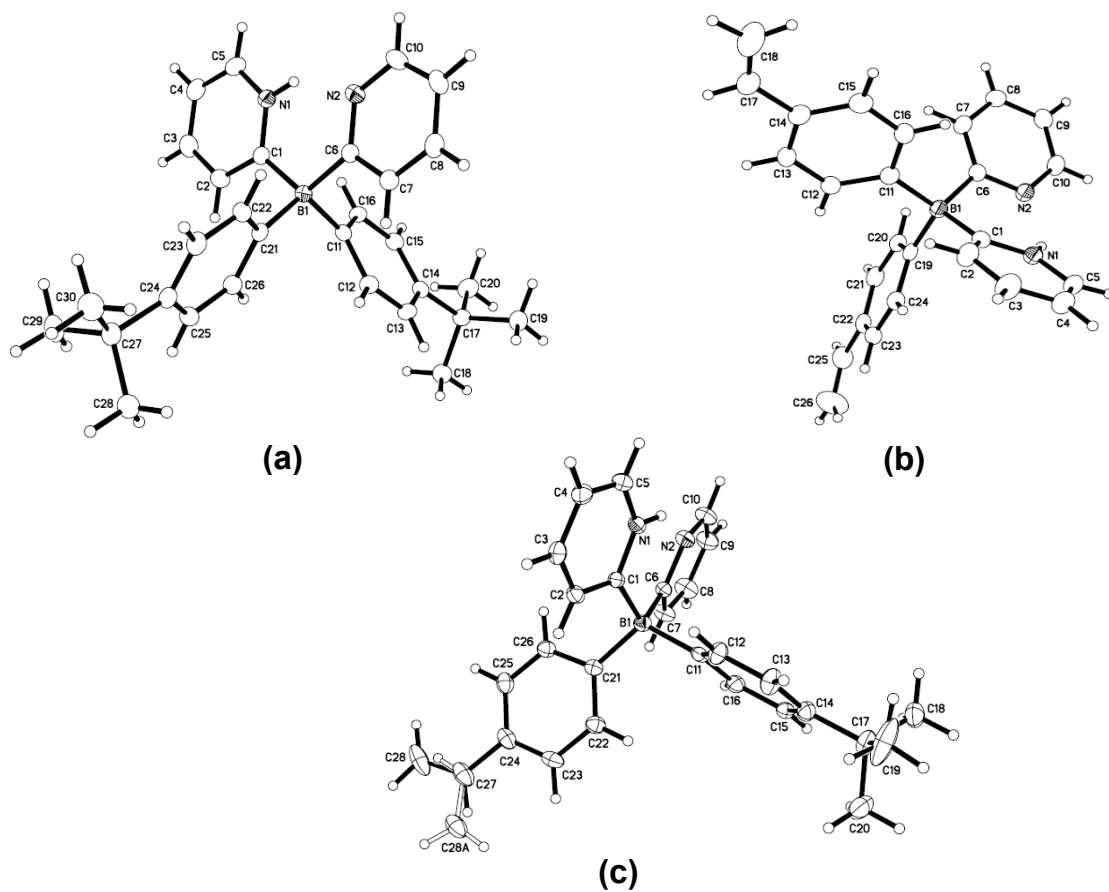


**Figure D16.** ORTEP view of diarylbis(2-pyridyl)borate free acids (50% probability). (a)

**D41; (b) D42; (c) D43.**



Made from **D37** and **D39**, both Fe(II) complexes (**D46** and **D45**) appear as red crystals. As the NMR studies suggested them to be diamagnetic in solution, single crystal X-ray diffraction was used to study the coordination environment about the Fe atom in the solid state. Bis-coordinated structures were revealed in both Fe(II) complexes. The structure of Fe(II) complex **D46** showed one main molecule and one toluene solvent molecule in the unit cell (Figure D17), whereas two independent molecules of Fe(II) complex and one toluene solvent molecule were found for **D45** (Figure D18). The geometry about the Fe atoms in the two complexes was again tetragonally distorted octahedral. For **D46**, two Fe-N bond lengths were ca. 1.99 Å, whereas the other Fe-N was found to be much shorter with a length of ca. 1.97 Å. For **D45**, for both independent molecules, two Fe-N bond lengths of ca. 2.00 Å were slightly longer than the other bond length of ca. 1.98 Å. The average Fe-N bond lengths of these two Fe(II) complexes are 1.983 Å and 1.990 Å, respectively, for **D46** and **D45**. The B-C bond lengths of the three pyridine rings in each complex were found in a narrow range from 1.625(4) to 1.642(4) Å. All the N-Fe-N angles were close to 90° with a maximum deviation of 0.7°. Interestingly, in a similar Fe(II) complex with a methyltris(2-pyridyl)aluminate tripod ligand,<sup>139</sup> the average Fe-N bond length is 2.054 Å, which is significantly longer than the Fe-N bond lengths of the Fe(II) complexes with pyridylborate ligands. The Fe-N bond length is indicative of the ligand field strength which decides the spin state and the magnetic properties of the Fe complexes.<sup>155</sup> Indeed, with longer Fe-N bond lengths the methyltris(2-pyridyl)aluminate

Fe(II) complex was found to be paramagnetic. It is worth noting that the tris(2-pyridyl)borate Fe complexes have comparable Fe-N bond lengths with the ones for the tris(2-pyridyl) ligand  $[\{N(2-py)_3\}_2Fe]^{2+}$  with N atom as bridge head (Fe-N range 1.970-1.961 Å), whereas they are significantly longer than the tris(2-pyridyl) ligand  $[\{HOC(2-py)_3\}_2Fe]$  with C atom as bridge head (Fe-N range 1.947-1.954 Å).<sup>153</sup> The short bond lengths in both tris(2-pyridyl)borate Fe(II) complexes suggest that they are diamagnetic in the solid state at the temperature used to acquire X-ray data (100K).

The planes described by three pyridine nitrogens of each t-butylphenyltris(2-pyridyl)borate ligand in **D46** are parallel with a distance of 2.288 Å. For **D45**, the distances between the two parallel planes described by three pyridine nitrogens of each tripod ligand in one molecule were found to be 2.289 Å and 2.314 Å, respectively, for the two crystallographically independent molecules. These distances are longer than the one in the tris(2-pyridyl)aluminate ligand (2.190 Å),<sup>139</sup> which reflects the trigonal compression of the latter. The phenyl rings in **D46** were also found to be coplanar with a distance of 0.965 Å. In comparison, the two phenyl rings in the independent molecules of **D45** were found to be coplanar with distances of 1.411 Å and 0.926 Å, respectively.

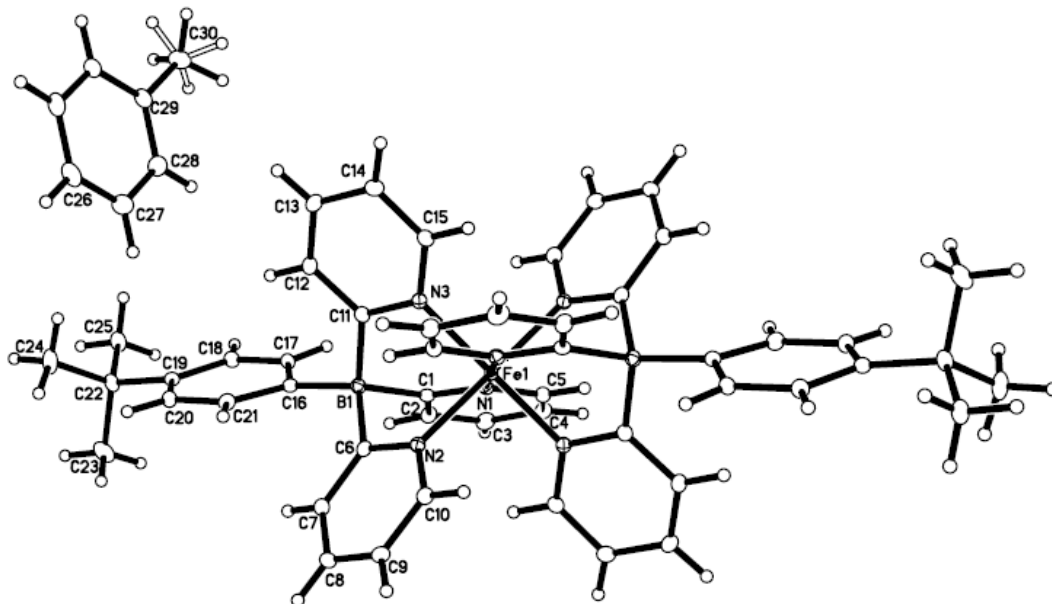


**Figure D17.** ORTEP view of Fe (II) complex **D46** (40% probability).

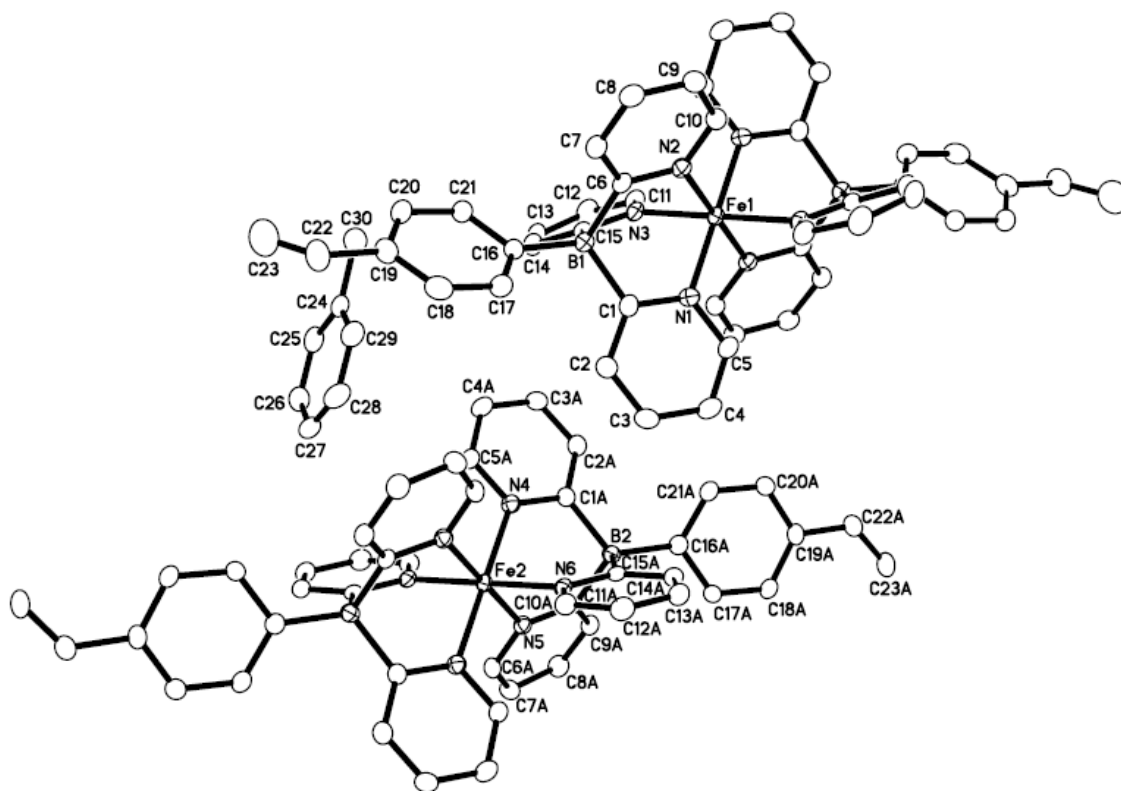


**Figure D18.** ORTEP view of Fe (II) complex **D45** (50% probability).

**Table D5.** Selected bond lengths (Å) and angles (deg) for Fe (II) complexes of **D46** and **D45**.

<b>D46</b>		<b>D45</b>	
		<b>Molecule 1</b>	<b>Molecule 2</b>
Fe(1)-N(1)	1.9883(13)	Fe(1)-N(1)	2.0031(19)
Fe(1)-N(2)	1.9906(13)	Fe(1)-N(2)	1.9707(19)
Fe(1)-N(3)	1.9691(13)	Fe(1)-N(3)	1.9929(19)
B(1)-C(16)	1.633(2)	B(1)-C(16)	1.632(3)
B(1)-C(1)	1.638(2)	B(1)-C(1)	1.635(4)
B(1)-C(6)	1.642(2)	B(1)-C(6)	1.636(4)
B(1)-C(11)	1.642(2)	B(1)-C(15)	1.625(4)
N(1)-C(1)	1.362(2)	N(1)-C(1)	1.362(3)
N(2)-C(6)	1.364(2)	N(2)-C(6)	1.361(3)
N(3)-C(11)	1.360(2)	N(3)-C(15)	1.366(3)
N(1)-Fe(1)-N(1)#1	180	N(1)#1-Fe(1)-N(1)	179.998(1)
N(2)-Fe(1)-N(2)#1	180	N(2)#1-Fe(1)-N(2)	179.997(1)
		Fe(2)-N(4)	2.0021(19)
		Fe(2)-N(5)	1.9927(18)
		Fe(2)-N(6)	1.9793(19)
		B(2)-C(16A)	1.634(3)
		B(2)-C(1A)	1.642(4)
		B(2)-C(10A)	1.639(4)
		B(2)-C(15A)	1.635(4)
		N(4)-C(1A)	1.369(3)
		N(5)-C(10A)	1.361(3)
		N(6)-C(15A)	1.363(3)
		N(4)-Fe(2)-N(4)#2	180
		N(5)-Fe(2)-N(5)#2	180

D46		D45	
	Molecule 1	Molecule 2	
N(3)-Fe(1)-N(3)#1	180	N(3)#1-Fe(1)-N(3)	180
N(1)-Fe(1)-N(2)	89.81(5)	N(1)-Fe(1)-N(2)	90.18(8)
N(1)-Fe(1)-N(2)#1	90.20(5)	N(1)#1-Fe(1)-N(2)	89.82(8)
N(1)-Fe(1)-N(3)	90.25(5)	N(1)-Fe(1)-N(3)	89.79(8)
N(1)#1-Fe(1)-N(3)	89.75(5)	N(1)#1-Fe(1)-N(3)	90.21(8)
N(2)-Fe(1)-N(3)	90.03(5)	N(2)-Fe(1)-N(3)	90.56(8)
N(2) #1-Fe(1)-N(3)	89.97(5)	N(2)-Fe(1)-N(3)#1	89.43(8)
C(1)-B(1)-C(6)	101.70(13)	C(1)-B(1)-C(16)	115.6(2)
C(1)-B(1)-C(11)	109.29(13)	C(1)-B(1)-C(6)	109.22(19)
C(1)-B(1)-C(16)	115.60(13)	C(1)-B(1)-C(15)	99.55(18)
C(6)-B(1)-C(16)	115.13(13)	C(6)-B(1)-C(15)	110.6(2)
C(6)-B(1)-C(11)	106.61(12)	C(6)-B(1)-C(16)	107.58(19)
C(11)-B(1)-C(16)	108.02(13)	C(15)-B(1)-C(16)	114.1(2)
		N(6)-Fe(2)-N(6)#2	180.000(1)
		N(4)#2-Fe(2)-N(5)	90.64(8)
		N(4)-Fe(2)-N(5)	89.36(8)
		N(4)#2-Fe(2)-N(6)	90.58(8)
		N(4)-Fe(2)-N(6)	89.42(8)
		N(5)#2-Fe(2)-N(6)	89.90(8)
		N(5)-Fe(2)-N(6)	90.10(8)
		C(1A)-B(2)-C(16A)	117.0(2)
		C(1A)-B(2)-C(15A)	107.48(18)
		C(1A)-B(2)-C(10A)	101.72(19)
		C(10A)-B(2)-C(15A)	109.15(19)
		C(10A)-B(2)-C(16A)	113.35(19)
		C(15A)-B(2)-C(16A)	107.82(19)

The preparative oxidation of **D46** with  $\text{FeCl}_3$  led to an Fe(III) complex **D47** with an  $\text{FeCl}_4^-$  counter anion as confirmed by single crystal X-ray analysis (Figure D19, Table D6). The geometry about the Fe(III) center is a distorted octahedron with an average Fe-N bond length of 1.991 Å, which is quite close to that for the neutral Fe(II) complex **D46**. However, the Fe-N bond lengths in the Fe(III) complex (**D47**) are less evenly distributed from 1.965(3) Å to 2.011(3) Å, reflecting the significant distortion of the octahedral geometry about the Fe atom. A small angle of 1.27° was found between the planes described by the three pyridine nitrogens of the tris(2-pyridyl)borate ligands. And the angle between the phenyl rings was found to be 3.90°. Moreover, the B-C bond to each of the phenyl rings was found to be significantly bent out of the plane of the phenyl ring. The angles between the B-C bond to the phenyl ring and the line described by *ipso* carbon and the centroid center of the phenyl ring are 168.87° and 169.79°, respectively, for each of the t-butylphenyltris(2-pyridyl)borate ligands.

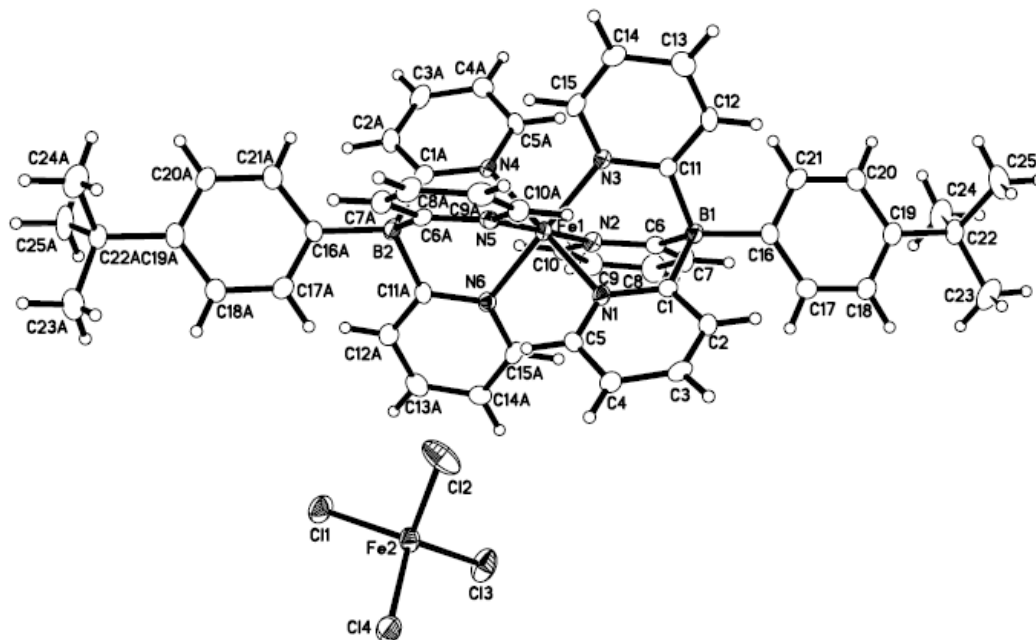


**Figure D19.** ORTEP view of Fe(III) complex **D47** (40% probability).

**Table D6.** Selected bond lengths (Å) and angles (deg) for Fe(III) complex **D47**.

Fe(1)-N(1)	1.996(3)	Fe(1)-N(4)	2.011(3)
Fe(1)-N(2)	1.965(3)	Fe(1)-N(5)	1.991(3)
Fe(1)-N(3)	1.990(3)	Fe(1)-N(6)	1.990(2)
B(1)-C(16)	1.613(5)	B(2)-C(16A)	1.621(5)
B(1)-C(1)	1.636(5)	B(2)-C(1A)	1.637(5)
B(1)-C(6)	1.633(5)	B(2)-C(6A)	1.635(5)
B(1)-C(11)	1.632(5)	B(2)-C(11A)	1.622(5)
N(1)-C(1)	1.361(4)	N(4)-C(1A)	1.356(4)
N(2)-C(6)	1.354(4)	N(5)-C(6A)	1.360(4)

N(3)-C(11)	1.357(4)	N(6)-C(11A)	1.355(4)
C(1)-B(1)-C(6)	107.3(3)	C(1A)-B(2)-C(6A)	106.6(3)
C(1)-B(1)-C(11)	99.4(3)	C(1A)-B(2)-C(11A)	100.8(3)
C(1)-B(1)-C(16)	117.4(3)	C(1A)-B(2)-C(16A)	118.8(3)
C(6)-B(1)-C(11)	109.9(3)	C(6A)-B(2)-C(11A)	109.7(3)
C(6)-B(1)-C(16)	107.6(3)	C(6A)-B(2)-C(16A)	106.4(3)
C(11)-B(1)-C(16)	114.8(3)	C(11A)-B(2)-C(16A)	114.1(3)
N(1)-Fe(1)-N(2)	90.65(12)	N(2)-Fe(1)-N(5)	178.81(13)
N(1)-Fe(1)-N(3)	89.18(11)	N(2)-Fe(1)-N(6)	88.80(11)
N(1)-Fe(1)-N(4)	179.40(12)	N(3)-Fe(1)-N(4)	90.23(11)
N(1)-Fe(1)-N(5)	90.07(11)	N(3)-Fe(1)-N(5)	89.60(11)
N(1)-Fe(1)-N(6)	90.16(11)	N(3)-Fe(1)-N(6)	179.32(11)
N(2)-Fe(1)-N(3)	91.35(11)	N(4)-Fe(1)-N(5)	89.80(12)
N(2)-Fe(1)-N(4)	89.49(11)	N(4)-Fe(1)-N(6)	90.44(11)
		N(5)-Fe(1)-N(6)	90.25(10)

### D.3 Free Radical Polymerizations of Styryltris(2-pyridyl)borate Free Acid (D39)

The styryltris(2-pyridyl)borate monomer (**D39**) shows good stability and no self-initiated polymerization was found when stored at ambient temperature. Standard free radical polymerization was used to prove that it is indeed a polymerizable monomer. A DMF

solution of styryltris(2-pyridyl)borate free acid and AIBN, the molarities of which were 0.43 M and 0.74 M, respectively, was thoroughly degassed. The mixture was then heated to 90 °C for 40 hours. A white solid product was isolated by precipitation of the reaction solution into diethyl ether and further purified twice by precipitation from a dichloromethane solution into diethyl ether. The white solid (**D48**) was collected and dried under high vacuum at 65 °C (60% yield).

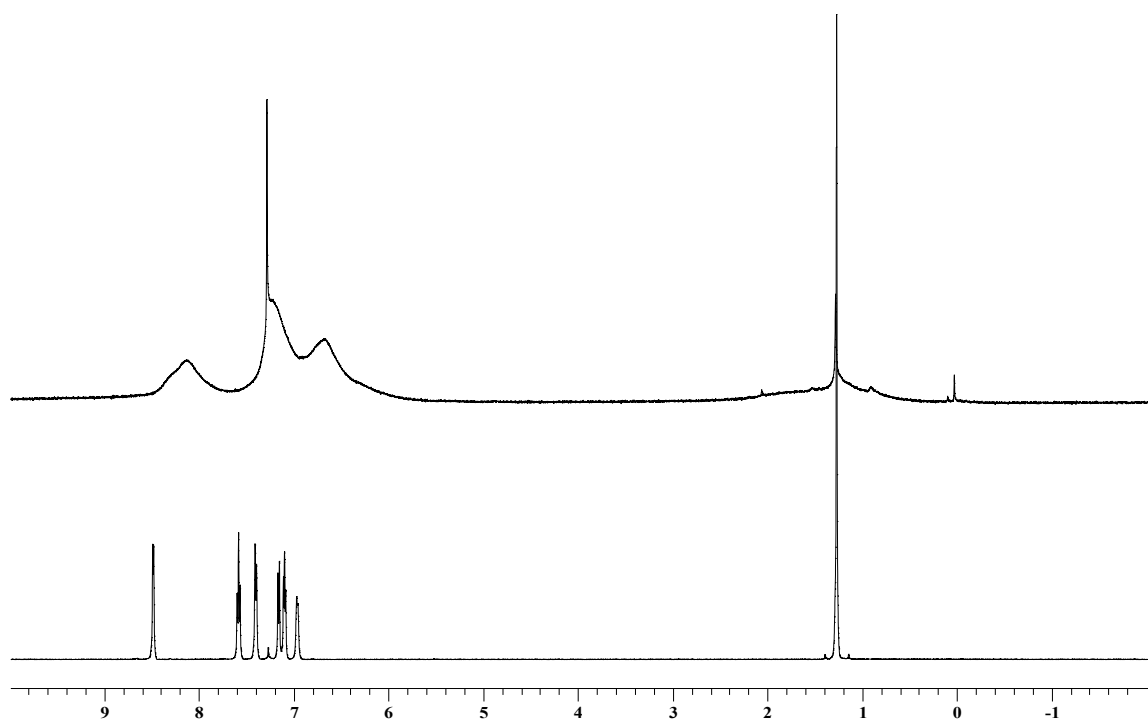


**Figure D20.** An overlay of  $^1\text{H}$  NMR of the homopolymer (**D48**) and model compound (**D37**).

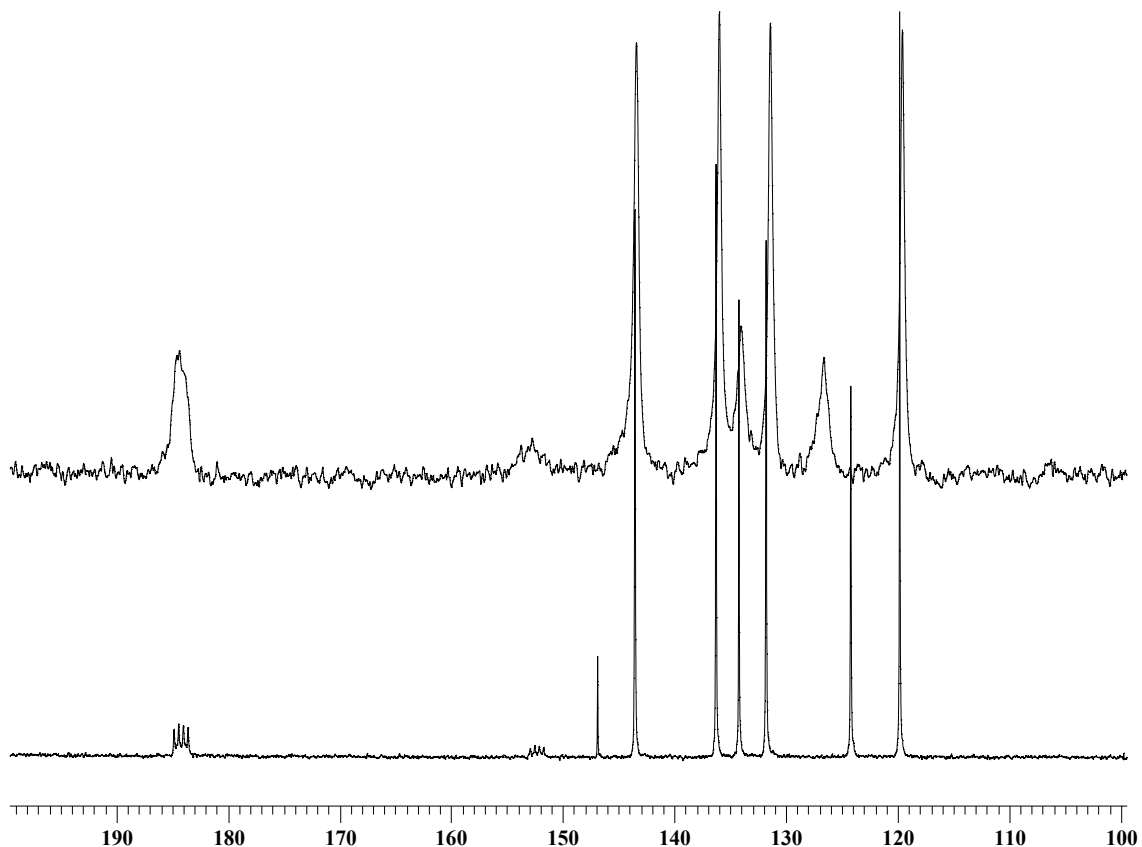


**Figure D21.** An overlay of <sup>13</sup>C NMR of the homopolymer (**D48**) and model compound (**D37**).

<sup>1</sup>H NMR analysis (Figure D20) showed broad peaks typical of the formation of an atactic polymer, which can be ascribed to the non-stereospecific nature of the free radical polymerization process. <sup>11</sup>B NMR showed a relatively broad peak at -11 ppm which is almost identical to that of the molecular tris(2-pyridyl)borate ligand. In the <sup>13</sup>C spectra, two broad peaks at 184 ppm and 153 ppm of different intensities were assigned to the *ipso* carbons of the respective pyridine and phenyl rings. The signals of the polymer (**D48**) were fairly consistent with the ones for the molecular species (**D37**) (Figure D21).

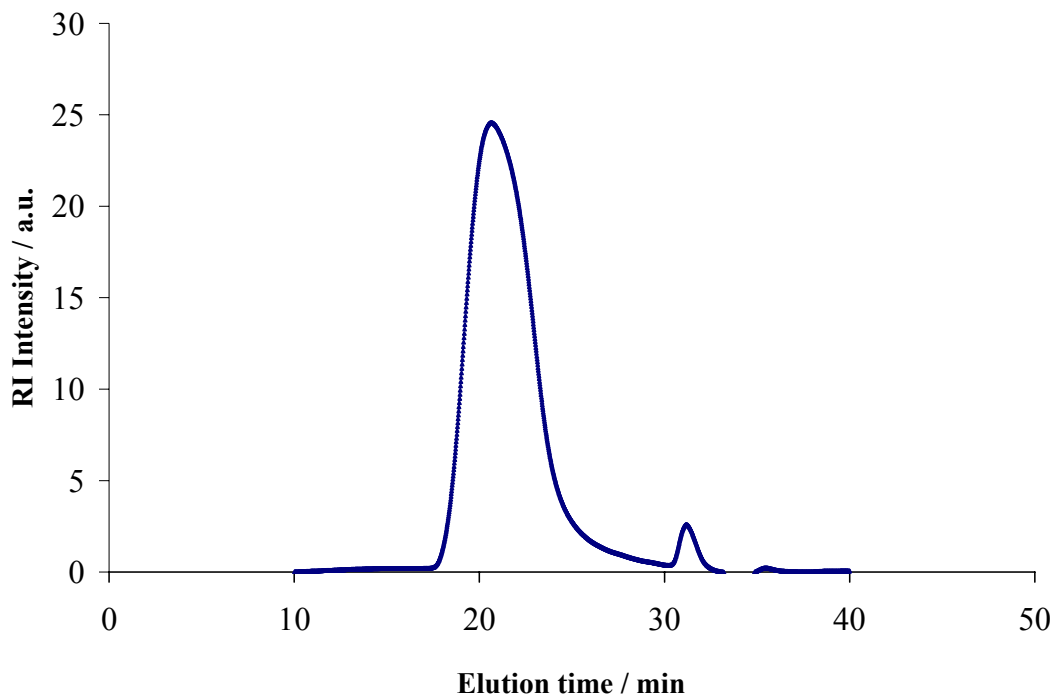


**Figure D22.** GPC trace for polymer (**D48**) (recorded in DMF/20mM  $\text{NH}_4[\text{PF}_6]$  at 60 °C).

The novel tripodal tris(2-pyridyl)borate functionalized polymer (**D48**), was further studied by gel permeation chromatography (GPC) in DMF containing 20 mM  $\text{NH}_4[\text{PF}_6]$  at 60 °C. The GPC trace (Figure D22) showed a main peak, which is relatively broad (PDI = 1.57) due to the non-controlled fashion of the free radical polymerization method used. The number average molecular weight ( $M_n$ ) was up to 35 k relative to narrow PS standards. It can be assumed that **D48** tends to have stronger interactions than the PS standards with the GPC column (crosslinked polyvinyl alcohol), so that the true  $M_n$  could be even higher than the one from calibration with PS standards. The high molecular weight obtained through free radical polymerization confirms that the styryltris(2-

pyridyl)borate free acid is indeed a polymerizable monomer and suggests that controlled polymerization of this monomer may also be possible.

#### **D.4 Conclusions**

2-Pyridyl magnesium chloride has been prepared and isolated in form of a dimeric structure, in which the pyridyl nitrogens bind to magnesium intramolecularly. The dimeric Grignard reagent is soluble and stable in dichloromethane and toluene and therefore has been successfully used to react with arylbromoboranes in the synthesis of a variety of multidentate pyridine-based borate ligands. The nitrogen-magnesium bonding is believed to be critical for overcoming interference due to strong complexation between the Lewis basic pyridine and highly Lewis acidic boron center of arylbromoboranes.

Tris(2-pyridyl)borate ligands were synthesized as the first tripod tris(2-pyridyl) ligands with a boron atom as the bridge head. Of great significance, the trispyridylborates with their pyridine rings bonded to boron through strong B-C bonds can be expected to be much more stable than the analogous well known scorpionate trispyrazolylborate (Tp) ligands, in which pyrazole rings are linked to boron with relatively polar B-N bonds. Tris(2-pyridyl)borate ligands are promising as novel chelating ligands, in analogy to Tp ligands, in various applications such as coordination, organometallic and bioinorganic chemistry. The magnesium and iron complexes of tris(2-pyridyl)borate ligands have been prepared. The iron complexes lend themselves to further investigation of their magnetic

properties. Upon complexation of different metals, novel coordination compounds can be expected to be synthesized and studied for different applications such as catalysis.

Attachment of the novel tris(2-pyridyl)borate ligands to polystyrene has been achieved by free radical polymerization of styryl tris(2-pyridyl)borate monomer. This type of novel polydentate boron containing polymer may be further explored for applications such as pH stimuli materials (pyridine quaternization at low pH), as a universal precursors for the synthesis of a plethora of metal containing polymers through metal ion complexation and possibly for selective metal ion extraction.

Controlled/living radical polymerizations of styryl tris(2-pyridyl)borate monomer is also attractive for the preparation of novel block copolymers, which can assemble into nano-structured materials with pH stimuli-responsive properties.

## **D.5 Experimental Part**

### **Synthesis of 2-Pyridyl Grignard Reagent (D34).**

To a freshly prepared solution of *i*PrMgCl in tetrahydrofuran (400 mL, 345 mmol), neat 2-bromopyridine (30.0 mL, 313 mmol) was added through a syringe. The resulting dark red reaction solution was kept stirring for 5 h and then connected to vacuum to evaporate the solvent until a dense yellow slurry formed suddenly. The slurry was carefully transferred under nitrogen protection to a fritted addition funnel and dry tetrahydrofuran

(ca. 150 mL) was used to help complete the transfer of the solids. Dry tetrahydrofuran was continuously passed through the filter cake until it was white and the filtrate colorless. The solid was dried under high vacuum at room temperature for 6 h and then further dried under high vacuum at 65 °C for 12 h. Yield of  $(\text{PyMgCl})_2 \cdot (\text{THF})_{3.5}$ : 63 g (76%).  $^1\text{H}$  NMR (499.973 MHz,  $\text{CD}_2\text{Cl}_2$ )  $\delta$  = 8.60 (br s), 7.87 (br s), 7.45 (br s), 7.01 (br s), 3.76 (br m, thf), 1.84 (br m, thf).

### Synthesis of Styryldibromoborane (D36).

To a solution of 4-trimethylsilylstyrene (9.50 g, 53.9 mmol) in toluene (100 mL) was slowly added a solution of boron tribromide (13.5 g, 53.9 mmol) in toluene (50 mL) and the mixture was kept stirring for 5 h. The solvent was removed under high vacuum and the oily residue was subjected to sublimation under high vacuum at 85-90 °C. The product was stored at -18 °C under  $\text{N}_2$  atmosphere. Yield: 8.1 g (55%).  $^1\text{H}$  NMR (499.973 MHz,  $\text{CDCl}_3$ )  $\delta$  = 8.20 (d,  $^3\text{J}$  = 8.0 Hz, 2H, styryl-H2,6), 7.49 (d,  $^3\text{J}$  = 8.0 Hz, 2H, styryl-H3,5), 6.78 (dd,  $^3\text{J}_{\text{trans}}$  = 17.5 Hz,  $^3\text{J}_{\text{cis}}$  = 11.0 Hz, 1H, =CH), 5.98 (d,  $^3\text{J}$  = 17.5 Hz, 1H, =CHH), 5.50 (d,  $^3\text{J}$  = 11.0 Hz, 1H, =CHH).  $^{13}\text{C}$  NMR (125.718 MHz,  $\text{CDCl}_3$ )  $\delta$  = 144.4 (styryl-C4), 138.4 (styryl-C2,6), 136.3 (vinyl-CH), 127.7 (styryl-C1), 126.1 (styryl-C3,5), 118.2 (vinyl- $\text{CH}_2$ ).  $^{11}\text{B}$  NMR (1260.386 MHz,  $\text{CDCl}_3$ )  $\delta$  = 51 ( $w_{1/2}$  = 170 Hz).

**Synthesis of 4-Trimethylstannylstyrene (D44).**

Chlorostyrene (23.0 g, 166 mmol) in THF (100 mL) was added dropwise to a flask containing magnesium (6.0 g, 247 mmol) in THF (250 mL) and dibromoethane (1 mL). The reaction mixture was kept stirring for 3 h and then cooled to 0 °C. A solution of trimethyltin chloride (33.1 g, 166 mmol) in THF (100 mL) was added to the reaction mixture. The resulting white slurry was slowly warmed to room temperature and then gently refluxed for 30 min. An aqueous solution of  $\text{NH}_4\text{HCO}_3$  was added to the reaction mixture and the product was subsequently extracted with diethyl ether (3×200 mL). The combined organic layer was dried on sodium sulfate and then concentrated with rotary evaporator to give an oil, which was distilled under high vacuum. Yield: 33.8 g (76%).

$^1\text{H}$  NMR (499.973 MHz,  $\text{CDCl}_3$ )  $\delta$  = 8.20 (d,  $^3\text{J}$  = 7.5 Hz, 2H, styryl-H<sub>2,6</sub>), 7.49 (d,  $^3\text{J}$  = 8.0 Hz, 2H, styryl-H<sub>3,5</sub>), 6.72 (dd,  $^3\text{J}_{\text{trans}}$  = 17.5 Hz,  $^3\text{J}_{\text{cis}}$  = 11.0 Hz, 1H, =CH), 5.78 (d,  $^3\text{J}$  = 17.5 Hz, 1H, =CHH), 5.25 (d,  $^3\text{J}$  = 11.0 Hz, 1H, =CHH).

**Synthesis of *t*-Butylphenyltris(2-pyridyl)borate Free Acid (D37).**

*t*-Butylphenyl dibromoborane (5.00 g, 16.5 mmol) in  $\text{CH}_2\text{Cl}_2$  (30 mL) was added dropwise to a solution of pyridyl Grignard (14.5 g, 27.2 mmol) in  $\text{CH}_2\text{Cl}_2$  (50 mL). The resulting dark red mixture was kept stirring for 5 h. The reaction mixture was poured into an aqueous  $\text{Na}_2\text{CO}_3$  solution (30 g in 250 mL  $\text{H}_2\text{O}$ ) to give a slurry which was stirred for 30 min. Extraction with  $\text{CH}_2\text{Cl}_2$  (3×200 mL) gave a brown organic phase that was dried

over Na<sub>2</sub>SO<sub>4</sub>. The solvents were removed under vacuum to give an oil that was redissolved in acetone (100 mL), filtered and brought to dryness. The crystalline solid residue was washed with cold acetone (5 mL) leaving behind a white crystalline product with a yellow tint. The product was further purified by chromatography on silica with a 1 to 1 mixture of hexanes and acetone containing 1% (v/v) triethylamine as the eluent. The product was dried under vacuum at 60 °C for 10 h to give a white solid. Yield: 3.4 g (54%). Single crystals for X-ray diffraction analysis were obtained by slow solvent evaporation of a toluene solution. <sup>1</sup>H NMR (499.973 MHz, CDCl<sub>3</sub>) δ = 19.5 (br s, 1H, pyridyl N-H), 8.49 (d, <sup>3</sup>J = 5.0 Hz, 3H, pyridyl-H6), 7.58 (pst, <sup>3</sup>J = 7.5 Hz, 3H, pyridyl-H4), 7.40 (d, <sup>3</sup>J = 7.5 Hz, 3H, pyridyl-H3), 7.16 (d, <sup>3</sup>J = 7.5 Hz, 2H, tPh-H3,5), 7.10 (pst, <sup>3</sup>J = 6.3 Hz, 3H, pyridyl-H5), 6.96 (br d, <sup>3</sup>J = 6.0 Hz, 2H, tPh-H2,6), 1.27 (s, 9H, *t*-Bu). <sup>13</sup>C NMR (125.718 MHz, CDCl<sub>3</sub>) δ = 184.2 (q, <sup>1</sup>J<sub>C-B</sub> = 53.1 Hz, pyridyl-C2), 152.3 (q, <sup>1</sup>J<sub>C-B</sub> = 50.0 Hz, tPh-C1), 146.9 (tPh-C4), 143.6 (pyridyl-C6), 136.3 (pyridyl-C4), 134.2 (pyridyl-C3), 131.8 (tPh-C2,6), 124.2 (tPh-C3,5), 119.8 (pyridyl-C5), 34.3 (C(CH<sub>3</sub>)<sub>3</sub>), 31.7 (C(CH<sub>3</sub>)<sub>3</sub>). <sup>11</sup>B NMR (160.386 MHz, CDCl<sub>3</sub>) δ = -10.8 (w<sub>1/2</sub> = 13 Hz). Elemental analysis: calcd for C<sub>25</sub>H<sub>26</sub>BN<sub>3</sub>: C 79.16, H 6.91, N 11.08%; found C 78.92, H 6.94, N 11.08%. MALDI-TOF (benzo[a]pyrene): m/z = 380.2333 (calcd for <sup>12</sup>C<sub>25</sub><sup>1</sup>H<sub>26</sub><sup>11</sup>B<sup>14</sup>N<sub>3</sub>+H 380.2298).

**Synthesis of Styryltris(2-pyridyl)borate Free Acid (D39).**

To a solution of pyridyl Grignard (49.6 g, 93.1 mmol) in  $\text{CH}_2\text{Cl}_2$  (150 mL), a solution of styryl dibromoborane (16.1 g, 58.8 mmol) in  $\text{CH}_2\text{Cl}_2$  (50 mL) was slowly added by syringe at 0 °C. The dark red reaction solution was stirred for 1 h at 0 °C, allowed to warm to room temperature and kept stirring for 5 h. The mixture was poured into an aqueous  $\text{Na}_2\text{CO}_3$  solution (50 g, 500 mL of  $\text{H}_2\text{O}$ ), the resulting slurry was stirred for 1 h and then extracted with  $\text{CH}_2\text{Cl}_2$  (4×150 mL). The organic layers were combined, dried over  $\text{Na}_2\text{SO}_4$  and evaporated using a rotary evaporator. The oily residue was redissolved in acetone (100 mL) and filtered. Solvent evaporation gave a dark brown solid, which was further purified by chromatography on silica gel with eluents being varied from dichloromethane to acetone. Solvent evaporation on a rotary evaporator resulted in fractions consisting of yellow oils or white crystalline solids. The yellow oily material can be titrated with hexanes to give a white solid. The combined solid products were subjected to recrystallization by slow solvent evaporation of a concentrated acetone solution. The white solid product was dried under high vacuum at 60 °C for 10 h. Yield: 11.4 g (56%). The product was subjected to an additional chromatography using a short column of silica gel prior to use in radical polymerizations. Single crystals for X-ray diffraction analysis were obtained by slow solvent evaporation of a toluene solution.  $^1\text{H}$  NMR (499.973 MHz,  $\text{CDCl}_3$ )  $\delta$  = 17.3 (br s, 1H, pyridyl N-H), 8.68 (d,  $^3\text{J}$  = 5.0 Hz, 3H, pyridyl-H6), 7.86 (pst,  $^3\text{J}$  = 7.3 Hz, 3H, pyridyl-H4), 7.58 (d,  $^3\text{J}$  = 7.5 Hz, 3H,

pyridyl-H3), 7.41 (pst,  $^3J = 6.0$  Hz, 3H, pyridyl-H5), 7.29 (d,  $^3J = 8.0$  Hz, 2H, styryl-H3,5), 7.07 (br d,  $^3J = 7.5$  Hz, 2H, styryl-H2,6), 6.69 (dd,  $^3J_{\text{trans}} = 17.5$  Hz,  $^3J_{\text{cis}} = 11.0$  Hz, 1H, =CH), 5.70 (d,  $^3J = 17.5$  Hz, 1H, =CHH), 5.18 (d,  $^3J = 11.0$  Hz, 1H, =CHH).  $^{13}\text{C}$  NMR (125.718 MHz,  $\text{CDCl}_3$ )  $\delta = 184.1$  (q,  $^1J_{\text{C-B}} = 52.9$  Hz, pyridyl-C2), 156.8 (q,  $^1J_{\text{C-B}} = 50.2$  Hz, styryl-C1), 143.7 (pyridyl-C6), 137.8 (vinyl-CH), 136.2 (styryl-C2,6), 134.9 (pyridyl-C4), 133.9 (styryl-C4), 131.7 (pyridyl-C3), 125.3 (styryl-C3,5), 119.8 (pyridyl-C5), 111.7 (vinyl- $\text{CH}_2$ ).  $^{11}\text{B}$  NMR (125.718 MHz,  $\text{CDCl}_3$ )  $\delta = -11.0$  ( $w_{1/2} = 11$  Hz). MALDI-TOF (benzo[a]pyrene):  $m/z = 350.1703$  (calcd for  $^{12}\text{C}_{23}^{1}\text{H}_{20}^{11}\text{B}^{14}\text{N}_3+\text{H}$  350.1829).

**Alternative Procedure:** To a solution of 4-trimethylsilylstyrene (10.0 g, 56.7 mmol) in toluene (150 mL) was slowly added a solution of boron tribromide (14.1 g, 56.3 mmol) in toluene (50 mL) and the mixture was kept stirring for 5 h. The reaction mixture was slowly transferred to a solution of pyridyl Grignard (46.0 g, 86.3 mmol) in toluene (200 mL). The resulting red brown suspension was kept stirring for 5 h. The purification was performed in a similar way as described in the previous procedure. During column chromatography, the magnesium sandwich complex, bis(styryltris(2-pyridyl)borate) magnesium, was obtained as a side product with  $\text{CH}_2\text{Cl}_2$  as the first eluent. Styryltris(2-pyridyl)borate free acid was then obtained with acetone as the eluent. Yield: 4.2 g (21%) for the free acid; 1.9 g (9.4%) for the magnesium sandwich complex.

Attempted purification of the sandwich magnesium compound by column chromatography on silica with  $\text{CH}_2\text{Cl}_2$  containing 1% of triethylamine resulted in conversion to the pure free acid. During the initial chromatography step, the presence of basic pyridine-containing impurities might have prevented the dissociation of the magnesium sandwich complex on the silica gel.

#### **Synthesis of Di(*t*-butylphenyl)bis(2-pyridyl)borate Free Acid (D41).**

To a solution of *t*-butylphenyldibromoborane (0.50 g, 1.6 mmol) in  $\text{CH}_2\text{Cl}_2$  (15 mL) was added a pre-cooled solution ( $-18\text{ }^\circ\text{C}$ ) of *t*-butylphenyltrimethyltin (0.51 g, 1.7 mmol) in  $\text{CH}_2\text{Cl}_2$  (15 mL) at  $-18\text{ }^\circ\text{C}$ . The mixture was allowed to warm to room temperature, kept stirring for 5 h, and then kept under vacuum to remove all the volatile components. The white residue was redissolved in  $\text{CH}_2\text{Cl}_2$  (30 mL) and transferred into a solution of pyridyl Grignard (0.92 g, 1.7 mmol) in  $\text{CH}_2\text{Cl}_2$  (10 mL) at  $0\text{ }^\circ\text{C}$ . The reaction mixture was allowed to warm to room temperature and kept stirring for 10 h. The dark red-brown suspension was poured into an aqueous solution of  $\text{Na}_2\text{CO}_3$ , and the slurry was stirred for 30 min and extracted with  $\text{CH}_2\text{Cl}_2$  ( $3\times 100\text{ mL}$ ). The combined organic layers were dried over  $\text{Na}_2\text{SO}_4$  and the solvents removed using a rotary evaporator. The oily residue was redissolved in acetone (100 mL), filtered and evaporated to dryness. The resulting solid residue was purified by column chromatography on silica gel with solvent gradients being varied from hexanes to acetone containing 1% (v/v) triethylamine. A white solid

was obtained and dried under vacuum at 60 °C for 10 h. Yield: 0.30 g (42%). Recrystallization from toluene by slow evaporation gave a clear crystal that was used for single crystal X-ray diffraction analysis. <sup>1</sup>H NMR (499.973 MHz, CDCl<sub>3</sub>) δ = 19.9 (br s, 1H, pyridyl N-H), 8.42 (d, <sup>3</sup>J = 5.5 Hz, 2H, pyridyl-H6), 7.65 (pst, <sup>3</sup>J = 7.8 Hz, 2H, pyridyl-H4), 7.58 (d, <sup>3</sup>J = 8.0 Hz, 2H, pyridyl-H3), 7.16 (m, 6H, pyridyl-H5, tPh-H3,5), 7.01 (d, <sup>3</sup>J = 7.0 Hz, 4H, tPh-H2,6), 1.29 (s, 18H, *t*-Bu). <sup>13</sup>C NMR (125.718 MHz, CDCl<sub>3</sub>) δ = 187.4 (q, <sup>1</sup>J<sub>C-B</sub> = 51.8 Hz, pyridyl-C2), 154.5 (q, <sup>1</sup>J<sub>C-B</sub> = 51.0 Hz, tPh-C1), 146.8 (tPh-C4), 142.1 (pyridyl-C6), 138.1 (pyridyl-C4), 135.5 (tPh-C2,6), 133.0 (pyridyl-C3), 124.4 (tPh-C3,5), 120.8 (pyridyl-C5), 34.7 (C(CH<sub>3</sub>)<sub>3</sub>), 32.0 (C(CH<sub>3</sub>)). <sup>11</sup>B NMR (160.386 MHz, CDCl<sub>3</sub>) δ = -11.0 (w<sub>1/2</sub> = 18 Hz). Elemental analysis: calcd for C<sub>30</sub>H<sub>35</sub>BN<sub>2</sub>: C 82.94, H 8.12, N 6.45%; found C 82.24, H 8.20, N 6.44%

#### **Synthesis of Distyrylbis(2-pyridyl)borate Free Acid (D42).**

To a solution of styryltrimethyltin (7.22 g, 27.0 mmol) in CH<sub>2</sub>Cl<sub>2</sub> (20 mL) was cooled to -18 °C, a solution of styryldibromoborane (7.00 g, 25.6 mmol) in CH<sub>2</sub>Cl<sub>2</sub> (20 mL) (pre-cooled to -18 °C) was slowly added. The reaction solution was allowed to warm to room temperature and kept stirring for 5 h. All volatile components were removed under high vacuum and the white residue was then redissolved in CH<sub>2</sub>Cl<sub>2</sub> (40 mL). The solution was cooled to 0 °C and added into a solution of pyridyl Grignard (15.7 g, 29.5 mmol) in CH<sub>2</sub>Cl<sub>2</sub> (50 mL). The resulting dark brown suspension was allowed to warm to room

temperature, kept stirring for 10 h, and then poured into an aqueous  $\text{Na}_2\text{CO}_3$  solution. The resulting slurry was stirred for 30 min and then extracted with  $\text{CH}_2\text{Cl}_2$  (3×200 mL). The combined organic layers were dried over  $\text{Na}_2\text{SO}_4$  and the solvents were removed using a rotary evaporator to give an oil, which was redissolved in acetone (100 mL), filtered and evaporated to dryness. The solid residue was purified by column chromatography on silica gel with solvent gradient being varied from hexanes to acetone containing 1% (v/v) triethylamine. The product was obtained as a white powdery solid, which was dried under high vacuum at 60 °C for 10 h. Yield: 3.6 g (37%).  $^1\text{H}$  NMR (499.973 MHz,  $\text{CDCl}_3$ )  $\delta$  = 20.0 (br s, 1H, pyridyl N-H), 8.44 (d,  $^3\text{J}$  = 5.5 Hz, 2H, pyridyl-H6), 7.66 (pst,  $^3\text{J}$  = 7.8 Hz, 2H, pyridyl-H4), 7.57 (d,  $^3\text{J}$  = 8.0 Hz, 2H, pyridyl-H3), 7.24 (d,  $^3\text{J}$  = 8.0 Hz, 4H, styryl-H3,5), 7.20 (pst,  $^3\text{J}$  = 6.5 Hz, 2H, pyridyl-H5), 7.11 (d,  $^3\text{J}$  = 6.5 Hz, 4H, styryl-H2,6), 6.70 (dd,  $^3\text{J}_{\text{trans}}$  = 18.0 Hz,  $^3\text{J}_{\text{cis}}$  = 11.0 Hz, 2H, =CH), 5.68 (d,  $^3\text{J}$  = 18.0 Hz, 2H, =CHH), 5.12 (d,  $^3\text{J}$  = 11.0 Hz, 2H, =CHH).  $^{13}\text{C}$  NMR (125.719 MHz,  $\text{CDCl}_3$ )  $\delta$  = 186.4 (q,  $^1\text{J}_{\text{C-B}}$  = 49.9 Hz, pyridyl-C2), 157.2 (q,  $^1\text{J}_{\text{C-B}}$  = 50.2 Hz, styryl-C1), 140.6 (pyridyl-C6), 137.9 (vinyl-CH), 137.5 (pyridyl-C4), 135.2 (styryl-C2,6), 133.9 (styryl-C4), 132.7 (pyridyl-C3), 125.2 (styryl-C3,5), 120.1 (pyridyl-C5), 111.7 (vinyl- $\text{CH}_2$ ).  $^{11}\text{B}$  NMR (160.386 MHz,  $\text{CDCl}_3$ )  $\delta$  = -10.9 ( $w_{1/2}$  = 15 Hz). MALDI-TOF (benzo[a]pyrene):  $m/z$  = 374.2020 (calcd for  $^{12}\text{C}_{26}^{1}\text{H}_{23}^{11}\text{B}^{14}\text{N}_2$  374.1954).

**Synthesis of Styryl(*t*-butylphenyl)bis(2-pyridyl)borate Free Acid (D43).**

A solution of styryldibromoborane (0.50 g, 1.8 mmol) in CH<sub>2</sub>Cl<sub>2</sub> (15 mL) was slowly added a pre-cooled solution (-18 °C) of *t*-butylphenyltrimethyltin (0.55 g, 1.85 mmol) in CH<sub>2</sub>Cl<sub>2</sub> (15 mL) at -18 °C. The mixture was allowed to warm to room temperature, kept stirring for 5 h, and then kept under vacuum to remove all the volatile components. The white residue was redissolved in CH<sub>2</sub>Cl<sub>2</sub> (30 mL) and transferred into a solution of pyridyl Grignard (1.0 g, 1.9 mmol) in CH<sub>2</sub>Cl<sub>2</sub> (10 mL) at 0 °C. The reaction mixture was allowed to warm to room temperature and kept stirring for 10 h. The dark red-brown solution was poured into an aqueous Na<sub>2</sub>CO<sub>3</sub> solution resulting a slurry, which was stirred for 30 min and extracted with CH<sub>2</sub>Cl<sub>2</sub> (3×100 mL). The combined organic layers were dried over Na<sub>2</sub>SO<sub>4</sub> and the solvents were removed using a rotary evaporator. The oily residue was redissolved in acetone (100 mL), filtered and evaporated to dryness. The solid residue was purified by column chromatography on silica gel with solvent gradients being varied from hexanes to acetone containing 1% (v/v) triethylamine. A white solid was obtained and dried under high vacuum at 60 °C for 10 h. Yield: 0.25 g (34%). <sup>1</sup>H NMR (499.973 MHz, CDCl<sub>3</sub>) δ = 20.0 (br s, 1H, pyridyl N-H), 8.43 (d, <sup>3</sup>J = 5.5 Hz, 2H, pyridyl-H6), 7.65 (pst, <sup>3</sup>J = 7.5 Hz, 2H, pyridyl-H4), 7.57 (d, <sup>3</sup>J = 8.0 Hz, 2H, pyridyl-H3), 7.23 (d, <sup>3</sup>J = 6.5 Hz, 2H, styryl-H3,5), 7.18 (pst, <sup>3</sup>J = 6.8 Hz, 2H, pyridyl-H5), 7.17 (d, <sup>3</sup>J = 8.0 Hz, 2H, tPh-H3,5), , 7.10 (d, <sup>3</sup>J = 6.0 Hz, 2H, styryl-H2,6), 7.06 (d, <sup>3</sup>J = 6.5 Hz, 2H, tPh-H2,6), 6.69 (dd, <sup>3</sup>J<sub>trans</sub> = 17.5 Hz, <sup>3</sup>J<sub>cis</sub> = 11.0 Hz, 1H, =CH),

5.66 (d,  $^3J = 17.5$  Hz, 1H, =CHH), 5.10 (d,  $^3J = 11.0$  Hz, 1H, =CHH), 1.29 (s, 9H, *t*-Bu).  $^{13}\text{C}$  NMR (125.718 MHz,  $\text{CDCl}_3$ )  $\delta = 186.7$  (q,  $^1J_{\text{C-B}} = 50.0$  Hz, pyridyl-C2), 157.8 (q,  $^1J_{\text{C-B}} = 50.7$  Hz, styryl-C1), 152.9 (q,  $^1J_{\text{C-B}} = 50.7$  Hz, tPh-C1), 146.7 (tPh-C4), 140.5 (pyridyl-C6), 137.9 (vinyl-CH), 137.3 (pyridyl-C4), 135.3 (styryl-C2,6), 134.5 (tPh-C2,6), 133.7 (styryl-C4), 132.7 (pyridyl-C3), 125.0 (styryl-C3,5), 124.0 (tPh-C3,5), 119.9 (pyridyl-C5), 111.5 (vinyl-CH<sub>2</sub>), 34.3 ( $\text{C}(\text{CH}_3)_3$ ), 31.7( $\text{C}(\text{CH}_3)_3$ ).  $^{11}\text{B}$  NMR (160.411 MHz,  $\text{CDCl}_3$ )  $\delta = -11.0$  ( $w_{1/2} = 19$  Hz).

#### Synthesis of Bis(*t*-butylphenyltris(2-pyridyl)borate) Magnesium (D38).

A solution of *t*-butylphenyl dibromoborane (1.0 g, 3.3 mmol) in toluene (15 mL) was slowly added to a solution of pyridyl Grignard (2.9 g, 5.4 mmol) in toluene (40 mL). The reaction mixture was stirred for 12 h and then brought to dryness under high vacuum to give a white solid residue. Methanol (300 mL) was added and the mixture was refluxed for 1 h. The product was isolated as a white solid by filtration. Yield of first crop: 0.45 g (35%).  $^1\text{H}$  NMR (499.973 MHz,  $\text{CDCl}_3$ )  $\delta = 7.97$  (d,  $^3J = 7.5$  Hz, 4H, styryl-H2,6), 7.70 (d,  $^3J = 8.0$  Hz, 6H, pyridyl-H3), 7.58 (d,  $^3J = 5.5$  Hz, 6H, pyridyl-H6), 7.56 (d,  $^3J = 8.0$  Hz, 4H, styryl-H3,5), 7.39 (pst,  $^3J = 7.5$  Hz, 6H, pyridyl-H4), 6.64 (pst,  $^3J = 6.3$  Hz, 6H, pyridyl-H5), 1.51 (s, 18H, *t*-Bu).  $^{13}\text{C}$  NMR (125.718 MHz,  $\text{CDCl}_3$ )  $\delta = 184.8$  (q,  $^1J_{\text{C-B}} = 51.5$  Hz, pyridyl-C2), 150.2 (q,  $^1J_{\text{C-B}} = 54.5$  Hz, styryl-C1), 148.4 (pyridyl-C6), 147.2 (styryl-C4), 137.0 (styryl-C2,6), 134.9 (pyridyl-C4), 129.9 (pyridyl-C3), 124.3

(styryl-C3,5), 118.7 (pyridyl-C5), 34.6 ( $C(CH_3)_3$ ), 32.0 ( $C(CH_3)_3$ ).  $^{11}B$  NMR (160.411 MHz,  $CDCl_3$ )  $\delta = -9.4$  ( $w_{1/2} = 16$  Hz). Elemental analysis: calcd for  $C_{50}H_{50}B_2MgN_6$ : C 76.90, H 6.45, N 10.76%; found C 76.44, H 6.45, N 10.68%. MALDI-TOF (benzo[a]pyrene):  $m/z = 780.4146$  (calcd for  $^{12}C_{50}^{1}H_{50}^{11}B_2^{24}Mg^{14}N_6$  780.4134). The methanol filtrate was concentrated to ca. 10 mL and then  $CH_2Cl_2$  (100 mL) was added. The resulting solution was poured into an aqueous  $Na_2CO_3$  solution (20 g, 150 mL), the organic layer was isolated and the aqueous layer was further extracted with  $CH_2Cl_2$  (2 $\times$ 50 mL). The combined organic layers were dried over  $Na_2SO_4$ , concentrated and purified by column chromatography on silica with solvent gradients ranging from hexanes to acetone containing 1% (v/v) triethylamine. This second crop was isolated by evaporation of the solvents and identified by NMR spectroscopy as the corresponding free acid. Yield: 0.25 g (20%).

#### **Synthesis of Bis(styryltris(2-pyridyl)borate) Magnesium (D40).**

A solution of styryl dibromoborane (1.0 g, 3.7 mmol) in toluene (15 mL) was slowly added to a solution of pyridyl Grignard (3.6 g, 6.8 mmol) in toluene (50 mL). The reaction mixture was stirred for 12 h and then brought to dryness under high vacuum to give a white solid residue. Methanol (300 mL) was added and the mixture was refluxed for 1 h. The product was isolated as a white solid by filtration and dried under high vacuum at 60 °C for 10 h. Yield of the first crop: 0.38 g (29%).  $^1H$  NMR (499.973 MHz,

CDCl<sub>3</sub>)  $\delta$  = 8.04 (d,  $^3J$  = 7.0 Hz, 4H, styryl-H2,6), 7.69 (d,  $^3J$  = 8.0 Hz, 6H, pyridyl-H3), 7.63 (d,  $^3J$  = 7.5 Hz, 4H, styryl- H3,5), 7.58 (d,  $^3J$  = 5.0 Hz, 6H, pyridyl-H6), 7.41 (pst,  $^3J$  = 7.8 Hz, 6H, pyridyl- H4), 6.94 (dd,  $^3J_{\text{trans}}$  = 17.8 Hz,  $^3J_{\text{cis}}$  = 10.8 Hz, 2H, vinyl-CH), 6.66 (pst,  $^3J$  = 6.0 Hz, 6H, pyridyl-H5), 5.91 (d,  $^3J_{\text{trans}}$  = 17.5 Hz, 2H, vinyl-CH<sub>2</sub>), 5.29 (d,  $^3J_{\text{cis}}$  = 11.0 Hz, 2H, vinyl-CH<sub>2</sub>). <sup>13</sup>C NMR (125.718 MHz, CDCl<sub>3</sub>)  $\delta$  = 184.4 (q,  $^1J_{\text{C-B}}$  = 51.9 Hz, pyridyl-C2), 153.6 (q,  $^1J_{\text{C-B}}$  = 54.9 Hz, styryl-C1), 148.4 (pyridyl-C6), 138.1 (styryl-C4), 137.6 (styryl-C2,6), 135.1 (pyridyl-C4), 134.0 (vinyl-CH), 129.8 (pyridyl-C3), 125.4 (styryl-C3,5), 118.8 (pyridyl-C5), 112.0 (vinyl-CH<sub>2</sub>). <sup>11</sup>B NMR (160.411 MHz, CDCl<sub>3</sub>)  $\delta$  = -9.1 ( $w_{1/2}$  = 13 Hz). MALDI-TOF (benzo[a]pyrene):  $m/z$  = 720.3169 (calcd for <sup>12</sup>C<sub>46</sub><sup>1</sup>H<sub>38</sub><sup>11</sup>B<sub>2</sub><sup>24</sup>Mg<sup>14</sup>N<sub>6</sub> 720.3194). The methanol filtrate was concentrated to ca. 10 mL and CH<sub>2</sub>Cl<sub>2</sub> (100 mL) was added. The resulting solution was poured into an aqueous Na<sub>2</sub>CO<sub>3</sub> solution (20 g, 150 mL), the organic layer was isolated and the aqueous layer was further extracted with CH<sub>2</sub>Cl<sub>2</sub> (2×50 mL). The combined organic layers were dried over Na<sub>2</sub>SO<sub>4</sub>, concentrated and purified by column chromatography on silica gel with solvent gradients being varied from hexanes to acetone containing 1% (v/v) triethylamine. This second crop was isolated by evaporation of the solvents and identified by NMR spectroscopy as the corresponding free acid. Yield: 0.27 g (21%).

### Synthesis of Bis(styryltris(2-pyridyl)borate) Iron(II) (D45).

The product was prepared in analogy to the procedure for bis(*t*-butylphenyltris(2-pyridyl)borate) iron(II), from FeCl<sub>2</sub> (0.50 g, 3.94 mmol), triethylamine (1.0 mL, 7.18 mmol) and styryltris(2-pyridyl)borate free acid (2.50 g, 7.16 mmol) in tetrahydrofuran. Yield for C<sub>46</sub>H<sub>38</sub>B<sub>2</sub>FeN<sub>6</sub>·(C<sub>7</sub>H<sub>8</sub>)<sub>0.5</sub>: 2.35 g (82%). <sup>1</sup>H NMR (499.973 MHz, CDCl<sub>3</sub>) δ = 8.15 (d, <sup>3</sup>J = 7.0 Hz, styryl-H<sub>2,6</sub>), 7.67 (d, <sup>3</sup>J = 7.5 Hz, styryl-H<sub>3,5</sub>), 7.58 (d, <sup>3</sup>J = 7.5 Hz, pyridyl-H<sub>3</sub>), 7.29 (pst, <sup>3</sup>J = 8.0 Hz, pyridyl-H<sub>4</sub>), 7.16 (d, <sup>3</sup>J = 5.5 Hz, pyridyl-H<sub>6</sub>), 6.94 (dd, <sup>3</sup>J<sub>trans</sub> = 17.5 Hz, <sup>3</sup>J<sub>cis</sub> = 11.0 Hz, 2H, vinyl-CH), 6.46 (pst, <sup>3</sup>J = 6.3 Hz, 6H, pyridyl-H<sub>5</sub>), 5.95 (d, <sup>3</sup>J<sub>trans</sub> = 17.5 Hz, 2H, vinyl-CH<sub>2</sub>), 5.31 (d, <sup>3</sup>J<sub>cis</sub> = 11.0 Hz, 2H, vinyl-CH<sub>2</sub>). <sup>13</sup>C NMR (125.718 MHz, CDCl<sub>3</sub>) δ = 187.3 (q, <sup>1</sup>J<sub>C-B</sub> = 49.7 Hz, pyridyl-C<sub>2</sub>), 158.2 (pyridyl-C<sub>6</sub>), 153.6 (q, <sup>1</sup>J<sub>C-B</sub> = 44.7 Hz, styryl-C<sub>1</sub>), 138.0 (styryl-C<sub>4</sub>), 137.2 (styryl-C<sub>2,6</sub>), 134.2 (vinyl-CH), 132.3 (pyridyl-C<sub>4</sub>), 125.6 (pyridyl-C<sub>3</sub>), 125.4 (styryl-C<sub>3,5</sub>), 119.6 (pyridyl-C<sub>5</sub>), 112.2 (vinyl-CH<sub>2</sub>). <sup>11</sup>B NMR (160.411 MHz, CDCl<sub>3</sub>) δ = -7.4 (w<sub>1/2</sub> = 16 Hz). UV-VIS (25 °C, CH<sub>2</sub>Cl<sub>2</sub>): λ<sub>max</sub> = 480 nm. CV: E<sub>1/2</sub> = -328 mV, ΔE<sub>p</sub> = 119 mV (1 mM with 0.1 M [Bu<sub>4</sub>N]PF<sub>6</sub> in CH<sub>2</sub>Cl<sub>2</sub> as the supporting electrolyte; scan rate 100 mV/s). MALDI-TOF (benzo[a]pyrene): m/z = 752.2642 (calcd for <sup>12</sup>C<sub>46</sub><sup>1</sup>H<sub>38</sub><sup>11</sup>B<sub>2</sub><sup>56</sup>Fe<sup>14</sup>N<sub>6</sub> 752.2693).

### Synthesis of Bis(*t*-butylphenyltris(2-pyridyl)borate) Iron(II) (D46).

To a mixture of FeCl<sub>2</sub> (0.10 g, 0.79 mmol) and triethylamine (0.20 mL, 1.43 mmol) in dry tetrahydrofuran (15 mL) was added a solution of *t*-butylphenyltris(2-pyridyl)borate free acid (0.50 g, 1.32 mmol) in dry tetrahydrofuran (15 mL) under nitrogen protection. The resulting red suspension was kept stirring for 3 h, brought to dryness and then extracted with dry toluene (3×100 mL). The reaction mixture was loaded onto a silica gel column and eluted with dry hexanes under nitrogen protection. Solvent evaporation gave a red solid product which was dried under high vacuum at RT for 1 h. Yield for C<sub>50</sub>H<sub>50</sub>B<sub>2</sub>FeN<sub>6</sub>·(C<sub>7</sub>H<sub>8</sub>): 0.45 g (75%). <sup>1</sup>H NMR (499.973 MHz, CDCl<sub>3</sub>) δ = 8.09 (d, <sup>3</sup>J = 7.5 Hz, 4H, tPh-H2,6), 7.60 (d, <sup>3</sup>J = 8.0 Hz, 4H, tPh-H3,5), 7.59 (d, <sup>3</sup>J = 9.0 Hz, 6H, pyridyl-H3), 7.27 (pst, <sup>3</sup>J = 7.5 Hz, 6H, pyridyl-H4), 7.11 (d, <sup>3</sup>J = 5.5 Hz, 6H, pyridyl-H6), 6.44 (pst, <sup>3</sup>J = 6.5 Hz, 6H, pyridyl-H5), 1.52 (s, 18H, *t*-Bu). <sup>13</sup>C NMR (125.718 MHz, CDCl<sub>3</sub>) δ = 188.0 (q, <sup>1</sup>J<sub>C-B</sub> = 49.6 Hz, pyridyl-C2), 158.3 (pyridyl-C6), 149.2 (q, <sup>1</sup>J<sub>C-B</sub> = 57.3 Hz, tPh-C1), 147.4 (tPh-C4), 136.7 (tPh-C2,6), 132.0 (pyridyl-C4), 125.7 (pyridyl-C3), 124.5 (tPh-C3,5), 119.7 (pyridyl-C5), 34.7 (C(CH<sub>3</sub>)<sub>3</sub>), 32.0 (C(CH<sub>3</sub>)<sub>3</sub>). <sup>11</sup>B NMR (160.411 MHz, CDCl<sub>3</sub>) δ = -7.5 (w<sub>1/2</sub> = 21 Hz). Elemental analysis: calcd for C<sub>50</sub>H<sub>50</sub>B<sub>2</sub>FeN<sub>6</sub>·C<sub>7</sub>H<sub>8</sub>: C 75.68, H 6.46, N 9.29%; found C 75.61, H 6.46, N 9.24%. UV-VIS (25 °C, CH<sub>2</sub>Cl<sub>2</sub>): λ<sub>max</sub> = 480 nm. CV: E<sub>1/2</sub> = -352 mV, ΔE<sub>p</sub> = 84 mV (1 mM with 0.1 M [Bu<sub>4</sub>N]PF<sub>6</sub> in CH<sub>2</sub>Cl<sub>2</sub> as the supporting electrolyte; scan rate 100 mV/s).

MALDI-TOF (benzo[a]pyrene):  $m/z = 812.3564$  (calcd for  $^{12}\text{C}_{50}^{1}\text{H}_{50}^{11}\text{B}_2^{56}\text{Fe}^{14}\text{N}_6$  812.3632).

**Synthesis of Bis(t-butylphenyltris(2-pyridyl)borate)iron(III) Tetrachloroferrate(III) (D47).**

A red solution of bis(t-butylphenyltris(2-pyridyl)borate) iron(II)·(toluene) (0.20 g, 0.22 mmol) in  $\text{CH}_2\text{Cl}_2$  (10 mL) was layered with a solution of  $\text{FeCl}_3$  (0.12 g, 0.74 mmol) in  $\text{H}_2\text{O}$  (10 mL). The reaction mixture was shaken vigorously for 5 min. The organic layer was collected and dried over  $\text{Na}_2\text{SO}_4$ . A dark purple solid was obtained after solvent evaporation and repeated precipitation of its dichloromethane solution into diethyl ether afforded was applied for further purification. The solid was dried under high vacuum at 60 °C. Yield: 0.18 g (81%).  $^1\text{H}$  NMR (499.973 MHz,  $\text{CDCl}_3$ )  $\delta = 22.7$  (s 4H, tPh-H2,6), 21.9 (s 6H, pyridyl-H6), 13.5 (s 4H, tPh-H3,5), 4.37 (s 9H, *t*-Bu), -6.91 (s pyridyl-H4), -8.06 (s pyridyl-H5), -79.19 (br s, 6H, pyridyl-H3).  $^{11}\text{B}$  NMR (160.411 MHz,  $\text{CDCl}_3$ )  $\delta = -30$  ( $w_{1/2} = 123$  Hz). Single crystals of the Fe(III) complex for single crystal X-ray diffraction was obtained by slow solvent evaporation of a ethanol solution.

**Standard Free Radical Polymerization of Styryltris(2-pyridyl)borate Free Acid.**

A mixture of styryltris(2-pyridyl)borate free acid (0.35 g, 1.0 mmol) and AIBN (1.7 mg, 0.010mmol) in DMF (2.3 mL) was sealed with a rubber septa in a 15 mL Schlenk flask

and degassed by nitrogen sparging for 30 min. The flask was then immersed into an oil bath preset at 90 °C. The mixture was kept stirring for 40 h. The polymer solution was precipitated into diethyl ether, the crude product was reprecipitated twice from dichloromethane into diethyl ether and dried under high vacuum at 65 °C. Yield: 0.21g (60%). <sup>1</sup>H NMR (499.973 MHz, CDCl<sub>3</sub>) δ = 10 (br, pyridyl N-H and H<sub>2</sub>O), 8.12 (br, 3H, pyridyl-H6), 7.25 (br, 6H, pyridyl-H3,4), 7.16 (br m, 7H, styryl-H2-6, pyridyl-H5), 2.7-0.2 (br m, 3H, CHCH<sub>2</sub>). <sup>13</sup>C NMR (125.718 MHz, CDCl<sub>3</sub>) δ = 184 (br, m, pyridyl-C2), 153 (br, m, styryl-C1), 144 (br, styryl-C4), 143.5 (pyridyl-C6), 136.1 (pyridyl-C4), 134.2 (pyridyl-C3), 131.5 (styryl-C2,6), 126.7 (styryl-C3,5), 119.7 (pyridyl-C5), 48-36 (br m, CHCH<sub>2</sub>). <sup>11</sup>B NMR (160.411 MHz, CDCl<sub>3</sub>) δ = -10.8 (w<sub>1/2</sub> = 40 Hz). Elemental analysis: calcd for C<sub>23</sub>H<sub>20</sub>BN<sub>3</sub>: C 79.10, H 5.77, N 12.03; GPC-RI (DMF/20mM NH<sub>4</sub>[PF<sub>6</sub>], 60 °C) M<sub>n</sub> = 35 k, M<sub>w</sub> = 55 k, PDI = 1.57.

## D.6 References

- 1.(a)Trofimenko, S., *J. Am. Chem. Soc.* **1966**, 88 1842-1844,(b)Trofimenko, S., *J. Coord. Chem.* **1972**, 2, 75-77.
- 2.(a)Trofimenko, S., *Chem. Rev.* **2002**, 93, 943-980, (b)Marques, N.; Sella, A.; Takats, J., *Chem. Rev.* **2002**, 102, 2137-2160, (c)Dias, H. V. R.; Lovely, C. J., *Chem. Rev.* **2008**, 108, 3223-3238, (d)Trofimenko, S., *Polyhedron* **2004**, 23, 197-203.
- 3.Pettinari, C., *Inorg. Chim. Acta* **2009**, 362, 4273-4275.
- 4.Trofimenko, S., *Scorpionates: Polypyrazolylborate Ligands and Their Coordination Chemistry*. Imperial College Press: London, 1999.
- 5.Trofimenko, S., *Chem. Rev.* **1993**, 93, 943-980.
- 6.Sohrin, Y.; Kokusen, H.; Matsui, M., *Inorg. Chem.* **2002**, 34, 3928-3934.

7. Oliver, J. D.; Mullica, D. F.; Hutchinson, B. B.; Milligan, W. O., *Inorg. Chem.* **1980**, *19*, 165-169.
8. Trofimenko, S.; Calabrese, J. C.; Domaille, P. J.; Thompson, J. S., *Inorg. Chem.* **2002**, *28*, 1091-1101.
9. Szczepura, L. F.; Witham, L. M.; Takeuchi, K. J., *Coord. Chem. Rev.* **1998**, *174*, 5-32.
10. Garcia, F.; Hopkins, A. D.; Humphrey, S. M.; McPartlin, M.; Rogers, M. C.; Wright, D. S., *Dalton Transactions* **2004**, 361-362.
11. Garcia, F.; Hopkins, A. D.; Kowenicki, R. A.; McPartlin, M.; Rogers, M. C.; Wright, D. S., *Organometallics* **2004**, *23*, 3884-3890.
12. Beswick, M. A.; Belle, C. J.; Davies, M. K.; Halcrow, M. A.; Raithby, P. R.; Steiner, A.; Wright, D. S., *Dalton Trans.* **2004**, 361 - 362.
13. Garcia, F.; Hopkins, A. D.; Kowenicki, R. A.; McPartlin, M.; Rogers, M. C.; Silvia, J. S.; Wright, D. S., *Organometallics* **2006**, *25*, 2561-2568.
14. Beswick, M. A.; Davies, M. K.; Raithby, P. R.; Steiner, A.; Wright, D. S., *Organometallics* **1997**, *16*, 1109-1110.
15. López-Linares, F.; Fuentes, A.; Tenia, R.; Martinez, M.; Karam, A., *Reaction Kinetics and Catalysis Letters* **2007**, *92*, 285-292.
16. Hodgkins, T. G.; Powell, D. R., *Inorg. Chem.* **1996**, *35*, 2140-2148.
17. Garcia, F.; Hopkins, A. D.; Kowenicki, R. A.; McPartlin, M.; Silvia, J. S.; Rawson, J. M.; Rogers, M. C.; Wright, D. S., *Chem. Commun.* **2007**, 586-588.
18. Khaskin, E.; Zavalij, P. Y.; Vedernikov, A. N., *J. Am. Chem. Soc.* **2006**, *128*, 13054-13055.
19. (a) Bullock, T. H.; Chan, W. T. K.; Wright, D. S., *Dalton Transactions* **2009**, 6709-6711, (b) Bullock, T. H.; Chan, W. T. K.; Eisler, D. J.; Streib, M.; Wright, D. S., *Dalton Transactions* **2009**, 1046-1054.
20. Alvarez, C. S.; García, F.; Humphrey, S. M.; Hopkins, A. D.; Kowenicki, R. A.; McPartlin, M.; Layfield, R. A.; Raja, R.; Rogers, M. C.; Woods, A. D.; Wright, D. S., *Chem. Commun.* **2005**, 198 - 200.
21. Fox, J. D.; Rowan, S. J., *Macromolecules* **2009**, *42*, 6823-6835.
22. Bergbreiter, D. E., *Chem. Rev.* **2002**, *102*, 3345-3384.
23. (a) Hofmeier, H.; Schubert, U. S., *Chem. Soc. Rev.* **2004**, *33*, 373-399, (b) Schubert Ulrich, S.; Eschbaumer, C., *Angew. Chem. Int. Ed.* **2002**, *41*, 2892-2926.
24. (a) Dobrawa, R.; Lysetska, M.; Ballester, P.; Gruene, M.; Wuerthner, F., *Macromolecules* **2005**, *38*, 1315-1325, (b) Gohy, J. F.; Lohmeijer, B. G. G.; Varshney, S. K.; Schubert, U. S., *Macromolecules* **2002**, *35*, 7427-7435.
25. Gohy, J.-F.; Lohmeijer, B. G. G.; Alexeev, A.; Wang, X.-S.; Manners, I.; Winnik, M. A.; Schubert, U. S., *Chem. Eur. J.* **2004**, *10*, 4315-4323.
26. Balzani, V.; Juris, A.; Venturi, M.; Campagna, S.; Serroni, S., *Chem. Rev.* **1996**, *96*, 759-834.

27. Shunmugam, R.; Tew, G. N., *J. Polym. Sci., Part A: Polym. Chem.* **2005**, *43*, 5831-5843.
28. Shunmugam, R.; Tew, G. N., *Polym. Adv. Technol.* **2008**, *19*, 596-601.
29. Heller, M.; Schubert, U. S., *Macromol. Rapid Comm.* **2002**, *23*, 411-415.
30. (a) F. F. de Biani; Jäkle, F.; Spiegler, M.; Wagner, M.; Zanello, P., *Inorg. Chem.* **1997**, *36*, 2103-2111, (b) Guo, S. L.; Peters, F.; de Biani, F. F.; Bats, J. W.; Herdtweck, E.; Zanello, P.; Wagner, M., *Inorg. Chem.* **2001**, *40*, 4928-4936.
31. Qin, Y.; Cui, C.; Jäkle, F., *Macromolecules* **2008**, *41*, 2972-2974.
32. (a) Trécourt, F.; Breton, G.; Bonnet, V.; Mongin, F.; Marsais, F.; Quéguiner, G., *Tetrahedron Lett.* **1999**, *40*, 4339-4342, (b) Martin, G. J.; Mechin, B.; Leroux, Y.; Paulmier, C.; Meunier, J. C., *Journal of Organometallic Chemistry* **1974**, *67*, 327-339, (c) Krasovskiy, A.; Knochel, P., *Angewandte Chemie International Edition* **2004**, *43*, 3333-3336.
33. Churakov, A. V.; Krut'ko, D. P.; Borzov, M. V.; Kirsanov, R. S.; Belov, S. A.; Howard, J. A. K., *Acta Cryst. E* **2006**, *62*, m1094-m1096.
34. Qin, Y.; Cheng, G.; Sundararaman, A.; Jäkle, F., *J. Am. Chem. Soc.* **2002**, *124*, 12672-12673.
35. Anderson, P. A.; Astley, T.; Hitchman, M. A.; Keene, F. R.; Moubaraki, B.; Murray, K. S.; Skelton, B. W.; Tiekink, E. R. T.; Toftlund, H.; White, A. H., *J. Chem. Soc., Dalton Transactions* **2000**, 3505-3512.
36. Moore, E. A.; Abel, E. W.; Janes, R., *Metal-Ligand Bonding*. The Open University: Milton Keynes, United Kingdom, 2004; p 104.
37. Sohrin, Y.; Kokusen, H.; Matsui, M., *Inorg. Chem.* **1995**, *34*, 3928-3934.

## Appendix

**Appendix A.1** The following tables are supplementary materials for the X-ray crystal structure of compound D37 and D39. The data of fractional atomic coordinates and equivalent isotropic displacement parameters, anisotropic displacement parameters, bond lengths and bond angles are listed.

### Crystal Data and Structure Refinement Details for D37 and D39

	D37	D39
Empirical formula	C <sub>25</sub> H <sub>26</sub> B N <sub>3</sub>	C <sub>23</sub> H <sub>20</sub> B N <sub>3</sub>
$M_r$	379.30	349.23
T, K	100(2)	100(2)
Wavelength, Å	1.54178	1.54178
Crystal system	Triclinic	Monoclinic
Space group	P-1	P 21/n
$a$ , Å	9.5834(2)	11.8959(2)
$b$ , Å	13.3508(3)	9.1565(2)
$c$ , Å	17.3829(4)	17.3296(3)
$\alpha$ , °	86.769(1)	90°.
$\beta$ , °	86.723(1)	97.688(1)°.
$\gamma$ , °	70.469(1)	90°
$V$ , Å <sup>3</sup>	2091.03(8)	1870.66(6)
$Z$	4	4
$\rho_{\text{calc}}$ , g/cm <sup>-3</sup>	1.205	1.240
$\mu(\text{CuK}\alpha)$ , mm <sup>-1</sup>	0.540	0.565
F(000)	808	736
Crystal size, mm <sup>3</sup>	0.50 x 0.15 x 0.10	0.33 x 0.16 x 0.15

$\theta$ range, °	2.55 to 67.95	4.26 to 67.21
Index ranges	-11 $\leq$ h $\leq$ 11	-14 $\leq$ h $\leq$ 14
	-16 $\leq$ k $\leq$ 14	-10 $\leq$ k $\leq$ 10
	-20 $\leq$ l $\leq$ 20	-20 $\leq$ l $\leq$ 20
Reflections collected	14577	14455
Independent reflections	7078 [R(int) = 0.0200]	3234 [R(int) = 0.0408]
Absorption correction	Numerical	Numerical
Refinement method	Full-matrix least-squares on F2	Full-matrix least-squares on F2
Data / restraints / parameters	7078 / 0 / 530	3234 / 0 / 245
Goodness-of-fit on F2	1.019	1.072
Final R indices [I $>$ 2 $\sigma$ (I)][a]	R1 = 0.0410, wR2 = 0.1074	R1 = 0.0354, wR2 = 0.0897
R indices (all data) [a]	R1 = 0.0446, wR2 = 0.1107	R1 = 0.0382, wR2 = 0.0927
Peak/hole (e $\text{\AA}^{-3}$ )	0.326 and -0.184	0.320 and -0.256

### Fractional Atomic Coordinates ( $\times 10^4$ ) and Equivalent Isotropic Displacement

Parameters ( $\text{\AA}^2 \times 10^3$ ) of D37 where  $U(\text{eq}) = (1/3) \sum_j U_{jj} a_j a_j a_j$

	x	y	z	U(eq)
B(1)	6857(2)	8225(1)	3906(1)	21(1)
N(1)	4338(1)	8818(1)	4689(1)	23(1)
N(2)	5986(1)	10233(1)	3529(1)	25(1)
N(3)	6879(1)	8533(1)	5349(1)	24(1)
C(1)	5063(2)	8471(1)	4016(1)	22(1)
C(2)	4184(2)	8363(1)	3430(1)	27(1)
C(3)	2679(2)	8579(1)	3548(1)	30(1)

C(4)	2003(2)	8927(1)	4261(1)	29(1)
C(5)	2868(2)	9045(1)	4825(1)	27(1)
C(6)	7114(2)	9300(1)	3515(1)	21(1)
C(7)	8511(2)	9275(1)	3201(1)	27(1)
C(8)	8745(2)	10194(1)	2916(1)	33(1)
C(9)	7579(2)	11145(1)	2941(1)	33(1)
C(10)	6233(2)	11118(1)	3246(1)	30(1)
C(11)	7682(2)	8046(1)	4727(1)	21(1)
C(12)	9205(2)	7514(1)	4793(1)	26(1)
C(13)	9887(2)	7507(1)	5475(1)	29(1)
C(14)	9043(2)	8032(1)	6096(1)	29(1)
C(15)	7548(2)	8525(1)	6010(1)	28(1)
C(16)	7523(1)	7225(1)	3344(1)	21(1)
C(17)	7949(2)	6158(1)	3614(1)	23(1)
C(18)	8432(2)	5316(1)	3123(1)	24(1)
C(19)	8515(1)	5480(1)	2322(1)	22(1)
C(20)	8079(1)	6534(1)	2046(1)	22(1)
C(21)	7607(1)	7373(1)	2542(1)	22(1)
C(22)	9084(2)	4542(1)	1786(1)	26(1)
C(23)	8071(2)	3862(2)	1873(1)	45(1)
C(24)	9158(2)	4919(1)	945(1)	37(1)
C(25)	10664(2)	3857(1)	2002(1)	37(1)
B(2)	2640(2)	7927(1)	899(1)	23(1)
N(1A)	-81(1)	9156(1)	781(1)	27(1)
N(2A)	3502(1)	8055(1)	-501(1)	30(1)
N(3A)	1835(1)	9788(1)	1479(1)	28(1)

C(1A)	948(2)	8223(1)	614(1)	23(1)
C(2A)	455(2)	7537(1)	207(1)	30(1)
C(3A)	-1000(2)	7819(1)	4(1)	33(1)
C(4A)	-1993(2)	8814(1)	182(1)	32(1)
C(5A)	-1506(2)	9480(1)	574(1)	32(1)
C(6A)	3738(2)	7431(1)	154(1)	24(1)
C(7A)	4830(2)	6433(1)	137(1)	37(1)
C(8A)	5664(2)	6074(2)	-534(1)	44(1)
C(9A)	5390(2)	6715(1)	-1191(1)	35(1)
C(10A)	4310(2)	7689(1)	-1143(1)	33(1)
C(11A)	2973(2)	8971(1)	1190(1)	25(1)
C(12A)	4416(2)	9016(1)	1205(1)	30(1)
C(13A)	4677(2)	9862(1)	1522(1)	35(1)
C(14A)	3490(2)	10681(1)	1817(1)	33(1)
C(15A)	2096(2)	10616(1)	1777(1)	32(1)
C(16A)	2843(2)	7092(1)	1645(1)	22(1)
C(17A)	4223(2)	6638(1)	1977(1)	26(1)
C(18A)	4438(2)	5952(1)	2621(1)	28(1)
C(19A)	3275(2)	5675(1)	2981(1)	27(1)
C(20A)	1888(2)	6135(1)	2671(1)	28(1)
C(21A)	1687(2)	6820(1)	2021(1)	26(1)
C(22A)	3521(2)	4954(1)	3717(1)	33(1)
C(23A)	3424(2)	5665(2)	4399(1)	44(1)
C(24A)	5057(2)	4099(1)	3689(1)	44(1)
C(25A)	2352(3)	4417(2)	3843(1)	84(1)

---

**Bond Lengths [Å] and Angles [deg] of D37**

B(1)-C(16)	1.628(2)	C(9)-C(10)	1.377(2)
B(1)-C(11)	1.6380(19)	C(11)-C(12)	1.4014(19)
B(1)-C(1)	1.6407(19)	C(12)-C(13)	1.384(2)
B(1)-C(6)	1.6410(19)	C(13)-C(14)	1.385(2)
N(1)-C(5)	1.3483(18)	C(14)-C(15)	1.375(2)
N(1)-C(1)	1.3491(18)	C(16)-C(21)	1.3974(18)
N(2)-C(10)	1.3426(19)	C(16)-C(17)	1.4053(19)
N(2)-C(6)	1.3490(19)	C(17)-C(18)	1.3867(19)
N(3)-C(15)	1.3442(18)	C(18)-C(19)	1.3984(19)
N(3)-C(11)	1.3539(18)	C(19)-C(20)	1.392(2)
C(1)-C(2)	1.4012(19)	C(19)-C(22)	1.5342(19)
C(2)-C(3)	1.379(2)	C(20)-C(21)	1.3897(19)
C(3)-C(4)	1.394(2)	C(22)-C(24)	1.525(2)
C(4)-C(5)	1.368(2)	C(22)-C(23)	1.531(2)
C(6)-C(7)	1.4071(19)	C(22)-C(25)	1.539(2)
C(7)-C(8)	1.380(2)	B(2)-C(1A)	1.635(2)
C(8)-C(9)	1.384(2)	B(2)-C(16A)	1.6384(19)
B(2)-C(6A)	1.642(2)	N(1)-C(5)-C(4)	120.18(13)
B(2)-C(11A)	1.643(2)	N(2)-C(6)-C(7)	119.57(13)
N(1A)-C(1A)	1.3402(19)	N(2)-C(6)-B(1)	119.34(12)
N(1A)-C(5A)	1.351(2)	C(7)-C(6)-B(1)	121.01(13)
N(2A)-C(10A)	1.339(2)	C(8)-C(7)-C(6)	120.76(15)
N(2A)-C(6A)	1.3563(18)	C(7)-C(8)-C(9)	118.89(14)
N(3A)-C(15A)	1.3487(19)	C(10)-C(9)-C(8)	117.70(14)
N(3A)-C(11A)	1.354(2)	N(2)-C(10)-C(9)	124.25(15)

C(1A)-C(2A)	1.401(2)	N(3)-C(11)-C(12)	118.87(12)
C(2A)-C(3A)	1.379(2)	N(3)-C(11)-B(1)	117.86(12)
C(3A)-C(4A)	1.390(2)	C(12)-C(11)-B(1)	122.89(12)
C(4A)-C(5A)	1.362(2)	C(13)-C(12)-C(11)	120.71(13)
C(6A)-C(7A)	1.392(2)	C(12)-C(13)-C(14)	119.15(14)
C(7A)-C(8A)	1.390(2)	C(15)-C(14)-C(13)	118.04(13)
C(8A)-C(9A)	1.371(2)	N(3)-C(15)-C(14)	123.09(13)
C(9A)-C(10A)	1.369(2)	C(21)-C(16)-C(17)	114.96(12)
C(11A)-C(12A)	1.405(2)	C(21)-C(16)-B(1)	121.66(12)
C(12A)-C(13A)	1.385(2)	C(17)-C(16)-B(1)	123.21(11)
C(13A)-C(14A)	1.384(2)	C(18)-C(17)-C(16)	122.49(12)
C(14A)-C(15A)	1.373(2)	C(17)-C(18)-C(19)	121.70(13)
C(16A)-C(21A)	1.3959(19)	C(20)-C(19)-C(18)	116.43(12)
C(16A)-C(17A)	1.4007(19)	C(20)-C(19)-C(22)	122.38(12)
C(17A)-C(18A)	1.384(2)	C(18)-C(19)-C(22)	121.19(12)
C(18A)-C(19A)	1.393(2)	C(21)-C(20)-C(19)	121.51(12)
C(19A)-C(20A)	1.391(2)	C(20)-C(21)-C(16)	122.90(13)
C(19A)-C(22A)	1.5373(19)	C(24)-C(22)-C(23)	109.25(13)
C(20A)-C(21A)	1.393(2)	C(24)-C(22)-C(19)	111.58(12)
C(22A)-C(25A)	1.520(2)	C(23)-C(22)-C(19)	109.97(12)
C(22A)-C(24A)	1.532(2)	C(24)-C(22)-C(25)	107.52(13)
C(22A)-C(23A)	1.539(2)	C(23)-C(22)-C(25)	109.37(14)
C(16)-B(1)-C(11)	113.47(11)	C(19)-C(22)-C(25)	109.09(11)
C(16)-B(1)-C(1)	107.77(10)	C(1A)-B(2)-C(16A)	108.15(11)
C(11)-B(1)-C(1)	112.97(11)	C(1A)-B(2)-C(6A)	106.20(11)
C(16)-B(1)-C(6)	111.13(11)	C(16A)-B(2)-C(6A)	113.53(12)

C(11)-B(1)-C(6)	103.93(10)	C(1A)-B(2)-C(11A)	112.23(12)
C(1)-B(1)-C(6)	107.42(11)	C(16A)-B(2)-C(11A)	106.44(11)
C(5)-N(1)-C(1)	124.51(12)	C(6A)-B(2)-C(11A)	110.38(11)
C(10)-N(2)-C(6)	118.82(13)	C(1A)-N(1A)-C(5A)	125.39(13)
C(15)-N(3)-C(11)	120.12(12)	C(10A)-N(2A)-C(6A)	119.14(13)
N(1)-C(1)-C(2)	115.77(12)	C(15A)-N(3A)-C(11A)	120.19(13)
N(1)-C(1)-B(1)	120.77(11)	N(1A)-C(1A)-C(2A)	115.51(13)
C(2)-C(1)-B(1)	123.45(12)	N(1A)-C(1A)-B(2)	120.56(12)
C(3)-C(2)-C(1)	121.50(13)	C(2A)-C(1A)-B(2)	123.91(13)
C(2)-C(3)-C(4)	119.67(13)	C(3A)-C(2A)-C(1A)	121.16(15)
C(5)-C(4)-C(3)	118.36(13)	C(2A)-C(3A)-C(4A)	119.85(15)
N(3A)-C(11A)-B(2)	119.10(12)	C(8A)-C(7A)-C(6A)	121.24(15)
C(12A)-C(11A)-B(2)	122.27(13)	C(9A)-C(8A)-C(7A)	118.98(16)
C(13A)-C(12A)-C(11A)	120.98(15)	C(10A)-C(9A)-C(8A)	117.49(15)
C(14A)-C(13A)-C(12A)	119.09(14)	N(2A)-C(10A)-C(9A)	124.52(14)
C(15A)-C(14A)-C(13A)	118.02(14)	N(3A)-C(11A)-C(12A)	118.46(13)
N(3A)-C(15A)-C(14A)	123.23(15)	C(20A)-C(19A)-C(18A)	116.75(13)
C(21A)-C(16A)-C(17A)	114.93(12)	C(20A)-C(19A)-C(22A)	122.49(13)
C(21A)-C(16A)-B(2)	124.18(12)	C(18A)-C(19A)-C(22A)	120.64(13)
C(17A)-C(16A)-B(2)	120.81(12)	C(19A)-C(20A)-C(21A)	121.26(13)
C(18A)-C(17A)-C(16A)	122.79(13)	C(20A)-C(21A)-C(16A)	122.77(13)
C(17A)-C(18A)-C(19A)	121.48(13)	C(25A)-C(22A)-C(24A)	108.94(17)
C(5A)-C(4A)-C(3A)	118.70(14)	C(25A)-C(22A)-C(19A)	111.81(12)
N(1A)-C(5A)-C(4A)	119.34(15)	C(24A)-C(22A)-C(19A)	111.06(13)
N(2A)-C(6A)-C(7A)	118.62(13)	C(25A)-C(22A)-C(23A)	109.03(17)
N(2A)-C(6A)-B(2)	115.44(12)	C(24A)-C(22A)-C(23A)	108.69(13)

C(7A)-C(6A)-B(2)      125.91(13)      C(19A)-C(22A)-C(23A)      107.23(13)

**Anisotropic Displacement Parameters ( $\text{\AA}^2 \times 10^3$ ) of D37**

	<b>U11</b>	<b>U22</b>	<b>U33</b>	<b>U23</b>	<b>U13</b>	<b>U12</b>
B(1)	21(1)	23(1)	20(1)	-4(1)	1(1)	-8(1)
N(1)	23(1)	25(1)	22(1)	-4(1)	1(1)	-9(1)
N(2)	29(1)	23(1)	24(1)	-4(1)	1(1)	-9(1)
N(3)	28(1)	24(1)	21(1)	-4(1)	1(1)	-9(1)
C(1)	25(1)	18(1)	23(1)	-3(1)	2(1)	-9(1)
C(2)	28(1)	31(1)	24(1)	-7(1)	2(1)	-12(1)
C(3)	28(1)	35(1)	30(1)	-7(1)	-2(1)	-14(1)
C(4)	23(1)	33(1)	34(1)	-5(1)	3(1)	-13(1)
C(5)	26(1)	30(1)	26(1)	-5(1)	5(1)	-10(1)
C(6)	25(1)	23(1)	16(1)	-6(1)	0(1)	-8(1)
C(7)	26(1)	27(1)	28(1)	-4(1)	2(1)	-9(1)
C(8)	33(1)	39(1)	31(1)	-2(1)	4(1)	-19(1)
C(9)	44(1)	29(1)	31(1)	3(1)	-2(1)	-19(1)
C(10)	36(1)	23(1)	30(1)	-1(1)	-2(1)	-8(1)
C(11)	25(1)	20(1)	22(1)	-2(1)	1(1)	-10(1)
C(12)	25(1)	30(1)	23(1)	-5(1)	2(1)	-10(1)
C(13)	25(1)	34(1)	29(1)	-1(1)	-3(1)	-10(1)
C(14)	34(1)	33(1)	21(1)	-1(1)	-5(1)	-14(1)
C(15)	33(1)	30(1)	20(1)	-5(1)	0(1)	-11(1)
C(16)	18(1)	24(1)	22(1)	-5(1)	0(1)	-8(1)
C(17)	24(1)	27(1)	20(1)	-3(1)	1(1)	-11(1)
C(18)	25(1)	22(1)	27(1)	-2(1)	-1(1)	-10(1)

C(19)	18(1)	25(1)	25(1)	-6(1)	0(1)	-9(1)
C(20)	20(1)	27(1)	19(1)	-4(1)	0(1)	-8(1)
C(21)	21(1)	21(1)	23(1)	-2(1)	-2(1)	-7(1)
C(22)	29(1)	24(1)	26(1)	-7(1)	0(1)	-9(1)
C(23)	52(1)	40(1)	52(1)	-23(1)	12(1)	-27(1)
C(24)	49(1)	29(1)	28(1)	-10(1)	0(1)	-5(1)
C(25)	37(1)	31(1)	35(1)	-11(1)	-2(1)	-2(1)
B(2)	24(1)	22(1)	23(1)	-2(1)	-1(1)	-7(1)
N(1A)	26(1)	22(1)	30(1)	-4(1)	3(1)	-6(1)
N(2A)	33(1)	28(1)	27(1)	-1(1)	3(1)	-9(1)
N(3A)	34(1)	26(1)	26(1)	-6(1)	7(1)	-13(1)
C(1A)	26(1)	22(1)	19(1)	0(1)	1(1)	-5(1)
C(2A)	28(1)	29(1)	29(1)	-8(1)	-3(1)	-4(1)
C(3A)	31(1)	39(1)	28(1)	-8(1)	-4(1)	-9(1)
C(4A)	24(1)	38(1)	28(1)	4(1)	-2(1)	-5(1)
C(5A)	27(1)	27(1)	37(1)	2(1)	4(1)	-3(1)
C(6A)	25(1)	24(1)	25(1)	-3(1)	-1(1)	-10(1)
C(7A)	42(1)	32(1)	29(1)	-1(1)	1(1)	0(1)
C(8A)	40(1)	39(1)	39(1)	-9(1)	3(1)	6(1)
C(9A)	29(1)	44(1)	30(1)	-11(1)	7(1)	-10(1)
C(10A)	37(1)	37(1)	26(1)	-1(1)	4(1)	-15(1)
C(11A)	31(1)	24(1)	20(1)	0(1)	0(1)	-10(1)
C(12A)	30(1)	27(1)	34(1)	-2(1)	0(1)	-9(1)
C(13A)	35(1)	34(1)	38(1)	-1(1)	-4(1)	-17(1)
C(14A)	47(1)	32(1)	28(1)	-6(1)	2(1)	-21(1)
C(15A)	42(1)	30(1)	28(1)	-8(1)	11(1)	-16(1)

C(16A)	25(1)	21(1)	21(1)	-5(1)	-1(1)	-8(1)
C(17A)	23(1)	31(1)	26(1)	-1(1)	0(1)	-11(1)
C(18A)	26(1)	32(1)	28(1)	0(1)	-6(1)	-11(1)
C(19A)	33(1)	29(1)	22(1)	0(1)	-6(1)	-15(1)
C(20A)	28(1)	33(1)	27(1)	2(1)	-2(1)	-17(1)
C(21A)	24(1)	28(1)	29(1)	0(1)	-5(1)	-10(1)
C(22A)	35(1)	42(1)	26(1)	8(1)	-10(1)	-19(1)
C(23A)	39(1)	53(1)	24(1)	0(1)	-5(1)	8(1)
C(24A)	67(1)	27(1)	30(1)	3(1)	-3(1)	-7(1)
C(25A)	94(2)	126(2)	68(1)	71(2)	-53(1)	-88(2)

---

**Fractional Atomic Coordinates ( $\times 10^4$ ) and Equivalent Isotropic Displacement**

**Parameters ( $\text{\AA}^2 \times 10^3$ ) of D39 where  $U(\text{eq}) = (1/3) \sum_j U_{jj} a_j a_j$**

	<b>x</b>	<b>y</b>	<b>z</b>	<b>U(eq)</b>
B(1)	9280(1)	5917(2)	6672(1)	19(1)
N(1)	8389(1)	5434(1)	7913(1)	18(1)
N(2)	9242(1)	3288(1)	7204(1)	19(1)
N(3)	7311(1)	6953(1)	6132(1)	24(1)
C(1)	8885(1)	6436(1)	7496(1)	18(1)
C(2)	8967(1)	7847(1)	7806(1)	20(1)
C(3)	8564(1)	8170(1)	8497(1)	21(1)
C(4)	8063(1)	7083(1)	8898(1)	23(1)
C(5)	7984(1)	5707(1)	8586(1)	21(1)
C(6)	9580(1)	1893(1)	7279(1)	22(1)
C(7)	10425(1)	1317(1)	6898(1)	23(1)

C(8)	10948(1)	2247(1)	6424(1)	24(1)
C(9)	10608(1)	3690(1)	6353(1)	22(1)
C(10)	9743(1)	4223(1)	6748(1)	18(1)
C(11)	8146(1)	5991(1)	6019(1)	18(1)
C(12)	8043(1)	5137(1)	5343(1)	21(1)
C(13)	7096(1)	5245(2)	4787(1)	26(1)
C(14)	6247(1)	6216(2)	4913(1)	29(1)
C(15)	6395(1)	7038(2)	5588(1)	28(1)
C(16)	10267(1)	6989(1)	6418(1)	18(1)
C(17)	10152(1)	7764(1)	5717(1)	19(1)
C(18)	11019(1)	8623(1)	5495(1)	19(1)
C(19)	12055(1)	8763(1)	5970(1)	18(1)
C(20)	12188(1)	8001(1)	6679(1)	21(1)
C(21)	11320(1)	7146(1)	6890(1)	20(1)
C(22)	12940(1)	9711(1)	5723(1)	21(1)
C(23)	13997(1)	9870(2)	6065(1)	29(1)

---

**Bond Lengths [Å] and Angles [deg] of D39**


---

B(1)-C(1)	1.6336(17)	C(7)-C(8)	1.3873(18)
B(1)-C(16)	1.6352(18)	C(8)-C(9)	1.3827(18)
B(1)-C(11)	1.6411(17)	C(9)-C(10)	1.3985(17)
B(1)-C(10)	1.6448(17)	C(11)-C(12)	1.4008(17)
N(1)-C(5)	1.3436(16)	C(12)-C(13)	1.3840(18)
N(1)-C(1)	1.3508(16)	C(13)-C(14)	1.384(2)
N(2)-C(6)	1.3398(16)	C(14)-C(15)	1.381(2)
N(2)-C(10)	1.3564(16)	C(16)-C(17)	1.3971(17)

N(3)-C(15)	1.3448(17)	C(16)-C(21)	1.4088(17)
N(3)-C(11)	1.3606(16)	C(17)-C(18)	1.3920(17)
C(1)-C(2)	1.3976(17)	C(18)-C(19)	1.3930(17)
C(2)-C(3)	1.3799(18)	C(19)-C(20)	1.4036(17)
C(3)-C(4)	1.3928(18)	C(19)-C(22)	1.4716(17)
C(4)-C(5)	1.3699(18)	C(20)-C(21)	1.3834(17)
C(6)-C(7)	1.3792(18)	C(22)-C(23)	1.3237(18)
C(5)-N(1)-C(1)	124.83(11)	C(1)-B(1)-C(16)	111.16(10)
C(6)-N(2)-C(10)	120.58(10)	C(1)-B(1)-C(11)	106.54(9)
C(15)-N(3)-C(11)	118.38(11)	C(16)-B(1)-C(11)	110.08(10)
N(1)-C(1)-C(2)	115.79(11)	C(1)-B(1)-C(10)	109.65(10)
N(1)-C(1)-B(1)	117.87(10)	C(16)-B(1)-C(10)	110.08(10)
C(2)-C(1)-B(1)	126.28(11)	C(11)-B(1)-C(10)	109.26(10)
N(2)-C(10)-B(1)	118.28(10)	C(14)-C(13)-C(12)	118.61(12)
C(9)-C(10)-B(1)	123.39(11)	C(15)-C(14)-C(13)	118.07(12)
N(3)-C(11)-C(12)	119.81(11)	N(3)-C(15)-C(14)	124.16(13)
N(3)-C(11)-B(1)	118.44(10)	C(17)-C(16)-C(21)	115.39(11)
C(12)-C(11)-B(1)	121.70(10)	C(17)-C(16)-B(1)	123.24(11)
C(13)-C(12)-C(11)	120.98(12)	C(21)-C(16)-B(1)	121.33(10)
C(3)-C(2)-C(1)	121.15(12)	C(18)-C(17)-C(16)	122.51(11)
C(2)-C(3)-C(4)	120.08(11)	C(17)-C(18)-C(19)	121.23(11)
C(5)-C(4)-C(3)	118.15(11)	C(18)-C(19)-C(20)	117.28(11)
N(1)-C(5)-C(4)	119.99(12)	C(18)-C(19)-C(22)	119.62(11)
N(2)-C(6)-C(7)	123.13(12)	C(20)-C(19)-C(22)	123.09(11)
C(6)-C(7)-C(8)	117.56(11)	C(21)-C(20)-C(19)	120.82(11)
C(9)-C(8)-C(7)	119.31(12)	C(20)-C(21)-C(16)	122.78(11)

C(8)-C(9)-C(10)	121.08(12)	C(23)-C(22)-C(19)	127.48(12)
N(2)-C(10)-C(9)	118.31(11)		

---

**Anisotropic Displacement Parameters ( $\text{\AA}^2 \times 10^3$ ) of D39**

	<b>U11</b>	<b>U22</b>	<b>U33</b>	<b>U23</b>	<b>U13</b>	<b>U12</b>
B(1)	21(1)	17(1)	19(1)	0(1)	5(1)	0(1)
N(1)	19(1)	15(1)	21(1)	-1(1)	4(1)	1(1)
N(2)	21(1)	16(1)	21(1)	-1(1)	4(1)	-2(1)
N(3)	22(1)	20(1)	29(1)	1(1)	2(1)	1(1)
C(1)	14(1)	18(1)	20(1)	3(1)	1(1)	2(1)
C(2)	20(1)	18(1)	24(1)	2(1)	5(1)	1(1)
C(3)	20(1)	18(1)	25(1)	-3(1)	2(1)	4(1)
C(4)	24(1)	25(1)	20(1)	0(1)	5(1)	7(1)
C(5)	21(1)	22(1)	21(1)	4(1)	6(1)	4(1)
C(6)	26(1)	16(1)	24(1)	0(1)	4(1)	-2(1)
C(7)	28(1)	16(1)	25(1)	-2(1)	2(1)	2(1)
C(8)	26(1)	23(1)	24(1)	-3(1)	6(1)	5(1)
C(9)	26(1)	21(1)	21(1)	1(1)	7(1)	0(1)
C(10)	18(1)	18(1)	16(1)	-1(1)	0(1)	-1(1)
C(11)	19(1)	14(1)	22(1)	4(1)	7(1)	-3(1)
C(12)	22(1)	21(1)	22(1)	2(1)	7(1)	-3(1)
C(13)	31(1)	28(1)	21(1)	1(1)	2(1)	-9(1)
C(14)	24(1)	30(1)	31(1)	8(1)	-5(1)	-6(1)
C(15)	23(1)	23(1)	38(1)	5(1)	0(1)	2(1)
C(16)	20(1)	13(1)	20(1)	-2(1)	5(1)	2(1)

C(17)	18(1)	18(1)	20(1)	-1(1)	1(1)	1(1)
C(18)	23(1)	17(1)	17(1)	1(1)	4(1)	1(1)
C(19)	19(1)	16(1)	21(1)	-3(1)	6(1)	2(1)
C(20)	18(1)	22(1)	22(1)	-1(1)	0(1)	2(1)
C(21)	24(1)	19(1)	18(1)	3(1)	3(1)	2(1)
C(22)	23(1)	19(1)	21(1)	-1(1)	6(1)	1(1)
C(23)	23(1)	31(1)	33(1)	5(1)	4(1)	-5(1)

**Appendix A.2** The following tables are supplementary materials for the X-ray crystal structure of compound D41 and D42. The data of fractional atomic coordinates and equivalent isotropic displacement parameters, anisotropic displacement parameters, bond lengths and bond angles are listed.

#### Crystal Data and Structure Refinement Details for D41 and D42

	D41	D42
Empirical formula	C <sub>30</sub> H <sub>35</sub> B N <sub>2</sub>	C <sub>26</sub> H <sub>23</sub> B N <sub>2</sub>
$M_r$	434.41	374.27
T, K	100(2)	100(2)
Wavelength, Å	1.54178	1.54178
Crystal system	Monoclinic	Monoclinic
Space group	P2(1)/c	P 21/n
$a$ , Å	9.9121(1)	10.9090(1)
$b$ , Å	18.3144(2)	9.2593(1)
$c$ , Å	13.8703(1)	20.7591(3)

$\alpha, ^\circ$	90	90
$\beta, ^\circ$	96.62	98.711(1)
$\gamma, ^\circ$	90	90
$V, \text{\AA}^3$	2501.15(4)	2072.68(4)
$Z$	4	4
$\rho_{\text{calc}}, \text{g/cm}^{-3}$	1.154	1.199
$\mu(\text{CuK}\alpha), \text{mm}^{-1}$	0.497	0.529
F(000)	936	792
Crystal size, $\text{mm}^3$	0.20 x 0.16 x 0.16	0.26 x 0.22 x 0.09
$\theta$ range, $^\circ$	4.01 to 67.99	4.31 to 67.35
Index ranges	-11 $\leq$ h $\leq$ 10 -21 $\leq$ k $\leq$ 21 -16 $\leq$ l $\leq$ 16	-13 $\leq$ h $\leq$ 12 -10 $\leq$ k $\leq$ 10 -23 $\leq$ l $\leq$ 24
Reflections collected	21765	16041
Independent reflections	4483 [R(int) = 0.0382]	3598 [R(int) = 0.0231]
Absorption correction	Numerical	Numerical
Refinement method	Full-matrix least-squares on $F^2$	Full-matrix least-squares on $F^2$
Data / restraints / parameters	4483 / 0 / 304	3598 / 0 / 263
Goodness-of-fit on $F^2$	1.042	1.058
Final R indices [I $>$ 2 $\sigma$ (I)] <sup>[a]</sup>	R1 = 0.0388, wR2 = 0.0965	R1 = 0.0351, wR2 = 0.0896
R indices (all data) <sup>[a]</sup>	R1 = 0.0430, wR2 = 0.1000	R1 = 0.0378, wR2 = 0.0920
Peak/hole ( $\text{e}\text{\AA}^{-3}$ )	0.318 and -0.231	0.294 and -0.181

---

**Fractional Atomic Coordinates ( $\times 10^4$ ) and Equivalent Isotropic Displacement**

**Parameters ( $\text{\AA}^2 \times 10^3$ ) of D41 where  $U(\text{eq}) = (1/3) \sum_j U^{jj} a_j a_j a_j$**

	<b>x</b>	<b>y</b>	<b>z</b>	<b>U(eq)</b>
B(1)	5530(1)	3334(1)	6849(1)	16(1)
N(1)	5818(1)	3549(1)	5033(1)	19(1)
N(2)	4838(1)	2302(1)	5581(1)	19(1)
C(1)	5965(1)	3820(1)	5944(1)	17(1)
C(2)	6522(1)	4524(1)	6042(1)	23(1)
C(3)	6863(1)	4908(1)	5252(1)	26(1)
C(4)	6666(1)	4597(1)	4328(1)	25(1)
C(5)	6148(1)	3907(1)	4241(1)	24(1)
C(6)	4847(1)	2545(1)	6504(1)	17(1)
C(7)	4286(1)	2098(1)	7181(1)	20(1)
C(8)	3754(1)	1421(1)	6921(1)	22(1)
C(9)	3765(1)	1184(1)	5970(1)	22(1)
C(10)	4306(1)	1641(1)	5330(1)	22(1)
C(11)	6913(1)	3142(1)	7570(1)	16(1)
C(12)	6888(1)	2976(1)	8556(1)	19(1)
C(13)	8020(1)	2717(1)	9139(1)	20(1)
C(14)	9257(1)	2607(1)	8775(1)	17(1)
C(15)	9315(1)	2796(1)	7807(1)	18(1)
C(16)	8171(1)	3054(1)	7229(1)	18(1)
C(17)	10472(1)	2286(1)	9428(1)	20(1)
C(18)	10800(1)	2782(1)	10317(1)	24(1)
C(19)	10094(1)	1520(1)	9767(1)	24(1)

C(20)	11737(1)	2216(1)	8899(1)	27(1)
C(21)	4425(1)	3823(1)	7360(1)	16(1)
C(22)	3026(1)	3752(1)	7098(1)	19(1)
C(23)	2068(1)	4206(1)	7456(1)	20(1)
C(24)	2466(1)	4767(1)	8103(1)	19(1)
C(25)	3861(1)	4835(1)	8391(1)	20(1)
C(26)	4804(1)	4380(1)	8034(1)	18(1)
C(27)	1478(1)	5322(1)	8462(1)	23(1)
C(28)	1626(1)	5333(1)	9577(1)	27(1)
C(29)	1835(2)	6085(1)	8099(1)	33(1)
C(30)	-3(1)	5152(1)	8089(1)	32(1)

---

**Bond Lengths [Å] and Angles [deg] of D41**

---

B(1)-C(21)	1.6374(17)	C(17)-C(20)	1.5292(18)
B(1)-C(1)	1.6386(17)	C(21)-C(22)	1.3985(17)
B(1)-C(11)	1.6389(16)	C(21)-C(26)	1.4053(16)
B(1)-C(6)	1.6432(17)	C(22)-C(23)	1.3955(17)
N(1)-C(1)	1.3486(15)	C(23)-C(24)	1.3910(17)
N(1)-C(5)	1.3512(16)	C(24)-C(25)	1.3996(18)
N(2)-C(10)	1.3500(16)	C(24)-C(27)	1.5346(16)
N(2)-C(6)	1.3543(15)	C(25)-C(26)	1.3867(17)
C(1)-C(2)	1.4020(17)	C(27)-C(30)	1.5317(19)
C(2)-C(3)	1.3772(18)	C(27)-C(28)	1.5371(17)
C(3)-C(4)	1.3953(19)	C(27)-C(29)	1.5400(18)
C(4)-C(5)	1.3632(19)	C(21)-B(1)-C(1)	106.43(9)
C(6)-C(7)	1.4078(17)	C(21)-B(1)-C(11)	114.05(9)

C(7)-C(8)	1.3782(17)	C(1)-B(1)-C(11)	107.97(9)
C(8)-C(9)	1.3896(18)	C(21)-B(1)-C(6)	109.49(9)
C(9)-C(10)	1.3734(18)	C(1)-B(1)-C(6)	112.98(9)
C(11)-C(16)	1.3937(17)	C(11)-B(1)-C(6)	106.06(9)
C(11)-C(12)	1.4039(16)	C(1)-N(1)-C(5)	124.92(11)
C(12)-C(13)	1.3892(17)	C(10)-N(2)-C(6)	119.87(11)
C(13)-C(14)	1.3938(18)	N(1)-C(1)-C(2)	115.34(11)
C(14)-C(15)	1.3934(17)	N(1)-C(1)-B(1)	120.55(10)
C(14)-C(17)	1.5384(16)	C(2)-C(1)-B(1)	124.11(10)
C(15)-C(16)	1.3938(17)	C(3)-C(2)-C(1)	121.46(12)
C(17)-C(18)	1.5358(17)	C(2)-C(3)-C(4)	120.07(12)
C(17)-C(19)	1.5394(17)	C(5)-C(4)-C(3)	118.07(12)
N(1)-C(5)-C(4)	120.11(12)	C(18)-C(17)-C(14)	108.97(10)
N(2)-C(6)-C(7)	118.65(11)	C(20)-C(17)-C(19)	108.18(10)
N(2)-C(6)-B(1)	121.48(10)	C(18)-C(17)-C(19)	109.32(10)
C(7)-C(6)-B(1)	119.85(10)	C(14)-C(17)-C(19)	109.13(10)
C(8)-C(7)-C(6)	121.13(11)	C(22)-C(21)-C(26)	114.90(11)
C(7)-C(8)-C(9)	118.99(12)	C(22)-C(21)-B(1)	121.99(10)
C(10)-C(9)-C(8)	118.01(11)	C(26)-C(21)-B(1)	122.93(10)
N(2)-C(10)-C(9)	123.34(12)	C(23)-C(22)-C(21)	123.19(11)
C(16)-C(11)-C(12)	115.03(10)	C(24)-C(23)-C(22)	121.02(11)
C(16)-C(11)-B(1)	122.42(10)	C(23)-C(24)-C(25)	116.61(11)
C(12)-C(11)-B(1)	122.21(10)	C(23)-C(24)-C(27)	123.70(11)
C(13)-C(12)-C(11)	122.47(11)	C(25)-C(24)-C(27)	119.61(11)
C(12)-C(13)-C(14)	121.60(11)	C(26)-C(25)-C(24)	121.90(11)
C(15)-C(14)-C(13)	116.68(11)	C(25)-C(26)-C(21)	122.34(11)

C(15)-C(14)-C(17)	123.12(11)	C(30)-C(27)-C(24)	112.21(11)
C(13)-C(14)-C(17)	120.20(10)	C(30)-C(27)-C(28)	108.60(11)
C(14)-C(15)-C(16)	121.16(11)	C(24)-C(27)-C(28)	110.14(10)
C(11)-C(16)-C(15)	122.98(11)	C(30)-C(27)-C(29)	108.81(11)
C(20)-C(17)-C(18)	108.97(10)	C(24)-C(27)-C(29)	108.41(10)
C(20)-C(17)-C(14)	112.23(10)	C(28)-C(27)-C(29)	108.61(11)

---

### Anisotropic Displacement Parameters ( $\text{\AA}^2 \times 10^3$ ) of D41

	U11	U22	U33	U23	U13	U12
B(1)	18(1)	16(1)	15(1)	0(1)	2(1)	0(1)
N(1)	21(1)	18(1)	18(1)	1(1)	1(1)	0(1)
N(2)	18(1)	19(1)	20(1)	-3(1)	2(1)	0(1)
C(1)	15(1)	19(1)	18(1)	1(1)	1(1)	4(1)
C(2)	28(1)	21(1)	21(1)	-1(1)	4(1)	-2(1)
C(3)	29(1)	19(1)	31(1)	3(1)	8(1)	-1(1)
C(4)	28(1)	26(1)	23(1)	8(1)	7(1)	3(1)
C(5)	26(1)	28(1)	17(1)	3(1)	3(1)	2(1)
C(6)	14(1)	17(1)	19(1)	0(1)	1(1)	3(1)
C(7)	20(1)	19(1)	20(1)	0(1)	2(1)	2(1)
C(8)	21(1)	19(1)	27(1)	5(1)	3(1)	0(1)
C(9)	19(1)	16(1)	32(1)	-3(1)	0(1)	0(1)
C(10)	21(1)	22(1)	24(1)	-7(1)	2(1)	1(1)
C(11)	18(1)	13(1)	17(1)	-2(1)	2(1)	-2(1)
C(12)	16(1)	22(1)	19(1)	0(1)	5(1)	1(1)
C(13)	22(1)	22(1)	15(1)	1(1)	3(1)	0(1)

C(14)	18(1)	15(1)	19(1)	-2(1)	0(1)	-1(1)
C(15)	16(1)	20(1)	20(1)	-1(1)	5(1)	-1(1)
C(16)	22(1)	19(1)	15(1)	0(1)	4(1)	-1(1)
C(17)	18(1)	22(1)	18(1)	-1(1)	1(1)	2(1)
C(18)	22(1)	25(1)	24(1)	-3(1)	-4(1)	3(1)
C(19)	25(1)	22(1)	25(1)	1(1)	-1(1)	3(1)
C(20)	19(1)	35(1)	26(1)	2(1)	1(1)	6(1)
C(21)	19(1)	14(1)	15(1)	3(1)	2(1)	0(1)
C(22)	21(1)	15(1)	19(1)	-1(1)	1(1)	-1(1)
C(23)	16(1)	19(1)	24(1)	4(1)	2(1)	0(1)
C(24)	23(1)	17(1)	18(1)	5(1)	6(1)	2(1)
C(25)	24(1)	16(1)	19(1)	-1(1)	4(1)	-2(1)
C(26)	18(1)	18(1)	19(1)	1(1)	2(1)	-2(1)
C(27)	25(1)	21(1)	22(1)	3(1)	7(1)	7(1)
C(28)	29(1)	28(1)	25(1)	2(1)	9(1)	8(1)
C(29)	44(1)	23(1)	34(1)	6(1)	16(1)	12(1)
C(30)	25(1)	40(1)	32(1)	-2(1)	6(1)	12(1)

**Fractional atomic Coordinates ( $\times 10^4$ ) and Equivalent Isotropic Displacement**

**Parameters ( $\text{\AA}^2 \times 10^3$ ) of D42 where  $U(\text{eq}) = (1/3) \sum_j U^{jj} a_j a_j a_j$**

	<b>x</b>	<b>y</b>	<b>z</b>	<b>U(eq)</b>
B(1)	7215(1)	9040(1)	1205(1)	21(1)
N(1)	7895(1)	11661(1)	1484(1)	21(1)
N(2)	8396(1)	9577(1)	2347(1)	23(1)
C(1)	7560(1)	10692(1)	1003(1)	21(1)

C(2)	7469(1)	11237(1)	372(1)	30(1)
C(3)	7690(1)	12677(1)	258(1)	34(1)
C(4)	8020(1)	13617(1)	776(1)	29(1)
C(5)	8130(1)	13067(1)	1394(1)	25(1)
C(6)	8163(1)	8573(1)	1864(1)	20(1)
C(7)	8720(1)	7217(1)	1961(1)	23(1)
C(8)	9521(1)	6899(1)	2526(1)	24(1)
C(9)	9770(1)	7953(1)	3000(1)	26(1)
C(10)	9181(1)	9266(1)	2891(1)	26(1)
C(11)	7317(1)	7958(1)	592(1)	21(1)
C(12)	6310(1)	7173(1)	271(1)	23(1)
C(13)	6401(1)	6299(1)	-265(1)	24(1)
C(14)	7511(1)	6158(1)	-512(1)	25(1)
C(15)	8539(1)	6917(1)	-191(1)	26(1)
C(16)	8438(1)	7783(1)	343(1)	24(1)
C(17)	7567(1)	5235(1)	-1086(1)	30(1)
C(18)	8519(2)	4987(2)	-1380(1)	59(1)
C(19)	5797(1)	9081(1)	1372(1)	20(1)
C(20)	5394(1)	8174(1)	1838(1)	23(1)
C(21)	4188(1)	8196(1)	1975(1)	27(1)
C(22)	3311(1)	9162(1)	1657(1)	26(1)
C(23)	3691(1)	10058(1)	1184(1)	24(1)
C(24)	4889(1)	10006(1)	1044(1)	22(1)
C(25)	2051(1)	9229(2)	1828(1)	35(1)
C(26)	1165(1)	10128(2)	1591(1)	54(1)

---

**Bond Lengths [Å] and Angles [deg] of D42**

B(1)-C(19)	1.6362(17)	N(1)-C(5)-C(4)	119.85(11)
B(1)-C(11)	1.6367(17)	N(2)-C(6)-C(7)	118.60(10)
B(1)-C(6)	1.6427(16)	N(2)-C(6)-B(1)	117.20(10)
B(1)-C(1)	1.6453(17)	C(7)-C(6)-B(1)	124.19(10)
N(1)-C(5)	1.3446(15)	C(8)-C(7)-C(6)	121.25(11)
N(1)-C(1)	1.3511(15)	C(7)-C(8)-C(9)	118.91(11)
N(2)-C(10)	1.3410(15)	C(10)-C(9)-C(8)	118.01(11)
N(2)-C(6)	1.3626(15)	N(2)-C(10)-C(9)	123.35(11)
C(1)-C(2)	1.3925(17)	C(12)-C(11)-C(16)	115.38(10)
C(2)-C(3)	1.3815(19)	C(12)-C(11)-B(1)	123.17(10)
C(3)-C(4)	1.3877(18)	C(16)-C(11)-B(1)	121.43(10)
C(4)-C(5)	1.3696(17)	C(13)-C(12)-C(11)	122.47(11)
C(6)-C(7)	1.3961(16)	C(19)-B(1)-C(11)	110.91(9)
C(7)-C(8)	1.3831(16)	C(19)-B(1)-C(6)	109.02(9)
C(8)-C(9)	1.3836(17)	C(11)-B(1)-C(6)	112.21(9)
C(9)-C(10)	1.3774(18)	C(19)-B(1)-C(1)	107.00(9)
C(11)-C(12)	1.3994(16)	C(11)-B(1)-C(1)	108.97(9)
C(11)-C(16)	1.4067(17)	C(6)-B(1)-C(1)	108.57(9)
C(12)-C(13)	1.3924(16)	C(5)-N(1)-C(1)	125.22(10)
C(13)-C(14)	1.3911(17)	C(10)-N(2)-C(6)	119.83(10)
C(14)-C(15)	1.4026(18)	C(14)-C(13)-C(12)	121.38(11)
C(14)-C(17)	1.4756(17)	C(13)-C(14)-C(15)	117.14(11)
C(15)-C(16)	1.3875(17)	C(13)-C(14)-C(17)	119.78(11)

C(17)-C(18)	1.301(2)	C(15)-C(14)-C(17)	123.08(11)
C(19)-C(20)	1.4003(16)	C(16)-C(15)-C(14)	120.96(11)
C(19)-C(24)	1.4045(16)	C(15)-C(16)-C(11)	122.64(11)
C(20)-C(21)	1.3884(18)	C(18)-C(17)-C(14)	127.86(13)
C(21)-C(22)	1.3999(18)	C(20)-C(19)-C(24)	115.37(11)
C(22)-C(23)	1.3963(17)	C(20)-C(19)-B(1)	122.52(10)
C(22)-C(25)	1.4724(18)	C(24)-C(19)-B(1)	122.09(10)
C(23)-C(24)	1.3825(17)	C(21)-C(20)-C(19)	122.66(11)
C(25)-C(26)	1.313(2)	C(20)-C(21)-C(22)	120.87(11)
N(1)-C(1)-C(2)	115.27(10)	C(23)-C(22)-C(21)	117.26(11)
N(1)-C(1)-B(1)	118.35(9)	C(23)-C(22)-C(25)	122.10(12)
C(2)-C(1)-B(1)	126.26(10)	C(21)-C(22)-C(25)	120.64(12)
C(3)-C(2)-C(1)	121.45(12)	C(24)-C(23)-C(22)	121.14(11)
C(2)-C(3)-C(4)	120.22(12)	C(23)-C(24)-C(19)	122.65(11)
C(5)-C(4)-C(3)	117.98(11)	C(26)-C(25)-C(22)	126.69(14)

### Anisotropic Displacement Parameters ( $\text{\AA}^2 \times 10^3$ ) of D42

	U11	U22	U33	U23	U13	U12
B(1)	24(1)	18(1)	19(1)	1(1)	-1(1)	0(1)
N(1)	24(1)	20(1)	18(1)	1(1)	1(1)	1(1)
N(2)	27(1)	20(1)	20(1)	1(1)	1(1)	0(1)
C(1)	19(1)	21(1)	22(1)	0(1)	0(1)	1(1)
C(2)	43(1)	23(1)	21(1)	0(1)	-2(1)	-2(1)
C(3)	51(1)	27(1)	22(1)	5(1)	2(1)	-2(1)

C(4)	37(1)	20(1)	30(1)	4(1)	3(1)	-3(1)
C(5)	30(1)	19(1)	25(1)	-1(1)	1(1)	0(1)
C(6)	20(1)	20(1)	20(1)	0(1)	3(1)	-2(1)
C(7)	29(1)	20(1)	20(1)	-1(1)	2(1)	-1(1)
C(8)	26(1)	21(1)	26(1)	5(1)	3(1)	3(1)
C(9)	29(1)	26(1)	21(1)	5(1)	-4(1)	-2(1)
C(10)	34(1)	22(1)	19(1)	0(1)	-2(1)	-4(1)
C(11)	27(1)	17(1)	18(1)	4(1)	-1(1)	2(1)
C(12)	24(1)	21(1)	21(1)	2(1)	0(1)	2(1)
C(13)	29(1)	21(1)	22(1)	0(1)	-4(1)	0(1)
C(14)	33(1)	21(1)	19(1)	3(1)	1(1)	4(1)
C(15)	28(1)	26(1)	25(1)	3(1)	6(1)	3(1)
C(16)	26(1)	22(1)	24(1)	1(1)	1(1)	-2(1)
C(17)	39(1)	27(1)	24(1)	-1(1)	1(1)	2(1)
C(18)	55(1)	72(1)	54(1)	-36(1)	24(1)	-17(1)
C(19)	25(1)	17(1)	17(1)	-5(1)	-1(1)	-2(1)
C(20)	28(1)	18(1)	23(1)	-1(1)	-1(1)	-1(1)
C(21)	32(1)	22(1)	27(1)	-1(1)	5(1)	-8(1)
C(22)	25(1)	25(1)	26(1)	-7(1)	1(1)	-5(1)
C(23)	25(1)	24(1)	21(1)	-4(1)	-3(1)	1(1)
C(24)	26(1)	21(1)	18(1)	-1(1)	0(1)	-1(1)
C(25)	30(1)	36(1)	40(1)	-3(1)	8(1)	-8(1)
C(26)	28(1)	67(1)	70(1)	15(1)	18(1)	4(1)

---

**Appendix A.3** The following tables are supplementary materials for the X-ray crystal structure of compound D38 and D40. The data of fractional atomic coordinates and

equivalent isotropic displacement parameters, anisotropic displacement parameters, bond lengths and bond angles are listed.

### Crystal Data and Structure Refinement Details for D38 and D40

	D38	D40
Empirical formula	C50 H50 B2 Mg N6	C53 H46 B2 Mg N6
$M_r$	780.89	812.89
T, K	100(2)	100(2)
Wavelength, Å	1.54178	1.54178
Crystal system	Rhombohedral	Triclinic
Space group	R-3	P-1
$a$ , Å	35.6690(6)	9.2796(2)
$b$ , Å	35.6690(6)	9.5310(2)
$c$ , Å	9.9695(5)	12.5635(2)
$\alpha$ , °	90	72.707(1)
$\beta$ , °	90	83.171(1)
$\gamma$ , °	120	88.764(1)
$V$ , Å <sup>3</sup>	10984.6(6)	1053.30(4)
Z	9	1
$\rho_{\text{calc}}$ , g/cm <sup>3</sup>	1.062	1.282
$\mu(\text{CuK}\alpha)$ , mm <sup>-1</sup>	0.595	0.715
F(000)	3726	428
Crystal size, mm <sup>3</sup>	0.40 x 0.18 x 0.10	0.20 x 0.16 x 0.16
$\theta$ range, °	2.48 to 68.06	3.71 to 67.04
Index ranges	-41 ≤ h ≤ 42	-10 ≤ h ≤ 10

	-42<=k<=42	-11<=k<=11
	-11<=l<=10	-14<=l<=14
Reflections collected	24780	7740
Independent reflections	4386 [R(int) = 0.0528]	3407 [R(int) = 0.0161]
Absorption correction	Numerical	Numerical
Refinement method	Full-matrix least-squares on $F^2$	Full-matrix least-squares on $F^2$
Data / restraints / parameters	4386 / 0 / 272	3407 / 0 / 295
Goodness-of-fit on $F^2$	1.080	1.069
Final R indices [ $I > 2\sigma(I)$ ] <sup>[a]</sup>	R1 = 0.0518, wR2 = 0.1483	R1 = 0.0408, wR2 = 0.1155
R indices (all data) <sup>[a]</sup>	R1 = 0.0637, wR2 = 0.1576	R1 = 0.0443, wR2 = 0.1192
Peak/hole ( $e\text{\AA}^{-3}$ )	0.606 and -0.239	0.437 and -0.206

### Fractional Atomic Coordinates ( $\times 10^4$ ) and Equivalent Isotropic Displacement

Parameters ( $\text{\AA}^2 \times 10^3$ ) of D38 where  $U(\text{eq}) = (1/3)\sum_j U_{jj} a_j a_j a_j$

	x	y	z	U(eq)
Mg(1)	5000	0	0	26(1)
B(1)	4786(1)	782(1)	412(2)	26(1)
N(1)	5457(1)	668(1)	319(2)	29(1)
N(2)	4678(1)	223(1)	-1399(2)	28(1)
N(3)	4619(1)	74(1)	1594(2)	27(1)
C(1)	5312(1)	954(1)	484(2)	26(1)
C(2)	5620(1)	1390(1)	718(2)	33(1)
C(3)	6058(1)	1528(1)	802(2)	37(1)
C(4)	6193(1)	1228(1)	647(2)	37(1)

C(5)	5884(1)	807(1)	400(2)	34(1)
C(6)	4576(1)	527(1)	-1006(2)	26(1)
C(7)	4267(1)	571(1)	-1758(2)	32(1)
C(8)	4082(1)	329(1)	-2896(2)	40(1)
C(9)	4212(1)	39(1)	-3309(2)	42(1)
C(10)	4505(1)	-4(1)	-2529(2)	35(1)
C(11)	4514(1)	392(1)	1493(2)	24(1)
C(12)	4154(1)	344(1)	2218(2)	28(1)
C(13)	3926(1)	-3(1)	3071(2)	31(1)
C(14)	4055(1)	-309(1)	3217(2)	30(1)
C(15)	4398(1)	-257(1)	2443(2)	30(1)
C(16)	4729(1)	1204(1)	640(2)	26(1)
C(17)	4683(1)	1343(1)	1916(2)	29(1)
C(18)	4655(1)	1713(1)	2118(2)	31(1)
C(19)	4675(1)	1977(1)	1052(2)	30(1)
C(20)	4745(1)	1858(1)	-213(2)	30(1)
C(21)	4772(1)	1486(1)	-404(2)	28(1)
C(22)	4625(1)	2373(1)	1311(2)	36(1)
C(23)	5018(1)	2709(1)	2123(2)	43(1)
C(24)	4600(1)	2582(1)	-5(3)	48(1)
C(25)	4211(1)	2242(1)	2106(3)	45(1)

---

**Bond Lengths [Å] and Angles [deg] of D38**


---

Mg(1)-N(1)	2.1322(16)	C(6)-C(7)	1.405(3)
Mg(1)-N(1)#1	2.1323(16)	C(7)-C(8)	1.379(3)
Mg(1)-N(3)#1	2.1909(16)	C(8)-C(9)	1.390(3)

Mg(1)-N(3)	2.1909(16)	C(9)-C(10)	1.370(3)
Mg(1)-N(2)	2.1945(16)	C(11)-C(12)	1.409(3)
Mg(1)-N(2)#1	2.1945(16)	C(12)-C(13)	1.381(3)
B(1)-C(16)	1.632(3)	C(13)-C(14)	1.389(3)
B(1)-C(11)	1.640(3)	C(14)-C(15)	1.379(3)
B(1)-C(6)	1.646(3)	C(16)-C(21)	1.402(3)
B(1)-C(1)	1.656(3)	C(16)-C(17)	1.405(3)
N(1)-C(5)	1.348(2)	C(17)-C(18)	1.387(3)
N(1)-C(1)	1.367(2)	C(18)-C(19)	1.396(3)
N(2)-C(10)	1.344(3)	C(19)-C(20)	1.392(3)
N(2)-C(6)	1.361(2)	C(19)-C(22)	1.535(3)
N(3)-C(15)	1.344(3)	C(20)-C(21)	1.391(3)
N(3)-C(11)	1.363(2)	C(22)-C(25)	1.528(3)
C(1)-C(2)	1.403(3)	C(22)-C(24)	1.533(3)
C(2)-C(3)	1.387(3)	C(22)-C(23)	1.541(3)
C(3)-C(4)	1.387(3)	N(1)-Mg(1)-N(1)#1	180
C(4)-C(5)	1.370(3)	N(1)-Mg(1)-N(3)#1	93.99(6)
N(1)#1-Mg(1)-N(3)#1	86.00(6)	C(5)-C(4)-C(3)	117.71(18)
N(1)-Mg(1)-N(3)	86.01(6)	N(1)-C(5)-C(4)	123.93(19)
N(1)#1-Mg(1)-N(3)	94.00(6)	N(2)-C(6)-C(7)	118.25(17)
N(3)#1-Mg(1)-N(3)	180.00(8)	N(2)-C(6)-B(1)	117.23(15)
N(1)-Mg(1)-N(2)	86.29(6)	C(7)-C(6)-B(1)	124.22(16)
N(1)#1-Mg(1)-N(2)	93.72(6)	C(8)-C(7)-C(6)	121.54(18)
N(3)#1-Mg(1)-N(2)	92.94(6)	C(7)-C(8)-C(9)	118.63(19)
N(3)-Mg(1)-N(2)	87.06(6)	C(10)-C(9)-C(8)	118.0(2)
N(1)-Mg(1)-N(2)#1	93.71(6)	N(2)-C(10)-C(9)	123.72(19)
N(1)#1-Mg(1)-N(2)#1	86.28(6)	N(3)-C(11)-C(12)	118.26(17)

N(3)#1-Mg(1)-N(2)#1	87.05(6)	N(3)-C(11)-B(1)	117.55(15)
N(3)-Mg(1)-N(2)#1	92.95(6)	C(12)-C(11)-B(1)	123.88(16)
N(2)-Mg(1)-N(2)#1	180.00(7)	C(13)-C(12)-C(11)	121.23(17)
C(16)-B(1)-C(11)	113.36(16)	C(12)-C(13)-C(14)	119.35(18)
C(16)-B(1)-C(6)	113.38(15)	C(15)-C(14)-C(13)	117.21(18)
C(11)-B(1)-C(6)	100.44(14)	N(3)-C(15)-C(14)	124.14(17)
C(16)-B(1)-C(1)	107.03(15)	C(21)-C(16)-C(17)	114.10(17)
C(11)-B(1)-C(1)	111.44(15)	C(21)-C(16)-B(1)	122.58(17)
C(6)-B(1)-C(1)	111.21(15)	C(17)-C(16)-B(1)	122.92(17)
C(5)-N(1)-C(1)	119.83(17)	C(18)-C(17)-C(16)	123.06(18)
C(5)-N(1)-Mg(1)	120.79(13)	C(17)-C(18)-C(19)	121.64(19)
C(1)-N(1)-Mg(1)	119.35(12)	C(20)-C(19)-C(18)	116.33(17)
C(10)-N(2)-C(6)	119.69(16)	C(20)-C(19)-C(22)	123.61(18)
C(10)-N(2)-Mg(1)	118.68(13)	C(18)-C(19)-C(22)	120.06(18)
C(6)-N(2)-Mg(1)	120.18(13)	C(21)-C(20)-C(19)	121.43(18)
C(15)-N(3)-C(11)	119.64(16)	C(20)-C(21)-C(16)	123.25(18)
C(15)-N(3)-Mg(1)	118.49(12)	C(25)-C(22)-C(24)	108.1(2)
C(11)-N(3)-Mg(1)	119.41(12)	C(25)-C(22)-C(19)	110.20(17)
N(1)-C(1)-C(2)	117.98(17)	C(24)-C(22)-C(19)	111.42(18)
N(1)-C(1)-B(1)	119.90(16)	C(25)-C(22)-C(23)	109.28(19)
C(2)-C(1)-B(1)	122.12(16)	C(24)-C(22)-C(23)	108.88(18)
C(3)-C(2)-C(1)	121.51(19)	C(19)-C(22)-C(23)	108.93(17)
C(2)-C(3)-C(4)	119.02(19)		

---

Symmetry transformations used to generate equivalent atoms: #1 -x+1,-y,-z

**Anisotropic Displacement Parameters ( $\text{\AA}^2 \times 10^3$ ) of D38**

Mg(1)	25(1)	31(1)	26(1)	-1(1)	0(1)	17(1)
B(1)	25(1)	30(1)	26(1)	-1(1)	-2(1)	15(1)
N(1)	25(1)	36(1)	26(1)	-1(1)	0(1)	16(1)
N(2)	30(1)	33(1)	25(1)	-3(1)	-2(1)	18(1)
N(3)	27(1)	30(1)	26(1)	0(1)	0(1)	16(1)
C(1)	27(1)	33(1)	19(1)	1(1)	0(1)	15(1)
C(2)	32(1)	34(1)	31(1)	0(1)	-1(1)	15(1)
C(3)	29(1)	37(1)	33(1)	0(1)	-1(1)	9(1)
C(4)	23(1)	50(1)	31(1)	0(1)	-1(1)	14(1)
C(5)	28(1)	47(1)	30(1)	-1(1)	0(1)	21(1)
C(6)	24(1)	28(1)	26(1)	1(1)	2(1)	13(1)
C(7)	32(1)	36(1)	32(1)	-4(1)	-5(1)	21(1)
C(8)	42(1)	47(1)	37(1)	-7(1)	-13(1)	28(1)
C(9)	53(1)	48(1)	31(1)	-13(1)	-14(1)	30(1)
C(10)	42(1)	40(1)	30(1)	-7(1)	-4(1)	26(1)
C(11)	24(1)	27(1)	23(1)	-5(1)	-6(1)	14(1)
C(12)	27(1)	30(1)	30(1)	-4(1)	-3(1)	16(1)
C(13)	27(1)	34(1)	30(1)	-3(1)	3(1)	14(1)
C(14)	32(1)	29(1)	25(1)	-1(1)	2(1)	13(1)
C(15)	34(1)	31(1)	28(1)	-1(1)	-1(1)	19(1)
C(16)	24(1)	27(1)	27(1)	-2(1)	-3(1)	12(1)
C(17)	32(1)	29(1)	25(1)	0(1)	-4(1)	14(1)
C(18)	38(1)	28(1)	23(1)	-3(1)	-3(1)	15(1)
C(19)	35(1)	25(1)	26(1)	-2(1)	-4(1)	13(1)
C(20)	33(1)	28(1)	25(1)	3(1)	-1(1)	13(1)

C(21)	29(1)	31(1)	24(1)	-1(1)	1(1)	14(1)
C(22)	52(1)	25(1)	31(1)	-4(1)	-5(1)	20(1)
C(23)	59(1)	28(1)	35(1)	-5(1)	-4(1)	16(1)
C(24)	79(2)	30(1)	40(2)	-2(1)	-9(1)	32(1)
C(25)	54(1)	36(1)	50(2)	-6(1)	-2(1)	28(1)

---

**Fractional Atomic Coordinates ( $\times 10^4$ ) and Equivalent Isotropic Displacement**

**Parameters ( $\text{\AA}^2 \times 10^3$ ) of D40 where  $U(\text{eq}) = (1/3) \sum_j U^{jj} a_j a_j a_j$**

	<b>x</b>	<b>y</b>	<b>z</b>	<b>U(eq)</b>
Mg(1)	5000	5000	5000	14(1)
N(1)	3100(1)	5918(1)	4235(1)	17(1)
N(2)	5689(1)	4485(1)	3452(1)	17(1)
N(3)	3773(1)	2902(1)	5564(1)	17(1)
C(1)	2344(2)	5089(2)	3770(1)	16(1)
C(2)	949(2)	5550(2)	3497(1)	20(1)
C(3)	361(2)	6816(2)	3673(1)	21(1)
C(4)	1174(2)	7661(2)	4115(1)	21(1)
C(5)	2528(2)	7166(2)	4381(1)	20(1)
C(6)	4758(2)	3858(2)	2962(1)	16(1)
C(7)	5318(2)	3375(2)	2046(1)	19(1)
C(8)	6773(2)	3555(2)	1629(1)	21(1)
C(9)	7692(2)	4223(2)	2131(1)	20(1)
C(10)	7101(2)	4665(2)	3036(1)	19(1)
C(11)	3265(2)	2370(2)	4781(1)	16(1)
C(12)	3078(2)	841(2)	5037(1)	19(1)

C(13)	3284(2)	-93(2)	6080(2)	22(1)
C(14)	3696(2)	489(2)	6888(2)	22(1)
C(15)	3953(2)	1984(2)	6579(1)	20(1)
C(16)	2059(2)	3041(2)	2761(1)	17(1)
C(17)	1040(2)	1881(2)	3094(1)	19(1)
C(18)	279(2)	1474(2)	2342(2)	20(1)
C(19)	465(2)	2229(2)	1198(1)	19(1)
C(20)	1376(2)	3472(2)	862(1)	20(1)
C(21)	2137(2)	3852(2)	1616(1)	19(1)
C(22)	-278(2)	1722(2)	404(2)	25(1)
C(23)	5(3)	2162(2)	-699(2)	39(1)
B(1)	3061(2)	3574(2)	3564(2)	16(1)
C(1A)	4601(4)	9275(4)	384(3)	33(1)
C(2A)	4069(2)	10717(3)	320(2)	40(1)
C(3A)	3457(5)	9528(6)	1024(4)	43(1)
C(3B)	4682(5)	11923(5)	-405(4)	38(1)
C(4A)	3949(3)	8028(3)	1121(2)	55(1)

---

**Bond Lengths [Å] and Angles [deg] of D40**

---

Mg(1)-N(1)#1	2.1527(13)	C(16)-C(17)	1.402(2)
Mg(1)-N(1)	2.1528(13)	C(16)-C(21)	1.411(2)
Mg(1)-N(2)	2.1656(13)	C(16)-B(1)	1.639(2)
Mg(1)-N(2)#1	2.1656(13)	C(17)-C(18)	1.391(2)
Mg(1)-N(3)#1	2.2047(13)	C(18)-C(19)	1.394(2)
Mg(1)-N(3)	2.2047(13)	C(19)-C(20)	1.400(2)
N(1)-C(5)	1.345(2)	C(19)-C(22)	1.472(2)

N(1)-C(1)	1.361(2)	C(20)-C(21)	1.379(2)
N(2)-C(10)	1.346(2)	C(22)-C(23)	1.318(3)
N(2)-C(6)	1.361(2)	C(1A)-C(3B)#2	1.303(6)
N(3)-C(15)	1.342(2)	C(1A)-C(3A)	1.317(6)
N(3)-C(11)	1.366(2)	C(1A)-C(4A)	1.371(5)
C(1)-C(2)	1.406(2)	C(1A)-C(2A)#2	1.429(5)
C(1)-B(1)	1.655(2)	C(1A)-C(2A)	1.433(5)
C(2)-C(3)	1.379(2)	C(1A)-C(1A)#2	1.572(8)
C(3)-C(4)	1.385(2)	C(2A)-C(3A)	1.305(5)
C(4)-C(5)	1.376(2)	C(2A)-C(3B)	1.325(5)
C(6)-C(7)	1.403(2)	C(2A)-C(1A)#2	1.429(5)
C(6)-B(1)	1.655(2)	C(3A)-C(4A)	1.467(6)
C(7)-C(8)	1.383(2)	C(3B)-C(1A)#2	1.303(6)
C(8)-C(9)	1.385(2)	C(3B)-C(4A)#2	1.459(5)
C(9)-C(10)	1.377(2)	C(4A)-C(3B)#2	1.459(5)
C(11)-C(12)	1.406(2)	N(1)#1-Mg(1)-N(1)	179.998(1)
C(11)-B(1)	1.644(2)	N(1)#1-Mg(1)-N(2)	93.82(5)
C(12)-C(13)	1.380(3)	N(1)-Mg(1)-N(2)	86.18(5)
C(13)-C(14)	1.386(2)	N(1)#1-Mg(1)-N(2)#1	86.18(5)
C(14)-C(15)	1.380(2)	N(1)-Mg(1)-N(2)#1	93.82(5)
N(2)-Mg(1)-N(2)#1	180.00(7)	C(17)-C(18)-C(19)	121.37(15)
N(1)#1-Mg(1)-N(3)#1	85.54(5)	C(18)-C(19)-C(20)	116.60(15)
N(1)-Mg(1)-N(3)#1	94.46(5)	C(18)-C(19)-C(22)	120.60(15)
N(2)-Mg(1)-N(3)#1	92.75(5)	C(20)-C(19)-C(22)	122.80(16)
N(2)#1-Mg(1)-N(3)#1	87.25(5)	C(21)-C(20)-C(19)	121.15(16)
N(1)#1-Mg(1)-N(3)	94.46(5)	C(5)-N(1)-C(1)	119.83(14)

N(1)-Mg(1)-N(3)	85.54(5)	C(20)-C(21)-C(16)	123.39(15)
N(2)-Mg(1)-N(3)	87.25(5)	C(23)-C(22)-C(19)	126.26(17)
N(2)#1-Mg(1)-N(3)	92.75(5)	C(16)-B(1)-C(11)	116.24(13)
N(3)#1-Mg(1)-N(3)	180.0	C(16)-B(1)-C(1)	107.55(13)
C(5)-N(1)-Mg(1)	120.64(11)	C(11)-B(1)-C(1)	109.57(13)
C(1)-N(1)-Mg(1)	118.55(10)	C(16)-B(1)-C(6)	110.13(13)
C(10)-N(2)-C(6)	119.92(14)	C(11)-B(1)-C(6)	101.85(12)
C(10)-N(2)-Mg(1)	118.55(11)	C(1)-B(1)-C(6)	111.49(12)
C(6)-N(2)-Mg(1)	121.23(10)	C(3B)#2-C(1A)-C(3A)	131.7(4)
C(15)-N(3)-C(11)	119.80(14)	C(3B)#2-C(1A)-C(4A)	66.1(3)
C(15)-N(3)-Mg(1)	117.71(10)	C(3A)-C(1A)-C(4A)	66.1(3)
C(11)-N(3)-Mg(1)	118.95(10)	C(3B)#2-C(1A)-C(2A)#2	57.8(3)
N(1)-C(1)-C(2)	118.05(14)	C(3A)-C(1A)-C(2A)#2	168.7(4)
N(1)-C(1)-B(1)	119.90(14)	C(4A)-C(1A)-C(2A)#2	123.9(3)
C(2)-C(1)-B(1)	122.05(14)	C(3B)#2-C(1A)-C(2A)	169.6(4)
C(3)-C(2)-C(1)	121.54(15)	C(3A)-C(1A)-C(2A)	56.4(3)
C(2)-C(3)-C(4)	119.11(15)	C(4A)-C(1A)-C(2A)	122.6(3)
C(5)-C(4)-C(3)	117.57(15)	C(2A)#2-C(1A)-C(2A)	113.4(3)
N(1)-C(5)-C(4)	123.84(15)	C(3B)#2-C(1A)-C(1A)#2	114.4(5)
N(2)-C(6)-C(7)	118.30(14)	C(3A)-C(1A)-C(1A)#2	112.8(5)
N(2)-C(6)-B(1)	117.36(13)	C(4A)-C(1A)-C(1A)#2	175.7(4)
C(7)-C(6)-B(1)	124.07(14)	C(2A)#2-C(1A)-C(1A)#2	56.8(3)
C(8)-C(7)-C(6)	121.36(15)	C(2A)-C(1A)-C(1A)#2	56.5(3)
C(7)-C(8)-C(9)	119.13(15)	C(3A)-C(2A)-C(3B)	179.4(3)
C(10)-C(9)-C(8)	117.67(15)	C(3A)-C(2A)-C(1A)#2	123.7(3)
N(2)-C(10)-C(9)	123.60(15)	C(3B)-C(2A)-C(1A)#2	56.3(3)

N(3)-C(11)-C(12)	117.95(15)	C(3A)-C(2A)-C(1A)	57.3(3)
N(3)-C(11)-B(1)	116.58(13)	C(3B)-C(2A)-C(1A)	122.7(3)
C(12)-C(11)-B(1)	125.23(15)	C(1A)#2-C(2A)-C(1A)	66.6(3)
C(13)-C(12)-C(11)	121.43(16)	C(2A)-C(3A)-C(1A)	66.3(3)
C(12)-C(13)-C(14)	119.24(15)	C(2A)-C(3A)-C(4A)	125.0(3)
C(15)-C(14)-C(13)	117.37(16)	C(1A)-C(3A)-C(4A)	58.7(3)
N(3)-C(15)-C(14)	123.89(16)	C(1A)#2-C(3B)-C(2A)	65.8(3)
C(17)-C(16)-C(21)	114.09(15)	C(1A)#2-C(3B)-C(4A)#2	59.2(3)
C(17)-C(16)-B(1)	127.09(15)	C(2A)-C(3B)-C(4A)#2	125.0(3)
C(21)-C(16)-B(1)	118.72(13)	C(1A)-C(4A)-C(3B)#2	54.7(3)
C(18)-C(17)-C(16)	122.95(16)	C(1A)-C(4A)-C(3A)	55.2(3)
		C(3B)#2-C(4A)-C(3A)	109.6(3)

Symmetry transformations used to generate equivalent atoms: #1  $-x+1,-y+1,-z+1$ ; #2  $-x+1,-y+2,-z$

#### Anisotropic Displacement Parameters ( $\text{\AA}^2 \times 10^3$ ) of D40

	U11	U22	U33	U23	U13	U12
Mg(1)	15(1)	13(1)	16(1)	-4(1)	-4(1)	-1(1)
N(1)	19(1)	15(1)	17(1)	-4(1)	-4(1)	0(1)
N(2)	17(1)	15(1)	18(1)	-3(1)	-3(1)	-1(1)
N(3)	17(1)	16(1)	18(1)	-4(1)	-5(1)	0(1)
C(1)	18(1)	15(1)	13(1)	-1(1)	-1(1)	-2(1)
C(2)	19(1)	20(1)	20(1)	-5(1)	-5(1)	-2(1)
C(3)	18(1)	22(1)	23(1)	-5(1)	-5(1)	3(1)
C(4)	25(1)	16(1)	23(1)	-6(1)	-3(1)	4(1)
C(5)	23(1)	17(1)	21(1)	-7(1)	-5(1)	-1(1)

C(6)	19(1)	11(1)	16(1)	0(1)	-5(1)	1(1)
C(7)	22(1)	17(1)	18(1)	-4(1)	-7(1)	2(1)
C(8)	26(1)	19(1)	18(1)	-5(1)	-1(1)	3(1)
C(9)	18(1)	19(1)	21(1)	-2(1)	0(1)	1(1)
C(10)	18(1)	17(1)	21(1)	-3(1)	-4(1)	-2(1)
C(11)	12(1)	18(1)	19(1)	-6(1)	-1(1)	0(1)
C(12)	19(1)	18(1)	21(1)	-6(1)	-5(1)	0(1)
C(13)	23(1)	15(1)	26(1)	-2(1)	-4(1)	-1(1)
C(14)	24(1)	21(1)	18(1)	0(1)	-6(1)	0(1)
C(15)	21(1)	21(1)	18(1)	-5(1)	-6(1)	-1(1)
C(16)	16(1)	15(1)	20(1)	-7(1)	-3(1)	3(1)
C(17)	19(1)	18(1)	18(1)	-5(1)	-3(1)	1(1)
C(18)	17(1)	16(1)	26(1)	-7(1)	-4(1)	-1(1)
C(19)	17(1)	20(1)	23(1)	-10(1)	-6(1)	4(1)
C(20)	22(1)	20(1)	18(1)	-3(1)	-4(1)	2(1)
C(21)	19(1)	16(1)	22(1)	-4(1)	-4(1)	-2(1)
C(22)	25(1)	24(1)	30(1)	-12(1)	-9(1)	0(1)
C(23)	55(1)	35(1)	30(1)	-11(1)	-16(1)	-10(1)
B(1)	18(1)	15(1)	17(1)	-5(1)	-3(1)	-1(1)
C(1A)	37(2)	34(2)	26(2)	-4(2)	-16(2)	-7(2)
C(2A)	34(1)	52(1)	41(1)	-24(1)	-12(1)	12(1)
C(3A)	32(2)	66(3)	41(2)	-30(2)	0(2)	-5(2)
C(3B)	47(2)	38(2)	38(2)	-18(2)	-24(2)	12(2)
C(4A)	61(2)	70(2)	40(1)	-16(1)	-23(1)	4(1)

---

**Appendix A.4** The following tables are supplementary materials for the X-ray crystal structure of compound D45 and D46. The data of fractional atomic coordinates and equivalent isotropic displacement parameters, anisotropic displacement parameters, bond lengths and bond angles are listed.

**Crystal Data and Structure Refinement Details for D45 and D46**

	D46	D45
Empirical formula	C57 H58 B2 Fe N6	C53 H46 B2 Fe N6
$M_r$	904.56	844.43
T, K	100(2)	100(2)
Wavelength, Å	1.54178	1.54178
Crystal system	Monoclinic	Triclinic
Space group	C2/c	P -1
$a$ , Å	18.0553(2)	12.5732(2)
$b$ , Å	10.0207(1)	13.3194(2)
$c$ , Å	26.1009(4)	13.3826(2)
$\alpha$ , °	90	89.972(1)
$\beta$ , °	105.384(1)	71.533(1)
$\gamma$ , °	90.	80.203(1)
$V$ , Å <sup>3</sup>	4553.15(10)	2091.32(6)
Z	4	2
$\rho_{\text{calc}}$ , g/cm <sup>3</sup>	1.320	1.341
$\mu(\text{CuK}\alpha)$ , mm <sup>-1</sup>	3.012	3,243
F(000)	1912	884
Crystal size, mm <sup>3</sup>	0.25 x 0.21 x 0.14	0.23 x 0.22 x 0.12

$\theta$ range, °	3.51 to 67.27	3.37 to 67.38
Index ranges	-21 ≤ h ≤ 20	-14 ≤ h ≤ 14
	-11 ≤ k ≤ 11	-15 ≤ k ≤ 15
	-30 ≤ l ≤ 30	-15 ≤ l ≤ 15
Reflections collected	17091	18432
Independent reflections	3962 [R(int) = 0.0272]	6822 [R(int) = 0.0287]
Absorption correction	Numerical	Numerical
Refinement method	Full-matrix least-squares on $F^2$	Full-matrix least-squares on $F^2$
Data / restraints / parameters	3962 / 0 / 305	6822 / 0 / 563
Goodness-of-fit on $F^2$	1.062	1.026
Final R indices [ $I > 2\sigma(I)$ ] <sup>[a]</sup>	R1 = 0.0325, wR2 = 0.0848	R1 = 0.0421, wR2 = 0.1089
R indices (all data) <sup>[a]</sup>	R1 = 0.0366, wR2 = 0.0873	R1 = 0.0549, wR2 = 0.1172
Peak/hole (eÅ <sup>-3</sup> )	0.323 and -0.371	0.982 and -0.441

### Fractional Atomic Coordinates ( $\times 10^4$ ) and Equivalent Isotropic Displacement

Parameters ( $\text{\AA}^2 \times 10^3$ ) of D46 where  $U(\text{eq}) = (1/3) \sum_j U^{jj} a_j a_j a_j$

	x	y	z	U(eq)
Fe(1)	2500	2500	0	12(1)
B(1)	2957(1)	2547(2)	1246(1)	16(1)
N(1)	3292(1)	1349(1)	471(1)	15(1)
N(2)	2913(1)	4070(1)	453(1)	15(1)
N(3)	1789(1)	2134(1)	439(1)	15(1)
C(1)	3475(1)	1490(2)	1009(1)	16(1)
C(2)	4120(1)	801(2)	1313(1)	20(1)

C(3)	4532(1)	-74(2)	1087(1)	22(1)
C(4)	4311(1)	-244(2)	540(1)	20(1)
C(5)	3700(1)	497(2)	250(1)	18(1)
C(6)	3152(1)	3963(2)	993(1)	16(1)
C(7)	3566(1)	5025(2)	1282(1)	19(1)
C(8)	3690(1)	6199(2)	1043(1)	21(1)
C(9)	3397(1)	6316(2)	496(1)	20(1)
C(10)	3026(1)	5230(2)	220(1)	18(1)
C(11)	2043(1)	2246(2)	977(1)	15(1)
C(12)	1507(1)	2106(2)	1278(1)	18(1)
C(13)	743(1)	1833(2)	1042(1)	19(1)
C(14)	506(1)	1673(2)	495(1)	19(1)
C(15)	1041(1)	1836(2)	210(1)	17(1)
C(16)	3105(1)	2538(2)	1891(1)	16(1)
C(17)	3312(1)	1397(2)	2207(1)	18(1)
C(18)	3410(1)	1393(2)	2755(1)	18(1)
C(19)	3287(1)	2533(2)	3026(1)	16(1)
C(20)	3027(1)	3655(2)	2712(1)	18(1)
C(21)	2937(1)	3652(2)	2168(1)	18(1)
C(22)	3455(1)	2606(2)	3633(1)	20(1)
C(23)	4247(1)	3269(2)	3849(1)	31(1)
C(24)	2838(1)	3439(2)	3793(1)	31(1)
C(25)	3476(1)	1226(2)	3890(1)	24(1)
C(26)	0	3551(3)	2500	28(1)
C(27)	637(1)	2854(2)	2445(1)	27(1)
C(28)	631(1)	1471(2)	2441(1)	24(1)

C(29)	0	749(2)	2500	21(1)
C(30)	0	-759(3)	2500	30(1)

---

**Bond Lengths [Å] and Angles [deg] of D46**

Fe(1)-N(3)	1.9691(13)	Fe(1)-N(2)#1	1.9907(13)
Fe(1)-N(3)#1	1.9692(13)	B(1)-C(1)	1.638(2)
Fe(1)-N(1)#1	1.9883(13)	B(1)-C(6)	1.642(2)
Fe(1)-N(1)	1.9883(13)	B(1)-C(11)	1.642(2)
Fe(1)-N(2)	1.9906(13)	B(1)-C(16)	1.633(2)
N(1)-C(5)	1.353(2)	N(3)-Fe(1)-N(2)#1	89.97(5)
N(1)-C(1)	1.362(2)	N(3)#1-Fe(1)-N(2)#1	90.03(5)
N(3)-C(15)	1.358(2)	N(1)#1-Fe(1)-N(2)#1	89.81(5)
N(3)-C(11)	1.360(2)	N(1)-Fe(1)-N(2)#1	90.20(5)
N(2)-C(10)	1.352(2)	N(3)#1-Fe(1)-N(1)#1	90.25(5)
N(2)-C(6)	1.364(2)	N(3)#1-Fe(1)-N(1)	89.75(5)
C(1)-C(2)	1.405(2)	N(3)-Fe(1)-N(2)	90.03(5)
C(2)-C(3)	1.380(2)	N(3)#1-Fe(1)-N(2)	89.97(5)
C(3)-C(4)	1.387(2)	N(1)#1-Fe(1)-N(2)	90.19(5)
C(4)-C(5)	1.378(2)	N(3)-Fe(1)-N(1)	90.25(5)
C(6)-C(7)	1.400(2)	C(11)-N(3)-Fe(1)	119.53(10)
C(7)-C(8)	1.378(2)	N(1)-C(1)-C(2)	118.07(14)
C(8)-C(9)	1.388(2)	N(1)-C(1)-B(1)	116.65(13)
C(9)-C(10)	1.378(2)	C(2)-C(1)-B(1)	125.11(14)
C(11)-C(12)	1.405(2)	C(3)-C(2)-C(1)	122.05(15)
C(12)-C(13)	1.381(2)	C(2)-C(3)-C(4)	118.52(15)
C(13)-C(14)	1.387(2)	C(5)-C(4)-C(3)	118.00(15)

C(14)-C(15)	1.375(2)	N(1)-C(5)-C(4)	123.58(15)
C(16)-C(17)	1.402(2)	N(2)-C(6)-C(7)	118.33(14)
C(16)-C(21)	1.406(2)	N(2)-C(6)-B(1)	116.08(13)
C(17)-C(18)	1.395(2)	C(7)-C(6)-B(1)	125.52(14)
C(18)-C(19)	1.391(2)	C(8)-C(7)-C(6)	122.12(15)
C(19)-C(20)	1.397(2)	C(7)-C(8)-C(9)	118.36(15)
C(19)-C(22)	1.534(2)	C(10)-C(9)-C(8)	118.08(15)
C(20)-C(21)	1.386(2)	N(2)-C(10)-C(9)	123.65(15)
C(22)-C(25)	1.534(2)	N(3)-C(11)-C(12)	118.39(14)
C(22)-C(24)	1.537(3)	N(3)-C(11)-B(1)	118.71(14)
C(22)-C(23)	1.540(3)	C(12)-C(11)-B(1)	122.90(14)
C(26)-C(27)#2	1.385(2)	C(13)-C(12)-C(11)	121.64(15)
C(26)-C(27)	1.385(2)	C(12)-C(13)-C(14)	118.75(15)
C(27)-C(28)	1.386(3)	C(15)-C(14)-C(13)	118.24(15)
C(28)-C(29)	1.393(2)	C(5)-N(1)-C(1)	119.60(13)
C(29)-C(28)#2	1.393(2)	C(5)-N(1)-Fe(1)	119.08(11)
C(29)-C(30)	1.512(3)	C(1)-N(1)-Fe(1)	121.05(10)
C(16)-B(1)-C(11)	108.02(13)	C(10)-N(2)-C(6)	119.21(13)
C(1)-B(1)-C(11)	109.29(13)	C(10)-N(2)-Fe(1)	119.31(10)
C(6)-B(1)-C(11)	106.61(12)	C(6)-N(2)-Fe(1)	121.19(10)
C(16)-B(1)-C(1)	115.60(13)	C(15)-N(3)-C(11)	119.71(13)
C(16)-B(1)-C(6)	115.13(13)	C(15)-N(3)-Fe(1)	120.69(11)
C(1)-B(1)-C(6)	101.70(13)	N(3)-C(15)-C(14)	123.20(15)
N(2)-Fe(1)-N(2)#1	180.0	C(19)-C(22)-C(24)	110.39(14)
N(1)#1-Fe(1)-N(1)	180.0	C(25)-C(22)-C(23)	108.41(14)
N(3)-Fe(1)-N(3)#1	180.0	C(17)-C(16)-B(1)	123.78(13)

N(3)-Fe(1)-N(1)#1	89.75(5)	C(21)-C(16)-B(1)	121.86(13)
N(1)-Fe(1)-N(2)	89.81(5)	C(18)-C(17)-C(16)	123.20(15)
C(19)-C(18)-C(17)	121.65(15)	C(25)-C(22)-C(19)	112.62(13)
C(18)-C(19)-C(20)	115.94(15)	C(25)-C(22)-C(24)	107.76(15)
C(17)-C(16)-C(21)	113.88(15)	C(27)#2-C(26)-C(27)	119.4(2)
C(20)-C(21)-C(16)	123.12(15)	C(26)-C(27)-C(28)	120.09(18)
C(21)-C(20)-C(19)	121.91(15)	C(27)-C(28)-C(29)	121.48(17)
C(18)-C(19)-C(22)	123.30(14)	C(28)#2-C(29)-C(28)	117.4(2)
C(20)-C(19)-C(22)	120.70(14)	C(28)#2-C(29)-C(30)	121.28(11)
C(19)-C(22)-C(23)	108.01(14)	C(28)-C(29)-C(30)	121.28(11)
C(24)-C(22)-C(23)			

---

**Anisotropic Displacement Parameters ( $\text{\AA}^2 \times 10^3$ ) of D46**

	U11	U22	U33	U23	U13	U12
Fe(1)	14(1)	12(1)	10(1)	0(1)	3(1)	0(1)
B(1)	17(1)	16(1)	13(1)	0(1)	3(1)	-1(1)
N(1)	16(1)	13(1)	15(1)	1(1)	4(1)	0(1)
N(2)	16(1)	15(1)	15(1)	0(1)	5(1)	0(1)
N(3)	17(1)	13(1)	14(1)	1(1)	4(1)	1(1)
C(1)	16(1)	14(1)	16(1)	1(1)	4(1)	-4(1)
C(2)	19(1)	24(1)	15(1)	2(1)	5(1)	0(1)
C(3)	19(1)	22(1)	24(1)	6(1)	5(1)	4(1)
C(4)	22(1)	15(1)	25(1)	0(1)	10(1)	2(1)
C(5)	21(1)	15(1)	18(1)	-1(1)	7(1)	-2(1)
C(6)	14(1)	18(1)	16(1)	0(1)	5(1)	2(1)

C(7)	19(1)	23(1)	16(1)	-3(1)	5(1)	-2(1)
C(8)	19(1)	21(1)	25(1)	-7(1)	8(1)	-5(1)
C(9)	21(1)	16(1)	25(1)	1(1)	10(1)	-2(1)
C(10)	19(1)	17(1)	17(1)	2(1)	6(1)	0(1)
C(11)	19(1)	10(1)	16(1)	1(1)	5(1)	2(1)
C(12)	22(1)	18(1)	15(1)	1(1)	6(1)	2(1)
C(13)	20(1)	18(1)	22(1)	2(1)	10(1)	2(1)
C(14)	16(1)	19(1)	23(1)	1(1)	3(1)	0(1)
C(15)	18(1)	16(1)	16(1)	0(1)	2(1)	0(1)
C(16)	13(1)	18(1)	15(1)	-1(1)	3(1)	-2(1)
C(17)	20(1)	16(1)	18(1)	-3(1)	6(1)	-1(1)
C(18)	22(1)	15(1)	16(1)	2(1)	5(1)	0(1)
C(19)	16(1)	19(1)	15(1)	0(1)	4(1)	-3(1)
C(20)	21(1)	16(1)	19(1)	-2(1)	8(1)	1(1)
C(21)	18(1)	18(1)	17(1)	3(1)	4(1)	2(1)
C(22)	29(1)	17(1)	14(1)	-1(1)	5(1)	-1(1)
C(23)	41(1)	26(1)	19(1)	0(1)	-2(1)	-6(1)
C(24)	52(1)	25(1)	19(1)	0(1)	16(1)	6(1)
C(25)	38(1)	22(1)	15(1)	1(1)	7(1)	0(1)
C(26)	44(2)	19(1)	19(1)	0	5(1)	0
C(27)	32(1)	27(1)	21(1)	5(1)	6(1)	-5(1)
C(28)	26(1)	26(1)	19(1)	5(1)	5(1)	3(1)
C(29)	25(1)	22(1)	13(1)	0	-1(1)	0
C(30)	24(1)	23(1)	38(2)	0	3(1)	0

---

**Fractional Atomic Coordinates ( $\times 10^4$ ) and Equivalent Isotropic Displacement**

**Parameters ( $\text{\AA}^2 \times 10^3$ ) of D45 where  $U(\text{eq}) = (1/3) \sum_j U^j a_j a_j$**

	<b>x</b>	<b>y</b>	<b>z</b>	<b>U(eq)</b>
Fe(1)	5000	5000	0	16(1)
B(1)	6383(2)	4848(2)	1574(2)	19(1)
N(1)	4444(2)	5657(2)	1463(2)	18(1)
N(2)	5586(2)	3714(1)	530(2)	17(1)
N(3)	6485(2)	5461(1)	-250(2)	17(1)
C(1)	5150(2)	5604(2)	2059(2)	19(1)
C(2)	4841(2)	6262(2)	2954(2)	23(1)
C(3)	3800(2)	6910(2)	3287(2)	27(1)
C(4)	3051(2)	6897(2)	2723(2)	26(1)
C(5)	3408(2)	6272(2)	1818(2)	23(1)
C(6)	6185(2)	3739(2)	1215(2)	18(1)
C(7)	6578(2)	2816(2)	1596(2)	22(1)
C(8)	6363(2)	1900(2)	1303(2)	23(1)
C(9)	5748(2)	1898(2)	608(2)	22(1)
C(10)	5387(2)	2811(2)	235(2)	20(1)
C(11)	6927(2)	5942(2)	-1132(2)	22(1)
C(12)	7767(2)	6511(2)	-1247(2)	26(1)
C(13)	8177(2)	6604(2)	-407(2)	26(1)
C(14)	7769(2)	6069(2)	472(2)	22(1)
C(15)	6947(2)	5462(2)	547(2)	18(1)
C(16)	7142(2)	4645(2)	2368(2)	19(1)
C(17)	6668(2)	4538(2)	3449(2)	23(1)

C(18)	7321(2)	4275(2)	4108(2)	27(1)
C(19)	8510(2)	4091(2)	3704(2)	27(1)
C(20)	9000(2)	4137(2)	2620(2)	24(1)
C(21)	8338(2)	4403(2)	1976(2)	22(1)
C(22)	9205(3)	3871(2)	4408(2)	38(1)
C(23)	10291(3)	3964(3)	4158(3)	62(1)
Fe(2)	5000	0	5000	15(1)
B(2)	3644(2)	307(2)	3380(2)	18(1)
N(4)	5599(2)	-484(1)	3475(2)	17(1)
N(5)	4319(2)	1339(1)	4600(2)	17(1)
N(6)	3583(2)	-526(1)	5136(2)	16(1)
C(1A)	4960(2)	-286(2)	2815(2)	17(1)
C(2A)	5489(2)	-542(2)	1738(2)	20(1)
C(3A)	6605(2)	-1027(2)	1330(2)	22(1)
C(4A)	7226(2)	-1253(2)	2021(2)	24(1)
C(5A)	6696(2)	-964(2)	3072(2)	21(1)
C(6A)	4456(2)	2211(2)	5016(2)	20(1)
C(7A)	4197(2)	3160(2)	4655(2)	23(1)
C(8A)	3802(2)	3214(2)	3792(2)	23(1)
C(9A)	3627(2)	2332(2)	3385(2)	20(1)
C(10A)	3842(2)	1387(2)	3816(2)	17(1)
C(11A)	3118(2)	-1068(2)	5967(2)	20(1)
C(12A)	2133(2)	-1448(2)	6108(2)	24(1)
C(13A)	1585(2)	-1268(2)	5357(2)	22(1)
C(14A)	2060(2)	-722(2)	4506(2)	19(1)
C(15A)	3065(2)	-340(2)	4385(2)	16(1)

C(16A)	2812(2)	458(2)	2649(2)	17(1)
C(17A)	1837(2)	1240(2)	2914(2)	17(1)
C(18A)	1074(2)	1378(2)	2351(2)	18(1)
C(19A)	1236(2)	733(2)	1472(2)	19(1)
C(20A)	2154(2)	-79(2)	1232(2)	20(1)
C(21A)	2897(2)	-218(2)	1815(2)	19(1)
C(22A)	492(2)	863(2)	804(2)	25(1)
C(23A)	-390(2)	1591(2)	891(2)	27(1)
C(24)	-118(2)	2965(2)	7944(2)	25(1)
C(25)	-485(2)	2043(2)	7922(2)	27(1)
C(26)	-45(2)	1375(2)	7033(2)	30(1)
C(27)	765(2)	1633(2)	6152(2)	31(1)
C(28)	1147(2)	2541(2)	6168(2)	32(1)
C(29)	714(2)	3205(2)	7060(2)	29(1)
C(30)	-611(2)	3691(2)	8915(2)	34(1)

---

**Bond Lengths [ $\text{\AA}$ ] and Angles [deg] of D45**

Fe(1)-N(2)#1	1.9707(19)	C(3)-C(4)	1.384(3)
Fe(1)-N(2)	1.9707(19)	C(4)-C(5)	1.375(3)
Fe(1)-N(3)#1	1.9929(19)	C(6)-C(7)	1.402(3)
Fe(1)-N(3)	1.9929(19)	C(7)-C(8)	1.377(4)
Fe(1)-N(1)#1	2.0030(19)	C(8)-C(9)	1.385(3)
Fe(1)-N(1)	2.0031(19)	C(9)-C(10)	1.375(3)
B(1)-C(15)	1.625(4)	C(11)-C(12)	1.372(4)
B(1)-C(16)	1.632(3)	C(12)-C(13)	1.391(4)

B(1)-C(1)	1.635(4)	C(13)-C(14)	1.377(4)
B(1)-C(6)	1.636(4)	C(14)-C(15)	1.396(3)
N(1)-C(5)	1.357(3)	C(16)-C(17)	1.396(3)
N(1)-C(1)	1.362(3)	C(16)-C(21)	1.406(3)
N(2)-C(10)	1.352(3)	C(17)-C(18)	1.392(3)
N(2)-C(6)	1.361(3)	C(18)-C(19)	1.397(4)
N(3)-C(11)	1.347(3)	C(19)-C(20)	1.391(4)
N(3)-C(15)	1.366(3)	C(19)-C(22)	1.473(3)
C(1)-C(2)	1.395(3)	C(20)-C(21)	1.384(3)
C(2)-C(3)	1.379(3)	C(22)-C(23)	1.326(5)
Fe(2)-N(6)#2	1.9793(19)	N(2)-Fe(1)-N(3)#1	89.43(8)
Fe(2)-N(6)	1.9793(19)	N(2)#1-Fe(1)-N(3)	89.43(8)
Fe(2)-N(5)	1.9927(18)	N(2)-Fe(1)-N(3)	90.56(8)
Fe(2)-N(5)#2	1.9927(18)	N(3)#1-Fe(1)-N(3)	180
Fe(2)-N(4)#2	2.0021(19)	N(2)#1-Fe(1)-N(1)#1	90.19(8)
Fe(2)-N(4)	2.0021(19)	N(2)-Fe(1)-N(1)#1	89.82(8)
B(2)-C(16A)	1.634(3)	N(3)#1-Fe(1)-N(1)#1	89.79(8)
B(2)-C(15A)	1.635(4)	N(3)-Fe(1)-N(1)#1	90.21(8)
B(2)-C(10A)	1.639(4)	N(2)#1-Fe(1)-N(1)	89.81(8)
B(2)-C(1A)	1.642(4)	N(2)-Fe(1)-N(1)	90.18(8)
N(4)-C(5A)	1.354(3)	N(3)#1-Fe(1)-N(1)	90.21(8)
N(4)-C(1A)	1.369(3)	N(3)-Fe(1)-N(1)	89.79(8)
N(5)-C(6A)	1.347(3)	N(1)#1-Fe(1)-N(1)	179.998(1)
N(5)-C(10A)	1.361(3)	C(15)-B(1)-C(16)	114.1(2)
N(6)-C(11A)	1.353(3)	C(15)-B(1)-C(1)	99.55(18)
N(6)-C(15A)	1.363(3)	C(16)-B(1)-C(1)	115.6(2)

C(1A)-C(2A)	1.397(3)	C(15)-B(1)-C(6)	110.6(2)
C(2A)-C(3A)	1.375(3)	C(16)-B(1)-C(6)	107.58(19)
C(3A)-C(4A)	1.390(3)	C(1)-B(1)-C(6)	109.22(19)
C(4A)-C(5A)	1.375(3)	C(5)-N(1)-C(1)	118.8(2)
C(6A)-C(7A)	1.378(3)	C(5)-N(1)-Fe(1)	119.88(16)
C(7A)-C(8A)	1.391(3)	C(1)-N(1)-Fe(1)	120.73(16)
C(8A)-C(9A)	1.375(3)	C(10)-N(2)-C(6)	119.7(2)
C(9A)-C(10A)	1.405(3)	C(10)-N(2)-Fe(1)	120.88(15)
C(11A)-C(12A)	1.376(3)	C(6)-N(2)-Fe(1)	119.36(16)
C(12A)-C(13A)	1.388(3)	C(11)-N(3)-C(15)	119.3(2)
C(13A)-C(14A)	1.378(3)	C(11)-N(3)-Fe(1)	119.66(15)
C(14A)-C(15A)	1.403(3)	C(15)-N(3)-Fe(1)	119.93(16)
C(16A)-C(21A)	1.400(3)	N(1)-C(1)-C(2)	119.1(2)
C(16A)-C(17A)	1.415(3)	N(1)-C(1)-B(1)	115.8(2)
C(17A)-C(18A)	1.385(3)	C(2)-C(1)-B(1)	124.7(2)
C(18A)-C(19A)	1.398(3)	C(3)-C(2)-C(1)	121.2(2)
C(19A)-C(20A)	1.394(3)	C(2)-C(3)-C(4)	119.0(2)
C(19A)-C(22A)	1.477(3)	C(5)-C(4)-C(3)	118.0(2)
C(20A)-C(21A)	1.386(3)	N(1)-C(5)-C(4)	123.4(2)
C(22A)-C(23A)	1.318(4)	N(2)-C(6)-C(7)	118.4(2)
C(24)-C(25)	1.387(4)	N(2)-C(6)-B(1)	118.3(2)
C(24)-C(29)	1.388(4)	C(7)-C(6)-B(1)	123.3(2)
C(24)-C(30)	1.514(4)	C(8)-C(7)-C(6)	121.7(2)
C(25)-C(26)	1.389(4)	C(7)-C(8)-C(9)	118.6(2)
C(26)-C(27)	1.380(4)	C(10)-C(9)-C(8)	118.4(2)
C(27)-C(28)	1.378(4)	N(2)-C(10)-C(9)	123.1(2)

C(28)-C(29)	1.388(4)	N(3)-C(11)-C(12)	123.4(2)
N(2)#1-Fe(1)-N(2)	179.997(1)	C(11)-C(12)-C(13)	118.4(2)
N(2)#1-Fe(1)-N(3)#1	90.57(8)	C(14)-C(13)-C(12)	118.2(2)
C(13)-C(14)-C(15)	122.0(2)	C(11A)-N(6)-Fe(2)	120.90(15)
N(3)-C(15)-C(14)	118.3(2)	C(15A)-N(6)-Fe(2)	119.74(16)
N(3)-C(15)-B(1)	116.3(2)	N(4)-C(1A)-C(2A)	118.3(2)
C(14)-C(15)-B(1)	125.0(2)	N(4)-C(1A)-B(2)	115.2(2)
C(17)-C(16)-C(21)	114.8(2)	C(2A)-C(1A)-B(2)	126.3(2)
C(17)-C(16)-B(1)	123.2(2)	C(3A)-C(2A)-C(1A)	122.5(2)
C(21)-C(16)-B(1)	121.3(2)	C(2A)-C(3A)-C(4A)	118.2(2)
C(18)-C(17)-C(16)	123.1(2)	C(5A)-C(4A)-C(3A)	118.1(2)
C(17)-C(18)-C(19)	120.7(3)	N(4)-C(5A)-C(4A)	123.8(2)
C(20)-C(19)-C(18)	117.2(2)	N(5)-C(6A)-C(7A)	123.8(2)
C(20)-C(19)-C(22)	122.0(3)	C(6A)-C(7A)-C(8A)	117.8(2)
C(18)-C(19)-C(22)	120.9(3)	C(9A)-C(8A)-C(7A)	118.6(2)
C(21)-C(20)-C(19)	121.3(2)	C(8A)-C(9A)-C(10A)	121.6(2)
C(20)-C(21)-C(16)	122.7(2)	N(5)-C(10A)-C(9A)	118.6(2)
C(23)-C(22)-C(19)	124.6(3)	N(5)-C(10A)-B(2)	116.93(19)
N(6)#2-Fe(2)-N(6)	180.000(1)	C(9A)-C(10A)-B(2)	124.4(2)
N(6)#2-Fe(2)-N(5)	89.90(8)	N(6)-C(11A)-C(12A)	123.6(2)
N(6)-Fe(2)-N(5)	90.10(8)	C(11A)-C(12A)-C(13A)	118.3(2)
N(6)#2-Fe(2)-N(5)#2	90.10(8)	C(14A)-C(13A)-C(12A)	118.2(2)
N(6)-Fe(2)-N(5)#2	89.90(8)	C(13A)-C(14A)-C(15A)	122.2(2)
N(5)-Fe(2)-N(5)#2	180	N(6)-C(15A)-C(14A)	118.3(2)
N(6)#2-Fe(2)-N(4)#2	89.42(8)	N(6)-C(15A)-B(2)	118.7(2)
N(6)-Fe(2)-N(4)#2	90.58(8)	C(14A)-C(15A)-B(2)	123.0(2)

N(5)-Fe(2)-N(4)#2	90.64(8)	C(21A)-C(16A)-C(17A)	114.3(2)
N(5)#2-Fe(2)-N(4)#2	89.36(8)	C(21A)-C(16A)-B(2)	124.6(2)
N(6)#2-Fe(2)-N(4)	90.58(8)	C(17A)-C(16A)-B(2)	120.6(2)
N(6)-Fe(2)-N(4)	89.42(8)	C(18A)-C(17A)-C(16A)	123.2(2)
N(5)-Fe(2)-N(4)	89.36(8)	C(17A)-C(18A)-C(19A)	120.7(2)
N(5)#2-Fe(2)-N(4)	90.64(8)	C(20A)-C(19A)-C(18A)	117.0(2)
N(4)#2-Fe(2)-N(4)	180	C(20A)-C(19A)-C(22A)	119.2(2)
C(16A)-B(2)-C(15A)	107.82(19)	C(18A)-C(19A)-C(22A)	123.8(2)
C(16A)-B(2)-C(10A)	113.35(19)	C(21A)-C(20A)-C(19A)	121.5(2)
C(15A)-B(2)-C(10A)	109.15(19)	C(20A)-C(21A)-C(16A)	122.9(2)
C(16A)-B(2)-C(1A)	117.0(2)	C(23A)-C(22A)-C(19A)	127.8(2)
C(15A)-B(2)-C(1A)	107.48(18)	C(25)-C(24)-C(29)	118.5(2)
C(10A)-B(2)-C(1A)	101.72(19)	C(25)-C(24)-C(30)	120.7(3)
C(5A)-N(4)-C(1A)	119.0(2)	C(29)-C(24)-C(30)	120.8(2)
C(5A)-N(4)-Fe(2)	118.67(15)	C(24)-C(25)-C(26)	121.2(3)
C(1A)-N(4)-Fe(2)	122.15(16)	C(27)-C(26)-C(25)	119.7(3)
C(6A)-N(5)-C(10A)	119.19(19)	C(28)-C(27)-C(26)	119.7(3)
C(6A)-N(5)-Fe(2)	119.65(15)	C(27)-C(28)-C(29)	120.6(3)
C(10A)-N(5)-Fe(2)	120.64(15)	C(28)-C(29)-C(24)	120.3(3)
C(11A)-N(6)-C(15A)	119.4(2)		

---

Symmetry transformations used to generate equivalent atoms: #1  $-x+1,-y+1,-z$ ; #2  $-x+1,-y,-z+1$

#### Anisotropic Displacement Parameters ( $\text{\AA}^2 \times 10^3$ ) of D45

---

	U11	U22	U33	U23	U13	U12
Fe(1)	15(1)	16(1)	17(1)	1(1)	-7(1)	-1(1)

---

B(1)	17(1)	19(1)	20(2)	0(1)	-7(1)	-1(1)
N(1)	19(1)	17(1)	17(1)	1(1)	-5(1)	-1(1)
N(2)	16(1)	17(1)	18(1)	1(1)	-6(1)	-1(1)
N(3)	14(1)	17(1)	20(1)	2(1)	-6(1)	-1(1)
C(1)	18(1)	18(1)	21(1)	5(1)	-9(1)	-4(1)
C(2)	26(1)	21(1)	25(1)	-1(1)	-13(1)	0(1)
C(3)	31(2)	25(1)	24(1)	-5(1)	-11(1)	3(1)
C(4)	23(1)	27(1)	26(2)	-1(1)	-8(1)	6(1)
C(5)	18(1)	26(1)	23(1)	1(1)	-9(1)	2(1)
C(6)	13(1)	22(1)	17(1)	1(1)	-4(1)	0(1)
C(7)	21(1)	23(1)	22(1)	2(1)	-10(1)	-1(1)
C(8)	25(1)	20(1)	23(1)	3(1)	-8(1)	1(1)
C(9)	23(1)	19(1)	24(1)	0(1)	-7(1)	-4(1)
C(10)	19(1)	21(1)	21(1)	0(1)	-7(1)	-3(1)
C(11)	20(1)	24(1)	22(1)	6(1)	-8(1)	-1(1)
C(12)	24(1)	29(2)	27(2)	12(1)	-8(1)	-6(1)
C(13)	20(1)	24(1)	38(2)	6(1)	-14(1)	-6(1)
C(14)	20(1)	21(1)	27(2)	2(1)	-11(1)	-3(1)
C(15)	16(1)	16(1)	22(1)	-2(1)	-8(1)	2(1)
C(16)	20(1)	14(1)	24(1)	1(1)	-11(1)	-2(1)
C(17)	24(1)	20(1)	26(2)	2(1)	-10(1)	0(1)
C(18)	40(2)	19(1)	23(1)	4(1)	-13(1)	-1(1)
C(19)	38(2)	14(1)	36(2)	3(1)	-24(1)	-1(1)
C(20)	23(1)	18(1)	34(2)	2(1)	-14(1)	-1(1)
C(21)	22(1)	19(1)	26(1)	1(1)	-11(1)	-2(1)
C(22)	49(2)	30(2)	45(2)	5(1)	-34(2)	-1(1)

C(23)	70(3)	60(2)	68(3)	-3(2)	-47(2)	3(2)
Fe(2)	15(1)	15(1)	16(1)	2(1)	-8(1)	0(1)
B(2)	19(2)	17(1)	17(2)	-1(1)	-7(1)	-1(1)
N(4)	18(1)	16(1)	16(1)	2(1)	-6(1)	-1(1)
N(5)	17(1)	15(1)	18(1)	1(1)	-7(1)	-2(1)
N(6)	14(1)	17(1)	17(1)	0(1)	-6(1)	1(1)
C(1A)	19(1)	12(1)	21(1)	3(1)	-9(1)	-3(1)
C(2A)	22(1)	19(1)	20(1)	5(1)	-10(1)	-4(1)
C(3A)	24(1)	23(1)	16(1)	0(1)	-4(1)	-2(1)
C(4A)	19(1)	23(1)	26(2)	1(1)	-6(1)	2(1)
C(5A)	19(1)	21(1)	22(1)	1(1)	-10(1)	2(1)
C(6A)	19(1)	24(1)	19(1)	1(1)	-9(1)	-4(1)
C(7A)	27(1)	18(1)	24(1)	-1(1)	-11(1)	-3(1)
C(8A)	25(1)	20(1)	24(1)	7(1)	-10(1)	-3(1)
C(9A)	19(1)	22(1)	18(1)	4(1)	-8(1)	-2(1)
C(10A)	13(1)	20(1)	17(1)	1(1)	-5(1)	0(1)
C(11A)	21(1)	20(1)	20(1)	3(1)	-8(1)	-1(1)
C(12A)	24(1)	24(1)	22(1)	4(1)	-5(1)	-4(1)
C(13A)	19(1)	20(1)	26(1)	1(1)	-7(1)	-3(1)
C(14A)	19(1)	16(1)	21(1)	0(1)	-9(1)	2(1)
C(15A)	16(1)	13(1)	18(1)	-3(1)	-6(1)	3(1)
C(16A)	19(1)	16(1)	18(1)	5(1)	-7(1)	-3(1)
C(17A)	18(1)	17(1)	17(1)	0(1)	-6(1)	-3(1)
C(18A)	16(1)	17(1)	22(1)	4(1)	-6(1)	-2(1)
C(19A)	19(1)	21(1)	21(1)	5(1)	-9(1)	-7(1)
C(20A)	21(1)	19(1)	22(1)	-1(1)	-7(1)	-4(1)

C(21A)	17(1)	17(1)	22(1)	3(1)	-7(1)	-1(1)
C(22A)	26(1)	26(1)	25(1)	-1(1)	-12(1)	-6(1)
C(23A)	27(2)	31(2)	30(2)	3(1)	-18(1)	-5(1)
C(24)	22(1)	25(1)	30(2)	0(1)	-15(1)	3(1)
C(25)	23(1)	32(2)	30(2)	8(1)	-13(1)	-4(1)
C(26)	31(2)	22(1)	42(2)	0(1)	-20(1)	-3(1)
C(27)	26(2)	32(2)	32(2)	-5(1)	-13(1)	9(1)
C(28)	26(2)	29(2)	35(2)	5(1)	-6(1)	2(1)
C(29)	28(2)	21(1)	41(2)	6(1)	-15(1)	-3(1)
C(30)	31(2)	37(2)	37(2)	-3(1)	-14(1)	-3(1)

---

**Appendix A.5** The following tables are supplementary materials for the X-ray crystal structure of compound D43 and D47. The data of fractional atomic coordinates and equivalent isotropic displacement parameters, anisotropic displacement parameters, bond lengths and bond angles are listed.

#### **Crystal Data and Structure Refinement Details for D47 and D43**

	<b>D47</b>	<b>D43</b>
Empirical formula	C <sub>50</sub> H <sub>50</sub> B <sub>2</sub> Cl <sub>4</sub> Fe <sub>2</sub> N <sub>6</sub>	C <sub>28</sub> H <sub>29</sub> B N <sub>2</sub>
$M_r$	1010.08	404.34
T, K	100(2)	100(2)
Wavelength, Å	1.54178	1.54178
Crystal system	Orthorhombic	Triclinic
Space group	P n a 21	P-1

$a$ , Å	27.5963(5)	9.4444(1)
$b$ , Å	12.7473(2)	11.5792(2)
$c$ , Å	13.6801(2)	11.6666(2)
$\alpha$ , °	90	103.667(1)
$\beta$ , °	90	107.340(1)
$\gamma$ , °	90	94.247(1)
$V$ , Å <sup>3</sup>	4812.36(14)	1168.93(3)
$Z$	4	2
$\rho_{\text{calc}}$ , g/cm <sup>-3</sup>	1.394	1.149
$\mu(\text{CuK}\alpha)$ , mm <sup>-1</sup>	7.199	0.500
F(000)	2088	432
Crystal size, mm <sup>3</sup>	0.24 x 0.16 x 0.13	0.17 x 0.14 x 0.10
$\theta$ range, °	3.20 to 67.54°	3.98 to 67.28°
Index ranges	-31 ≤ $h$ ≤ 32 -12 ≤ $k$ ≤ 14 -16 ≤ $l$ ≤ 16	-10 ≤ $h$ ≤ 10 -13 ≤ $k$ ≤ 13, -13 ≤ $l$ ≤ 13
Reflections collected	41914	9884
Independent reflections	8158 [R(int) = 0.0606]	3839 [R(int) = 0.0770]
Absorption correction	Numerical	Numerical
Refinement method	Full-matrix least-squares on $F^2$	Full-matrix least-squares on $F^2$
Data / restraints / parameters	8158 / 1 / 585	3839 / 0 / 294
Goodness-of-fit on $F^2$	1.022	1.073
Final R indices [ $I > 2\sigma(I)$ ] <sup>[a]</sup>	R1 = 0.0370, wR2 = 0.0808	R1 = 0.0469, wR2 = 0.1223
R indices (all data) <sup>[a]</sup>	R1 = 0.0451, wR2 = 0.0844	R1 = 0.0609, wR2 = 0.1303
Peak/hole (eÅ <sup>-3</sup> )	0.509 and -0.271	0.423 and -0.341

**Fractional Atomic Coordinates ( $\times 10^4$ ) and Equivalent Isotropic Displacement**

**Parameters ( $\text{\AA}^2 \times 10^3$ ) of D47 where  $U(\text{eq}) = (1/3) \sum_j U^{jj} a_j a_j a_j$**

	<b>x</b>	<b>y</b>	<b>z</b>	<b>U(eq)</b>
Fe(1)	8799(1)	7306(1)	6177(1)	15(1)
B(1)	9270(1)	6916(3)	4131(3)	17(1)
B(2)	8323(1)	7752(3)	8213(3)	18(1)
N(1)	8570(1)	6265(2)	5190(2)	16(1)
N(2)	8863(1)	8382(2)	5155(2)	17(1)
N(3)	9475(1)	6820(2)	5953(2)	17(1)
N(4)	9036(1)	8348(2)	7171(2)	18(1)
N(5)	8725(1)	6238(2)	7228(2)	16(1)
N(6)	8120(1)	7778(2)	6392(2)	16(1)
C(1)	8830(1)	6092(3)	4360(2)	17(1)
C(2)	8728(1)	5179(3)	3825(3)	19(1)
C(3)	8359(1)	4516(3)	4096(2)	20(1)
C(4)	8072(1)	4763(3)	4890(2)	20(1)
C(5)	8191(1)	5640(3)	5423(2)	18(1)
C(6)	9053(1)	8098(3)	4282(2)	18(1)
C(7)	9043(1)	8847(3)	3531(3)	25(1)
C(8)	8855(1)	9829(3)	3673(3)	30(1)
C(9)	8674(1)	10098(3)	4592(3)	26(1)
C(10)	8689(1)	9360(3)	5303(3)	22(1)
C(11)	9633(1)	6623(2)	5032(2)	15(1)
C(12)	10077(1)	6097(3)	4921(2)	20(1)
C(13)	10346(1)	5802(3)	5717(3)	24(1)

C(14)	10185(1)	6058(3)	6647(3)	24(1)
C(15)	9751(1)	6556(3)	6732(3)	20(1)
C(16)	9514(1)	6869(3)	3061(2)	19(1)
C(17)	9261(1)	6665(3)	2203(3)	21(1)
C(18)	9456(1)	6822(2)	1276(3)	21(1)
C(19)	9923(1)	7218(2)	1150(3)	20(1)
C(20)	10178(1)	7457(3)	2002(3)	19(1)
C(21)	9978(1)	7296(3)	2923(3)	21(1)
C(22)	10151(1)	7436(3)	154(3)	23(1)
C(23)	9826(2)	7079(3)	-690(3)	39(1)
C(24)	10240(2)	8608(3)	43(3)	35(1)
C(25)	10633(1)	6849(3)	76(3)	38(1)
C(1A)	8779(1)	8539(3)	7997(2)	17(1)
C(2A)	8894(1)	9421(3)	8555(3)	22(1)
C(3A)	9294(1)	10032(3)	8333(3)	25(1)
C(4A)	9576(1)	9766(3)	7533(2)	21(1)
C(5A)	9433(1)	8935(3)	6964(2)	19(1)
C(6A)	8529(1)	6556(3)	8090(2)	17(1)
C(7A)	8525(1)	5814(3)	8854(2)	21(1)
C(8A)	8708(1)	4829(3)	8741(3)	23(1)
C(9A)	8898(1)	4534(3)	7841(3)	23(1)
C(10A)	8893(1)	5264(3)	7101(3)	19(1)
C(11A)	7969(1)	8034(2)	7304(2)	17(1)
C(12A)	7541(1)	8609(2)	7402(3)	21(1)
C(13A)	7260(1)	8853(3)	6598(3)	23(1)
C(14A)	7404(1)	8519(3)	5680(3)	22(1)

C(15A)	7839(1)	7996(3)	5603(2)	19(1)
C(16A)	8060(1)	7799(3)	9273(2)	19(1)
C(17A)	7600(1)	7346(3)	9393(3)	20(1)
C(18A)	7385(1)	7198(3)	10302(3)	22(1)
C(19A)	7619(1)	7496(2)	11156(3)	21(1)
C(20A)	8075(1)	7934(2)	11056(3)	21(1)
C(21A)	8290(1)	8070(3)	10152(2)	21(1)
C(22A)	7386(1)	7364(3)	12178(3)	23(1)
C(23A)	6897(2)	6810(4)	12128(3)	45(1)
C(24A)	7721(2)	6721(3)	12838(3)	34(1)
C(25A)	7321(2)	8460(3)	12634(3)	35(1)
Fe(2)	6310(1)	6461(1)	6166(1)	21(1)
Cl(1)	6167(1)	7542(1)	7388(1)	32(1)
Cl(2)	7020(1)	5767(1)	6437(1)	46(1)
Cl(3)	6286(1)	7254(1)	4743(1)	38(1)
Cl(4)	5754(1)	5232(1)	6151(1)	33(1)

**Bond Lengths [Å] and Angles [deg] of D47**

Fe(1)-N(2)	1.965(3)	C(16)-C(21)	1.403(5)
Fe(1)-N(3)	1.990(3)	C(17)-C(18)	1.393(5)
Fe(1)-N(5)	1.991(3)	C(18)-C(19)	1.393(4)
Fe(1)-N(1)	1.996(3)	C(19)-C(20)	1.395(5)
Fe(1)-N(4)	2.011(3)	C(19)-C(22)	1.527(5)
Fe(1)-N(6)	1.990(2)	C(20)-C(21)	1.392(5)
B(1)-C(16)	1.613(5)	C(22)-C(24)	1.521(5)
B(1)-C(11)	1.632(5)	C(22)-C(25)	1.530(5)

B(1)-C(6)	1.633(5)	C(1A)-C(2A)	1.395(5)
B(1)-C(1)	1.636(5)	C(2A)-C(3A)	1.385(5)
B(2)-C(16A)	1.621(5)	C(3A)-C(4A)	1.385(5)
B(2)-C(11A)	1.622(5)	C(4A)-C(5A)	1.373(5)
B(2)-C(6A)	1.635(5)	C(6A)-C(7A)	1.410(5)
B(2)-C(1A)	1.637(5)	C(7A)-C(8A)	1.361(5)
N(1)-C(5)	1.351(4)	C(8A)-C(9A)	1.391(5)
N(1)-C(1)	1.361(4)	C(9A)-C(10A)	1.375(5)
N(2)-C(10)	1.351(4)	C(11A)-C(12A)	1.397(4)
N(2)-C(6)	1.354(4)	C(12A)-C(13A)	1.381(5)
N(3)-C(15)	1.353(4)	C(13A)-C(14A)	1.385(5)
N(3)-C(11)	1.357(4)	C(14A)-C(15A)	1.377(5)
N(4)-C(5A)	1.355(4)	C(16A)-C(21A)	1.404(5)
N(4)-C(1A)	1.356(4)	C(16A)-C(17A)	1.405(4)
N(5)-C(10A)	1.337(4)	C(17A)-C(18A)	1.389(5)
N(5)-C(6A)	1.360(4)	C(18A)-C(19A)	1.388(5)
N(6)-C(11A)	1.355(4)	C(19A)-C(20A)	1.384(4)
N(6)-C(15A)	1.356(4)	C(19A)-C(22A)	1.547(5)
C(1)-C(2)	1.404(5)	C(20A)-C(21A)	1.381(5)
C(2)-C(3)	1.375(5)	C(22A)-C(23A)	1.524(5)
C(3)-C(4)	1.381(5)	C(22A)-C(24A)	1.531(5)
C(4)-C(5)	1.375(5)	C(22A)-C(25A)	1.541(5)
C(6)-C(7)	1.404(5)	Fe(2)-Cl(2)	2.1804(10)
C(7)-C(8)	1.369(5)	Fe(2)-Cl(3)	2.1941(12)
C(8)-C(9)	1.395(5)	Fe(2)-Cl(4)	2.1943(9)
C(9)-C(10)	1.354(5)	Fe(2)-Cl(1)	2.2018(11)

C(11)-C(12)	1.406(5)	N(2)-Fe(1)-N(6)	88.80(11)
C(12)-C(13)	1.370(5)	N(2)-Fe(1)-N(3)	91.35(11)
C(13)-C(14)	1.388(5)	N(6)-Fe(1)-N(3)	179.32(11)
C(14)-C(15)	1.360(5)	N(2)-Fe(1)-N(5)	178.81(13)
C(16)-C(17)	1.390(5)	N(6)-Fe(1)-N(5)	90.25(10)
N(3)-Fe(1)-N(5)	89.60(11)	C(5)-C(4)-C(3)	117.7(3)
N(2)-Fe(1)-N(1)	90.65(12)	N(1)-C(5)-C(4)	122.7(3)
N(6)-Fe(1)-N(1)	90.16(11)	N(2)-C(6)-C(7)	117.1(3)
N(3)-Fe(1)-N(1)	89.18(11)	N(2)-C(6)-B(1)	120.0(3)
N(5)-Fe(1)-N(1)	90.07(11)	C(7)-C(6)-B(1)	122.8(3)
N(2)-Fe(1)-N(4)	89.49(11)	C(8)-C(7)-C(6)	121.7(3)
N(6)-Fe(1)-N(4)	90.44(11)	C(7)-C(8)-C(9)	119.2(3)
N(3)-Fe(1)-N(4)	90.23(11)	C(10)-C(9)-C(8)	117.7(3)
N(5)-Fe(1)-N(4)	89.80(12)	N(2)-C(10)-C(9)	123.0(3)
N(1)-Fe(1)-N(4)	179.40(12)	N(3)-C(11)-C(12)	117.9(3)
C(16)-B(1)-C(11)	114.8(3)	N(3)-C(11)-B(1)	117.5(3)
C(16)-B(1)-C(6)	107.6(3)	C(12)-C(11)-B(1)	124.3(3)
C(16)-B(1)-C(1)	117.4(3)	C(13)-C(12)-C(11)	121.2(3)
C(11)-B(1)-C(6)	109.9(3)	C(12)-C(13)-C(14)	119.3(3)
C(11)-B(1)-C(1)	99.4(3)	C(15)-C(14)-C(13)	118.1(3)
C(6)-B(1)-C(1)	107.3(3)	N(3)-C(15)-C(14)	123.1(3)
C(16A)-B(2)-C(11A)	114.1(3)	C(17)-C(16)-C(21)	114.6(3)
C(16A)-B(2)-C(6A)	106.4(3)	C(17)-C(16)-B(1)	124.3(3)
C(11A)-B(2)-C(6A)	109.7(3)	C(21)-C(16)-B(1)	119.3(3)
C(16A)-B(2)-C(1A)	118.8(3)	C(16)-C(17)-C(18)	123.2(3)
C(11A)-B(2)-C(1A)	100.8(3)	C(19)-C(18)-C(17)	121.4(3)

C(6A)-B(2)-C(1A)	106.6(3)	C(18)-C(19)-C(20)	116.3(4)
C(5)-N(1)-C(1)	120.6(3)	C(18)-C(19)-C(22)	123.9(3)
C(5)-N(1)-Fe(1)	118.5(2)	C(20)-C(19)-C(22)	119.8(3)
C(1)-N(1)-Fe(1)	120.3(2)	C(21)-C(20)-C(19)	121.5(3)
C(10)-N(2)-C(6)	121.1(3)	C(20)-C(21)-C(16)	122.8(3)
C(10)-N(2)-Fe(1)	120.4(2)	C(24)-C(22)-C(19)	109.6(3)
C(6)-N(2)-Fe(1)	118.4(2)	C(24)-C(22)-C(25)	109.4(3)
C(15)-N(3)-C(11)	120.3(3)	C(19)-C(22)-C(25)	109.4(3)
C(15)-N(3)-Fe(1)	119.0(2)	C(24)-C(22)-C(23)	108.2(3)
C(11)-N(3)-Fe(1)	120.1(2)	C(19)-C(22)-C(23)	112.2(3)
C(5A)-N(4)-C(1A)	119.9(3)	C(25)-C(22)-C(23)	108.1(3)
C(5A)-N(4)-Fe(1)	119.1(2)	N(4)-C(1A)-C(2A)	118.7(3)
C(1A)-N(4)-Fe(1)	120.7(2)	N(4)-C(1A)-B(2)	116.3(3)
C(10A)-N(5)-C(6A)	121.9(3)	C(2A)-C(1A)-B(2)	124.8(3)
C(10A)-N(5)-Fe(1)	120.4(2)	C(3A)-C(2A)-C(1A)	121.0(3)
C(6A)-N(5)-Fe(1)	117.5(2)	C(4A)-C(3A)-C(2A)	118.9(3)
C(11A)-N(6)-C(15A)	120.5(3)	C(5A)-C(4A)-C(3A)	118.4(3)
C(11A)-N(6)-Fe(1)	119.9(2)	N(4)-C(5A)-C(4A)	122.7(3)
C(15A)-N(6)-Fe(1)	118.8(2)	N(5)-C(6A)-C(7A)	116.5(3)
N(1)-C(1)-C(2)	117.7(3)	N(5)-C(6A)-B(2)	120.4(3)
N(1)-C(1)-B(1)	116.5(3)	C(7A)-C(6A)-B(2)	123.1(3)
C(2)-C(1)-B(1)	125.5(3)	C(8A)-C(7A)-C(6A)	122.1(3)
C(3)-C(2)-C(1)	121.1(3)	C(7A)-C(8A)-C(9A)	119.3(3)
C(2)-C(3)-C(4)	119.8(3)	C(10A)-C(9A)-C(8A)	117.7(3)
N(5)-C(10A)-C(9A)	122.4(3)	C(24A)-C(22A)-C(25A)	108.5(3)
N(6)-C(11A)-C(12A)	118.3(3)	C(23A)-C(22A)-C(19A)	112.2(3)

N(6)-C(11A)-B(2)	117.9(3)	C(21A)-C(16A)-C(17A)	114.1(3)
C(12A)-C(11A)-B(2)	123.5(3)	C(21A)-C(16A)-B(2)	125.0(3)
C(13A)-C(12A)-C(11A)	121.1(3)	C(17A)-C(16A)-B(2)	119.6(3)
C(12A)-C(13A)-C(14A)	119.4(3)	C(18A)-C(17A)-C(16A)	123.1(3)
C(15A)-C(14A)-C(13A)	117.9(3)	C(19A)-C(18A)-C(17A)	121.2(3)
N(6)-C(15A)-C(14A)	122.4(3)	C(24A)-C(22A)-C(19A)	109.9(3)
C(20A)-C(19A)-C(18A)	116.7(4)	C(25A)-C(22A)-C(19A)	108.4(3)
C(20A)-C(19A)-C(22A)	120.7(3)	Cl(2)-Fe(2)-Cl(3)	111.42(5)
C(18A)-C(19A)-C(22A)	122.6(3)	Cl(2)-Fe(2)-Cl(4)	109.86(4)
C(21A)-C(20A)-C(19A)	122.0(3)	Cl(3)-Fe(2)-Cl(4)	107.46(5)
C(20A)-C(21A)-C(16A)	122.8(3)	Cl(2)-Fe(2)-Cl(1)	106.59(5)
C(23A)-C(22A)-C(24A)	108.3(3)	Cl(3)-Fe(2)-Cl(1)	112.33(5)
C(23A)-C(22A)-C(25A)	109.5(3)	Cl(4)-Fe(2)-Cl(1)	109.18(4)

#### Anisotropic Displacement Parameters ( $\text{\AA}^2 \times 10^3$ ) of D47

	U11	U22	U33	U23	U13	U12
Fe(1)	16(1)	16(1)	12(1)	-1(1)	1(1)	0(1)
B(1)	19(2)	20(2)	13(2)	-1(2)	0(2)	-1(2)
B(2)	20(2)	20(2)	13(2)	-1(2)	-1(2)	3(2)
N(1)	17(2)	17(2)	15(2)	-5(1)	0(1)	4(1)
N(2)	20(2)	16(2)	16(2)	0(1)	0(1)	0(1)
N(3)	17(1)	21(2)	12(2)	0(1)	0(1)	-1(1)
N(4)	17(2)	24(2)	13(2)	-6(1)	-1(1)	1(1)
N(5)	13(2)	17(2)	17(2)	2(1)	-1(1)	-1(1)
N(6)	17(1)	17(2)	14(2)	1(1)	1(1)	-1(1)

C(1)	14(2)	22(2)	15(2)	-1(1)	-2(1)	3(1)
C(2)	18(2)	26(2)	14(2)	-1(1)	1(1)	5(1)
C(3)	23(2)	16(2)	19(2)	-2(1)	-7(2)	0(1)
C(4)	20(2)	24(2)	17(2)	-1(1)	-1(1)	-2(1)
C(5)	14(2)	26(2)	15(2)	2(1)	2(1)	-1(1)
C(6)	15(2)	21(2)	16(2)	2(1)	-1(1)	-2(1)
C(7)	29(2)	33(2)	14(2)	1(2)	4(2)	5(2)
C(8)	39(2)	22(2)	29(2)	7(2)	2(2)	6(2)
C(9)	28(2)	22(2)	29(2)	1(2)	1(2)	4(2)
C(10)	19(2)	24(2)	23(2)	-4(1)	4(2)	2(1)
C(11)	16(2)	17(2)	13(2)	1(1)	1(1)	-4(1)
C(12)	23(2)	22(2)	15(2)	-1(1)	6(1)	0(1)
C(13)	23(2)	25(2)	26(2)	3(2)	2(2)	2(1)
C(14)	23(2)	30(2)	17(2)	4(2)	-5(2)	-1(2)
C(15)	26(2)	21(2)	12(2)	-1(1)	-1(2)	-1(1)
C(16)	18(2)	20(2)	18(2)	-3(1)	2(1)	3(1)
C(17)	19(2)	22(2)	22(2)	-3(1)	-1(2)	1(1)
C(18)	23(2)	24(2)	16(2)	-1(2)	0(2)	1(1)
C(19)	25(2)	18(2)	17(2)	-1(2)	0(2)	6(1)
C(20)	21(2)	17(2)	21(2)	1(1)	3(2)	0(1)
C(21)	26(2)	22(2)	17(2)	-3(1)	-3(2)	1(1)
C(22)	27(2)	24(2)	17(2)	0(2)	6(2)	0(2)
C(23)	55(3)	52(3)	11(2)	3(2)	2(2)	-11(2)
C(24)	52(3)	34(2)	20(2)	6(2)	10(2)	-1(2)
C(25)	42(3)	49(3)	23(2)	10(2)	14(2)	18(2)
C(1A)	18(2)	17(2)	15(2)	2(1)	-1(1)	1(1)

C(2A)	25(2)	23(2)	16(2)	0(2)	5(2)	-1(2)
C(3A)	34(2)	22(2)	18(2)	-7(1)	-1(2)	-4(2)
C(4A)	20(2)	22(2)	21(2)	2(1)	1(2)	-5(1)
C(5A)	18(2)	23(2)	16(2)	1(1)	6(1)	-2(1)
C(6A)	16(2)	23(2)	14(2)	-3(1)	-2(1)	-5(1)
C(7A)	22(2)	24(2)	16(2)	1(1)	1(2)	-1(1)
C(8A)	29(2)	22(2)	17(2)	8(2)	-5(2)	-1(2)
C(9A)	22(2)	19(2)	28(2)	1(2)	-3(2)	0(1)
C(10A)	20(2)	18(2)	19(2)	-5(1)	-1(2)	0(1)
C(11A)	19(2)	18(2)	14(2)	1(1)	4(2)	-2(1)
C(12A)	23(2)	20(2)	20(2)	-5(2)	2(2)	-1(1)
C(13A)	20(2)	20(2)	30(2)	0(2)	4(2)	4(1)
C(14A)	17(2)	29(2)	21(2)	6(2)	-4(2)	2(1)
C(15A)	26(2)	19(2)	12(2)	1(1)	0(2)	-1(1)
C(16A)	17(2)	23(2)	15(2)	-1(1)	3(1)	3(1)
C(17A)	23(2)	18(2)	18(2)	-3(1)	-2(2)	0(1)
C(18A)	22(2)	25(2)	19(2)	2(1)	2(2)	-1(1)
C(19A)	24(2)	21(2)	17(2)	-2(2)	4(2)	4(1)
C(20A)	26(2)	22(2)	15(2)	-2(1)	0(2)	3(1)
C(21A)	24(2)	21(2)	19(2)	-2(1)	4(2)	-3(1)
C(22A)	24(2)	31(2)	14(2)	2(2)	3(2)	0(2)
C(23A)	39(3)	70(3)	24(2)	6(2)	9(2)	-15(2)
C(24A)	47(3)	31(2)	22(2)	5(2)	1(2)	5(2)
C(25A)	46(3)	41(3)	18(2)	2(2)	13(2)	13(2)
Fe(2)	25(1)	18(1)	21(1)	-1(1)	4(1)	0(1)
Cl(1)	38(1)	32(1)	27(1)	-12(1)	-1(1)	3(1)

Cl(2)	27(1)	32(1)	79(1)	11(1)	13(1)	7(1)
Cl(3)	62(1)	28(1)	23(1)	4(1)	4(1)	-11(1)
Cl(4)	38(1)	36(1)	24(1)	-1(1)	3(1)	-16(1)

**Fractional Atomic Coordinates ( $\times 10^4$ ) and Equivalent Isotropic Displacement**

**Parameters ( $\text{\AA}^2 \times 10^3$ ) of D43 where  $U(\text{eq}) = (1/3) \sum_j U^{jj} a_j a_j a_j$**

	x	y	z	U(eq)
B(1)	4170(2)	7622(2)	6053(2)	22(1)
N(1)	4285(2)	5526(1)	6437(1)	23(1)
N(2)	6759(2)	6913(1)	6693(1)	26(1)
C(1)	3449(2)	6412(1)	6301(1)	20(1)
C(2)	1980(2)	6157(2)	6284(2)	23(1)
C(3)	1426(2)	5056(2)	6378(2)	26(1)
C(4)	2342(2)	4184(2)	6503(2)	28(1)
C(5)	3794(2)	4446(2)	6541(2)	28(1)
C(6)	6008(2)	7867(2)	6655(2)	22(1)
C(7)	6840(2)	9019(2)	7026(2)	31(1)
C(8)	8387(2)	9194(2)	7393(2)	37(1)
C(9)	9125(2)	8211(2)	7409(2)	34(1)
C(10)	8269(2)	7097(2)	7071(2)	32(1)
C(11)	3774(2)	7369(1)	4536(2)	21(1)
C(12)	2772(2)	6394(2)	3654(2)	27(1)
C(13)	2478(2)	6202(2)	2377(2)	33(1)
C(14)	3191(2)	6974(2)	1898(2)	27(1)
C(15)	4205(2)	7951(2)	2771(2)	25(1)

C(16)	4476(2)	8140(2)	4036(2)	25(1)
C(17)	2933(2)	6797(2)	504(2)	35(1)
C(18)	4412(2)	6661(2)	244(2)	38(1)
C(19)	1765(3)	5717(2)	-284(2)	75(1)
C(20)	2408(3)	7933(2)	141(2)	55(1)
C(21)	3446(2)	8760(1)	6642(2)	22(1)
C(22)	2482(2)	9385(2)	5942(2)	26(1)
C(23)	1864(2)	10334(2)	6489(2)	30(1)
C(24)	2180(2)	10708(2)	7776(2)	29(1)
C(25)	3142(2)	10098(2)	8488(2)	28(1)
C(26)	3753(2)	9160(2)	7936(2)	25(1)
C(27)	1516(2)	11708(2)	8355(2)	38(1)
C(28)	1717(4)	12155(3)	9566(4)	53(1)
C(28A)	468(6)	12245(5)	7788(6)	40(2)

---

**Bond Lengths [Å] and Angles [deg] of D43**

B(1)-C(21)	1.631(2)	C(6)-C(7)	1.397(2)
B(1)-C(1)	1.636(2)	C(7)-C(8)	1.378(2)
B(1)-C(6)	1.641(2)	C(8)-C(9)	1.379(3)
B(1)-C(11)	1.644(2)	C(9)-C(10)	1.375(3)
N(1)-C(5)	1.345(2)	C(11)-C(12)	1.393(2)
N(1)-C(1)	1.351(2)	C(11)-C(16)	1.403(2)
N(2)-C(10)	1.345(2)	C(12)-C(13)	1.390(2)
N(2)-C(6)	1.359(2)	C(13)-C(14)	1.392(3)
C(1)-C(2)	1.390(2)	C(14)-C(15)	1.395(2)
C(2)-C(3)	1.384(2)	C(14)-C(17)	1.532(2)

C(3)-C(4)	1.384(2)	C(15)-C(16)	1.379(2)
C(4)-C(5)	1.367(2)	C(17)-C(19)	1.508(3)
C(17)-C(18)	1.527(3)	C(10)-C(9)-C(8)	117.72(16)
C(17)-C(20)	1.546(3)	N(2)-C(10)-C(9)	123.68(17)
C(21)-C(22)	1.398(2)	C(12)-C(11)-C(16)	114.67(15)
C(21)-C(26)	1.403(2)	C(12)-C(11)-B(1)	124.51(15)
C(22)-C(23)	1.393(2)	C(16)-C(11)-B(1)	120.81(15)
C(23)-C(24)	1.391(3)	C(13)-C(12)-C(11)	122.90(17)
C(24)-C(25)	1.392(3)	C(12)-C(13)-C(14)	121.59(17)
C(24)-C(27)	1.477(2)	C(13)-C(14)-C(15)	116.16(16)
C(25)-C(26)	1.383(2)	C(13)-C(14)-C(17)	123.94(16)
C(27)-C(28A)	1.305(6)	C(15)-C(14)-C(17)	119.89(16)
C(27)-C(28)	1.333(4)	C(16)-C(15)-C(14)	121.76(17)
C(21)-B(1)-C(1)	108.59(13)	C(15)-C(16)-C(11)	122.91(16)
C(21)-B(1)-C(6)	111.06(13)	C(19)-C(17)-C(18)	110.06(18)
C(1)-B(1)-C(6)	111.31(14)	C(19)-C(17)-C(14)	111.72(17)
C(21)-B(1)-C(11)	112.14(14)	C(18)-C(17)-C(14)	109.58(15)
C(1)-B(1)-C(11)	107.15(13)	C(19)-C(17)-C(20)	109.08(19)
C(6)-B(1)-C(11)	106.54(13)	C(18)-C(17)-C(20)	107.35(16)
C(5)-N(1)-C(1)	125.06(15)	C(14)-C(17)-C(20)	108.94(16)
C(10)-N(2)-C(6)	119.54(15)	C(22)-C(21)-C(26)	115.22(15)
N(1)-C(1)-C(2)	115.43(15)	C(22)-C(21)-B(1)	124.70(15)
N(1)-C(1)-B(1)	118.76(14)	C(26)-C(21)-B(1)	120.07(14)
C(2)-C(1)-B(1)	125.58(14)	C(23)-C(22)-C(21)	122.44(17)
C(3)-C(2)-C(1)	121.41(16)	C(24)-C(23)-C(22)	121.18(17)
C(2)-C(3)-C(4)	120.02(16)	C(23)-C(24)-C(25)	117.20(15)

C(5)-C(4)-C(3)	118.33(17)	C(23)-C(24)-C(27)	121.20(17)
N(1)-C(5)-C(4)	119.73(16)	C(25)-C(24)-C(27)	121.60(18)
N(2)-C(6)-C(7)	118.51(15)	C(26)-C(25)-C(24)	121.17(17)
N(2)-C(6)-B(1)	119.10(14)	C(25)-C(26)-C(21)	122.79(16)
C(7)-C(6)-B(1)	122.12(14)	C(28A)-C(27)-C(28)	104.8(3)
C(8)-C(7)-C(6)	121.35(17)	C(28A)-C(27)-C(24)	127.2(3)
C(7)-C(8)-C(9)	119.16(17)	C(28)-C(27)-C(24)	127.5(2)

### Anisotropic Displacement Parameters ( $\text{\AA}^2 \times 10^3$ ) of D43

	U11	U22	U33	U23	U13	U12
B(1)	23(1)	20(1)	22(1)	6(1)	6(1)	4(1)
N(1)	23(1)	22(1)	26(1)	7(1)	10(1)	6(1)
N(2)	23(1)	24(1)	31(1)	7(1)	9(1)	6(1)
C(1)	24(1)	19(1)	14(1)	2(1)	4(1)	7(1)
C(2)	24(1)	24(1)	21(1)	4(1)	7(1)	7(1)
C(3)	26(1)	30(1)	21(1)	3(1)	9(1)	0(1)
C(4)	36(1)	20(1)	31(1)	8(1)	14(1)	3(1)
C(5)	35(1)	21(1)	33(1)	9(1)	14(1)	10(1)
C(6)	25(1)	21(1)	21(1)	6(1)	8(1)	7(1)
C(7)	26(1)	24(1)	40(1)	8(1)	8(1)	7(1)
C(8)	28(1)	27(1)	49(1)	6(1)	9(1)	-1(1)
C(9)	20(1)	35(1)	44(1)	10(1)	7(1)	4(1)
C(10)	24(1)	30(1)	42(1)	10(1)	9(1)	9(1)
C(11)	21(1)	20(1)	24(1)	5(1)	7(1)	9(1)
C(12)	25(1)	31(1)	25(1)	7(1)	9(1)	-2(1)

C(13)	29(1)	39(1)	23(1)	2(1)	5(1)	-6(1)
C(14)	24(1)	35(1)	25(1)	9(1)	9(1)	7(1)
C(15)	30(1)	20(1)	28(1)	9(1)	13(1)	9(1)
C(16)	31(1)	18(1)	26(1)	4(1)	9(1)	6(1)
C(17)	33(1)	47(1)	23(1)	8(1)	9(1)	0(1)
C(18)	48(1)	38(1)	31(1)	4(1)	19(1)	7(1)
C(19)	80(2)	100(2)	22(1)	-2(1)	12(1)	-48(2)
C(20)	50(1)	89(2)	38(1)	35(1)	16(1)	26(1)
C(21)	19(1)	19(1)	25(1)	6(1)	6(1)	2(1)
C(22)	25(1)	23(1)	26(1)	5(1)	6(1)	4(1)
C(23)	25(1)	23(1)	42(1)	11(1)	9(1)	9(1)
C(24)	26(1)	18(1)	42(1)	3(1)	17(1)	1(1)
C(25)	32(1)	23(1)	29(1)	1(1)	14(1)	1(1)
C(26)	27(1)	22(1)	26(1)	7(1)	8(1)	5(1)
C(27)	36(1)	22(1)	61(1)	4(1)	26(1)	4(1)
C(28)	47(2)	37(2)	74(3)	-10(2)	38(2)	5(2)
C(28A)	38(3)	26(3)	66(4)	13(3)	30(3)	9(2)

---

## List of Publications

1. "Organoboronium-functionalized Polystyrenes as a New Class of Polycations"  
**Cui, C.**; Jäkle, F. *Chemical Communications*, **2009**, 2744-2746.
2. "Organoboronium Amphiphilic Block Copolymers" **Cui, C.**; Qin, Y.; Bonder, E. M.; Jäkle, F. *Journal of Polymer Science Part A: Polymer Chemistry*, **2009**, *47*, 6612-6618.
3. "Weakly-coordinating Organoborate Polymers and Amphiphilic Block-Copolymers." **Cui, C.**; Qin, Y.; Bonder, E. M.; Jäkle, F. submitted for publication.
4. "Synthesis and pH-dependent Micellization of the Amphiphilic Block Copolymer Poly(styrene boronic acid)-block-Polystyrene in Water." **Cui C.**; Qin, Y.; Bonder, E. M.; Jäkle, F. submitted for publication.
5. "Tris(1-pyrazolyl)borate (Scorpionate) Functionalized Polymers as Scaffolds for Metallopolymers." Qin, Y.; **Cui, C.**; Jäkle, F. *Macromolecules* **2008**, *41*, 2972-2974.
6. "Silylated Initiators for the Efficient Preparation of Borane-End-Functionalized Polymers via ATRP." Qin, Y.; **Cui, C.**; Jäkle, F. *Macromolecules* **2007**, *40*, 1413-1420.

7. "Preparation of Organoboron Block Copolymers via ATRP of Silicon and Boron-Functionalized Monomers." Qin, Y.; Sukul, V.; Pagakos, D.; Cui, C.; Jäkle, F. *Macromolecules* **2005**, *38*, 8987-8990.

## VITA

### Chengzhong Cui

**Date of Birth:** January 7<sup>th</sup>, 1974

**Place of Birth** Shenyang, Liaoning, China

**Name of the Father** Shushen Cui

**Name of the Mother** Jinfeng Wang

#### Educational background

1992-1996 Department of Chemical Engineering,  
Nanjing University of Science & Technology, Nanjing, Jiangsu, China.  
Degree achieved:  
B. S. in Polymer Science and Engineering.

2002-2003 Department of Physics,  
New Jersey Institute of Technology, Newark, NJ, USA  
Degree achieved:  
M.S. in Materials Science and Engineering.

2004-present Department of Chemistry,  
Rutgers University-Newark, Newark, NJ, USA  
Degree sought:  
Ph.D. in Chemistry. Advisor: Frieder Jäkle.